POLITECNICO DI MILANO
DEPARTMENT OF CIVIL AND ENVIRONMENTAL ENGINEERING
DOCTORAL PROGRAM IN ENVIRONMENTAL AND INFRASTRUCTURE ENGINEERING
ENVIRONMENTAL TECHNOLOGIES AREA

# WATER INDIRECT REUSE: FROM AN UNPLANNED RISK TO A PLANNED RESOURCE

Doctoral dissertation of:
**Riccardo Delli Compagni**

Supervisor:
**Prof. Manuela Antonelli**
Co-supervisor:
**Dr. Andrea Turolla**
Tutor:
**Prof. Francesca Malpei**
The chair of the doctoral program:
**Prof. Riccardo Barzaghi**

32th cycle
2016 - 2019

# Acknowledgments

I am sincerely and heartily grateful to Prof. Manuela Antonelli, for being more than a supervisor, for her patient guidance, encouragement and advice she has provided throughout my PhD. I would also like to thank my assistant supervisor: Dr. Andrea Turolla for the time and help given throughout, and his precious pieces of advice.

I am very grateful to Dr. Fabio Polesel, an invaluable person from a human and professional point of view, for being essential in defining my research activities and for being always present for discussions and suggestions.

I would like to express my gratitude for Prof. Luca Vezzaro and Prof. Stefan Trapp for their enthusiastic supervision during my stay at DTU, for providing substantial inputs to my research and sharing with me their wide knowledge in mathematical modelling.

I wish to thank Dr. Christoph Ort and Dr. Frank Blumensaat for the critical and fruitful discussions at Eawag.

One special thought goes to all my colleagues at Polimi, DTU and Eawag, for making this journey so memorable.

And finally but by no means least, special thanks goes to my family, especially to my aunt Elena Delli Compagni for her patience and support on so many occasions.

# Abstract

Reuse of reclaimed wastewater (RWW) in agriculture has recently received increasing attention as a possible solution to water scarcity in many parts of the world. However, RWW can still contains a large variety of contaminants of emerging concern (CECs), which can seep into the soil and enter into the food chain through uptake of edible plants, posing a risk to the environment and human health. Quantification of the risk consists of understanding the level of exposure concentrations with respect to safety thresholds derived from ecotoxicological studies. Historically, determination of exposure concentrations depended essentially on measurements. However, the monitoring of thousands of CECs in different environmental compartments is unfeasible (both economically and physically). Moreover, measurements are discontinuous in-time, site/person-specific and do not allow extrapolating contamination levels to others systems. Developing of reliable modelling tools can help to overcome these challenges.

The purpose of this PhD thesis is to contribute to filling the knowledge gaps in the field of risk assessment related to spread of CECs in RWW reuse systems. Specifically, the thesis aims at developing a modelling framework capable of supporting policy-makers to assess the environmental and human health risk of current and future water reuse management strategies. Moreover, the framework is indented for the planning of measuring campaigns to collect samples with high representativeness in order to allow a proper evaluation of compliance with current and forthcoming standards. In this work, the RWW reuse system was considered as made of 5 elements: (i) CECs sources (e.g. cities, industries, hospitals), (ii) combined sewer network, (iii) conventional wastewater treatment plant (WWTP), (iv) surface water and (v) irrigation system. Within this framework, dynamic deterministic conceptual models (both lump and distributed), have been combined with advanced statistical methods (i.e. cluster analysis, uncertainty analysis, stochastic generators, etc.) to make the best use of heterogeneous data sources (e.g. georeferenced information, sales data, etc.) to predict CECs exposure concentrations in target environmental compartments (surface water and edible plant organs). Risk assessment was mainly investigated due to: discharge of treated and untreated wastewater (during rain events) into receiving water system (i.e. environmental risk) and, (ii) human consumption of contaminated edible plants irrigated with RWW (i.e. human health risk).

The fate of down-the-drain CECs (e.g. pharmaceutical active compounds - PhACs, personal care products, etc.) from emission sources to the WWTP was first investigated. Within this context, a new systematic approach, combining GIS-based information and a Gaussian mixture model, was developed to identify the optimal structure of a multi-catchment conceptual model to simulate the fate of CECs in large urban catchments. The approach was tested in a catchment located in a highly urbanized Italian city and model performance compared against a traditional single-catchment conceptual model. Results showed that the multi-catchment model allows for a successful simulation of dry weather flow patterns and for an improved simulation of CECs fate compared to the classical single-catchment model.

Secondly, an existing micropollutants fate model library (IUWS_MP) was extended to simulate the fate of PhACs with different properties across the whole Integrated Urban Wastewater and Stormwater systems (IUWS – drainage systems, wastewater treatment plants, receiving water bodies). Extensions included specific PhACs fate processes (deconjugation) and a consumption-excretion model to allow simulation of seldom monitored PhAC fractions (e.g. metabolites and fractions entrapped within the faecal matter) along the whole system, thus refining fate and risk assessment in RWW system. PhACs process descriptions was based on simple equations (e.g. first-order kinetics rates to describe deconjugation) and easily retrievable input-parameters (e.g. inherent chemical-physical properties, consumption data, etc.) to minimize the need of data collection for model calibration (except for validation). Model predictions were tested in two different real case studies (i.e. Italian and Danish ones) under dry-weather conditions for 5 highly-consumed PhACs (i.e. carbamazepine, diclofenac, ibuprofen, furosemide and paracetamol). Predictions showed good agreements with measurements at various comparison points (e.g. WWTP inlet and outlet). Possible model implications included: (i) identification of potential environmental risks due to non-compliance of PhACs with existing or proposed environmental quality standards at the WWTP/sewer outlet and (ii) evaluation of the effects of different control strategies in reducing risks for the aquatic environment.

Then, the fate of PhACs under wet weather conditions was assessed to: (i) evaluate the impact of combined sewer overflows (CSOs) on surface water streams and (ii) identify optimal sampling strategies (i.e. type of composite, frequency and duration) to sample CSO concentration as much representative as possible. Specifically, a dynamic distributed model was coupled with stochastic PhAC loads generator to make the best use of census and georeferenced data (e.g. number of people per household, age and sex, house location) as proxy variables of unknown/confidential information (e.g., location of the person taking a certain drug, prescribed posology) to simulate realistic PhACs dynamics in sewer systems. Model prediction capabilities were tested in a small Swiss catchment where high-frequency measurements for diclofenac were available during wet-weather conditions. Results showed a proper match between model predictions and measurements. The model was then used to predict diclofenac concentrations at the CSO location during different rain events. Results highlighted that diclofenac concentrations can exceed the quality standard (i.e. the chronic standard was used since an acute standard is not available yet) in the sewage flow discharging to the water stream, posing a risk for the environment. Simulations also showed that flow-proportional mode with a high sampling frequency (2-5 minutes) is the most appropriate way to capture most of the diclofenac load passing through the CSO structure.

Lastly, the extended IUWS_MP was coupled with a dynamic plant uptake model to predict the fate of CECs beyond wastewater treatments. The modelled system included a discharge channel and cultivation area where four different types of crops were irrigated with RWW. The model showed capability and flexibility in describing the fate of 13 CECs (clarithromycin, sulfamethoxazole, diclofenac, ibuprofen, paracetamol, carbamazepine, furosemide, 17α-ethinylestradiol, 17β-estradiol, estrone, perfluorooctanoic acid, perfluorooctane sulfonate and triclosan), covering a wide range of physicochemical properties, across different compartments and over long-time intervals. Model predictions were generally verified with measured data,

thus allowing for the evaluation of ecological and human health risk. A negligible risk was predicted for most CECs, while sulfamethoxazole and 17α-ethinylestradiol exhibited the highest risk for consumers. Model predictions identified conventional wastewater treatments as an efficient barrier to reduce the overall risk of simulated CECs, although further reduction can be obtained by adopting more efficient irrigation practices.

# Contents

# Chapter 1

## Introduction

A micropollutant (MP) is any substance that is present in the (aquatic) environment at trace level (e.g. μg $l^{-1}$ or ng $l^{-1}$) due to anthropogenic activities (Stamm et al., 2016), and whose concentration is well above the environmental background level. Thousands of substances belong to this definition, and among them the so called "contaminants of emerging concern" (CECs) have garnered much attention from scientists in the last years. Particularly, CECs can be defined as MPs, whose presence in the environment is likely to affect negatively the metabolism of a living being (Sauvé and Desrosiers, 2014). The term CECs does not necessarily refer to new substances, but can also refers to MPs whose presence have been known for long times, but negative effects on environment/human health have only recently come into focus (Sauvé and Desrosiers, 2014). Consequently, CECs can include well known MPs such as heavy metals, insecticides and herbicides, but also others types of MPs such as personal care products and pharmaceuticals.

A wide range of diffuse and point sources (e.g. highly populated cities, industries, agriculture, landfills, etc.) are responsible of introducing MPs into the environment through different paths (e.g. runoff, leachate, direct discharge, etc.), with wastewater being one of the main transport media. Concentrations in wastewater can generally vary from 1 ng $l^{-1}$ to 1000 μg $l^{-1}$, and the most commonly detected CECs are pharmaceutical active compounds (PhACs) such as analgesic and anti-inflammatory drugs, antibiotics, diuretics, psychiatric drugs, antidiabetics and antihistamines (Luo et al., 2014). Removal in conventional wastewater treatment plants (WWTPs) varies greatly (0% to 100%) (Margot et al., 2015) and mainly occurs by biodegradation/biotransformation and sorption (Verlicchi et al., 2012), and volatilization and abiotic degradation. Negative removal efficiencies were observed for some PhACs such as the anti-inflammatory drug diclofenac, the antiepileptic drug carbamazepine and sulphonamides, a class of antibiotic drugs. Possible explanations include retransformation (i.e. deconjugation) of metabolites, which are by-products produced by the human metabolization of the original molecule (also known as parent fraction), and direct release from feces particles (Luo et al., 2014). However, erroneous sampling methods and analytic uncertainties can also partly explain negative values (Aymerich et al., 2017; Majewsky et al., 2011; Ort et al., 2010; Verlicchi and Ghirardini, 2019), especially in large WWTPs. The advanced tertiary treatments such as activated carbon and ozone have shown very high removal efficiencies (i.e. > 90%) for a broad range of CECs (Margot et al., 2015). However, very few countries (e.g. Switzerland and parts of Germany) have systematically implemented these technologies (Eggen et al., 2014) due to the high costs and undefined discharge limits.

CECs are frequently detected in different environmental compartments (e.g. soil, sediment, surface water, groundwater and even drinking water) (Margot et al., 2015), including even the most biodegradable ones (e.g. the anti-inflammatory paracetamol, one of the most consumed PhACs), due to their continuous emission which compensate the removal. Although acute

toxicity is unlikely, in the long run a constant exposure to low level of CECs may trigger negative chronic effects such as feminization of fish, intersex and reproductive disruption, alteration of macroinvertebrate, etc. (Margot et al., 2015).
To limit the environmental risk, in 2008 the European legislation (Directive 2008/105/EU and Directive 2013/39/UE) established the concept of environmental quality standards (EQSs), defining a maximum allowable concentration (MAC-EQS) and an annual average concentration (AA-EQS) which should not be exceeded in the receiving water to limit acute and chronic effects, respectively. Limits were identified for some MPs including herbicides, fungicides, surfactants, metals and polycyclic aromatic hydrocarbons, while determination of EQSs for a list of target CECs is now in progress. Particularly, a watch-list mechanism (Decision 2015/495/EU and Decision 2018/495/EU) was established to gather high-quality monitoring data across the European Union with the intent to elucidate the extent of the spatial contamination and associated risk. Included CECs were: the natural and synthetic hormones (17α-ethinylestradiol, 17β-estradiol and estrone), antibiotics (clarithromycin, erythromycin, azithromycin, amoxicillin and ciprofloxacin), pesticides (methiocarb, imidacloprid, etc.), UV filters (2-ethylhexyl 4-methoxycinnamate), non-steroidal anti-inflammatory drugs (diclofenac), etc. So far, no decision has been taken about setting new EQSs.

Besides the environmental risk, highly persistent CECs (e.g. the antiepileptic carbamazepine is one of the most studied for its poor biodegradability and sorption affinity) can naturally find their way to humans through indirect exposure routes (e.g. food chain), posing a human health risk (René et al., 2006). Nowadays, indirect exposure to these substances is also enforced in many arid and semi-arid regions of the world where reclaimed wastewater (RWW) is reused for irrigation to alleviate fresh water depletion (COM/2015/614). For example, in California and Israel, RWW already accounts for 6% to 50% of the total irrigation-water demand (Goldstein et al., 2014), and also in some European countries (e.g. Spain and Italy) RWW reuse is becoming a common practice. Consequently, an unintended human exposure to these substances can originate due to their high potential of accumulating in edible plant organs such as leaves and fruits (Goldstein et al., 2014). Specifically, non-negligible concentrations of carbamazepine and associated metabolites were recently found in urine of adults who consumed vegetables irrigated with RWW (Paltiel et al., 2016). Authors concluded that clinical effects are unlikely since concentration levels were four order of magnitude lower than therapeutic concentrations; however chronic effects are still unknown and a possible health risk might be present for the most sensitive targets (e.g. children, pregnant women and the elderly). Furthermore, authors investigated the fate of carbamazepine only, while a mixture of CECs is generally taken up by plants, which additive or synergic effects can lead to stronger consequences on human health (Brian et al., 2005). Finally, little is known about the uptake of PhACs metabolites, which in some cases were found to be more toxic than the corresponding parent fraction (Hermida and Tutor, 2003; Malchi et al., 2015).

For these reasons, indirect human exposure assessment to CECs in RWW reuse systems is fundamental. A recent European proposal identifies the need of assessing the risk associated to PhACs in RWW reuse system (COM/2018/337), acknowledging the need of a science-based risk assessment framework, which scope is to identify case-specific limits and preventing measures.

Quantification of the risk consists of understanding the level of exposure concentrations with respect to safety thresholds derived from ecotoxicological studies. Historically, determination of exposure concentrations depended essentially on measurements. However, today it is well-recognized that monitoring of thousands of CECs, in different environmental compartments and matrixes, with all associated metabolites and physical forms (e.g. particulate, dissolved, etc.) is either economically and physically not feasible. Moreover, measurements are discontinuous in-time, site/person-specific and do not allow extrapolating contamination levels to others systems.
Within this context, modelling tools can help to overcome this lack of knowledge and contribute significantly with valuable complementary information (e.g. filling temporal gaps between measurements, estimate concentrations of unmeasured fractions, etc.), also accounting for the influence of site-specific conditions. Moreover, statistical indicators (e.g. percentiles) of the predicted exposure concentrations can then be used to infer useful information such as probability of exceedance of certain threshold (e.g. MAC-EQS) for a better quantification of the risk. In environmental modelling, deterministic conceptual models generally predominate over mechanistic and/or stochastic models, mainly due to limited data availability and the need of simplifying complex systems. Model state variables (e.g. concentrations and flow) are typically distributed in time (i.e. lump model) rather than both in time and space (i.e. distributed model) since model solutions in each part of the system might not always be necessary (Vanrolleghem et al., 2002). Furthermore, dynamic models are generally preferred over steady-state models, mainly due to intrinsic dynamicity of the modelled phenomena.
Historically, modelling efforts focused on the single elements of the urban wastewater system (e.g. WWTP and surface water system) resulting in state-of-the-art models (e.g. the activated sludge model, river water quality model, etc.) that aimed at predicting conventional pollutant dynamics (e.g. COD, TSS, nitrogen and phosphorus, etc.). Only recently, some of these models were modified to include CECs processes (Plósz et al., 2013). However, limited CECs data availability for model input and parameter identifiability still make the use of these models limited to few well-known CECs (e.g. carbamazepine and diclofenac). There is currently high need to identify relevant and general fate processes and system conceptualization approaches to predict CECs fate with the minimum degree of model structure complexity and data requirement (Pomiès et al., 2013). Moreover, modelling integration is required to simulate CECs fate from sources to the final receptor (i.e. environment and/or human) as well as to evaluate alternative scenarios (e.g. risk management strategies, cost-effective control options, etc.) considering all multiple (re)uses of the water resource in each element.

The first idea of integrated model was proposed more than 40 years ago (Beck, 1976) and since then, there have been many successful attempts of integration of various elements of the Integrated Urban storm water and Wastewater System (IUWS) (Bach et al., 2014). Modelled IUWS elements mainly included the sewer system, the WWTP, and the receiving surface water, with the latter considered as endpoint. For example, in the work of De Keyser et al. (2010) an integrated model showed the ability of evaluating the impacts of discharges from storm- and wastewater system on the chemical status of surface water for a hypothetical case study. Recently, an integrated model (Polesel et al., 2015) was developed to simulate the CECs fate from excretion to crop irrigation, expanding the traditional boundaries of the IUWS system for

evaluating human health risk under worst-case scenarios in semi-steady state conditions. Dynamic models are often required to evaluate the effect of specific events such combined sewer overflows, CECs source emissions, diurnal and seasonal patterns in wastewater discharges, which are intrinsically dynamic. Also, dynamic models can support the planning of future measuring campaigns, indicating what kind of fluctuations are expected in order to optimize sampling modes to collect samples with high representativeness. The ScorePP project (Source Control Options for Reducing Emissions of Priority Pollutants - 2006-2009) investigated different MP control options, and a dynamic model library (IUWS_MP library, Vezzaro et al. 2014) was specifically developed for simulating the fate of priority MPs (e.g. herbicides, fungicides, surfactants, metals and polycyclic aromatic hydrocarbons) in the IUWS system. Due to data scarcity, the library has been used only for ideal scenarios, lacking a full-scale validation with real catchments. Furthermore, many CECs such as PhACs are substantially different from MPs that were originally investigated by the IUWS model library, as they show additional release pathways and fate processes (i.e. deconjugation, ionization-driven sorption affinity, etc.).

In conclusion, there is currently a high need of a reliable and robust dynamic model capable of estimating CECs concentrations (and associated risk) in different interconnected environmental compartments (surface water, soil, crops) under different reuse scenarios and environmental conditions.

# Chapter 2

## Design of the research

Reclaimed wastewater (RWW) reuse in agriculture is becoming a valid option to replace fresh water in many arid and semi-arid regions of the world. However, the environment and humans might be unintended exposed to CECs, which persist to wastewater treatments, and enter the food chain through uptake of edible plants.

Whether a risk exists depends on understanding if CECs exposure concentrations exceed a tolerable threshold. The scope of ecotoxicological studies is to identify such threshold, while measurements might determine the level of exposure. However, monitoring of thousands of CECs is impractical if not impossible. Moreover, measurements are discontinuous in-time, site/person-specific and do not allow extrapolating contamination levels to others systems.

The overall objective of the thesis was to develop a flexible integrated model to predict CECs fate in different types of RWW reuse systems, irrespective of size and complexity, that could support decision-makers in evaluating the impact (i.e. the risk) of RWW practices on both environment and human health. Moreover, the model is intended to be a supporting tool for planning measuring campaigns, suggesting where (i.e. in which environmental compartment) and when (i.e. with which frequency) a certain CEC is expected.

In this thesis, the whole integrated model is subdivided in four parts (i.e. chapters), each one following a scientific article-base structured and published/intended for publication on an international peer-reviewed scientific journal. A schematic overview of the thesis chapters is given in Figure 1, and their content is briefly described in the following.

- *Chapter 3:* a new, systematic and fast approach is presented to support the construction of conceptual models for predicting in-sewer CECs fate in large urban catchments. The method relies on GIS information (e.g. consumer locations and sewer network), quantitative data (e.g. water consumption and WWTP inflow data) and advanced statistical techniques (cluster analysis) to cluster areas of the urban catchment based on similar hydraulic residence time (HRT). As a result, a multi-catchment conceptual model (i.e. with a discrete HRT distribution) is obtained. The approach was tested for a large urban catchment and its performance was compared against a traditional single-catchment model (i.e. one HRT) for three scenarios: (i) CECs undergoing biodegradation; (ii) CECs undergoing biodegradation and retransformation; (iii) CECs emissions from a point source at different locations in the catchment, i.e. with different distance and transport time to the receiving WWTP.

- *Chapter 4:* a dynamic model library, originally developed to estimate the fate of priority substances (i.e. herbicides, fungicides, surfactants, metals and polycyclic aromatic hydrocarbons) in an integrated urban wastewater system, was modified to simulate the fate of PhACs (e.g., anti-inflammatory substances and antibiotics), which are the most

consumed CECs on the market. Specifically, model modifications included: (i) integration with a consumption-excretion model to generate initial concentrations of PhAC fractions at the urban catchment scale, (ii) new fate processes (e.g. deconjugation and sequestration in fece particles) and, (iii) redefinition of existing fate processes (e.g. sorption to account for ionization). Prediction capabilities of the dynamic model were verified under dry-weather conditions against measurements in two urban wastewater systems (an Italian and a Danish system) with different characteristics (i.e. different structure of the sewer network, presence and absence of a wastewater treatment plant, etc.).

- *Chapter 5:* the PhACs fate under wet-weather conditions was evaluated by means of a new modelling framework, which combines accessible census and georeferenced data with a complex hydrodynamic storm water model. The framework was verified with measurements and used to perform an environmental risk assessment in a small urban catchment in Switzerland, where combined sewer overflows are discharged into a receiving water system. Moreover, the framework was used to plan future sampling campaigns.

- *Chapter 6:* a river water quality model, included in the dynamic model library developed in chapter 4, was combined with a coupled soil-plant model to describe CECs fate in the generic agricultural irrigation system. The integrated model was applied to a real Italian RWW reuse scenario, comprising a discharge channel and cultivation of four different types of crops (silage maize, rice, wheat and ryegrass) and verified with site-specific measurements (where available) and literature data in different compartments. Human health risk following the ingestion of irrigated crops was evaluated and alternative risk management and minimization scenarios compared.

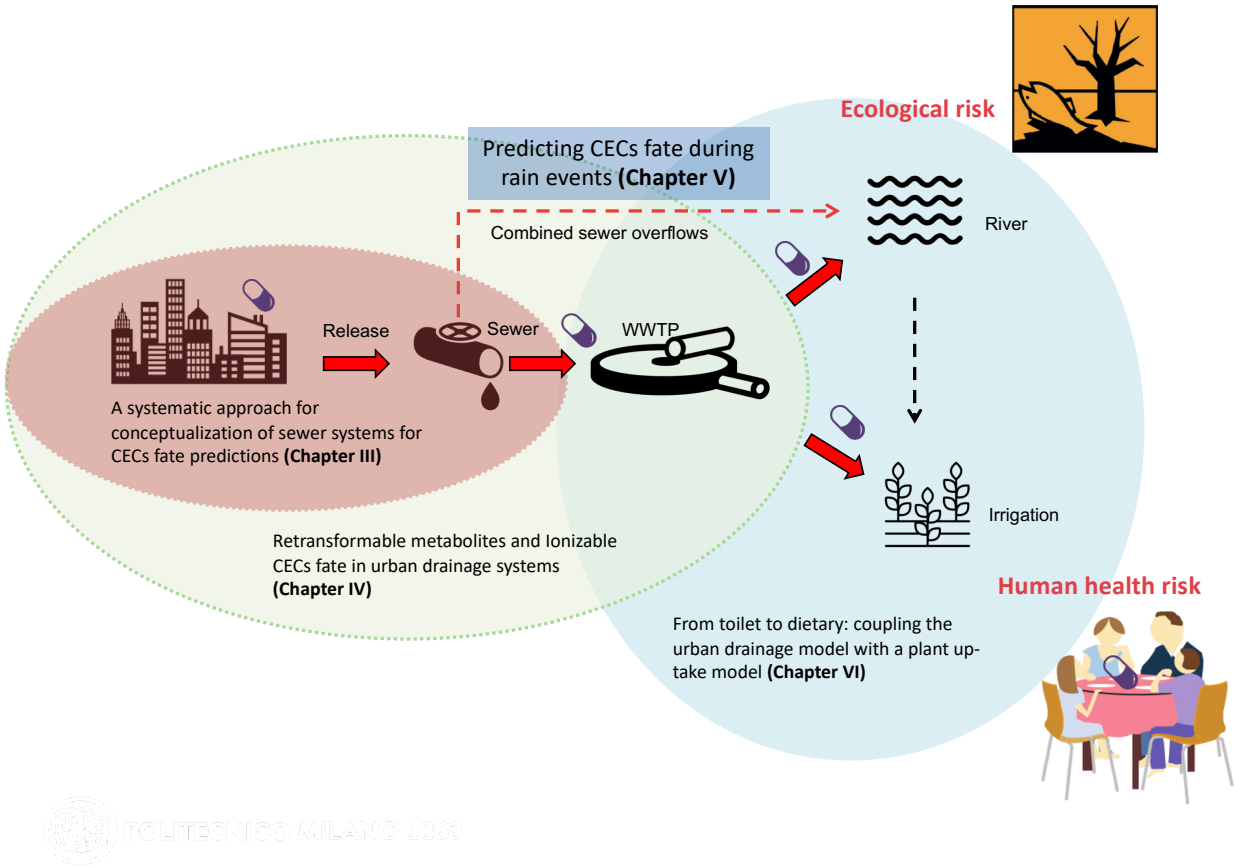


**Figure 1:** Schematic overview of the thesis chapters and their focus on each part of the wastewater reuse system.

# Chapter 3

# Modelling micropollutant fate in sewer systems – A new systematic approach to support conceptual model construction based on in-sewer hydraulic retention time

**Abstract:** Conceptual sewer models are useful tools to assess the fate of micropollutants (MPs) in integrated wastewater systems. However, the definition of their model structure is highly subjective, and obtaining a realistic simulation of the in-sewer hydraulic retention time (*HRT*) is a major challenge without detailed hydrodynamic information or with limited measurements from the sewer network. This study presents an objective approach for defining the structure of conceptual sewer models in view of modelling MP fate in large urban catchments. The proposed approach relies on GIS-based information and a Gaussian mixture model to identify the model optimal structure, providing a multi-catchment conceptual model that accounts for *HRT* variability across urban catchment. This approach was tested in a catchment located in a highly urbanized Italian city and it was compared against a traditional single-catchment conceptual model (using a single average *HRT*) for the fate assessment of reactive MPs. Results showed that the multi-catchment model allows for a successful simulation of dry weather flow patterns and for an improved simulation of MP fate compared to the classical single-catchment model. Specifically, results suggested that a multi-catchment model should be preferred for (i) degradable MPs with half-life lower than the average *HRT* of the catchment and (ii) MPs undergoing formation from other compounds (e.g. human metabolites); or (iii) assessing MP loads entering the wastewater treatment plant from point sources, depending on their location in the catchment. Overall, the proposed approach is expected to ease the building of conceptual sewer models, allowing to properly account for *HRT* distribution and consequently improving MP fate estimation.

**Keywords:** geographical information system, cluster analysis, sewer system modelling, wastewater-based epidemiology, emerging contaminants.

The research work presented in this chapter was carried out during a research stay period of 8 months at the Technical University of Denmark (Denmark). The research work was carried out with the valuable support of Prof. Luca Vezzaro (Technical University of Denmark) and Dr. Fabio Polesel (DHI A/S) and the help of two MSc students, Kerstin von Borries and Zheng Zhang.

This chapter has been published in "Journal of Environmental Management[1]"

[1] Delli Compagni, R., Polesel, F., von Borries, K.J.F., Zhang, Z., Turolla, A., Antonelli, M., Vezzaro, L., 2019. Modelling micropollutant fate in sewer systems – A new systematic approach to support conceptual model construction based on in-sewer hydraulic retention time. J. Environ. Manage. 246, 141–149. https://doi.org/10.1016/J.JENVMAN.2019.05.13

# 1. Introduction

Organic micropollutants (MPs) have been recognized as a concern for the environment and human health due to the detrimental effects (e.g. toxicity, estrogenicity) they can pose even at low concentrations (ng $L^{-1}$ to µg $L^{-1}$) (Galus et al., 2013; Fent et al., 2006; Daughton and Ternes, 1999). Several MPs (e.g. pharmaceuticals and personal care products) enter the water cycle through wastewater discharges flowing along sewer systems to wastewater treatment plants (WWTPs), where they are not entirely removed and consequently discharged into environmental recipients (Petrie et al., 2015). In sewer systems, MPs can undergo degradation (biotic and abiotic), adsorption and retransformation – from other excreted metabolites (Bahlmann et al., 2014), remobilisation of sewer deposit (Launay et al., 2016), abiotic formation from other MPs (Sengeløv et al., 2003). The importance of these processes depends on the MP properties, environmental and hydraulic conditions (D'Ascenzo et al., 2003; Gomes et al., 2009; Plósz et al., 2012; Thai et al., 2014; Ramin et al., 2016; McCall et al., 2016; Menzies et al., 2017). Combining the abovementioned processes with the hydrodynamics of the sewer itself is a challenging modelling task. Nevertheless, MP fate models can be highly beneficial for (i) providing high-frequency input data to assess performances of WWTP models (i.e. to assess MP discharge into the environment) when full-scale measurements are scarce (e.g. Snip et al., 2014); (ii) evaluating possible mitigation strategies within the urban drainage system taking into account interactions with the WWTP system (e.g. Eriksson et al., 2011); and (iii) back-calculating consumption of chemicals in upstream catchments using wastewater-based epidemiology approaches while considering in-sewer losses (e.g. McCall et al., 2017).

In sewer systems, water transport is usually modelled by using distributed hydrodynamic or conceptual models (Obropta and Kardos, 2007; Zoppou, 2001). Hydrodynamic models are computationally demanding and require detailed information about the network (number of pipes, slopes, diameters, etc.) to explicitly describe the hydraulic conditions (e.g. water level, flow velocity, etc.) in each part of the system. On the other hand, conceptual models lump parts of the system into simple units, while flow routing is described by using continuously stirred tank reactors (CSTRs) in series (Saagi et al., 2016). These models use general information such as the average hydraulic residence time (*HRT*) to describe water dynamics at specific points of the system (e.g. the sewer outlet, overflow structure). The loss of details is balanced by the increase of computational speed, making conceptual models ideal for simulating water quality, both for traditional water quality indicators (Flores-Alsina et al., 2014; Martin and Vanrolleghem, 2014) and MPs (De Keyser et al., 2010; Snip et al., 2016; Mannina et al., 2017). Although alternative approaches have been also tested to simulate the stochastic behaviour of specific MP sources (Ort et al., 2005; Pouzol et al., 2018), conceptual models are often applied in a deterministic manner (i.e. MP sources are modelled as deterministic).

The realistic description of in-sewer *HRT* represents a major challenge for the development of conceptual models for large urban catchment. Moreover, *HRT* can strongly influence the extent of in-sewer MP processes and their overall attenuation, and it should therefore be carefully considered during model construction (Jelic et al., 2015; Polesel et al., 2016; Ramin et al., 2016, McCall et al., 2017; Li et al., 2018). Typically, one of the first steps during model construction consists of subdividing the urban catchment into smaller sub-catchments in a heuristic or empirical manner, where *HRTs* are defined based on the available information of the area (e.g.

geographical maps, topography, distances). However, this step is highly subjective and requires several trial-and-error iterations. To make this step objective, automatic algorithms have been proposed for hydrological models (Davidsen et al., 2017; Wolfs et al., 2013), while tools supporting the building of conceptual models focusing on water quality are still missing. Alternative approaches have been developed to define *HRT* as a probability density distribution, which was derived using road network as proxy variable for sewer network (Kapo et al., 2017) or by running complex hydrodynamic models (McCall et al., 2017). To date, however, an automated procedure for constructing a conceptual model is still lacking.
This study aimed at developing a new, systematic and fast approach to support the construction of conceptual models for predicting in-sewer MP fate in large urban catchments. The method relies on GIS information (e.g. consumer locations and sewer network), quantitative data (e.g. water consumption and WWTP inflow data) and advanced statistical techniques (cluster analysis) in order to cluster areas of the urban catchment based on similar *HRT*. As a result, a multi-catchment conceptual model (i.e. with a discrete *HRT* distribution) is obtained. The approach was tested for a large urban catchment and its performance was compared against a traditional single-catchment model (i.e. one *HRT*) for three scenarios: (i) MP undergoing biodegradation; (ii) MP undergoing biodegradation and retransformation; (iii) MP emissions from a point source at different locations in the catchment, i.e. with different distance and transport time to the receiving WWTP.

## 2. Materials and methods

### 2.1. Case study

The modelling approach was developed for a large urban catchment in Northern Italy (total area of 69 $km^2$ with approximately 1.250.000 inhabitants with a negligible industrial contribution. The catchment is relatively flat (maximum elevation change of 40 meters over about 10 km) and all the wastewater flow is gravity driven, without pumps along the sewer network. No detailed hydrodynamic model of the catchment was available during the study. Relevant data for the area were provided by the local water utility, and they included shape files of the gravity sewer network, boundaries of the catchment area, geographical location of potable water consumption points along the distribution system (around 28,000 points), and the potable water consumption for each point over a reference period (1 year, from January to December 2016). WWTP influent flow data (at 5-minute resolution) were also available for the study period. The average potable water consumption in the study area is 0.22 $m^3$ $inh^{-1}$ $d^{-1}$ (ISTAT, 2018).

### 2.2. The approach

#### *2.2.1. Identification of sub-catchments*

The wastewater discharge points (assumed to coincide with the GIS location of potable water consumption points) were grouped into sub-catchments based on three steps:

i) the shortest in-sewer distance between each point and the WWTP was calculated using the Dijkstra's algorithm (Cormen, 2001; see Supplementary Information for more information on the algorithm), available in ArcGIS 10.3 (ESRI);
ii) distances were input to the iterative Expectation-Maximation (EM) algorithm to fit a Gaussian mixture model (Reynolds, 2015), optimizing the likelihood function of a number of probability density functions (we called them as virtual sub-catchments due to their mathematical nature). The number *n* of virtual sub-catchments was varied from 1 to 30 (considered as the highest number feasibly described by a conceptual model), and the number that minimised the Bayesian Information Criterion (BIC) was selected;
iii) each wastewater discharge point was assigned to the virtual sub-catchment that maximised its probability density function, providing a geographical representation.

Step ii and iii were coded in Matlab R2016a (Mathworks).

### *2.2.2. Estimation of dry-weather flow parameters*

Two dry-weather parameters were estimated, namely the in-sewer flow velocity *v* and the total infiltration flow $Q_{inf,tot}$. The in-sewer flow velocity *v* [m $s^{-1}$], assumed constant in the catchment due to the flat characteristic of the urban area, is linked to the *HRT* in each sub-catchment (Eq.1):

$$HRT_i = \frac{d_i}{v} \qquad \text{Eq. 1}$$

where $d_i$ [m] is the average in-sewer distance of the $i^{th}$ sub-catchment.
The optimization relied on a simple simplex search algorithm (Nelder et al., 1964) and minimized the root mean square error (RMSE) between the Measured Flow Pattern (*MFP*) and the calculated wastewater flow at the inlet of the WWTP (eq. 2):

$$\min_{v,Q_{inf,tot}} RMSE\left(\sum_{i=1}^{n} Q_{PW,i}(t + HRT_i)(1-\alpha) + Q_{inf,tot}, MFP(t)\right) \qquad \text{Eq. 2}$$

where $Q_{PW,i}\ (t)$ [$m^3\ s^{-1}$] is the potable water consumption of the $i^{th}$ sub-catchment (*n* in total), calculated as the sum of the potable water consumed by all points within the $i^{th}$ sub-catchment and normalized by a typical daily consumption profile (Candelieri and Archetti, 2014), α [-] is the water loss factor (due to e.g. gardening), assumed equal to 0.02 (Butler et al., 2004), and $Q_{inf,tot}$ [$m^3\ s^{-1}$] is the total infiltration flow considering the entire catchment. *MFP(t)* was obtained by aggregating dry-weather flow data (excluding weekends and holiday periods) on an hourly basis to generate a daily flow pattern with its confidence interval ($5^{th}$ and $95^{th}$ percentile).

### *2.2.3. Building the conceptual model*

The conceptual model was built by combining elements of the IUWS_MP library (Vezzaro et al., 2014), implemented in WEST 2014® (DHI A/S, Denmark). The elements allow simulating wastewater/MPs generation at the household level (source), wastewater transport and MP transformation processes (e.g. volatilization, sorption, aerobic biodegradation, etc.) in different parts of the urban drainage system (e.g. sewer, WWTP, river). For our case study, each sub-catchment was modelled as a wastewater source and a sewer system. Wastewater generation is simulated by considering the main characteristics of the systems (population density, capita daily wastewater production, groundwater infiltration, etc. – see Supplementary Information). The sewer system was modelled as a series of CSTRs, whose number was iteratively adjusted to match the $HRT_i$ obtained from section 2.2.2 (see Supplementary Information). Verification of the multi-catchment model was performed by comparing the simulated dry weather flow (sum of the contributions of each sub-catchment) at the WWTP location with flow measurements (the *MFP(t)* pattern obtained in section 2.2.2 was used).

## 2.3. Scenario analysis

### *2.3.1. Comparison of conceptual model structures*

The performance of the multi-catchment model in simulating in-sewer MP fate was compared against a classical single-catchment model. The latter was built using a single series of CSTRs, whose number was adjusted to simulate an average *HRT** defined as the flow-weighted average of the $HRT_i$ of each sub-catchment. Model verification was also performed with flow measurements at the WWTP as for the multi-catchment model (see section 2.2.2).
The fate of an ideal reactive non-sorptive MP, which can undergo biodegradation and retransformation, was simulated with both models for two types of inputs:

i) a pulse input (less than 1 hour), which refers to a compound with a relative small usage and/or discharged predominantly from few points (e.g. hospital or manufacturing facility);
ii) a continuous input (over 24 hours following the same flow pattern), which refers to a substance with a relatively high consumption. An average concentration of $\sim 2.5$ μg $L^{-1}$ was selected as representative (Galus et al., 2013; Fent et al., 2006; Daughton and Ternes, 1999) to be emitted (where the sum of the individual contributions of each sub-catchment, proportionally to its size, was equal to the total contribution from discharge in the single-catchment).

The model output was calculated for the inlet of the WWTP. Five performance indicators, four for the pulse input (eq. 3, 4, 5 and 6) and one for the continuous input (eq. 7) were derived in Matlab 2016a: 1) the *cumulative load* [g] entering the WWTP (eq. 3); 2) the *removal efficiency* [%] during in-sewer transport (eq. 4); 3) the *peak delay* [min] (eq. 5); the *pulse duration* [min] (eq. 6); and the *average concentration* $\bar{C}$ [μg $L^{-1}$] derived to mimic a 24-hour flow-proportional composite sampler with 10-minute sampling frequency (eq. 7).

$$Cumulative\ load\ = \int_{t_{start}}^{t_{end}} C(t)Q(t)\ dt \quad \text{Eq. 3}$$

$$Removal\ efficiency\ = \frac{pulse\ input - cumulative\ load}{pulse\ input} \quad \text{Eq. 4}$$

$$Peak\ delay\ = t(C_{\max}) - t_{release} \quad \text{Eq. 5}$$

$$Pulse\ duration\ = t(C_{99}) - t(C_1) \quad \text{Eq. 6}$$

$$\overline{C} = \frac{\sum C(t)Q(t)}{\sum Q(t)} \quad \text{Eq. 7}$$

where $C$ [µg $L^{-1}$] stands for the MP concentration and $C_{max}$, $C_1$ and $C_{99}$ are the maximum, 1st and 99th percentile concentrations, respectively; $Q$ [$m^3$ $d^{-1}$] is the wastewater flow; $t_{start}$ and $t_{end}$ [min] are the initial and final time of the simulation, respectively and, $t_{release}$ [min] is the releasing time of the pulse.
The comparison between the two conceptual models was based on the percentage *deviation* [%] between values of the above indicators derived for the single-catchment and the multi-catchment model (eq. 8):

$$Deviation = \frac{indicator_{multi-catchment} - indicator_{single-catchment}}{indicator_{single-catchment}} \quad \text{Eq. 8}$$

*2.3.2. Simulated scenarios*

Three scenarios were investigated, focusing on the effect of biodegradation kinetics (Scenario 1), simultaneous biodegradation and retransformation kinetics (Scenario 2) and geographical location of point sources of emission (Scenario 3):

- *Scenario 1: Effect of biodegradation.* Six biodegradation half-life values of 12 min, 20 min, 2.5 h, 4.5 h, 40 h and 1000 h were chosen to mimic the behaviour of a broad range of easily (e.g. ibuprofen), moderately (e.g. furosemide) and not biodegradable/recalcitrant (e.g. carbamazepine) substances. The selected half-life values lump the biodegradation by suspended microorganisms and biofilms in sewer, which have found to be both active in the biodegradation of MPs (Thai et al., 2014; Ramin et al., 2016, 2017; McCall et al., 2016; O'Brien et al., 2017).

- *Scenario 2: Effect of complex retransformation pathways.* We evaluated the impact of retransformation processes on model predictions for MPs that simultaneously undergo biodegradation. In the IUWS_MP library, we implemented retransformation as reported in Equations 9 and 10, similarly to the approach used by Plósz et al. (2010, 2012):

$$\frac{dS_{MP_{ret}}}{dt} = -k_{ret}S_{MP_{ret}} \quad \text{Eq. 9}$$

$$\frac{dS_{MP}}{dt} = -kS_{MP} + k_{ret}S_{MP_{ret}} \quad \text{Eq. 10}$$

where $k_{ret}$ [$d^{-1}$] and $k$ [$d^{-1}$] are the first-order rate of retransformation and biodegradation, respectively; $S_{MP}$ [g $m^{-3}$] and $S_{MPret}$ [g $m^{-3}$] are the concentrations of the parent and retransformable fractions, respectively. Three half-life values for retransformation (20 min, 2.5 h and 40 h, were selected to mimic retransformable fractions that can quickly transform back to their respective parent compounds (e.g. glucuronide conjugates) or are relatively stable (e.g. sulphate conjugates) (Gomes et al., 2009). Two types of proportions (1 and 10) between the released concentration of the parent MP and its retransformable fractions were selected, based on typical values found in raw wastewater (Khan and Ongerth, 2003; Bahlmann et al., 2014). All the possible combinations between the above-mentioned parameters were tested (see Table S3 in SI).

- *Scenario 3: Effect of location of point sources.* Two sub-catchments (A and F) were chosen as location of a point source discharging an easily (half-life = 12 min), moderately (half-life = 2.5 h) and hardly biodegradable (half-life = 40 h) MP.

## 3. Results and discussion

### 3.1. Conceptual model structure

#### *3.1.1. Identification of sub-catchments*

The cluster analysis resulted in the identification of six virtual sub-catchments (Figure 1a), for a minimum BIC value of $3.10 \cdot 10^5$ (ranging from $3.13 \cdot 10^5$ to $3.11 \cdot 10^5$ for 1 and 30 catchments, respectively). Figure 1b shows the geographical representation of the sub-catchments based on the location of the wastewater discharge points. The usefulness of an objective over a heuristic approach can be appreciated when considering sub-catchments C and D. While their geographical location (Figure 1b) would suggest considering them as unique catchment, the cluster analysis clearly highlighted two distinct *HRT* peaks of 150 and 180 min (Figure 1a). This 30-minute difference may influence fate estimations for degradable MPs (half-life ≤ 1 h).

#### *3.1.2. Dry weather flow parameters*

The calibration of dry-weather *MFP* (RMSE value of 0.16 $m^3$ $s^{-1}$) resulted in a total infiltration flow $Q_{inf,tot}$ and in-sewer flow velocity $v$ of 1.0 $m^3$ $s^{-1}$ and 0.8 m $s^{-1}$, respectively. $Q_{inf,tot}$ corresponded to 24% of the dry-weather flow and $v$ fell within typical ranges for gravity sewer systems (Butler et al., 2004). The estimated *HRT* distribution had a flow-weighted average of 150 min (equal to *HRT**) and $HRT_i$ values were placed at seemingly rather regular intervals (on average 40 min), ranging from 78 to 278 min (Figure 1a). These intervals depend on the shape of the *HRT* distribution (unique for every urban catchment) and should not be extrapolated for sub-catchment identification in other urban catchments.

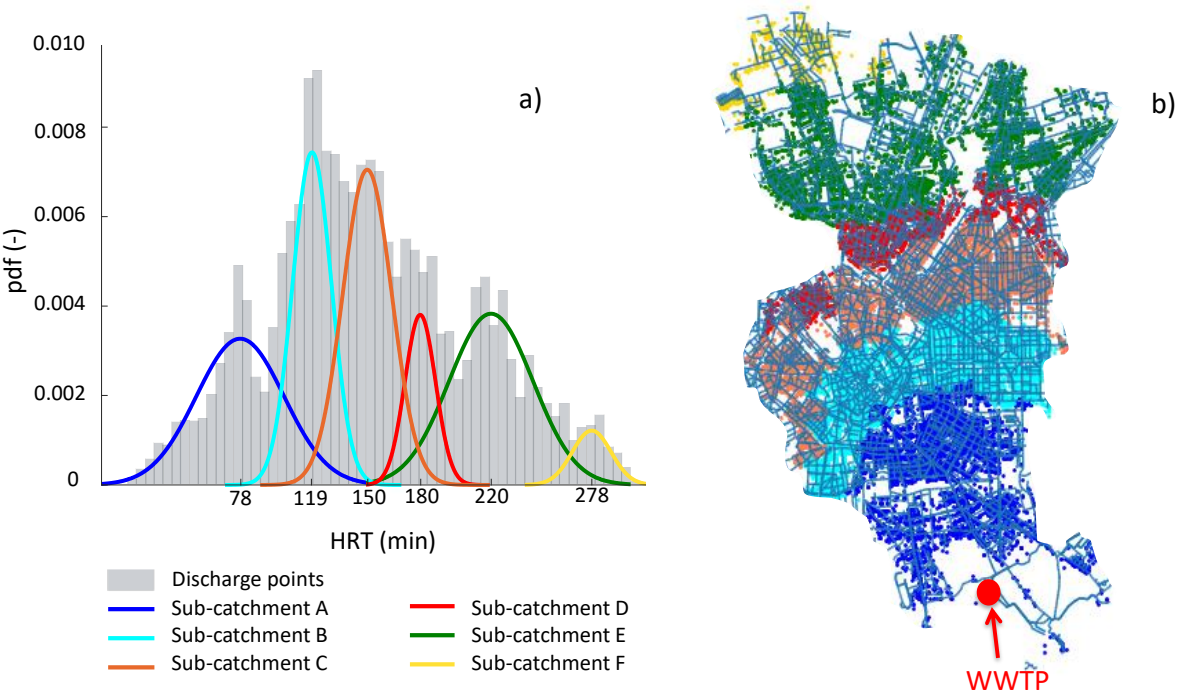


**Figure 1**. (a) Results of the cluster analysis with identification of the virtual sub-catchments. (b) Geographical representation of the virtual sub-catchments based on the location of the wastewater discharge points.

### *3.1.3. Development of the conceptual model*

A multi-catchment model (Figure 2a) was developed based on the results of the previous two steps. Model parameters were set as described in section 2.2.3 and reported in Table 1 where population density $\rho$ (18816 inh km$^{-2}$), wastewater production *WWP* (0.218 m$^3$ inh$^{-1}$ d$^{-1}$) and infiltration flow *Ifl* (0.145 m$^3$ s$^{-1}$ km$^{-2}$) were equal in each sub-catchment. The relative deviation between simulated and estimated $HRT_i$ was small (< 6%) for each sub-catchment, indicating a proper fit (see Table S2). As for the single-catchment model, model parameters are also reported in Table 1, and the relative deviation between simulated and estimated *HRT** and the relative deviation was also small (3%).

Model verification using measured and simulated flow data can be seen in Figure 2b. The simulated dry-weather flow was within the confidence interval of the measured flow data, indicating an adequate description of the influent flow by both models.

**Table 1.** Conceptual model parameters

| | Multi-catchment | | | | | | Single-catchment |
|---|---|---|---|---|---|---|---|
| Sub-catchment | A | B | C | D | E | F | - |
| A (km$^2$) | 13.1 | 16.4 | 17.5 | 6.6 | 13.8 | 2.2 | 69 |
| Number of tanks | 5 | 8 | 9 | 10 | 12 | 12 | 12 |

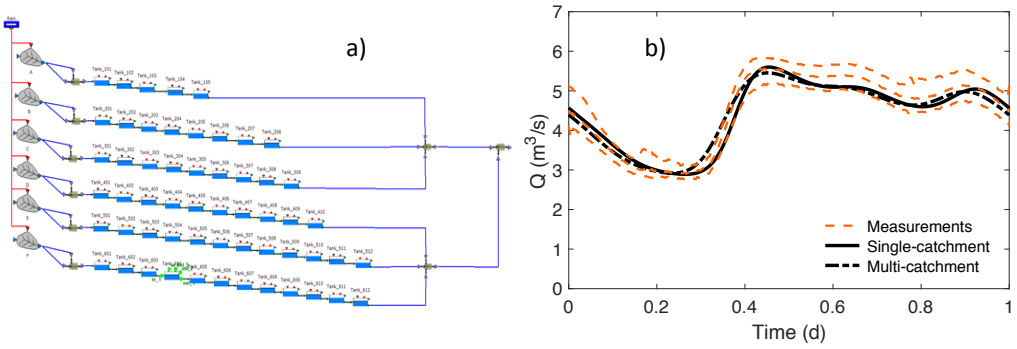


**Figure 2**. (a) Conceptual model in WEST®. (b) Model verification: measurements median and 5th and 95th percentiles (dashed orange line), and model simulations (solid and dash black line).

## 3.2. Scenario analysis

### *3.2.1. Scenario 1 – Effect of degradation*

*Pulse source.* The results from the simulations of a moderately biodegradable MP (half-life = 2.5 h) are shown in Figure 3a. The pulse input resulted in bell-shaped curves, where the simulation of advection and biodegradation led to a reduction of the area below the curves. The estimated cumulative load and removal efficiency, and the corresponding deviation, for the whole range of tested biodegradation half-lives is shown in Figure 3c and 3e, respectively. The cumulative load deviation ranged from 0% to 312% (Figure 3c), being larger than 10% for MPs with half-lives ≤ 2.5 h and negligible or null value (5%, 1% and 0%) for the more recalcitrant MPs. Hence, the predicted loads entering the WWTP were overall higher for the multi-catchment model. As to in-sewer removal efficiency, deviations ranged from -15% to 0% (Figure 3e), showing that the multi-catchment model predicted lower removal efficiencies than the single-catchment model, especially for MPs with half-lives = 2.5 h and 4.5 h. The analysis of the peak delay indicator (Figure S1) showed that the multi-catchment model predicts the peak load entering the WWTP earlier than the single-catchment model (deviation ranging from -9% to -6%, corresponding to a difference between the models of 70 to 50 minutes). This is mainly due to the contribution of the closest sub-catchment to the WWTP (indicated in blue in Figure 1b), for which MP release occurs sooner than the other sub-catchments due to its short *HRT* (78 min). Deviations for the pulse duration (see Figure S1) indicated that the a pulse takes longer to be completely release for the multi-catchment model (deviation ranging from 6% to 21%, corresponding to 20 to 90 minutes differences between the models).

*Continuous source.* The model results for a continuous input of a moderately biodegradable MP (half-life equal to 2.5 h) are shown in Figure 3b. The 24-h composite concentration and the deviation for all the whole range of substances (from easily biodegradable to recalcitrant) are shown in Figure 3d. The models predicted different concentrations for half-life lower than 2.5 h (deviation equal to ~ 10%), with a maximum deviation of 350% for half-life of 0.2 h. In these cases, the percentage deviation between the two models was higher than the uncertainty typically associated to analytics, quantifiable in 20–30% (Ort et al., 2009; Castiglioni et al., 2012), thus indicating a considerably lower estimated concentrations at the WWTP inlet with the single-catchment model. Notably, a high deviation (e.g., 350%) corresponded to small

concentration differences (e.g. < 0.2 µg $L^{-1}$) due to the low input concentrations (~ 2.5 µg $L^{-1}$) that were used for simulations. On the other hand, higher input concentrations (e.g. ~ 100 µg $L^{-1}$) would lead, for the same deviation, to higher concentration differences (e.g. < 8 µg $L^{-1}$). Predicted removal efficiencies were generally in good agreement with measurements from pilot- and full-scale sewer studies with degradable and persistent MPs (Table S4). Findings of both scenarios highlighted how the proposed approach supported the development of an appropriate model structure for predictions of biodegradable MPs with half-life close to or below the average *HRT* of the catchment (150 min).

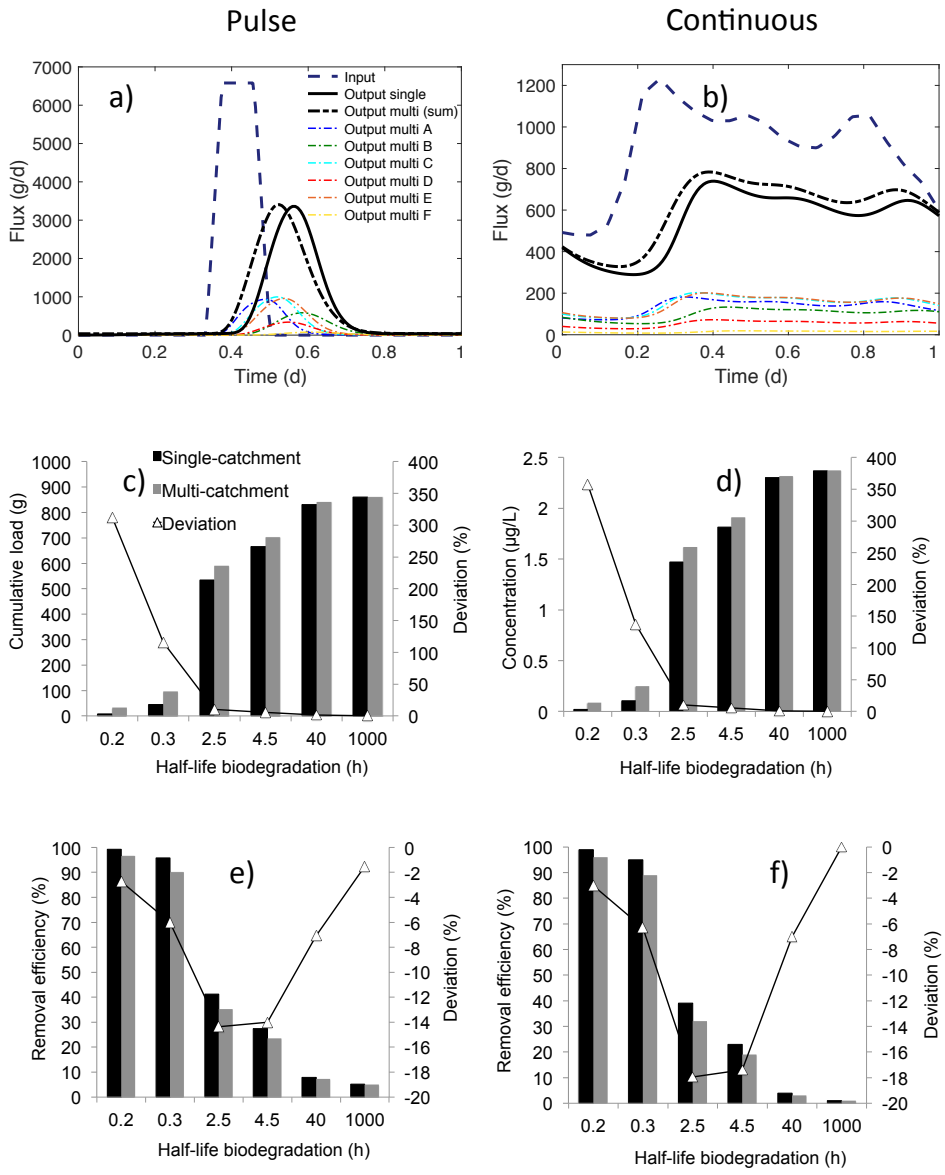


**Figure 3**. Model response for a moderately biodegradable MP (half-life of 2.5 h) for (a) pulse input and (b) continuous input. Calculated (c) cumulative load, (d) average concentration and (e and f) removal efficiency for the single catchment model (black bar) and multi-catchment model (grey bar) with the corresponding percentage deviation (solid triangle) for different half-life.

### *3.2.2. Scenario 2 – Effect of complex transformation pathways*

The impact of retransformation on single- and multi-catchment model predictions was assessed for parent MPs with biodegradation half-life equal to 2.5 h and 40 h. These two values were selected to describe easily-to-moderately biodegradable and recalcitrant, MPs, respectively. Furthermore, results from Scenario 1 showed that deviation between model predictions for these half-lives was ≤10%, hence retransformation may potentially increase such deviation.

*Pulse source.* The effect of simultaneous biodegradation and formation in the sewer on the fate of MPs was assessed by considering the removal efficiency as relevant indicator (Figure 4). Nearly all simulations predicted negative removal efficiency (Figure 4a), suggesting that retransformation can strongly affect MP fate during in-sewer transport. Very low values, ranging from -950% and -400%, were estimated for MPs which undergo retransformation rapidly (half-life ≤ 2.5 h) and when high retransformable fractions were present. When retransformation was slow (half-life = 40 h) or retransformable fractions were comparable to the one of parent compound, removal efficiencies ranged from -100 % to 35 %. This suggests a minor but not negligible effect of retransformable fractions on the parent compound estimation. Figure 4c presents the comparison between multi- and single-catchment predictions in terms of deviation of removal efficiency. For moderately biodegradable MPs (biodegradation half-life = 2.5 h) the deviation was around -7% on average (with a minimum of -35%), indicating that lower MP loads were estimated with the single-catchment model. Conversely, the deviation for hardly biodegradable MPs (biodegradation half-life = 40 h) was 16% on average (with a maximum of 50%), suggesting that the single-catchment model provided higher estimation of the MP loads entering the WWTP.

*Continuous source.* Predicted influent concentrations by multi-catchment and single-catchment models are presented in Figure 4b. A wide range of concentrations (3–26 μg $L^{-1}$) was obtained. Specifically, the faster the retransformable fractions retransform, the more important is the effect of the retransformation and retransformable fraction initial concentration on the parent compound concentration. For example, when the retransformation half-life was 0.3 h, parent MP concentrations differed significantly depending on biodegradable half-life and initial proportion, while almost no differences in concentrations were observed for a retransformation half-life of 40 h.

Deviations between multi-catchment and single-catchment predictions (Figure 4d) ranged between 10% and -12%, exhibiting higher values than the ones reported for the continuous source in the scenario 1 (section 3.2.1).

Notably, negative removal efficiencies (down to -66%) have been also measured in pilot- and full-scale sewer studies (Table S4). The availability of empirical data is nevertheless limited as compared to Scenario 1, as most studies have been relied on spiking of parent MPs alone.

Findings of both scenarios suggested that deviations between the models increased when retransformation processes were considered. Specifically, the single-catchment model provided either higher or lower estimation of removal efficiency/concentration without following any particular trend, probably due to the non-linear interactions between the investigated parameters.

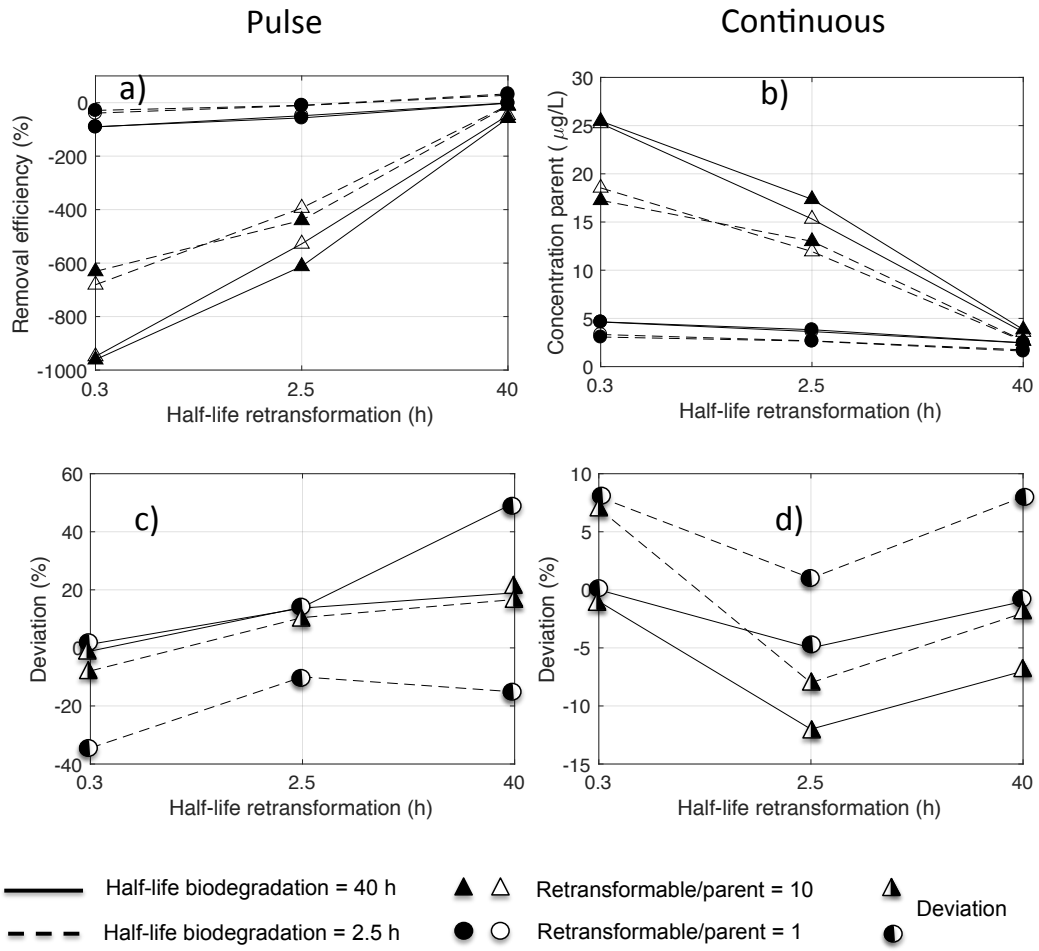


**Figure 4.** (a) Calculated removal efficiency and (b) average parent concentration by single-catchment (black triangle and black circle) and multi-catchment (white triangle and white circle) models for different initial conditions. Deviation for (c) removal efficiency and (d) average parent concentration.

### *3.2.3. Scenario 3 – Effect of point source location*

Simulation results for easily (half-life = 12 min), moderately (half-life = 2.5 h) and hardly biodegradable (half-life = 40 h) MPs discharged from two different locations in the catchment are shown in Figure 5. Corresponding removal efficiencies, and their comparison with efficiencies derived from the single-catchment model, are reported in Table S5 (SI).

Results show that both location and MP biodegradability affected the MP loads entering the WWTP. The impact of point source location significantly affected the removal efficiency for easily and especially moderately biodegradable MPs (from 19% to 46% change), for which a considerable deviation was also shown from the single-catchment prediction (-49–24%). Conversely, discharge from different locations had a limited impact on in-sewer removal efficiencies for a hardly biodegradable compound (2%–5%).

Overall, these results indicate that the extent of in-sewer attenuation processes for degradable MPs is associated with the spatial distribution of discharge sources. In this context, point sources of discharge require special consideration, and limited in-sewer attenuation may be

decisive for the implementation of an *in situ* pre-treatment to minimize MP loads to WWTPs (Scott et al., 2018).

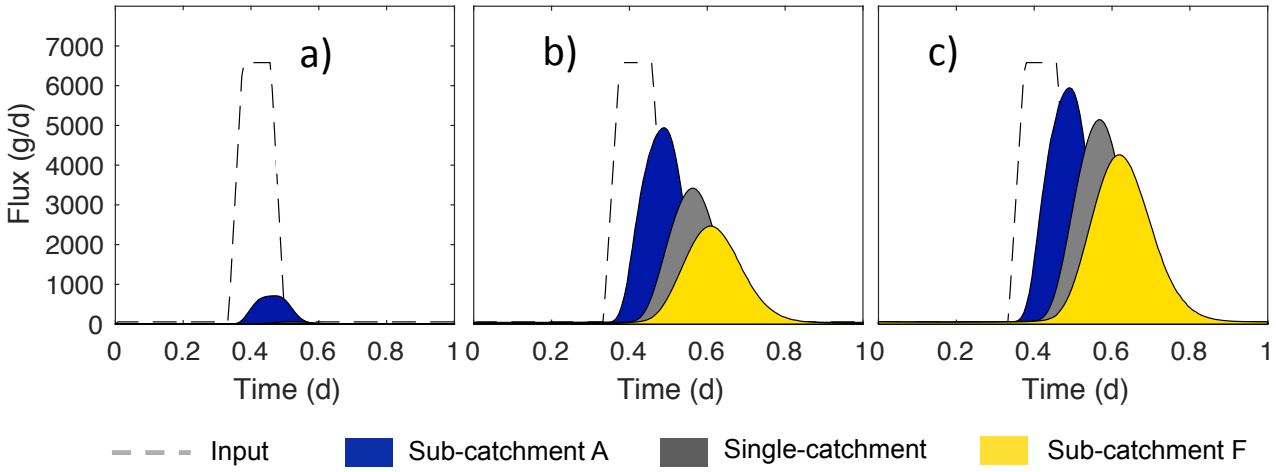


**Figure 5.** Estimated flux entering the WWTP of (a) a readily biodegradable, (b) moderately and (c) hardly biodegradable MP, based on point source location (sub-catchment A and F) and model conceptualization (multi-catchment and single-catchment).

### 3.3. Applicability, data requirements and future perspectives

This study presents a methodology for systematic construction of conceptual sewer models in large urban catchments with the intent of simulating the fate of reactive, non-sorptive MPs. The approach can be held valid under dry-weather conditions and during small rain events, i.e. when *HRT* is not significantly different. The applicability to medium events (resulting e.g. in combined sewer overflows (CSO), or wastewater detention in storage basins) would require a model structure including the addition of the most relevant points of the network. Moreover, the model can thus be used as decision-support on whether pre-treatment at the point source is needed before discharge or in-sewer attenuation is sufficient to reduce MP loads to WWTP.
As for the data requirement, the method required the location of the wastewater discharge points along the sewer network. In this work, we used the location of potable water consumption points (28,000) as proxy variable for the position of the wastewater discharge points. Alternatively, nodes of the sewer network (McCall et al., 2017) or the centroids of the census block polygons (Kapo et al., 2017) can be used. The sewer network structure is also required, although road networks are a valid alternative as suggested by Kapo et al. (2017). As for the in-sewer flow velocity, an average value was estimated, matching the simulated wastewater flow (derived from potable water consumption) against measurements at the inlet of the WWTP. Alternatively, a design standard velocity could be used (Kapo et al., 2017), although the topography of the area should be carefully considered. In our study, given the flat characteristics of urban area, a unique value was assumed across the catchment. However, different in-sewer flow velocities should be assigned (e.g. to each sub-catchments) to account for different altitudes (resulting in different *HRTs*).

Overall, the above-mentioned assumptions can affect the sub-catchment identification and further investigation should be done to assess their sensitivity. Further investigations should also include:

- *Wet-weather conditions.* Wet-weather conditions are not expected to be relevant when assessing the overall MP loads to the WWTP over long time periods, since they typically represent a minor (<10%) fraction of the total WWTP operating time. However, the presence of wet-weather discharges (CSO, WWTP bypass) might require a redefinition of the model structure in order to fully investigate the impacts on the receiving waters.
- *Complexity of the biochemical model*. A first-order kinetic for both biodegradation and retransformation process was assumed in the IUWS_MP library. It should be investigated if more complex process description can improve the estimation of the MP fate (e.g. biodegradation rates dependence on total suspended solids—TSS).
- *Integration with other elements of the wastewater system.* Since the proposed approach can be extended to predict MP fate across the whole integrated wastewater system (including WWTP and recipients), the scenarios investigated in this study (e.g. location of MP point sources) should possibly be replicated with an integrated model. The integrated assessment should mainly focus on moderately-to-hardly biodegradable MPs that are subjected to retransformation processes, for which poor removal in the WWTP or persistence in the environment can pose a risk to receiving water bodies.

## 4. Conclusions

In this study, we present a new systematic approach combining GIS-based information and statistical analysis to identify the optimal structure of a conceptual model for simulating in-sewer *HRT* in a large urban catchment, while keeping model complexity as simple as possible. The approach was developed to improve fate predictions of down-the-drain MPs that undergo degradation and/or formation during transport in sewers. Findings from the study allowed reaching the following conclusions:

- The conceptual modelling approach allowed deriving a multi-catchment model, and the large catchment was subdivided into sub-catchments, each characterized by a typical *HRT*. The obtained model allowed for successful simulation of dry weather flow and is applicable (i) in the absence of a complex hydrodynamic model and (ii) when a single-catchment model (with one average *HRT*) is not representative of large urban areas.
- The multi-catchment model should be preferred over a single-catchment model for simulating the fate of (i) biodegradable MPs with half-life lower than the average *HRT* of the catchment and (ii) MPs that undergo rapid formation (half-life < 2.5 h) in the presence of high concentrations of retransformable compounds (e.g., conjugated metabolites).
- The multi-catchment model allowed assessing the importance of point source location within the catchment, providing decision-support on whether pre-treatment at the source is needed before discharge or in-sewer attenuation is sufficient to reduce MP loads to WWTP.

Overall, the proposed approach is expected to ease the building of conceptual sewer water quality models, allowing for a broader implementation of integrated models (sewer, WWTP, receiving

## Supplementary information

### Materials and methods

*Identification of sub-catchments*

The Dijkstra's algorithm (taking its name from the inventor, Edsger W. Dijkstra), is used to find the shortest path between nodes in a graph or a network by solving an optimization problem (Cormen, 2001). In the current study, we used the algorithm to identify the shortest in-sewer path from each discharge point to the wastewater treatment plant.

*Building the conceptual model*

Table S1 describes the calculations utilized to define the structure and the parameters of each sub-catchment. These values are utilized in the different blocks from the IUWS_MP library.

**Table S1:** Conceptual model parameters for each sub-catchment; n.d. stands for not defined.

| | Population density $\rho$ [inh km$^{-2}$] | Wastewater production $WWP$ [m$^3$ inh$^{-1}$ s$^{-1}$] | Infiltration flow rate $Ifr$ [m$^3$ s$^{-1}$ km$^{-2}$] | Area $A_i$ [km$^2$] | Hourly peak factors for WW release $PF$ [-] | Number of in-series CSTR [-] |
|---|---|---|---|---|---|---|
| Source | $= \frac{1.250.000^{a}}{69^{b}}$ | $= \frac{0.22^{c} * (1-\alpha^{d})}{Cf^{e}}$ | $= \frac{Q_{inf,tot}{}^{f}}{69^{b}}$ | $= \frac{Q_{PW,i}{}^{g}\ (1-\alpha^{d})}{\rho * WWP}$ | $pattern^{h}$ | n.d. |
| Sewer | n.d. | n.d. | n.d. | n.d. | n.d. | Iteratively adjusted to minimise $\frac{\lvert HRT_i^{f} - HRT_{simulated}\rvert^{l}}{HRT_{simulated}}$ |

[a] Total number of inhabitants in the area

[b] Total urban area in km$^2$

[c] Average potable water consumption in the study area in m$^3$ inh$^{-1}$ d$^{-1}$ (ISTAT, 2018)

[d] Water losses (Butler et al., 2004)

[e] Conversion factor equals to 86400 s d$^{-1}$

[f] Estimated from section 2.2.2; see equation 1-2

[g] Sum of the potable water consumption of all the points within the i$^{th}$ sub-catchment, in m$^3$ s$^{-1}$

[h] Normalized daily potable water consumption pattern for workdays (Monday to Friday) reported by Candelieri and Archetti (2014)

[l] Formula of the relative deviation

Equation S1 describes how the dry weather flow for each i$^{th}$ catchment (sum of wastewater flow $Q_{ww,i}$ and infiltration flow $Q_{inf,i}$) is calculated by the WEST model.

$$Q_{dwf,i} = Q_{ww,i} + Q_{inf,i} = \rho * WWP * A_i * PF + Ifr * A_i \quad \text{Eq. S1}$$

where ρ [inh km$^{-2}$] is the population density, *WWP* [m$^3$ inh$^{-1}$ s$^{-1}$] the per capita wastewater production, $A_i$ [km$^2$] the area of the i$^{th}$ sub-catchment and, *PF* the peak factors to introduce flow temporal variability; *Ifr* [m$^3$ s$^{-1}$ km$^{-2}$]is the groundwater infiltration rate.
Table S2 indicates the number of tanks (in the IUWS_MP library indicated as pipes) and the corresponding length after model calibration. The relative deviation was calculated according to the equation reported in Table S1. The volume of each pipe, obtained as product of the surface and length of the pipe, was initially fixed (~ 1750 m$^3$) and slightly tuned for minor adjustments once the optimal number of CSTRs was found.

**Table S2.** Model parameters and performance indicator for each sub-catchment.

| Sub-catchment | Number of tanks (-) | Length of each pipe (m) | Relative deviation (%) |
|---|---|---|---|
| A | 5 | 600 | 3.1 |
| B | 8 | 600 | 5.3 |
| C | 9 | 650 | 0.2 |
| D | 10 | 500 | 2.5 |
| E | 12 | 650 | 2.5 |
| F | 12 | 475 | 0.8 |

*Scenario 2: Effect of complex retransformation pathways.*
Table S3 shows the parameters combinations (12 in total) that were tested in scenario 2. The third column indicates the proportion between the release concentration of the parent micropollutant and its retransformable fractions.

**Table S3:** parameter combination for each simulation for scenario 2.

| Half-life biodegradation | Half-life retransformation | Retransformable fraction/parent | Simulation number |
|---|---|---|---|
| 2.5 h | 20 min | 1 | 1 |
| | | 10 | 2 |
| 2.5 h | 2.5 h | 1 | 3 |
| | | 10 | 4 |
| 2.5 h | 40 h | 1 | 5 |
| | | 10 | 6 |
| 40 h | 20 min | 1 | 7 |
| | | 10 | 8 |
| 40 h | 2.5 h | 1 | 9 |
| | | 10 | 10 |
| 40 h | 40 h | 1 | 11 |
| | | 10 | 12 |

**Results and discussion**

*Scenario analysis*

*Scenario 1 – Effect of degradation*

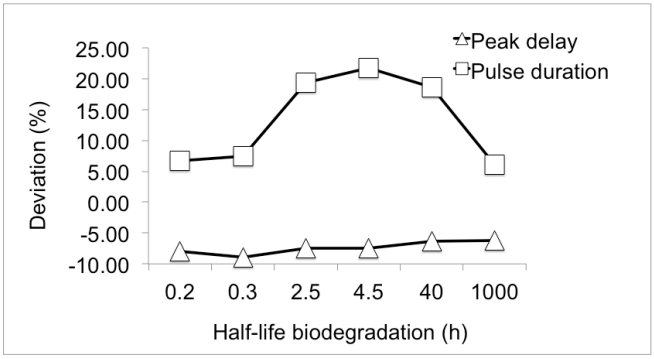


**Figure S1.** Deviation for the peak delay and pulse duration between the multi-catchment model and the single-catchment model for different biodegradable half-lives.

*Scenario 2 – Effect of complex transformation pathways*

**Table S4.** Comparison between predicted and measured in-sewer removal efficiencies for MPs. Characteristics of investigated sewers are provided for literature studies.

| | **In-sewer removal efficiency (%)** | |
|---|---|---|
| | **Predicted (this study)** | **Measured (literature)** |
| **Scenario 1 (biodegradation)** | 1% to 32% (half-life > 2.5 h) | 0 to 60% (Jelic et al., 2015: pressurized sewer, HRT = 21 h)<br>0% to 35% (Gao et al., 2018: pilot gravity sewer, HRT = 2.5 h)<br>20% to 60% [cocaine]; 25% to 70% [6-AM]; 20% to 80% [methadone] (Li et al., 2018: pressurized sewer, HRT > 3.5 h)<br>25% [cocaine]; 15% [MDMA]; 20% [methadone](Li et al., 2019: gravity sewer, HRT = 2-3 h) |
| **Scenario 2 (biodegradation and retransformation )** | -950% to 0% | -66% to 0% (Jelic et al., 2015: pressurized sewer, HRT = 21 h)<br>-15% [benzoylecgonine](Li et al., 2019: gravity sewer, HRT = 2-3 h) |

*Scenario 3 – Effect of point source location*

**Table S5.** Simulated removal efficiencies by the multi-catchment model and the single-catchment model for different point source locations and biodegradable half-lives.

| Half-life | Single-catchment | Sub-catchment F | Sub-catchment A |
|---|---|---|---|
| 12 min | 99 | 99 | 88 |
| 2.5 h | 37 | 46 | 19 |
| 40 h | 4 | 5 | 2 |

# Chapter 4

# Modelling the fate of pharmaceuticals in integrated urban wastewater systems – extending the applicability of the IUWS_MP model library

**Abstract:** Pharmaceutical active compounds (PhACs) are a new category of micropollutants (MP) frequently detected across Integrated Urban Wastewater and Stormwater systems (IUWS – drainage systems, wastewater treatment plants, receiving water bodies). PhACs are characterized by fate processes (consumption-excretion, deconjugation) and fractions (metabolites, sequestrated fraction) which were not available in the existing MP fate model library (IUWS_MP), limiting its field of applicability. Thus, this was extended to simulate the fate of PhACs with different properties (e.g. carbamazepine, ibuprofen, diclofenac, paracetamol, furosemide) across IUWS systems. The extended library was tested in two different IUWS systems, and result uncertainty was estimated by applying a forward Monte-Carlo approach. Despite data uncertainty and the simplicity of the modelling approach to minimize data requirements, there was a good agreement between model prediction bounds and available measurements across the simulated systems. Possible applications of the extended library are presented, illustrating how this tool can support urban water managers in reducing environmental impacts from PhACs discharges.

**Keywords:** Integrated water quality modelling; watch-list; micropollutants control strategies; xenobiotics; emerging contaminants.

The research work presented in this chapter was carried out during a research stay period of 8 months at the Technical University of Denmark (Denmark). The research work was carried out with the valuable support of Prof. Luca Vezzaro (Technical University of Denmark), Dr. Fabio Polesel (DHI A/S) and the help of two MSc students, Kerstin von Borries and Zheng Zhang.

This chapter has been submitted for publication to "Journal of Environmental Modelling & Software"

# 1. Introduction

Micropollutants (MPs) released from urban areas into surface waters might pose an important environmental risk (Gosset et al., 2017; Johnson et al., 2017; Letsinger and Kay, 2019). MPs are typically discharged from the Integrated Urban Wastewater and Stormwater (IUWS) systems in dry and wet weather, i.e. from outlets of wastewater treatment plants (WWTPs) (Luo et al., 2014; Margot et al., 2015; Rogowska et al., 2019), separate storm sewer outlets (e.g. Zgheib et al., 2012; Brudler et al., 2019) and combined sewer overflows (e.g. Gasperi et al., 2012; Launay et al., 2016). MPs have been targeted by existing environmental legislations for almost two decades. For example, the European legislation (Water Framework Directive (European Commission, 2000); and following directives (European Commission, 2013, 2008) established environmental quality standards (EQS) for 33 (later extended to 45) priority substances, including herbicides, fungicides, surfactants, metals and polycyclic aromatic hydrocarbons.
Cost-effective MP control strategies need to be implemented to (i) reduce MP emissions, (ii) meet the desired EQS, and (iii) achieve good chemical status in natural waters. The ScorePP project (Source Control Options for Reducing Emissions of Priority Pollutants - 2006-2009-www.scorepp.eu) investigated different MP control options, and a dynamic model library (IUWS_MP, Vezzaro et al., 2014) was specifically developed. The IUWS_MP library was designed to support water managers in developing MP control strategies (e.g Delli Compagni et al., 2020; Eriksson et al., 2011) by: (i) simulating MP fluxes across the IUWS, (ii) supporting the development of monitoring campaigns, and (iii) evaluating the compliance of different strategies with EQS and/or with risks for the environment and human health.
The IUWS_MP library uses simple process descriptions, with an approach derived from chemical fate assessment. The fate of a specific MP is predicted based on inherent chemical-physical properties and first-order kinetics rates (e.g. to describe biodegradation), which can easily be retrieved from existing databases and literature results. This minimizes the need for parameter calibration, and it allows simulating the fate of a wide range of MPs in the different elements of IUWS with the same model library. However, the ranges of MP properties in literature show high variability, which needs to be propagated to obtain representative results. Parameter uncertainty in integrated MP models has been investigated in few studies, focusing on single elements of the system (Vezzaro et al., 2011) or on a single MP (Mannina et al., 2017). Thus, an overall quantification of the influence of parameters uncertainty on results in different elements of the IUWS and for MPs with different properties is still missing.
Recently, a new range of MPs has recently come into focus (the EU "watch list", European Commission, 2015), i.e. pharmaceutically active compounds (PhACs, such as anti-inflammatory substances, antibiotics and hormones). PhACs are the most sold chemicals on the market and since they are designed to be biologically active they can have harmful effects on natural ecosystems (Bottoni et al., 2010). PhACs are characterized by different release pathways and behaviour compared to the MPs that were originally considered in the IUWS_MP library. For example, PhACs can be excreted as original molecules (also termed parent fraction) and metabolites, through faeces and/or urine, showing high variability in wastewater concentrations (Luo et al., 2014; Margot et al., 2015). Different studies (Letsinger and Kay, 2019; Andrew et al., 2004) included different MP release models in their simple mass balance calculations, or in more sophisticated models (Khan and Ongerth, 2004; Coutu et al., 2016). However, this has not been investigated through dynamic model in complex integrated systems

(i.e. source, sewer, WWTP and receiving water body) yet. Moreover, these models conceptualised the PhAC parent mass excreted through urine and faeces as one single flux, although the flux excreted by faeces might be partly enclosed in faeces particles (i.e. sequestration) and thereby less bioavailable (i.e. less subject to sorption/desorption equilibria and biodegradation processes) than the flux excreted through urine (i.e. fully bioavailable) (Gonzalez-Gil et al., 2018). Additionally, PhACs are generally ionisable substances and they can undergo retransformation processes, known as deconjugation (Plósz et al., 2012; Testa et al., 2012). These processes can play an important role for the PhACs fate in the different elements of the IUWS. For example, the ionisable status (i.e. positive, negative or both) of a PhAC affects its sorption affinity with solid matrices (raw wastewater solids, sludge, sediments). Also, retransformation of certain metabolites (i.e. glucuronide conjugates) can affect the fate of the parent PhACs fraction (Stadler et al., 2012).
During the last years there have been several monitoring activities, targeting a wide range of MPs, including PhACs (Kasprzyk-Hordern et al., 2009; Zuccato et al., 2010; Patrolecco et al., 2015; Castiglioni et al., 2018). Compared to previous modelling studies (De Keyser et al., 2010; Keller et al., 2007; Koormann et al., 2006; Schowanek et al., 2001; Vezzaro et al., 2014; Williams et al., 2009), data availability has thus improved, allowing for a more comprehensive evaluation of model performance.
This work presents: (i) the extension of the IUWS_MP library with additional release pathways (a consumption-excretion model was developed) and fate processes (deconjugation), allowing for simulation of PhACs across IUWS systems, (ii) the quantification of the model results uncertainty deriving from the high variability of PhACs inherent properties; (iii) the verification of the IUWS_MP prediction capabilities against measurements from two different IUWS systems where sufficient data (e.g., consumption data and PhACs measurements at the WWTP inlet and outlet) were available.

## 2. Materials and methods

### 2.1. The original IUWS_MP model library

The IUWS_MP library extended the traditional models from the ASM family (Henze et al., 2000; Reichert et al., 2001; Shanahan et al., 2001) with fate processes for MPs. As in Saagi et al. (2017), all the elements of the IUWS system (sewer pipes and detention basins, WWTP tanks, river stretches, etc.) are represented as continuously stirred tank reactors (CSTRs). Specifically, CSTRs provide a lump modelling approach which represent an optimal solution to describe MPs processes in time and space, keeping an affordable computational time with the minimum system information (e.g. sewer pipes and river stretches location) availability. In each tank, biochemical transformation of traditional pollutants (organic matter, nitrogen, phosphorous) are modelled by using widely applied models, such as the Activated Sludge Model no. 2d (ASM2d - Henze et al., 2000) for the WWTP and the River Water Quality Model no.1 (RWQM1s - Reichert et al., 2001; Shanahan et al., 2001; Vanrolleghem et al., 2001) for the receiving water body. MP fate processes (sorption/desorption, biodegradation, photolysis, hydrolysis, etc.) are modelled by using simple first-order kinetics, thus relying on half-life values available in literature and public databases. MPs are defined as present in two fractions: dissolved ($S_{MP}$ [$g_{MP}$

$m^{-3}$]) and particulate MP ($X_{MP}$ [$g_{MP}$ $m^{-3}$]). The IUWS_MP library is currently implemented in the WEST® software (www.mikepoweredbydhi.com), which employs solvers with variable time steps. Rainfall intensity is the major forcing function of the model, but other dynamic environmental constraints (e.g. air temperature) can also be provided to the model. Model outputs are generated at fixed time steps, which are defined by the user. For further details on the IUWS_MP library the reader is directed to Vezzaro et al. (2014).

## 2.2. The extended IUWS_MP library

In order to allow for the simulation of PhACs, the original IUWS_MP library was modified by including: i) a consumption-excretion model to generate initial concentrations of PhAC fractions at the urban catchment scale, ii) additional fate processes such as deconjugation, and iii) refining existing fate processes such as sorption to account for ionization.

### *2.2.1. Consumption-excretion model*

Similarly to the models presented in Khan and Ongerth (2004) and Coutu et al. (2016), we conceptualised the consumption-excretion phenomena to derive model state variables ($S_{MP}$, $X_{MP}$, $X_{MP,seq}$ and $S_{conj}$) from consumption data, minimizing the effort of pharmacokinetic data collection (i.e. using only excretion rate). Briefly, ingested PhAC mass is excreted as soluble parent fraction in urine ($S_{MP}$) and as particulate parent fraction sequestered in faeces ($X_{MP,seq}$). Different degrees of bioavailability (no bioavailable and fully bioavailable) were considered for $X_{MP,seq}$ depending on the adopted model structure (i.e. with and without sequestration, see paragraph 2.3.5). As for the metabolites, we focused on the fate of specific metabolites (i.e. glucuronide conjugates), whose deconjugation to parent fraction is well recognised (Gomes et al., 2009) (see paragraph 2.2.2). Glucuronide conjugates ($S_{MP\_conj}$) were considered as soluble due to their high water solubility (Celiz et al., 2009). The parent fraction sorbed on *TSS* was considered as particulate ($X_{MP}$) and defined though the partitioning coefficient (i.e. the solid-water partition coefficient $K_d$) (see paragraph 2.2.3). Figure 1 presents a schematic representation of the model, explained step by step in the following:

1. *Consumption (phase 1)*: Ingested mass $M_{ingested}$ [mg $inhab^{-1}$ $d^{-1}$] is derived as $M_{ingested} = DDD \cdot N \cdot 10^3$, where *DDD* is the defined daily dose (the average maintenance dose used per day for its main indication in adults) and *N* is the total number of *DDDs* sold per day every 1000 inhabitants.

2. *Excretion (phase 2):* $M_{ingested}$ is fractionated in parent PhAC excreted through urine and faeces ($M_{MP\_urine}$, $M_{MP\_feces}$) and conjugates ($M_{MP\_conj}$) by means of excretion rates ($f_{MP,urine}$, $f_{MP,feces}$ and $f_{MP\_conj}$).

3. *Dilution and partitioning (phase 3)*: wastewater concentrations ($C_{MP,urine}$, $C_{MP,feces}$ and $C_{MP\_conj}$) are obtained dividing excreted masses by the daily wastewater production (*WWP* [l $inhab^{-1}$ $d^{-1}$]). Partitioning between $S_{MP}$ and $X_{MP}$ was assumed to reach

equilibrium instantaneously after the discharge in the sewer and it was derived from equations: $S_{MP} = C_{MP\_urine}/(1+C_{TSS} \cdot K_d)$ and $X_{MP} = C_{MP\_urine} - S_{MP}$, where $C_{TSS}$ [$g_{TSS}$ $m^{-3}$] is the concentration of *TSS* and $K_d$ [$m^3$ $g_{TSS}^{-1}$] is the solid-water partition coefficient. When $X_{MP,seq}$ was not bioavailable (i.e. sequestration), $M_{MP,feces}$ was added to $M_{MP,urine,}$ before phase 3.

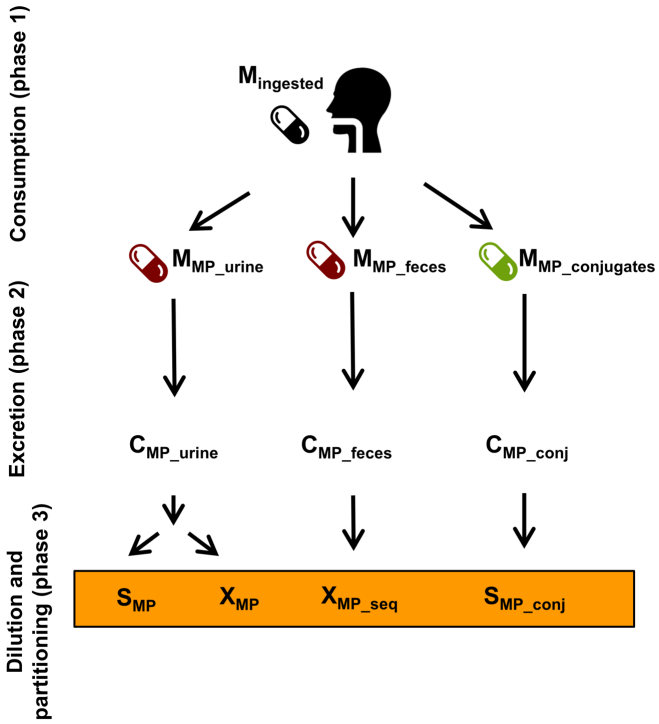


**Figure 1.** Schematic representation of the consumption-excretion model.

### *2.2.2. Deconjugation*

PhACs are biotransformed in the human body by adding or unmasking functional groups (phase I metabolitization) of the parent PhACs and/or adding a hydrophilic moiety (phase II metabolitization) to facilitate excretion (Polesel et al., 2016; Testa et al., 2012). In wastewater, phase II metabolites (also known as conjugates) can retransform back to the parent PhACs through cleavage of the conjugated moiety (e.g., glucuronide, acetyl, sulphate groups). This process, thereby defined as "deconjugation", was observed in laboratory-scale and/or full-scale treatment systems for non-steroidal anti-inflammatory drugs (diclofenac), antiepileptic drugs (carbamazepine), antibiotics (sulphonamides) and estrogens (estriol, estradiol and estrone) (Göbel et al., 2007; Luo et al., 2014). When not directly observed, deconjugation was also hypothesized for other PhACs to explain negative removal efficiencies (Luo et al., 2014; Stadler et al., 2012). Generally, glucuronide conjugates are the main excreted conjugates and they deconjugate rapidly following a pseudo-first or first order kinetics. Sulphate conjugates are also often detected in wastewater but are less abundant and more recalcitrant to deconjugate than glucuronide conjugates (Gomes et al., 2009).
The conjugates fraction dissolved into wastewater ($S_{MP\_conj}$ [g $m^{-3}$] - Figure 1) was added to the IUWS_MP library. The deconjugation process was implemented as first-order kinetics (similarly to Plósz et al., 2012, 2010) with rate $k_{dec}$ [$d^{-1}$] and a process rate $\rho_{conj}$ [g $l^{-1}$ $d^{-1}$]:

$$\rho_{conj} = k_{dec} S_{MP_{conj}} \quad \text{Eq. 1}$$

The stoichiometric coefficients describing the mass balance of $S_{MP\_conj}$ and $S_{MP}$ are shown in the Gujer matrix in Table 1, along with the main PhAC processes used in this work. For the complete Gujer matrix of the IUWS_MP library, the reader is directed to Vezzaro et al. (2014). The fraction of conjugates that deconjugates is defined by $f_{dec}$ [-], which was set to a different value (i.e. 0 and 1) depending on the adopted model structure (i.e. no deconjugation or complete deconjugation, see paragraph 2.3.5). The variable $S_{MP\_others}$ was also added in the Gujer matrix, representing transformation of $S_{MP\_conj}$ to other forms.

**Table 1.** Gujer matrix representing the processes in the extended IUWS_MP library used in this study to simulate PhAC fate.

| | $S_{MP}$ | $X_{MP}$ | $S_{MPconj}$ | $S_{MPothers}$[d] | Process rate [$g_{MP}$ $l^{-1}$ $d^{-1}$][b] |
|---|---|---|---|---|---|
| Deconjugation | $+f_{dec}$ | | -1 | $(1-f_{dec})$ | $k_{dec} S_{MP_{conj}}$ |
| Biodegradation[a] | -1 | | | | $k_{bio}\, S_{MP_{conj}}$ |
| Sorption[a] | -1 | +1 | | | $k_{sor}\, C_{TSS} S_{MP}$ |
| Desorption[a] | +1 | -1 | | | $\frac{k_{sor}}{K_d}\, X_{MP}$ |
| Aerobic biodegradation[a,c] | -1 | | | | $\alpha_{oxygen}\, k_{aer} S_{MP}$ |
| Anaerobic/anoxic biodegradation[a,c] | -1 | | | | $(1-\alpha_{oxygen})\, k_{anoxb} S_{MP}$ |

[a] Processes from the original IUWS_MP library (Vezzaro et al., 2014)

[b] The units for the process rates are $d^{-1}$ (for $k_{dec}$, $k_{bio}$, $k_{aer}$ and $k_{anoxb}$) and $m^3\ g_{TSS}^{-1}\ d^{-1}$ for $k_{sor}$

[c] In all the units where oxygen and nitrate are included as water components (e.g. WWTP), dependency from these components is accounted in the process rate as a Monod-type dependency (e.g. in the form $\frac{S_{O_2}}{S_{O_2}+K_{O_2}}$ for oxygen). Contrary, in the remaining units, in which oxygen and nitrate are not available as water components (e.g. sewer), the $\alpha_{oxygen}$ is fixed either to 1 (i.e. presence of oxygen) or 0 (i.e. no oxygen).

[d] $S_{MPothers}$ refers to conjugates that do not deconjugate to $S_{MP}$, but undertake transformation to other forms.

### *2.2.3. Ionisation-based partitioning to solids*

The IUWS_MP describes dynamic sorption/desorption processes based on the MP solid-water partition coefficient $K_d$ [$m^3\ g_{TSS}^{-1}$], describing sorption due to different mechanisms, such as lipophilicity and electrostatic interactions (Schwarzenbach et al., 2003):

$$K_d = f_{oc} * K_{OC} \quad \text{Eq. 2}$$

where $f_{OC}$ [$g\ g^{-1}$] is the organic carbon content of the solid matrix and $K_{OC}$ [$l\ kg^{-1}$] is the organic carbon-water partition coefficient.

For traditional MPs, i.e. neutral and hydrophobic substances, $K_{OC}$ can be expressed as a function of the octanol-water partition coefficient of the neutral molecule ($K_{OW}$, often reported in logarithmic form as $\log P_n$), and empirical regressions have been accordingly defined by technical guidance documents (European Commission, 2003). However, PhACs are generally ionisable, and their sorption is driven by a mix of electrostatic and lipophilic interactions

(MacKay and Vasudevan, 2012). Hence, the degree of ionization (fraction of ionized and neutral form in the solution) and type of speciation (acid or base) can affect the magnitude of the electrostatic interactions and thereby the partition coefficient. In consideration of this, Franco and Trapp (2008) and Franco et al., (2009) refined existing approaches by proposing empirical regressions to derive $K_{OC}$ of acids (Eq. 3) and bases (Eq. 4):

$$K_{OC,acid} = \phi_n 10^{0.54 \log P_n + 1.11} + \phi_i 10^{0.11 \log P_n + 1.54} \quad \text{Eq. 3}$$

$$K_{OC,base} = 10^{0.31 \log D_{OW} + 2.78} \quad \text{Eq. 4}$$

where $\phi_n$ and $\phi_i$ denote the fractions of neutral and ionized species at a reference $pH_{ref}$ (= environmental pH – 0.6) and they are calculated as a function of ionisation constants ($pK_a$) using Henderson-Hasselbach equations. $D_{OW}$ is the pH-dependent octanol-water distribution coefficient, which is also a function of $pK_a$ accordingly to equation: $logD_{OW} = logP_n - log[1 + 10^{(pk-pH)}]$. The refined $K_{OC}$ formulations described in Eq. 3 and 4 were applied to all units of the IUWS.

## 2.3. Testing the extended IUWS_MP library in real scenarios

### *2.3.1. Simulated case studies*

Two integrated urban wastewater systems (System A and B - Table 2) were selected for testing the extended IUWS_MP library. The systems were selected due to the availability of conventional parameters (flow, *TSS*) and PhAC measurements. Notably, the latter only reported the dissolved parent compounds, while no data were available for particulate and conjugated fractions. The models of the two systems differ both in terms of simulated IUWS elements and in how the sewer catchment models were conceptualized (Figure 2):

- The model of System A included emission sources and sewer catchment. System A was subdivided into 8 subcatchments, which were identified for testing Real-Time-Control strategies by using a detailed hydrodynamic model as starting point (Löwe et al., 2016). PhACs measurements were obtained from Naturstyrelsen (2015), reporting measurements collected at the outlet of the catchment over a 1-week sampling campaign in 2012.

- The model of System B included emission sources, sewer catchment and municipal WWTP. System B was subdivided into 6 subcatchments, identified based on the hydraulic retention time by using the automatic approach described in Delli Compagni et al. (2019). The WWTP was conceptualised as a single line, with volume and area corresponding to the volume and area of the whole plant. PhACs measurements were obtained from Castiglioni et al. (2018), who carried out a 1-week sampling campaign at the outlet of the catchment and of the WWTP in March 2011.

Both systems were implemented in WEST® and the models were run with a dynamic output of 2 minutes. Further details on the two systems can be found in SI.

**Table 2.** Characteristics of the modelled integrated systems

| *Integrated Urban Wastewater system* | Location | Inhabitants | Catchment area | Type of sewer system | WWTP included in the model |
|---|---|---|---|---|---|
| A | Denmark | 531.000 | 76 km$^2$ | Gravity/Pressurised | no |
| B | Italy | 1.200.000 | 69 km$^2$ | Gravity | yes |

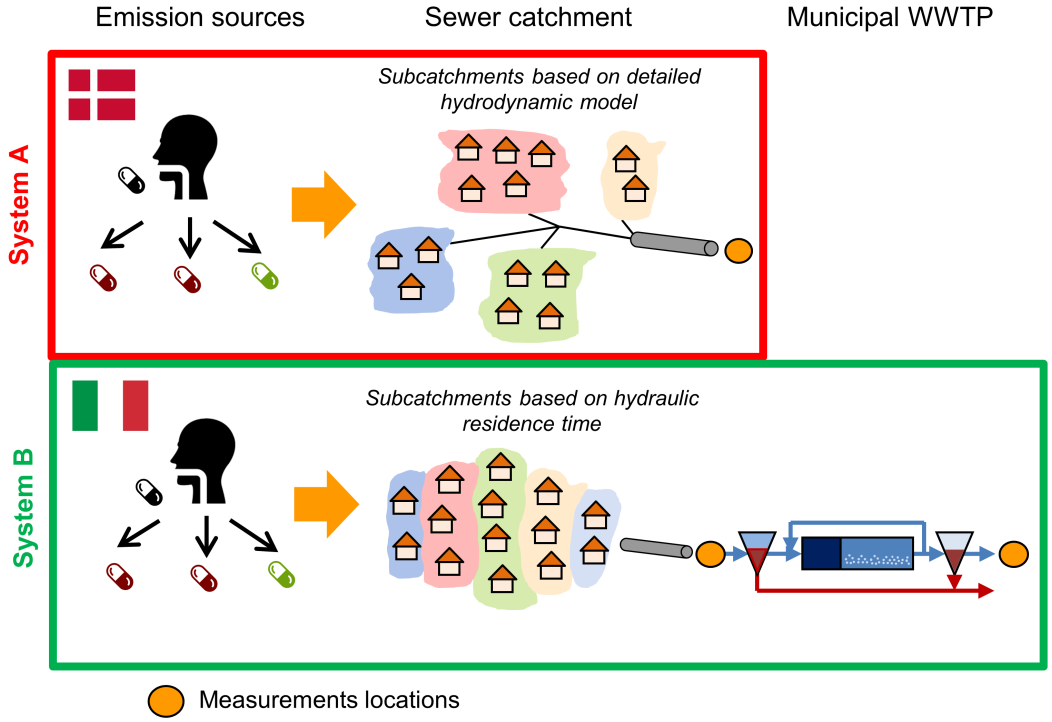


**Figure 2.** Schematic representation of the models of the two IUWS systems and locations where available measurements were collected.

*2.3.2. Calibration of the IUWS sub-models*

For both systems, the integrated models were calibrated for flow and conventional pollutants (*TSS, COD, $NH_4$, Total_P* and *Total_N*). The calibration procedure consisted of three steps, which are described in detail in SI:

1. *Calibration of wastewater quantity parameters.* Catchment quantity parameters (daily wastewater production *WWP* [l cap$^{-1}$ d$^{-1}$], in-sewer infiltration *Inf* [m$^3$ s$^{-1}$ km$^{-2}$], daily profiles, etc.) and sewer parameters (e.g. number of tanks used to simulate the sewer

network, storage constant, etc.) were estimated to simulate dry weather flow (*DWF*) at the sewer outlet.

2. *Calibration of influent quality.* Catchment quality parameters (e.g., average released concentrations of *TSS* and $NH_4$ [mg $l^{-1}$]) of the KOSIM-WEST® model, and WWTP fractionation parameters for ASM2d were estimated to simulate loads of conventional pollutants at the sewer outlet (i.e. WWTP inlet). Fractionation parameters were derived based on existing guidelines (Roeleveld and van Loosdrecht, 2002).

3. *Calibration of the solid balance and WWTP effluent concentrations.* Selected process and biokinetic parameters were estimated to simulate sludge production (mixed liquor suspended solids and solids retention time *SRT*), and conventional pollutants concentrations at the WWTP outlet.

### *2.3.3. Simulated pharmaceuticals*

Five highly consumed PhACs were chosen based on the following criteria: (i) availability of input data (consumption, fate parameters) and field measurements; (ii) significant excretion of conjugated metabolites ($f_{MP\_conj}$ > 10 %); (iii) different $f_{MP\_feces}$ excretion rate (0% - 35%).
The selected PhACs included three widely used nonsteroidal anti-inflammatory drugs (paracetamol-PCM, diclofenac-DCF and ibuprofen-IBU), one diuretic (furosemide-FSM) and one antiepileptic (carbamazepine-CBZ).

### *2.3.4. Model input and parameters*

Defined daily doses (*DDDs)* were obtained from the WHO Collaborating Center for Drug Statistics Methodology (WHO, 2009). National consumption values (defined by *N*) were obtained from sales databases, summarizing information on different distribution systems (over-the-counter, medical prescription, hospitals). Specifically, *N* was obtained from the Italian Annual Pharmaceutical Consumption report (OsMed, 2011) and the Danish MEDical STATistic database (MEDSTAT, 2014). Excretion rates were based on data retrieved from clinical studies. In this study, $f_{MP\_conj}$ refers specifically to glucuronic conjugates, for which data are available. First-order rates for deconjugation ($k_{dec}$) and biodegradation under aerobic ($k_{aer}$) and anoxic ($k_{anoxb}$) conditions were collected from literature studies, where batch/full-scale experiments were performed. The influence of biomass concentration on deconjugation and biodegradation kinetics was considered by adjusting first-order rates accordingly to the equation: $k_{adjusted} = k\ (C_{TSS\_measured} / C_{TSS\_simulated})$, where $C_{TSS\_measured}$ is the experimental *TSS* concentration and, $C_{TSS\_simulated}$ the simulated *TSS* concentration in the sewer/WWTP. When no empirical data were available for $k_{dec}$ and $k_{anoxb}$ for a specific PhAC, two assumptions were made: (i) $k_{dec}$ of another PhAC was used, and (ii) a $k_{anoxb}$ equals to 0.0001 was assumed (i.e. no degradation under anoxic conditions). Physical and chemical properties were retrieved from Advanced Chemistry Development Inc. (ACD/Labs) calculator or the Performs Automated Reasoning in Chemistry (SPARC) calculator. All collected data are reported in Table 3, where

rate constants were converted in half-lives ($t_{1/2\_aer}$, $t_{1/2\_anoxb}$ and $t_{1/2\_dec}$) according to $ln(2)/k_i$ with $k_i$ being $k_{aer}$, $k_{anoxb}$, $k_{dec}$, respectively.

### *2.3.5. Uncertainty analysis*

The high variability of the model input and parameters linked to PhACs (Table 3) was propagated to the results by using a forward Monte Carlo approach (1,000 simulations), similarly to Mannina et al. (2017). Depending on data availability, parameter probability distributions were considered to be uniform or triangular as also in Delli Compagni et al. (2020). Extremes of uniform distributions were assigned based on two criteria: (i) when the dataset included more than two values, the extremes were the maximum and the minimum, (ii) when the dataset included only one value, the extremes were calculated as a percentage variation (PV) from the value. Two PV were used: ± 10% and ± 50%, depending on the reliability of data source. Specifically, a PV = ± 10% was assigned to $N$ since values were obtained from well documented consumption data. Conversely, a PV of ± 50% was assigned to excretion rates ($f_{MP,urine}$, $f_{MP,feces}$ and $f_{MP\_conj}$) and half-lifes ($t_{1/2\_aer}$, $t_{1/2\_anoxb}$, $t_{1/2\_dec}$) since values were obtained from laboratory experiments where multiple factors (e.g., initial concentrations, type of biomass) could have made the results too laboratory-specific. Triangular probability distributions were used for skewed dataset: specifically, the median was set as mode, while and maximum and minimum values were used as extremes of the distribution. The physicochemical properties (molar mass, water solubility, Henry constant, log$P_n$ and $pK_a$) were assumed to be reliable and thus kept constant for all the simulations.

### *2.3.6. Model performance evaluation*

The effect of the new processes included in the extended IUWS_MP library (deconjugation, sequestration) was evaluated by looking at the predicted fate of carbamazepine (which is widely used as reference substance) against the available measurements in both systems. Three different model structure combinations (Table 4) were tested against the results of the original IUWS_MP library (Case 0). Based on these simulations, the model structure providing the best results (also in terms of uncertainty bounds) was applied to simulate the fate of the other four PhACs. Partitioning due to ionization processes (paragraph 2.2.3) was always included in all cases since its validity was already well verified.

**Table 4**. Overview of the four different model structures that were compared for simulation of CBZ: "-" and "+" stands for exclusion and inclusion of the specific process.

| | Case 0 | Case 1 | Case 2 | Case 3 |
|---|---|---|---|---|
| Deconjugation | - | + | - | + |
| Sequestration | - | - | + | + |

**Table 3.** Model inputs and parameters of the simulated PhACs

| | Source | | | | | Sewer | | WWTP | | | Generics[d] | | | | |
|---|---|---|---|---|---|---|---|---|---|---|---|---|---|---|---|
| | DDD [mg DDD$^{-1}$] | N°$_{DDD}$ [DDD $10^3$inhab$^{-1}$ d$^{-1}$] | $f_{MP\_urine}$ [-] | $f_{MP\_feces}$ [-] | $f_{conj}$ [-] | $T_{1/2\_aer}$ [d] | $T_{1/2\_dec}$ [d] | $T_{1/2\_aer}$ [d] | $T_{1/2\_anoxb}$ [d] | $T_{1/2\_dec}$ [d] | Molar mass [g mol$^{-1}$] | Water solubility [mg l$^{-1}$] | Vapor P [mmHg] | $LogP_n$ [-] | $pK_a$ [-] |
| PCM | 3000[c] | 68.4[a], 6.1[b] | 2, 2-5, 5 [1] | 0 [1] | 52, 55, 57 [2] | 0.06 [8] | 0.28 [9] | 0.003, 0.002 | 1000* | 0.02 [9] | 151.16 | 14000 | 1.43E-06 | 0.46 | 10.2 |
| DCF | 100[c] | -, 10[b] | 1, 6 [1,3] | 5, 25 [1] | 11 [4] | 1000 [8] | 0.28 [9] | 0.04, 0.2, 0.3, 1.8 | 4.6 | 0.02 [9] | 296.15 | 2.37 | 1.59E-07 | 4.51 | 4.4 |
| IBU | 1200[c] | 20.4[a], 4.3[b] | 1,10,11,12 [1,5] | 15, 35 [1] | 9,12 [1,5] | 13.3 [8] | 0.28 [9] | 0.005, 0.009, 0.009, 0.036 | 0.12 | 0.02 [9] | 206.28 | 21 | 1.39E-04 | 3.97 | 4.3 |
| FSM | 40[c] | 43.6[a], 19.2[b] | 9, 46, 89 [6] | 7, 9 [6] | 35 [6] | 0.24 [8] | 0.28 [9] | 0.10, 0.36 | 1000* | 0.02 [9] | 330.74 | 73.1 | 3.11E-11 | 2.03 | 3.5 |
| CBZ | 1000[c] | 0.84[a], 1.5[b] | 0.8 [7] | 13 [7] | 11 [7] | 6.3 [8] | 0.28 [9] | 0.9, 2.9, 3.0, 21.0 | 6.1 | 0.02 [9] | 236.27 | 17.7 | 5.78E-07 | 2.45 | 13.9 |

[1](Lienert et al., 2007), [2] (Mazaleuskaya et al., 2015), [3] (Zhang et al., 2008), [4] (Vieno and Sillanpää, 2014), [5] (Speight and Sjöqvist, 2006), [6] (Boles Ponto and Schoenwald, 1990), [7] (Bahlmann et al., 2014), [8] (O'Brien et al., 2017), [9] (Lee et al., 2012).

a Value for system A

b Values for the system B

c WHO Collaborating Centre for Drug Statistics Methodology, Oslo, Norway.

d ACD/Labs and SPARC

# 3. Results

## 3.1. Calibration of the IUWS sub-models

Simulated *DWF* at the catchment outlet (Figure S2) fell within uncertainty ranges of measurements, and estimated parameters resulted in *WWP* of 112 and 220 l $cap^{-1}$ $d^{-1}$ and *Inf* of 0.22 and 0.8 $m^3$ $s^{-1}$ for System A and B, respectively. At the WWTP inlet, the concentrations of conventional pollutants (Figure S3) were well described by simulation results by using parameters that were within typical literature ranges (both for the catchment description and for the wastewater fractionation; Table S2-S4).
In the WWTP (System B), *TSS* predictions in the aerated tank and in the returned sludge were in good agreement with measurements (Figure S4). Measured effluent concentrations of *COD*, *TSS*, total nitrogen, ammonium and total phosphorus were also well described by simulation results (Figure S5). These results were obtained by using default ASM2d parameter values (Henze et al., 2000) except for $\mu_{AUT}$ and $K_{NH}$, which were estimated to be 0.1 $d^{-1}$ and 0.3 mgN $l^{-1}$ (default value 0.05-0.15 and 1 respectively).

## 3.2. Effect of the new processes introduced in the extended model library

The dynamic CBZ concentrations from the 1,000 Monte Carlo simulations were aggregated in box-plots (Figure 3) to enable the comparison against measurements (which are mostly based on 24-h composite samples). The prediction bounds (i.e. width of the whiskers) shows the ranges of predicted CBZ concentrations over the week when samples were taken, while measured concentrations are shown as maximum, median and minimum values.
The concentrations predicted by the original model library (Case 0) systematically overestimated the measurements in all the sites. Specifically, predicted concentration median was 6 times higher than the measurements median in System A, while for System B it was about 3 times higher, both at the inlet and outlet of the WWTP.
Including only deconjugation in the model structure (Case 1) did not improve model performance. Predicted concentrations further increased with respect to Case 0, leading to further deviation from measurements. This aspect was particularly evident at the outlet the WWTP, where predicted median was about 7.5 times higher than the median of the measurements. The increase compared to Case 0 was due to the high concentration of conjugates that was predicted at the inlet of the WWTP, which would further deconjugate to parent CBZ during wastewater treatment.
Including only sequestration in the consumption-excretion model (Case 2) substantially changed the proportions of CBZ fractions released at the source, reducing the deviation in the predicted concentrations in both systems. In System B, for example, the parent CBZ released at the source ($C_{MP\_urine}$) decreased from about 0.9 μg $l^{-1}$ (Case 0-1) to about 0.05 μg $l^{-1}$ (Case 2); while the sequestered CBZ ($X_{MP\_seq}$) increased from 0.003 μg $l^{-1}$to 0.8 μg $l^{-1}$.
Including both sequestration and deconjugation (Case 3) led to the closest match between predictions and measurements, especially at the inlet of the WWTP. At the WWTP outlet, predictions overlapped with measurements although a slight discrepancy was observed. This

might suggest deconjugation of conjugated CBZ to other compounds than parent CBZ, which has been observed elsewhere (Zonja and Pe, 2015). This hypothesis was considered in additional simulations, whereby it was assumed that 50% of conjugated CBZ would retransform back to parent CBZ (i.e., $f_{dec}$ = 0.5) (Figure S6).

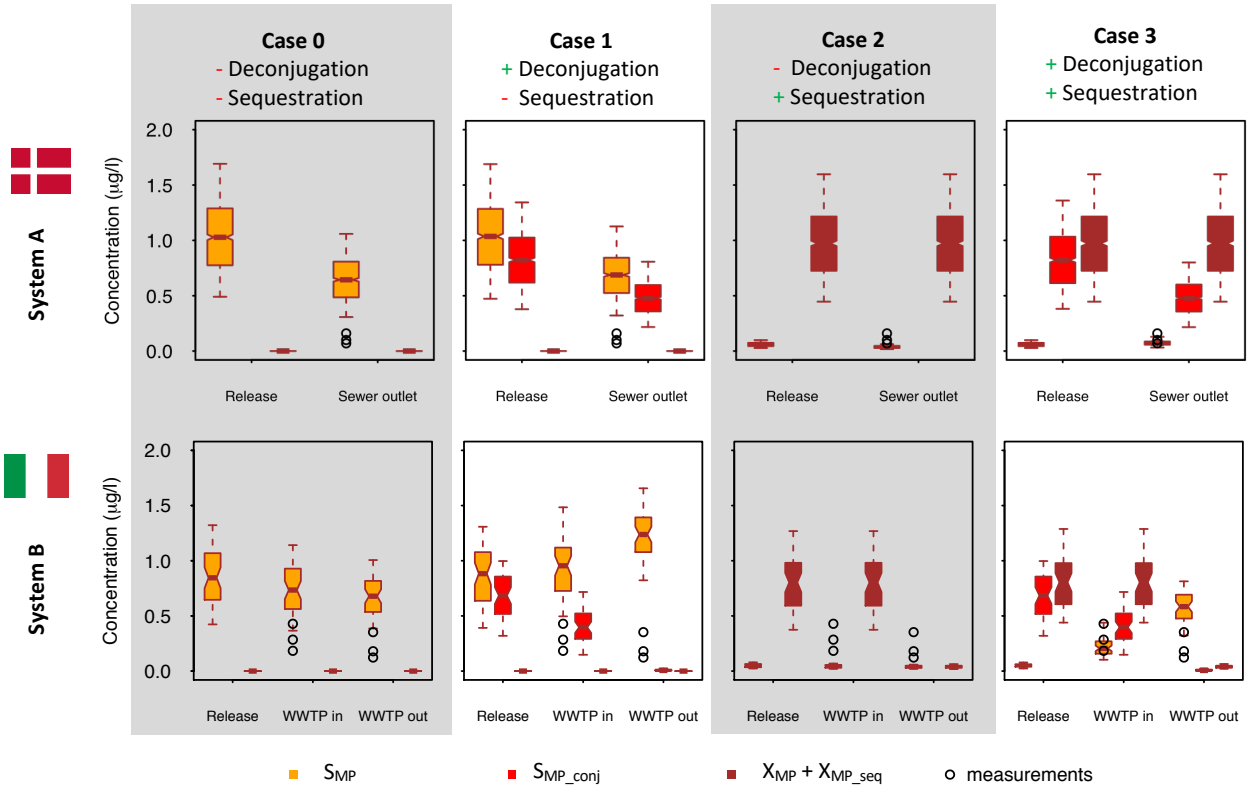


**Figure 3:** Comparison between CBZ measurements (dots representing maximum, median and minimum values) and different simulated fractions at the release point, at the outlet of the catchment (inlet of WWTP) and the WWTP outlet for four different model structures.

### 3.3. Performance of the model library in predicting the fate of other PhACs

Based on the performance analysis on CBZ predictions, the model structure including both deconjugation and sequestration (Case 3) was applied to simulate the remaining four PhACs (Figure 4).

At the sewer outlet of both systems, model predictions for IBU, FSM and PCM were in good agreement with measurements, showing an overlap between the uncertainty bounds of measurements and simulations. A good model prediction capability was also observed for PCM although predicted concentrations slightly overestimated measurements at the WWTP inlet, with a deviation between the predicted and the measured median concentrations of about 60 %. This could be explained by the fact that PCM has an in-sewer biodegradable half-life ($t_{1/2\_aerb}$ = 3.6 h) comparable with the average *HRT* of the system (i.e. around 3.5 h). This makes the estimation of PCM fate more sensitive to hydrodynamic parameters compared to the other PhACs. In this study, uncertainties associated to hydrodynamic parameters were not considered for two reasons: i) to keep computation burden within reasonable values and, ii) to

quantify model results uncertainty mainly due to uncertainties associated to the chemical characteristics of PhACs.

FSM predictions overestimated measurements at the WWTP outlet. This can be explained by an incomplete deconjugation of conjugates back to the parent FSM in the simulated system, as previously observed for CBZ (Figure 3). This process was included in new simulations by assuming that only 10% of the glucuronide conjugates (i.e., $f_{dec}$ = 0.1) eventually deconjugates. A better match for both FSM and CBZ was then obtained (Figure S6). Retransformation to other compounds than parent substances has been observed for a number of PhACs (Ramin et al., 2017). However, no evidence is currently available for the PhACs investigated in this study, and detailed experimental evaluation would be required to improve fate assessment.

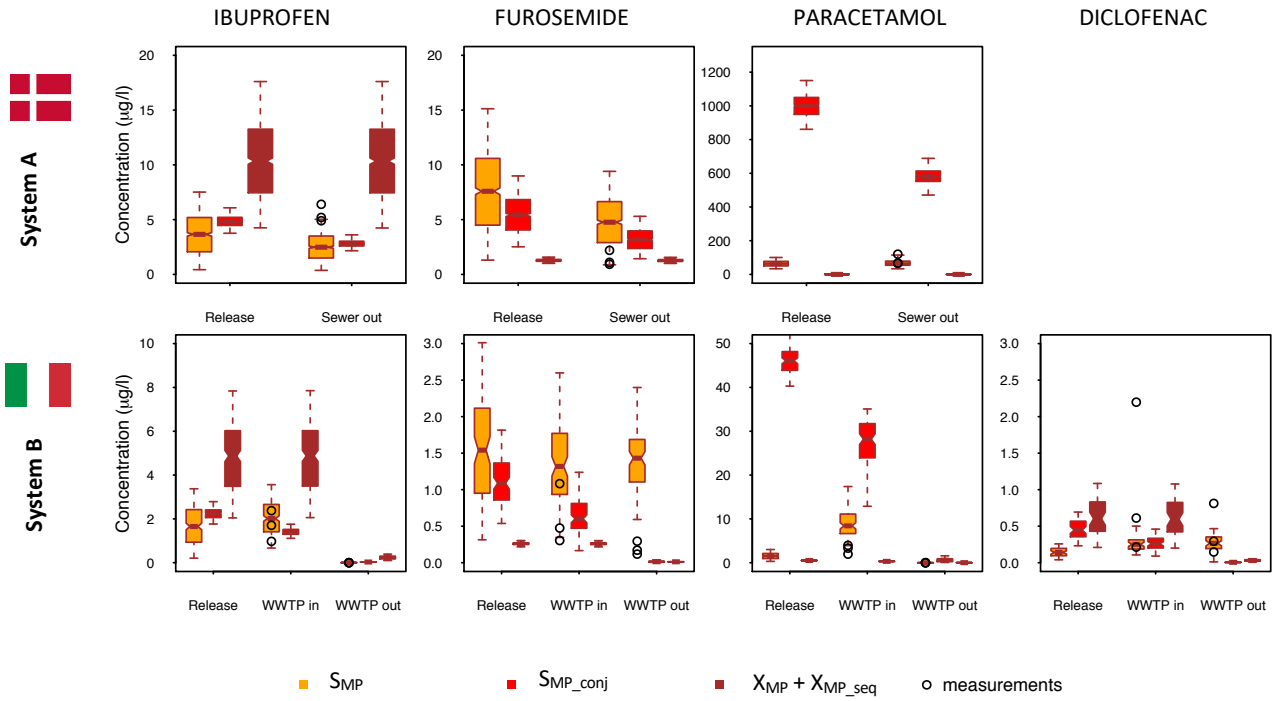


**Figure 4:** Comparison between measurements and model predictions for different fractions of PhACs at release point, sewer outlet (WWTP inlet) and WWTP outlet. Results were obtained by using model structure 3 (i.e. + deconjugation, + sequestration).

## 4. Discussion

Based on national/local consumption data and publicly available input data, the extended IUWS_MP library was capable of evaluating the fate of highly consumed PhACs in two different urban wastewater systems. Possible applications of the extended library are described below.

### 4.1. Identify potentially hazardous substances

The definition of Environmental Quality Standards for hazardous/priority MPs in environmental legislations requires implementation of specific actions when EQS are exceeded.

Identification of hotspots and testing of multiple scenarios (i.e. minimization strategies) within a complex, interconnected and dynamic IUWS system needs modelling tools that can provide a high level of system description while keeping a low computational burden. Within this context, the extended IUWS_MP library is a valuable compromise between multimedia compartment models (e.g. SimpleTreat), which are very fast but generally suitable for system under steady-state conditions, and complex hydrodynamic models (e.g. SWMM), which are very detailed but also highly computationally demanding. In this paragraph, we used the library to identify hazardous/priority MPs that will be likely to exceed forthcoming European limits. The WWTP in System B discharges to a small river that is often under low flow conditions, making the WWTP effluent its main flow contributor (see Delli Compagni et al., 2020). Predicted WWTP effluent concentrations for IBU and DCF were compared with the chronic quality standards that were recently proposed by the Swiss Ecotox Centre (i.e. 0.01 μg $l^{-1}$ and 0.05 μg $l^{-1}$ for IBU and DCF, respectively) (Oekotoxzentrum, 2019). We can conclude with a 95% confidence that median DCF concentrations would not comply with the proposed standard ($S_{MP}$ = 0.26 ± 0.03μg $l^{-1}$), while median IBU concentrations would be below the proposed standard ($S_{MP}$ = 0.003 ± 0.001 μg $l^{-1}$). However, maximum predicted concentrations would be above the standards for both PhACs, with concentrations of DCF and IBU from 1 to 8 times higher than the standards (0.46 μg $l^{-1}$ and 0.02 μg $l^{-1}$ for DCF and IBU, respectively). These results suggested that precautionary interventions (e.g., upgrading of the WWTP with a tertiary treatment) should be considered in future policies to comply with forthcoming European limits.

## 4.2. Understanding the fate of not routinely measured fractions

Monitoring of thousands of MPs present in different forms (e.g. parent fraction and metabolites) in all the environmental compartments is well-recognized to be economically or physically unfeasible.
Within this context, the extended IUWS_MP library can help understanding the fate of PhACs fractions that are not routinely measured and thus refining fate assessment.

1. *Assessment of the removal efficiency during wastewater treatments*. Generally, removal efficiency calculations are only based on the dissolved fraction of the target compounds (Stadler et al., 2012), especially when a low sorption capacity is expected. However, if large PhAC quantities are excreted through the faeces, sequestration might occur and a non-negligible fraction might exit the WWTP enclosed within the *TSS* independently from the sorption capacity (Luo et al., 2014). In this paragraph, the removal efficiency for IBU, which has a low sorption capacity but a great potential of undertaking sequestration ($f_{MP\_feces}$ ranging from 15% to 35%), was calculated by closing the mass balance on the WWTP by considering (i) both $S_{MP}$ and $X_{MP,seq}$ (i.e. total efficiency) or (ii) only $S_{MP}$ (i.e. apparent efficiency). Results showed that, with a *TSS* removal of 95% (obtained after the calibration of the WWTP submodel), the total and apparent removal efficiency were 96.4% and 99.8%, respectively. Thus, closing the mass balance with only $S_{MP}$ would lead to a 3.4% error in the efficiency calculation. Although this error might be considered negligible, this value can change depending on the *TSS* removal of a specific

WWTP and on the $f_{MP\_feces}$ of a target PhAC. For example, a total removal efficiency of 92.8% and 89.4% was obtained with *TSS* removal of 90% and 85%, with an error in the efficiency calculation of 7% and 10.4%, respectively.

2. *Environmental risk assessment.* Environmental risk assessment implies calculating the ratio between environmental concentration of a target PhAC and predicted non-effect concentration (*PNEC*). If the ratio is higher than 1, a risk for the environment is likely to occur. Environmental concentrations are either measured (*MEC*) or predicted through models (*PEC*), and they generally refer to the parent fraction, while metabolites are rarely considered. However, when metabolite such as glucuronides can deconjugate to the parent fractions (Göbel et al., 2007; Luo et al., 2014), their exclusion from the analysis can cause an underestimation of the risk. The case of PCM can be instrumental with this respect. At the WWTP outlet, predicted concentrations of glucuronic conjugates of PCM were, on average, 9600 times bigger than the parent concentrations ($S_{MP\_conj}$ and $S_{MP}$ equal to 0.6 and 0.00006 μg $l^{-1}$, respectively). This high discrepancy between the two fractions was due to: (i) the high biodegradability of the parent fraction ($t_{1/2\_aerb} \approx 0.072$ h), which led to very low concentrations and (ii) the large quantity of excreted glucuronide conjugates (in the range 40-52 μg $l^{-1}$ at the source) that do not totally deconjugate during in-sewer transit/wastewater treatments. Calculating the risk as $S_{MP}/PNEC$, where *PNEC* is equals to 0.367 μg $l^{-1}$ (Riva et al., 2019) would lead to 0.0002 (i.e. no risk). However, since glucuronic conjugates are still present at the WWTP outlet, deconjugation is likely to keep occurring after wastewater treatment and the risk quotient should be calculated as $((S_{MP} + S_{MP\_conj})/PNEC)$. In this case a value of 1.6 was obtained, highlighting a possible risk for the receiving water system.

### 4.3. Support the monitoring and design of sampling campaigns

PhACs concentrations in wastewater showed seasonal and daily temporal variability, which have been explained though seasonality in consumption data as well as PhAC posology (i.e. prescribed dose and administration time to treat an infection) (Coutu et al., 2013). Within this context, this *a priori* knowledge can be used as input to our modelling tool to derive expected PhAC dynamics over a defined period, supporting the planning of sampling campaigns at a certain location (e.g. WWTP, combined sewer overflows). For example, Figure 5 shows the hourly predicted concentrations of parent CBZ and its associate glucoronate conjugates along System B over 1-year. In this case, a constant time trend in the consumption data was assumed, since CBZ is expected to be constantly consumed by patients on a daily basis over a very long period. At the outlet of the WWTP, the predicted median concentration in March was double than in August, highlighting a monthly temporal variation mainly driven by the high in-sewer infiltration of the area. In this case, a sampling campaign during summer would fail to capture the highest concentrations, thus underestimating the annual average CBZ load entering the WWTP and consequently discharged into the recipient. As for the diurnal dynamics, predicted concentrations of parent CBZ followed a smoother dynamic than the conjugate fractions, especially at the WWTP inlet. Consequently, different sampling frequency should be used at the

WWTP inlet to determine conjugate concentrations as much representative as for the parent fraction.

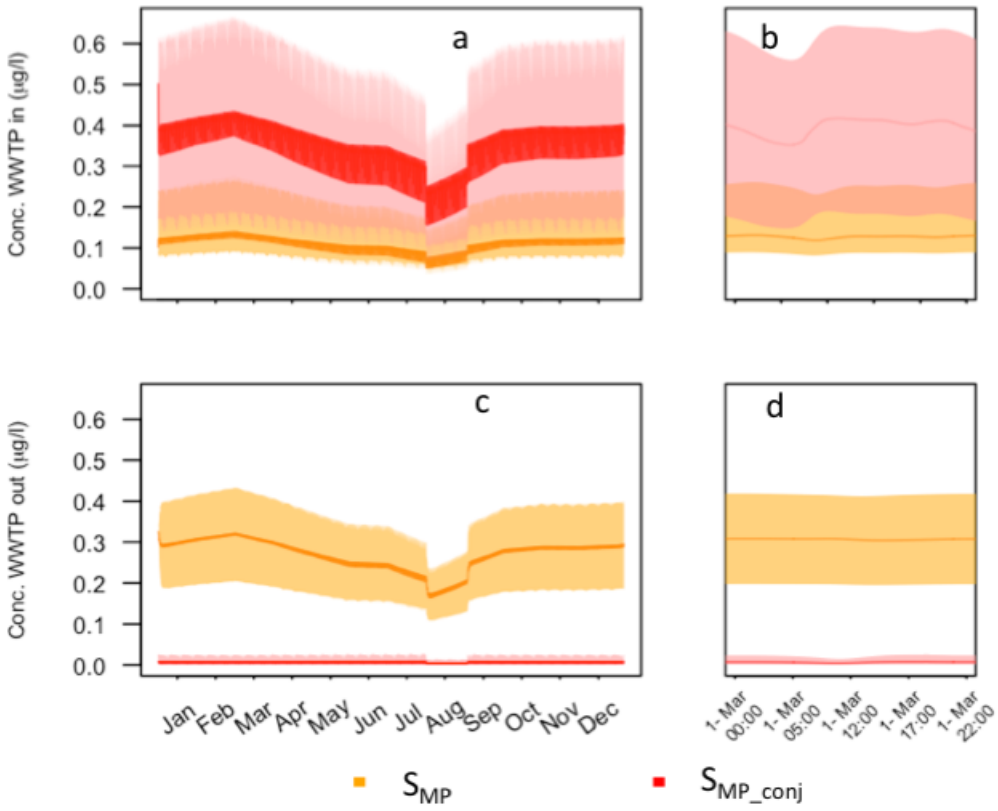


**Figure 5.** Simulated concentrations of carbamazepine at the WWTP inlet (a,b) and outlet (c,d) over a whole year (a, c) and over a single day (b, d). Solid lines: median value. Coloured bounds: 5-95% percentile of the model prediction bounds.

## 5. Conclusions

The IUWS_MP library was successfully extended with additional processes allowing for the simulation of pharmaceuticals (PhACs). As for the original library, the extended IUWS_MP library relies on information easily retrievable from existing databases and literature, such as local/national consumption data and, inherent PhACs physical-chemical properties and degradation rates. This allows for the simulation of a wide range of micropollutants without requiring site-specific data for parameter estimation, other than measurements of conventional indicators (flows, TSS, nitrogen, etc.).

Comparison of the library predictions for a range of widely consumed PhACs with different properties (i.e. carbamazepine, ibuprofen, diclofenac, paracetamol and furosemide) showed a good agreement with measurements. The additional processes (consumption-excretion, deconjugation) proved to be essential in order to allow for a realistic simulation of PhACs. Despite the great uncertainties linked to the process simplifications of the IUWS_MP library approach (first order rates, national emission rates, etc.), the median simulated values were in the same order of magnitude of the measurements. The robustness of the IUWS_MP approach was highlighted by the fact that the two simulated catchments were located in different

countries (i.e. different emission rates), and that the sewer catchment models were built using different approaches (based on the physical structure of the network in System A, or on the analysis of the hydraulic retention time in System B).
As for the extended library, possible applications include:

- Identification of potential environmental risks due to non-compliance of PhACs with existing or proposed environmental quality standards.
- Estimation of PhACs fate and total fluxes based on the simulation of seldom monitored fractions (e.g. glucuronide metabolites and parent fraction sequestered within the faecal matter). This is a specific feature of the extended library.
- Evaluation of the effects of different PhACs strategies in reducing risks for the aquatic environment and for the human health (as in water-reuse scenarios).
- Optimization of sampling campaigns, suggesting which compartment should be sampled and at which location and time.

The presented extension of the IUWS_MP library increased its range of applicability, allowing urban water manager not only to evaluate the effect of their efforts in reducing emission of already regulated substances, but also to investigate the potential risks linked to emissions of other emerging contaminants (such as PhACs). The extended library thus provides an essential modelling tool to tackle the future challenges in ensuring availability and sustainable management of water in urban areas.

## Supplementary information

### Materials and methods

*System conceptualization*

The two simulated IUWS systems were built in the WEST® environment by using elements of the IUWS_MP library (Figure S1). The PhAC fluxes were simulated from the sources (wastewater generation in each subcatchment) to the outlet of the sewer and to the outlet of the WWTP (only for System B).
System A includes the wastewater collection (combined sewer) of catchment in a large urban area in Denmark. Detailed information on the sewer system can be found in Löwe et al. (2016). The catchment is subdivided into 8 subcatchments, which were identified by looking at available control points for Real-Time-Control applications (i.e. subcatchment discharging to a detention basin or a pumping station). Conceptualization of sewer stretches (i.e. number of tanks for each connection) was performed by using results from a detailed hydrodynamic model (Mike Urban). The procedure was identical as in Löwe et al. (2016), where the conceptual model was built in the WaterAspects™ software.
System B includes both wastewater collection (combined sewer) and treatment systems of catchment in a large urban area in Northern Italy. Detailed information on the sewer system and its conceptualization can be found in Delli Compagni et. (2019). The catchment was divide into 6 subcatchments, identified based on the analysis of the hydraulic retention time. The WWTP consists of a primary treatment with coarse and fine screening, grit and grease removal, followed by biological treatment. The former consists of four modules, each one of eight lines including an anoxic and aerobic zone and a settler. Sandfilters and a disinfection step are also present after the settlers. Phosphorus removal is obtained by chemical precipitation before the sandfilter. The sludge treatment line consists of a thickener, a filter press and a sludge drying process. Model conceptualization of the WWTP is shown in Figure S1 and focused on the water line only, due to the focus on effluent quality and discharge to

water recipients. The plant was modelled as one line, with tank volumes and areas equal the sum of volumes and areas of tanks in the individual lines. In Table S1, all modelled units of the WWTP are reported with respective dimensions (where required). Based on measurements, recirculation and waste flows such as internal recycle (IR) of the mixed liquor, return activated sludge (RAS) and waste activated sludge (WAS) were set to be 1.5, 6.2 and 0.06 $m^3 s^{-1}$, respectively. The aerated activated sludge tank was additionally equipped with a controller for aeration, with dissolved oxygen (DO) set-point of 1.5 mg $l^{-1}$. For the sandfilter, backwash flow was set to 2 $m^3 s^{-1}$ and backwash intervals to 15 min. Disinfection was not included since affects little the simulated PhACs fate. All the data were either retrieved from the personnel or from the SCADA system of the plant.

**Table S1.** Dimension for each modelled unit of the WWTP.

| Treatment Unit | Dimensions |
|---|---|
| Coarse screen | - |
| Fine screen | - |
| Grit separator | - |
| Denitrifcation | V=50000 m3 |
| Nitrification | V=152000 m3 |
| Settler | A=175000 $m^3$ and H = 5.5 m |
| Sandfilter | A=2440 m2 and H = 1.5 m |

System A

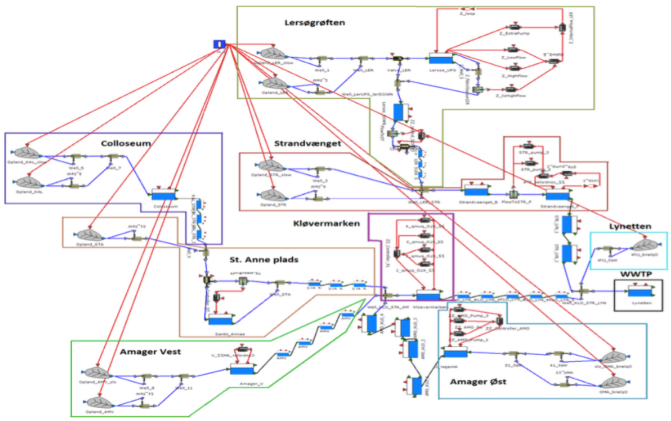


System B

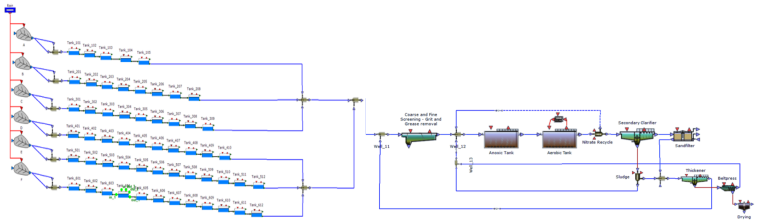

**Figure S1.** Screenshots of the implementation of the two simulated IUWS systems in WEST® environment. The eight subcatchments in System A are identified by different colours.

*Model calibration and performance evaluation*

*Calibration of wastewater quantity (WWTP influent).*

Each subcatchment in System A was calibrated against the data from the detailed hydrodynamic model, as done by Löwe et al. (2016) with the WaterAspects™ model. While the latter simulates transport among the points of the system as a transfer function, the IUWS_MP library require the definition of a specific number of non-linear tanks, and the calibration of the reservoirs' discharge constants. This was performed by using a simplex optimization in Matlab, where the parameters of each subcatchment were estimated in order to achieve the desired transport time among points of the system.

The per capita wastewater production *WWP* [l $cap^{-1}$ $d^{-1}$], in-sewer infiltration *Inf* [$m^3$ $s^{-1}$ $km^{-2}$], and associated and respective daily and seasonal profiles were estimated by using flow measurements at the catchment outlet (i.e. inlet of the local WWTP, which was not included in the IUWS model in this study). The flow data covered the five month period of the monitoring campaign carried out by Alferes et al. (2014): from these data, typical daily profiles for dry weather days were estimated. The daily profile in the IUWS_MP was calibrated against the median of these dry weather days (see Figure S2a). The same profile is assumed in all the subcatchments.

Similarly for System B, *WWP*, *Inf* and respective daily and seasonal profiles were estimated by looking at measurements at WWTP inlet. Specifically, *WWP* and *Inf* were automatically derived from the approach for model conceptualization developed by Delli Compagni et al., (2019). Hourly peak factors for *WWP* were based on the drinking water consumption patter found by Candelieri and Archetti (2014), while monthly peak factors for *Inf* were estimated to match both flow and concentration dynamics of conventional pollutants at the WWTP inlet.

*Calibration of wastewater quality parameters (WWTP influent).* This step consisted in the estimation of (i) catchment model inputs for water quality in the KOSIM-WEST® model (*TSS – total suspended solids*, $COD_S$ – soluble chemical oxygen demand, $COD_X$ – particulate chemical oxygen demand, $NH_4$ and $PO_4$) (Table S2), and (ii) WWTP fractionation parameters to convert catchment model state variables into ASM-type state variables (ASM2d). Since System A did not include the WWTP, only TSS were calibrated, since the other components do not affect the MP fate calculations.

In System B, the fractionation procedure was based on the work of Roeleveld and van Loodsrecht (2002) and the guidelines for using activate sludge model (Rieger, 2012). These two calibration steps were performed simultaneously due to their interdependence. This aspect can be noticed in the fractionation of total nitrogen (*Total_N*) (eq. S1) and phosphorous (*Total_P*) (eq. S2), where *Total_N* and *Total_P* depend on the COD fractionation ($S_F$, $X_S$, $S_I$, $X_I$, $X_{PP}$ and $X_H$) and on $S_{NH}$ and $S_{PO}$, the state variables of the catchment model.

$$Total\_N = S_{NH} + S_{NO} + i_{NSF} \cdot S_F + i_{NXS} \cdot X_S + i_{NSI} \cdot S_I + i_{NXI} \cdot X_I + i_{NB} \cdot X_H \quad \text{Eq. S1}$$

$$Total\_P = S_{PO} + i_{PSF} \cdot S_F + i_{PXS} \cdot X_S + i_{PSI} \cdot S_I + i_{PXI} \cdot X_I + X_{PP} + i_{PB} X_H \quad \text{Eq. S2}$$

Specifically, the followed procedure is reported and was based on measurements collected at the WWTP inlet:

- $COD_s$ and $COD_x$ were obtained according to equations:

$$COD_X = TSS / 0.85 \quad \text{(Eq. S3)}$$
$$COD_S = COD_{TOT} - COD_X \quad \text{(Eq. S4)}$$

where *TSS* and $COD_{tot}$ represent the average of the measured concentrations over 1-year time, and 0.85 (gTSS $gCOD^{-1}$) denotes the conversion factor from particulate COD to TSS.

- $COD_S$ and $COD_X$ were further fractionated into biodegradable, unbiodegradable and biomass fractions (Table S3).

**Table S2.** Comparison of calibrated catchment model inputs against typical literature range (Henze et al., 2008)

| Catchment model input | Literature range [mg/l] | Estimated value[mg/l] |
|---|---|---|
| TSS | 200 - 600 | 270 |
| $COD_{tot} = COD_s + COD_x$ | 200 - 1000 | = 67 + 323 |
| $NH_4$ | 20 - 75 | 21.5 |
| $PO_4$ | 6 - 25 | 1 |

**Table S3.** COD fractionation, default and estimated ASM values and literature ranges (Roeleveld and van Loodsrecht, 2002)

| | COD fraction | Calculation method | Default values | Typical range | Estimated value |
|---|---|---|---|---|---|
| $COD_S$ | Readily biodegradable ($S_S$) | $= S_A + S_F$ | 0.62 | 0.09-0.42 | 0.85 |
| | Inert ($SS_I$) | $= COD_{effluent,filt}$ | 0.37 | 0.03-0.1 | 0.15 |
| | (Volatile fatty acids) $S_A$ | $= 0.4 \cdot S_s$ | 0.25 | - | 0.34 |
| | (Fermantable organic matter) $S_F$ | $= 0.6 \cdot S_s$ | 0.37 | - | 0.51 |
| $COD_X$ | Slowly biodegradable matter ($X_S$) | $X_S = BCOD^a - S_S - X_H$ | 0.68 | 0.1-0.48 | 0.68 |
| | Heterotrophic biomass ($X_H$) | $X_H = 30$ | 0.16 | > 0.1 | 0.16 |
| | Inert particulate matter ($X_I$) | $X_I = COD_X - X_S - X_H$ | 0.16 | 0.23-0.5 | 0.16 |

[a] BCOD was calculated as $BOD_5/((1-e^{-5k})(1-f))$ where $BOD_5$ is the average of the measured concentrations over 1-year time and $k$ and $f$ are equals to 0.3 and 0.15, respectively. (Roeleveld and van Loosdrecht, 2002).

- Five target variables (i.e. *TSS, COD, $NH_4$, $PO_4$, Total_P* and *Total_N*) were chosen based on available measurements for calibration. Conversion factors for organic nitrogen and organic phosphorus fractions (Table S4) and catchment model inputs were manually adjusted until a proper match was reached between simulated target variables and measurements at the inlet of the WWTP. $S_{NO}$ (in eq. S1) was set as constant and equal to the average of the measured $NO_3^-$ concentrations over a 1-year time (0.8 mg $l^{-1}$).

*Calibration of the solid balance in WWTP and effluent concentrations of conventional pollutants.* Settling parameters (e.g. the non-settable fraction of suspended solid) were estimated to have a good match (± 10 %) between simulated *TSS* concentrations (both in the aerated zone and in the RAS flow) with available measurements. Biokinetic parameters were finally adjusted until a proper accuracy (± 5 mg $l^-$

[1]) between target variables and measured concentrations at the WWTP outlet, as suggested in guidelines for using activate sludge model (Rieger, 2012).

**Table S4.** Literature and estimated nitrogen and phosphorus coefficients for fractionation.

| Nitrogen fraction | Default value (gN/gCOD) | Literature range (gN/gCOD) | Estimated value |
|---|---|---|---|
| $i_{NSI}$ | 0.01 | 0.01-0.02 | 0.01 |
| $i_{NSA}$ | 0.00 | 0 | 0.00 |
| $i_{NSF}$ | 0.02 | 0.02-0.04 | 0.02 |
| $i_{NXI}$ | 0.02 | 0.01-0.06 | 0.02 |
| $i_{NXS}$ | 0.03 | 0.02-0.06 | 0.03 |
| $i_{BM}$ | 0.07 | - | 0.07 |
| Phosphorus fraction | gP/gCOD | gP/gCOD | |
| $i_{PSI}$ | 0.00 | 0.002-0.008 | 0.000 |
| $i_{PSA}$ | 0.00 | 0.000 | 0.000 |
| $i_{PSF}$ | 0.01 | 0.01-0.015 | 0.010 |
| $i_{PXI}$ | 0.005 | 0.005-0.01 | 0.005 |
| $i_{PXS}$ | 0.01 | 0.01-0.015 | 0.010 |
| $i_{BM}$ | 0.02 | - | 0.020 |

**Results and discussion**

**Calibration of the systems**

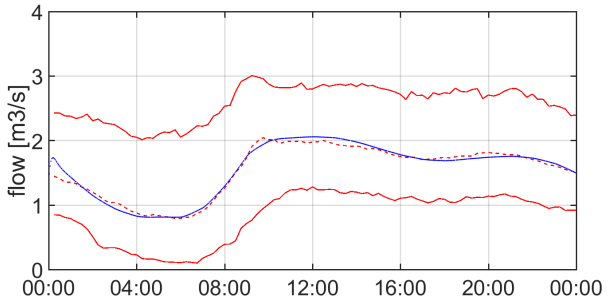


**Figure S2a.** Simulated (blue line) and measured (red line) flow at the outlet of System A for a typical dry weather day. Measured values are reported as 5%, 50% (dashed line), and 95% percentiles of flow data collected in dry weather.

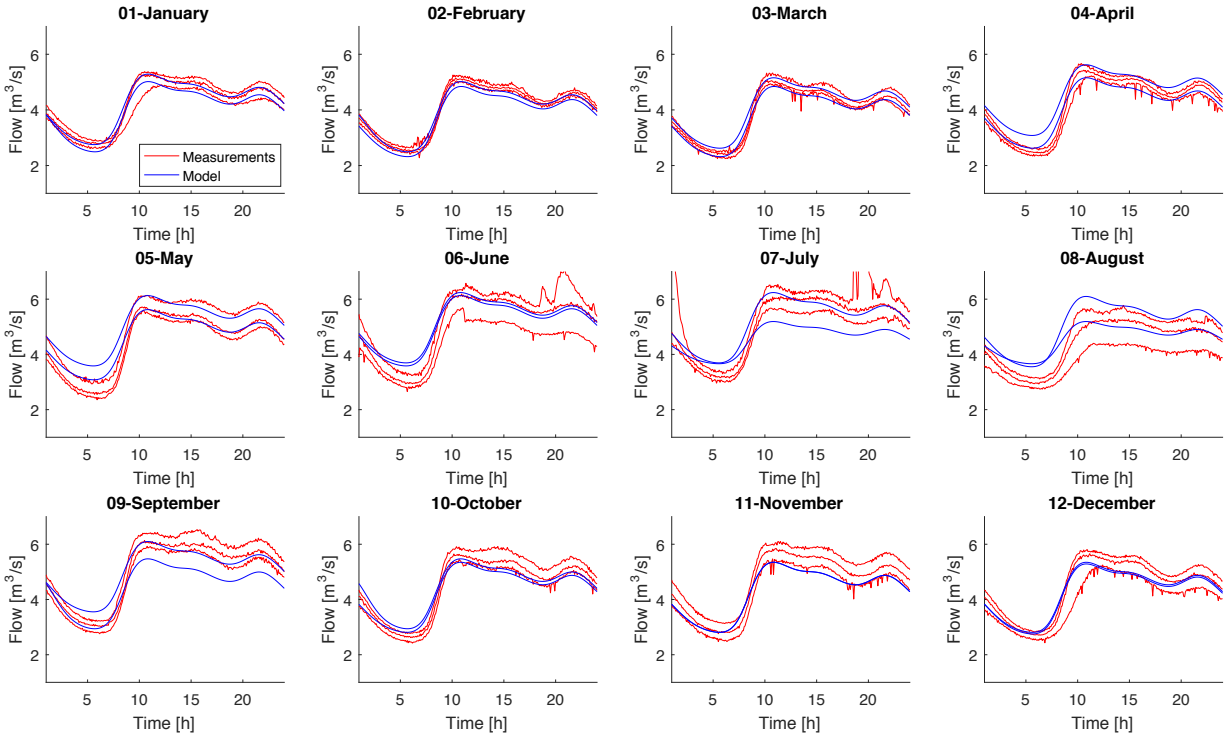


**Figure S2b.** Simulated daily dry weather flow at the first and last day of the simulated month (blue lines) in System B. Values are shown on a monthly basis to account for seasonal variations of groundwater infiltration. Measured values (red line) are reported as 5%, 50%, and 95% percentiles of data collected in dry weather.

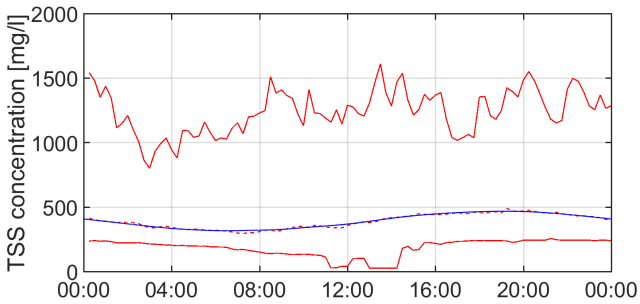


**Figure S3a.** Observed (red line) and simulated (blue line) TSS concentration at the outlet of System A for a typical dry weather day. Measured values are reported as 5%, 50% (dashed line), and 95% percentiles of the measurements collected by Alferes et al. (2014) in dry weather.

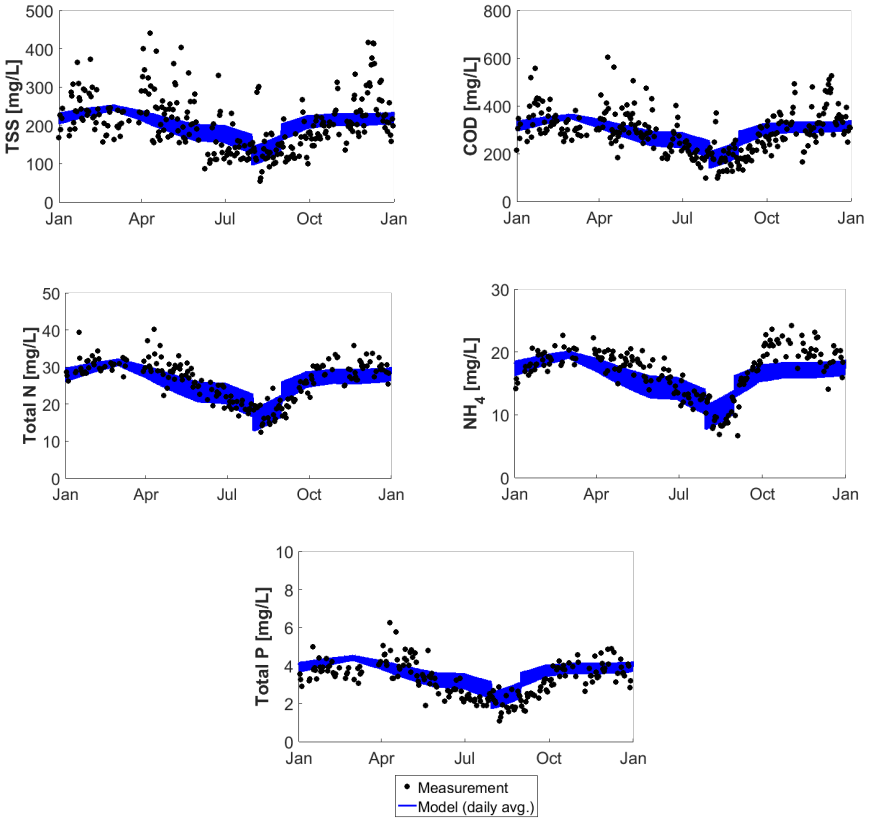


**Figure S3b.** System B: Observed (dots) and simulated (blue line) concentrations of conventional pollutants at the WWTP inlet. The modelled daily variations appear as bounds when a yearly scale is used.

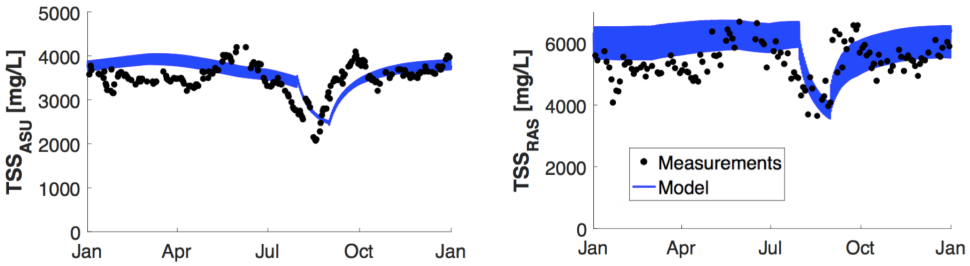


**Figure S4.** System B: Observed (dots) and simulated (blue line) concentrations of conventional pollutants in the aerated zone and RAS flow of the WWTP. The modelled daily variations appear as bounds when a yearly scale is used.

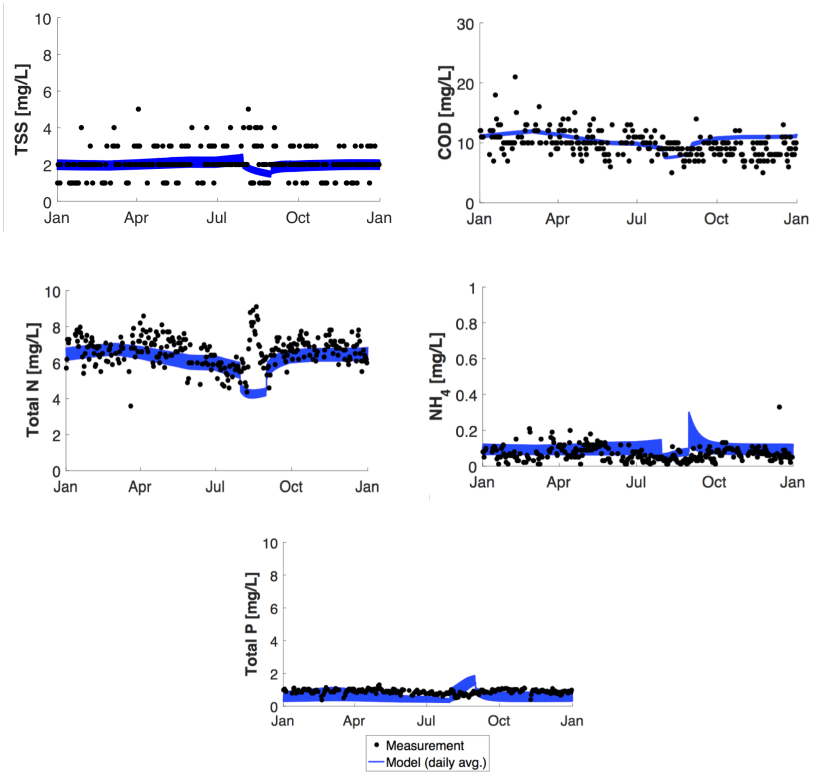


**Figure S5.** System B: Observed (dots) and simulated (blue line) concentrations of conventional pollutants at the outlet of the WWTP. The modelled daily variations appear as bounds when a yearly scale is used.

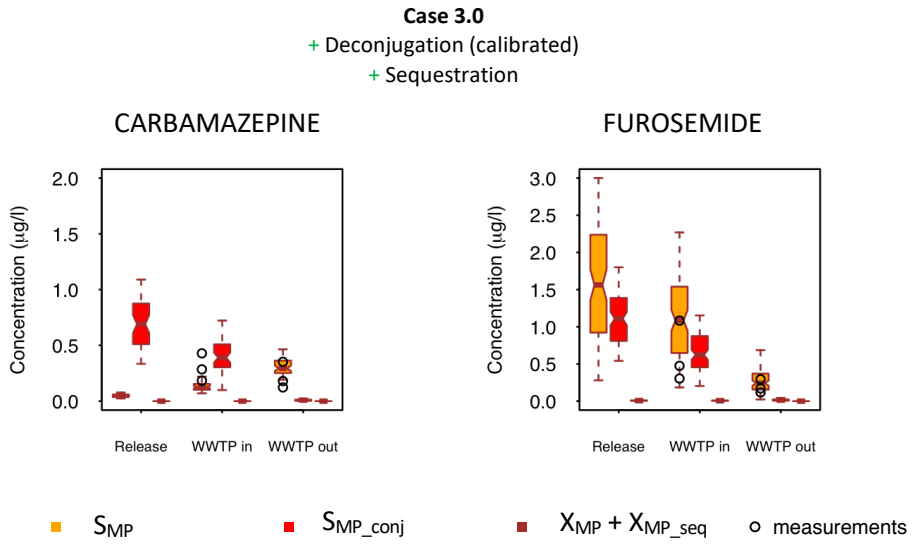


**Figure S6.** Model predictions (calibrated deconjugation) and measurements.

# Chapter 5

# Predicting pharmaceutical concentrations during combined sewer overflows using a census data driven model

**Abstract:** A new modelling framework was developed to predict more realistic concentration dynamics of pharmaceutically active compounds (PhACs) during combined sewer overflows (CSOs). The framework aims at (i) evaluating the impact of CSOs on surface water streams and (ii) identifying optimal sampling strategies (i.e. type of composite, frequency and duration) to sample CSO concentration as much representative as possible. Specifically, the framework uses census data (e.g. number of people per household, age and sex) and georeferenced data (e.g. house location) as proxy variables of unknown/confidential information (e.g., location of the person taking a certain drug, prescribed posology) to generate daily dynamic of PhACs loads as input to a mechanistic stormwater model. Model predictions for diclofenac (a highly consumed PhAC) were verified with 24 composite samples (sampling frequency dt=5 min, pooled to 20-minute composite samples) collected during a rain event in the combined sewer system of a small urban catchment in Switzerland. The framework was then used to predict diclofenac concentrations at CSO location during different rain events. Results highlighted that diclofenac concentrations can exceed the quality standard (i.e. the chronic standard was used since the acute standard is not available yet) in the sewage flow discharging to the receiving creek, posing a possible risk for the environment. Simulations also showed that flow-proportional mode with a high sampling frequency (2-5 minutes) is the most appropriate way to capture most of the diclofenac load discharged into the creek.

**Keywords:** pollutant load; river quality; sampling strategies; combined sewer overflow; census data; ecological risk assessment

The research work presented in this chapter was carried out during a research stay period of 6 months at the Swiss Federal Institute of Aquatic Science and Technology (Eawag), under the supervision of Dr. Christoph Ort and Dr. Frank Blumensaat.

This chapter, once integrated with further simulations, will be prepared for submission to a peer-review international journal.

## 1. Introduction

As a result of combined sewer overflows (CSOs), contaminants of emerging concern are frequently discharged in surface water bodies after rain events (Launay et al., 2016). Among all types of contaminants, many pharmaceutically active compounds (PhACs) are usually/always detected in municipal raw wastewater samples due to the high and continuous consumption from sick people and the elderly. Although PhAC concentrations in CSOs are expected to be diluted by surface runoff, in some cases PhAC concentrations were higher than concentrations in treated wastewater (Buser et al., 1999; Phillips et al., 2012). Thus PhAC concentrations in CSOs may exceed environmental quality standards in receiving water bodies, inducing detrimental effects on aquatic species (Bottoni et al., 2010). Assessing compliance with acute standards would require monitoring at high-temporal resolution to capture the expected short-term fluctuations (Ort et al., 2010a), making sampling economically not feasible on a regular basis for thousands of CSO sites in a country.

Therefore, models may be used to indicate where and what kind of fluctuations we would expect to prioritize locations, optimise sampling campaigns and perform risk assessments. However, the prediction of realistic exposure scenarios at high temporal resolution is highly challenging. In a recent work (Coutu et al., 2016), a stochastic model succeeded in predicting dry weather concentration dynamics of the antibiotic ciprofloxacin, on an hourly time scale in the sewer. Specifically, an ingestion-excretion model, based on retrievable model input-parameters (e.g. national sales data, pharmacokinetics parameters, etc.), provided dynamic inputs to a simplified sewer model, in which transport-degradation phenomena were simulated by a travel time density function (i.e. lump model). However, model predictions failed under wet-weather conditions. Possible reasons mentioned by the authors included the high uncertainties associated with monitoring data and the simplistic representation of the sewer network. We suppose that other possible reasons might be the lack of unknown and/or confidential information (e.g.: location of the person taking a certain drug, prescribed posology, that is the exact dose and number of times a certain drug is taken, etc.), which would provide valuable inputs for the model.

Nowadays, other types of information such as household location, age and sex of the population, are generally made available with different levels of aggregation (e.g., national, district, canton, neighbourhood, etc.,) in census database and may be a valuable alternative to the above-mentioned types of model inputs. In fact, prescribed posology is generally age-dependent (e.g. children usually take smaller doses than adults) and, the older the population of a certain area the higher the probability of having consumption of specific PhACs. Besides, the gender can indicate what type of PhACs are more likely to be consumed in the area. Consequently, national sales data can be weighted by local population age and sex to derive more precise information. In addition, locations of households can be used as proxy variable of point sources.

Moreover, distributed dynamic models can offer a very detailed representation of water transport phenomena, both in time and spatial dimension, diminishing uncertainties associated to in-sewer water transport predictions. However, these models require detail sewer information (e.g. pipe position and diameters, slopes, etc), and generally need high computational demand.

In this work we combine additional types of data (i.e. census data, geospatial house location) with a detailed hydrodynamic model to: i) setup and validate a census data driven model to realistically simulate PhAC concentrations (e.g. diclofenac, a well-known non-steriodal anti-inflammatory drugs) in CSOs, ii) assess the environmental impact of PhACs on river water quality during different rain events, and iii) verify optimal sampling strategies to collect samples with high representativeness.

## 2. Materials and methods

### 2.1. The modelling framework – the theory

#### *2.1.1. Wastewater and PhAC generator*

Every house was modelled as a point source consisting of a defined number of people (healthy and sick), of a defined age and sex, who discharge wastewater flow and PhAC loads to the closest sewer manhole. Wastewater flow was calculated for each house as the product of the number of people and an average daily drinking water consumption in this area. Flow dynamics was generated accordingly to the drinking water demand defined in the work of Candelieri and Archetti (2014). For each sick person, the daily ingested mass of a specific PhAC was assumed equal to the average maintenance dose used for main therapeutic indication in adults, also known as defined daily dose (DDD [mg $inhab^{-1}d^{-1}$]). This value was halved if the sick person was a child (i.e. age < 16). Excreted mass was than obtained by multiplying DDD by excretion rate *f* (-). Daily dynamic was generated by Sewage Pattern Generator (SPG, 2013) (Ort et al., 2005). Specifically, SPG generates a number of mass pulses [mg $s^{-1}$] accordingly to a non-homogeneous Poisson distribution, following *a priori* daily pattern profile. The Poisson parameter (i.e. process rate $\lambda$), which indicates the average number of pulses expected over the simulated period (i.e. 24 h), was calculated for every time step (i.e. 2 min) by weighting the expected number of daily pulses per person with respect to the daily pattern profile. In detail, a specific daily pattern profile was used depending on the typical intake profile of the simulated PhAC (e.g. antibiotics are generally administrated twice a day after eating). If no specific intake profile is available (e.g. nonsteroidal anti-inflammatory drugs are taken when an inflammatory disorder occurs), the number of mass pulses are generated accordingly to an ordinary (i.e. homogeneous) Poisson distribution. The expected number of daily pulses per person was set to 5, that is the average number of daily toilet flush per person as in Aymerich et al. (2017).
Effective mass pulses were then obtained from the generated ones depending on the PhAC elimination half-life in the human body. We assumed that, for PhACs with elimination half-life > 6 hours, all the generated pulses are representative of a realistic situation since the PhAC is generally found in the urine for the whole day; while for PhACs with an elimination half-life < 6 h, the whole PhAC mass is generally found within the first two times a sick person urinates, in this case we considered only the first two mass pulses.

#### *2.1.2 The Georeference generator*

Houses location was georeferenced accordingly to the spatial location of the sewer system structure. The Dijkstra's algorithm (Cormen et al., 2001) was then used to identify the closest

manhole to each house (detail in Figure 1). The number of people per house was sampled accordingly to a discrete distribution of 6 classes, which indicates the frequency of having a certain number of people per household unit (i.e. 1, 2, 3, 4, 5, and > 6). In this work, we assumed each house as consisted of a single household unit since most of the houses in the area are single family house. Age was assigned to each person following the same principle (i.e. three classes of 0-18, 19-60 and > 60), making sure that unrealistic situations (e.g. house of two people belonging to the class 0 -18) was not considered. Sex was than assigned to each people accordingly to a discrete Bernoulli distribution where the distribution parameter p was set accordingly to the frequency of having a male or female in the population area. Lastly, locations of a number of sick people were randomly selected.

### *2.1.3. Sewer model*

In-sewer water transport phenomena were simulated by full dynamic wave flow routing methods available in PySWMM, a newly developed Python language software that speeded up the simulation time if compared to the classical EPA Storm Water Management Model SWMM (EPA, 2018). First-order kinetic processes were also included to simulate PhACs biodegradation during in-sewer transit.

## 2.2. Case study

A small urban catchment (Figure 1) in Switzerland (about 400 inhabitants), for which a calibrated hydrodynamic sewer model was available, was selected for testing the framework. In the area, the sewer system combines wastewater and storm water and has a CSO that discharges into a receiving water system when the system capacity is overloaded during intense rain events. Three rain events were chosen for testing the framework: event 1, which was selected for model validation with respect to the available in-sewer measurements of flow and diclofenac concentration; events 2 and 3 which were used to predict flow and diclofenac concentration at the sewer overflow structure to perform the environmental risk assessment and optimisation of the sampling strategies (see paragraph 2.4).

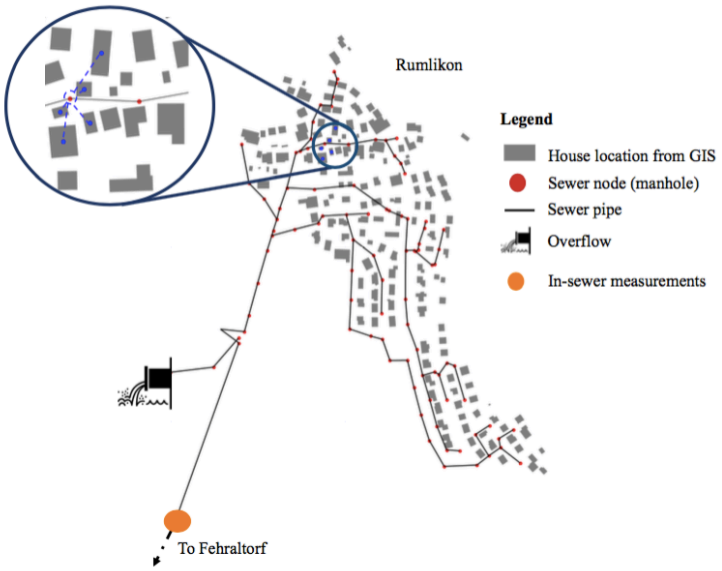


**Figure 1.** Georeferenced information about the Rumlikon neighbourhood in Switzerland. The detail shows an example of identification of the closest manhole (red dot) to each house.

## 2.3. Data collection

Census data (number of people per household, age and sex of the population) at different aggregation levels were retrieved from the Swiss Federal Statistical online database (STAT-TAB); local drug consumption data (number of people taking a certain drug) were collected from a public health report prepared by Helsana (Schneider *et al.*, 2018). Drug-specific information for diclofenac (e.g., DDD, excretion rate) was retrieved from the WHO Collaborating Centre for Drug Statistics Methodology (WHO, 2009) and literature data (Lienert et al., 2007; Zhang et al., 2008). No specific intake profile was used due to randomly usage of diclofenac during the day from sick people. Local drinking water consumption data were provided by the local utility. In the combined sewer system, 24 composite samples (sampling frequency dt=5 min, pooled to 20-minute composite samples) was collected as described in Mutzner et al. (2019). Precipitation data for the rain events were available from a nearby rain gauge and house locations were obtained from the open street map. Diclofenac environmental quality standard (equals to 0.05 µg $l^{-1}$, chronical, no acute available) was obtained from the proposal for acute and chronic quality standard issued by the Ecotox Centre (Switzerland) (Oekotoxzentrum, 2019).

## 2.4. Work objectives

The modelling framework was used with a three-fold objective:

i. Plausibility check: predicted diclofenac concentrations and flow were compared with real measurements in the sewer system during a short rain event (event 1) to verify model prediction capability.

ii. Environmental risk assessment: the ratio ($= \frac{C_{t_i}}{QS}$) was calculated for two rain events (event 2 and 3), where $C_{t_i}$ is the predicted diclofenac concentration at the CSO structure at the $i^{th}$ time step and $QS$ is the acute and/or chronic quality standard for aquatic systems; particularly, the ratio indicates the dilution required by the receiving water system to comply with the standard. Specifically, a ratio < 1 indicates that no dilution is needed while, a ratio > 1, for example equals to 2, indicates that the receiving water system should have a water flow at least as much as the discharged CSO to comply with the standard. If the receiving water system has a null or negligible flow, the ratio indicates directly the magnitude of the exceedance.

iii. Optimisation of composite sampling strategy (i.e. type of composite, frequency and duration) to collect samples as much representative of the CSO concentration as possible: different sampling strategies were tested (Table 1) during event 2 and 3 and derived concentrations compared with the "true" expected concentration, that is the average concentration calculated with the highest time step resolution (i.e. 2 min) as in Ort et al. (2010b). Relative sampling error ( $= \frac{\overline{C}_{true} - \overline{C}_{sample}}{\overline{C}_{true}}$) was then used as indicator to evaluate the error between different strategies.

Model simulations were repeated for 1,000 runs, leading to the distributions of predicted concentrations, environmental risk ratio and sampling error.

**Table 1.** Tested sampling strategies.

| Sampling strategy | Sampling mode | Composite duration [min] | Sampling frequency [min] |
|---|---|---|---|
| 1 | Flow-prop. | 20 | 15[a], 5, 2 |
| 2 | Flow-prop. | 10 | 8[a], 5, 2 |
| 3 | Volume-prop. | 20 | - |
| 4 | Volume-prop. | 10 | - |
| 5 | Time-prop. | 20 | 15[a], 5, 2 |
| 6 | Time-prop. | 10 | 8[a], 5, 2 |

[a] representative of a grab sampling mode

## 3. Preliminary results and discussion

### 3.1. Plausibility check

The calibrated hydrodynamic model was able to follow wastewater flow dynamics during the plausibility check phase (Figure 1, event 1), showing a satisfactory prediction capability. Specifically, the model reproduced well the flow dynamics under dry weather conditions (from 18:00 to 22:00 and from 02:00) and wet weather conditions (from 22:00 to 02:00). However, predicted flow peak slightly overestimated the measurements at midnight. As for diclofenac predicted concentrations, measurements fell within the confidence interval (99 %), showing a good agreement. During the flow peak caused by stormwater, predicted concentrations decreased, on average, by a factor 4 with respect to the dry weather conditions. The same dynamic was observed by the measurements, confirming the findings of Launay et al., 2019, who highlighted that diclofenac concentrations are generally diluted during rain events.

### 3.2. Environmental risk assessment

At the CSO structure, diclofenac concentrations were predicted during two short rain events (Figure 2, event 2 and 3). The ratio between the predicted concentration and the environmental quality standard was calculated to identify situations where river dilution would be required not to cause an ecological impact. Event 2 did not generate any risk, showing a ratio always below the threshold of 1. On the contrary, the second one would require to be diluted by the receiving water system to comply with the standard, although for a very short time. However, specific control actions (e.g. flow deviation to a storage tank) should be implemented to reduce peak concentrations.

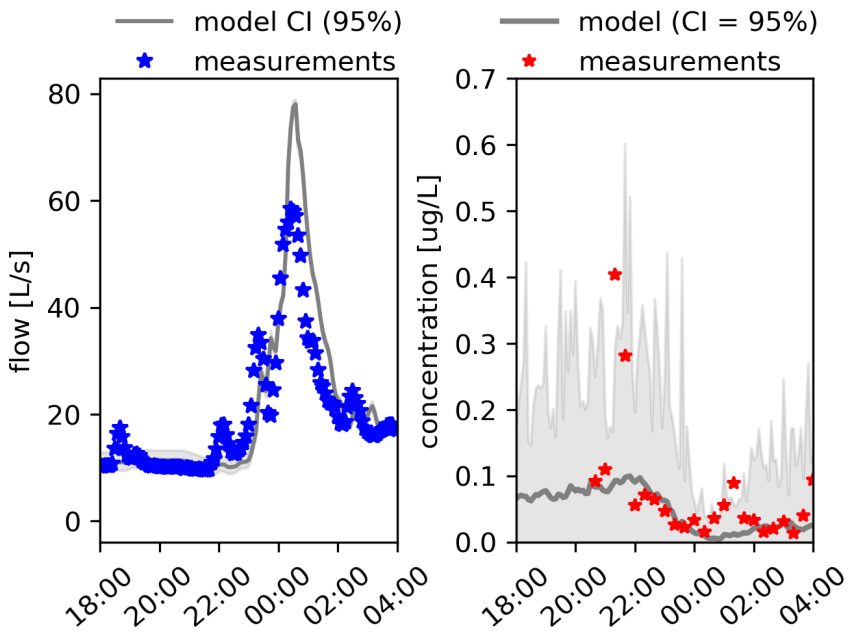


**Figure 1**. Measured and predicted flow (a) and diclofenac concentration (b) during rain event 1 (plausibility check).

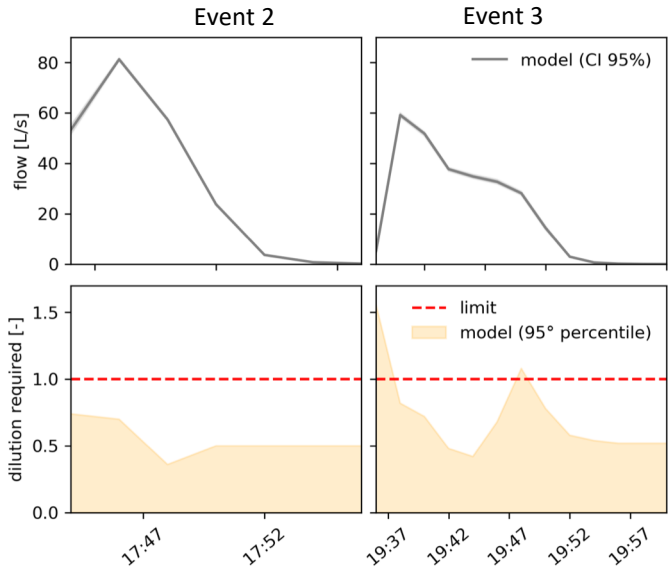


**Figure 2**. Predicted flow and diclofenac concentration (95° percentile) during events 2 and 3 at the CSO structure and ratio of predicted concentration and chronic quality standard. As for this ratio, the red dash line indicates the threshold above which dilution of the receiving water system is needed to comply with the standard.

### 3.3. Optimization of the sampling strategy

Distribution of the relative error between different sampling strategies is shown by box-plots (Figure 3). Looking at the results, very high sampling errors were obtained with the lowest sampling frequency (i.e. 15 and 8 min) independently from the composite duration (20 and 10 min, respectively) and sampling mode. This result was expected since only 1 sample was

collected during the simulated events, providing a water sample that is as much representative as a grab sample, which is the less recommended one. On the contrary, a sampling frequency of 2 minutes led to a negligible error using both the volume- and flow-proportional mode, independently from the composite duration. However, very high errors were obtained for the time-proportional mode, regardless the sampling frequency and composite duration. Probably due to the strong (negative) correlation of flow and concentration profiles.

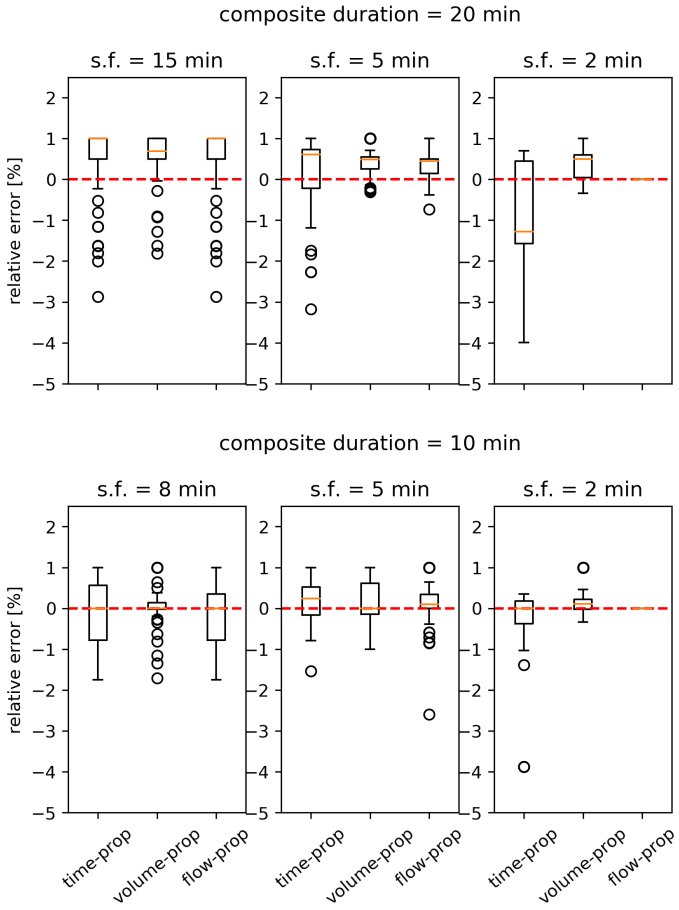


**Figure 3**. Box-plots representing the relative sampling error distribution using different sampling strategies; open circles represent values that were automatically identified by the software package as outliers. From an experimental point of view, outliers generally indicate possible erroneous values; however, in this case all the values were obtained through simulations and simply represent particular combinations of model input-parameters that led to relative errors significantly different from the others. The red dash line indicates the referenced relative error of zero.

## 3.4. Preliminary conclusions and future developments

With this study we proposed a new modelling framework to simulate realistic diclofenac dynamics concentrations during CSOs, combining census and geo-referenced data with a storm water model. The framework makes the best use of accessible input data and try to minimize the need of data collection for calibration (except for validation). Results showed that chronic

quality standard can be exceed for diclofenac and that flow-proportional mode with high sampling frequency (2-5 minutes) is the most appropriate way to capture most of the diclofenac load discharged into the water stream.
Future developments include:

- simulate multiple overflow events of various intensity to assess the indicators, i.e. predicted CSO concentration, the environmental risk and sampling error, in a more robust and reliable manner;
- investigate how other relevant PhACs, such as paracetamol, estrogen, carbamazepine, with different posology and gender usage affect the indicators;
- identification of effective control actions (e.g. storage tank) to limit the risk;
- expanding the spatial scope of the modelled system including the wastewater treatment plant where high-frequency PhACs measurements are available for model validation under both dry- and wet-weather periods.

# Chapter 6

# Risk assessment of contaminants of emerging concern in the context of wastewater reuse for irrigation: An integrated modelling approach

**Abstract:** Direct reuse of reclaimed wastewater (RWW) in agriculture has recently received increasing attention as a possible solution to water scarcity. The presence of contaminants of emerging concern (CECs) in RWW can be critical, as these chemicals can be uptaken in irrigated crops and eventually ingested during food consumption.
In the present study, an integrated model was developed to predict the fate of CECs in water reuse systems where RWW is used for edible crops irrigation. The model was applied to a case study where RWW (originating from a municipal wastewater treatment plant) is discharged into a water channel, with subsequent irrigation of silage maize, rice, wheat and ryegrass. Environmental and human health risks were assessed for 13 CECs, selected based on their chemical and hazard characteristics. Predicted CEC concentrations in the channel showed good agreement with available measurements, indicating potential ecotoxicity of some CECs (estrogens and biocides) due to their limited attenuation. Plant uptake predictions were in good agreement with existing literature data, indicating higher uptake in leaves and roots than fruits. Notably, high uncertainties were shown for weakly acidic CECs, possibly due to degradation in soil and pH variations inside plants. The human health risk due to the ingestion of wheat and rice was assessed using the threshold of toxicological concern and the hazard quotient. Both approaches predicted negligible risk for most CECs, while sulfamethoxazole and 17α-ethinylestradiol exhibited the highest risk for consumers. Alternative scenarios were evaluated to identify possible risk minimization strategies (e.g., adoption of a more efficient irrigation system).

**Keywords:** dietary intake; micropollutants; model-based risk assessment; plant uptake.

The research work presented in this chapter was carried out during a research stay period of 8 months at the Technical University of Denmark (Denmark). The research work was carried out with the valuable support of Prof. Luca Vezzaro (Technical University of Denmark), Prof. Stefan Trapp (Technical University of Denmark), Dr. Fabio Polesel (DHI A/S) and the help of MSc student Marco Gabrielli (Polietcnico di Milano).

This chapter has been published in the journal “Chemosphere[2]”

[2] Delli Compagni, R., Gabrielli, M., Polesel, F., Turolla, A., Trapp, S., Vezzaro, L., Antonelli, M., 2020. Risk assessment of contaminants of emerging concern in the context of wastewater reuse for irrigation: An integrated modelling approach. Chemosphere 242. https://doi.org/10.1016/j.chemosphere.2019.125185

# 1. Introduction

Water scarcity induces monetary and job losses throughout all continents (Asano, 2002; Ding et al., 2011) and the situation is expected to worsen due to population growth, increase of water use per capita, climate change and other stress factors (IPCC, 2014; Gosling and Arnell, 2016). Following circular economy principles, the reuse of reclaimed wastewater (RWW) originating from urban wastewater treatment plants (WWTPs) is identified as one of the main measures to alleviate fresh water depletion (COM/2015/614). This can be a valid alternative to water supply for agricultural irrigation, the largest source of freshwater consumption worldwide (COM/2015/614). This approach has recently been promoted by the European Union, which also proposed minimum requirements for a safe reuse (COM/2018/337). This document acknowledges the need of assessing the risk (where relevant) associated to contaminants of emerging concern (CECs), whose threat for environment and human health is well recognized (Daughton and Ternes, 1999; Monteiro and Boxall, 2010).

Existing WWTPs are typically not designed for removal of CECs (e.g. pharmaceuticals, estrogens, biocides), which are generally released from households into sewer systems (Luo et al., 2014; Castiglioni et al., 2018). Hence, some CECs persist in RWW and can reach agricultural fields through irrigation, leading to accumulation in soil (Durán-Alvarez et al., 2009; Gibson et al., 2010) and contamination of groundwater (Siemens et al., 2008; Lesser et al., 2018). Irrigated crops can also accumulate CECs in roots (Miller et al., 2016) and translocate them towards edible plant organs such as leaves and fruits (Goldstein et al., 2014; Christou et al., 2017). Consequently, potential exposure of humans and organisms living in environmental recipients to CECs requires a careful assessment, and adverse effects can be quantified based on the estimated exposure concentrations (Piña et al., 2018). Besides being discontinuous in time and subject to uncertainty (due to e.g. analytics), empirical measurements of environmental CEC levels are site-specific and do not allow extrapolating contamination levels to other RWW reuse systems. In this case, modeling tools can contribute with valuable complementary information (e.g. filling temporal gaps between measurements), and account for the influence of site-specific conditions. The use of complex modelling tools, especially for integrated systems, can be challenged by parameter identifiability (Voinov and Shugart, 2013; Bach et al., 2014) and limited input data availability. These sources of uncertainty can be addressed by using statistical analysis methods (e.g., sensitivity and uncertainty analysis), allowing the identification of important model factors and the quantification of results uncertainty. So far, integrated models have shown the ability of evaluating the impacts of discharges from storm- and wastewater system on the chemical status of surface water (De Keyser et al., 2010). However, a dynamic chemical fate model capable of estimating CEC concentrations (and thereby risk) in different environmental compartments (surface water, soil, crops) under different water management and reuse scenarios is currently in high need.

The objective of this work was to develop a flexible integrated model to predict CEC fate in different types of RWW reuse systems, irrespective of size and complexity, and to assess environmental and human health risks. The model was: (i) applied to a real RWW reuse scenario, comprising a discharge channel and cultivation of four different types of crops (silage maize, rice, wheat and ryegrass); (ii) verified with site-specific measurements, where available, and literature data in different compartments; (iii) used to estimate the environmental risk

associated to CEC occurrence in surface water, and human health risk following the ingestion of irrigated crops; (iv) used to evaluate alternative risk management and minimization scenarios, which were compared to the present situation and to a worst-case scenario (characterized by the absence of a WWTP).

## 2. Materials and methods

### 2.1. Fate model development and evaluation

A generic RWW reuse system was considered to include a surface water body, receiving RWW discharges, and cultivated fields with irrigation. The river water quality model extended with CEC fate processes (from the IUWS_MP library) (Vezzaro et al., 2014) and the coupled soil-plant model (CSPM) (Trapp and Matthies, 1998; Trapp, 2017) were identified as the state-of-the-art models (section 2.1.1) to describe CECs fate in the generic system. These models were extended (section 2.1.2) to increase their applicability and coupled (section 2.1.3). A sensitivity analysis (section 2.1.4) was also performed to identify the most significant parameters in the developed model.

#### *2.1.1. State of the art models*

The IUWS_MP library (Vezzaro et al., 2014) utilizes a conceptual approach to simulate river water quality, where water transport is simulated by a series of continuously stirred tanks reactors (CSTRs). Each CSTR consists of two compartments (bulk water and sediments), in which fate processes (abiotic and biotic degradation, sorption to suspended solids and colloids) occur.
The CSPM includes (i) a tipping bucket model to describe the movement of water and dissolved CECs through soil and (ii) a numerical four-compartment model to simulate CEC uptake and translocation through xylem and phloem flows, in roots, stem, leaves and fruits. Partitioning between plant tissues and soil, and xylem and phloem flows is described through a detailed intracellular model (Trapp, 2004; Trapp and Horobin, 2005; Trapp, 2009; Trapp 2017).

#### *2.1.2. Model extensions*

Many CECs are ionized at environmental pH, which affects their partitioning behavior (Franco et al., 2010). Hence, the equations described in Franco and Trapp (2008) were included in the IUWS_MP library to describe sorption of ionized monovalent acidic and basic compounds.
In the CSPM, phloem flow was introduced to improve the dynamics of the internal plant circulation, through which weakly acidic CECs translocate from leaves through stem to fruits and roots (Gonzalez-Garcia et al., 2019; Kleier & Hsu, 1996).
Model structures were further modified to accommodate for temporal and spatial dynamics of environmental conditions (e.g., air, soil and water temperature, water and soil pH, sunlight intensity, etc.), which can substantially affect CEC fate (Kunkel and Radke, 2011; Matamoros and Rodriguez, 2017). Moreover, the CSPM was also modified to simulate complex types of irrigational systems, in which water can partially submerge the cultivations (e.g. rice).

Particularly, the field capacity of the first soil layer was adjusted to simulate the saturation effect introduced by a standing water layer. The reader is referred to the Supplementary Material (SM) for a detailed description of the extensions of the IUWS_MP library and of CSPM model.

### *2.1.3. Model coupling and software selection*

Predicted CEC concentrations were obtained twice a day (noon and midnight) from the river model (implemented in WEST 2014®, DHI A/S, Denmark) to consider high and low peaks, and input to the CSPM (implemented in Microsoft Excel), which provided daily outputs.

### *2.1.4. Identification of influential parameters*

A sensitivity analysis (SA) was performed to identify: (i) the most influential model parameters for concentration predictions and (ii) non-sensitive model parameters uncertainties, which could be fixed to a default value without affecting model predictions uncertainties. As for the river model, a one-at-a-time (OAT) approach (Frey and Patil, 2002) was performed by varying each parameter ±5% from its default value. A total of 52 parameters were investigated. The variation in predicted concentrations was calculated as reported in Equation 1:

$$Deviation = \frac{1}{n}\sum_{i}^{n}\frac{y_i^{p,max} - y_i^{p,min}}{y_i^{p,default}} \qquad \text{(Eq. 1)}$$

where $y_i^{p,max}$, $y_i^{p,min}$, $y_i^{p,default}$ are the predicted concentrations obtained with the maximum, minimum and default values of the parameter $p$ for $i^{th}$ time step; $n$ is the number of time steps in the simulation. Three CECs (i.e. diclofenac, triclosan and carbamazepine, see section 2.2.1) and four conventional pollutants (ammonia, nitrite, nitrate and phosphorus) were chosen as benchmark for different physicochemical properties.
As for the SA of CSPM, partial rank correlation coefficients (PRCCs) (Saltelli et al., 1993) were calculated through the software Crystal Ball 11.1.2 (Oracle®). First, 1000 runs were conducted by varying separately plant and soil parameters. The parameters presenting |PRCCs| above 0.1 were selected and included into a second SA of 10000 runs. This time, parameters with |PRCCs| exceeding $\sqrt{1/n}$ (with $n$ being the number of parameters varied in each simulation) were identified as relevant. The validity of the PRCCs was checked through the $R^2$ between the two sets of ranks (Sin et al., 2011). The second SA was carried out both with and without degradation in soil to better highlight its sensitivity on model variations.

## 2.2. Model testing

The developed model was tested on an existing Italian case study, where RWW from a municipal WWTP (flow = 3.5 $m^3\ s^{-1}$) is the only source providing water through a surface water channel to subsequently irrigate crop fields. The channel extends for about 12 km and provides irrigation water for 90 farms with more than 40 $km^2$ of crop fields (Pizza, 2014). Cultivated

crops include winter wheat and rice, which are sold for human food consumption; and silage maize and ryegrass that are used for animal feed production. Irrigation systems included surface irrigation, the dominant form of irrigation in southern European countries (Masseroni et al., 2017) for all the crops but rice, which is grown in paddies. In the area, crop rotation is a standard procedure and is performed each season.

### *2.2.1. Chemicals*

Thirteen CECs of different classes of use were assessed: clarithromycin (CLA), sulfamethoxazole (SMX), diclofenac (DCF), ibuprofen (IBU), paracetamol (PAR), carbamazepine (CBZ), furosemide (FUR), 17-α ethinylestradiol (EE2), 17-β estradiol (E2), estrone (E1), perfluorooctanoic acid (PFOA), perfluorooctane sulfonate (PFOS) and triclosan (TCS). These CECs were selected from an initial group of 80 CECs, for which measurements were available at the outlet of the WWTP (Castiglioni et al., 2018a, 2018b). Specifically, two criteria were used: i) selected CECs had to cover a broad range of physicochemical properties in terms of: normalized organic carbon partitioning coefficients ($K_{oc}$) and ionization state at environmental pH; ii) selected CECs had to belong to different CEC classes (e.g. antibiotics, hormones, etc.) and to possibly exceed the predicted no-effect concentration (PNEC). Physicochemical properties (Table S2) and degradation rates (Tables S3-S15) of the selected CECs were collected from literature (see SM for sources) and/or retrieved from QSAR software (Advanced Chemistry Development Inc., 2015; National Food Institute, Technical University of Denmark, 2018).

### *2.2.2. System conceptualization*

The RWW reuse system was conceptualized as shown in Figure 1. The channel was described by the river modules from the IUWS_MP library, resulting in 11 in-series CSTRs, each one approximately 500 m long. This length was selected in agreement with Benedetti et al. (2004) as a compromise between the need of simulating temporal dynamics in a realistic way and the required computational effort. Within the channel, nine equidistant locations were selected, each having irrigation water withdrawal that was proportional to the required water demand to harvest the closest crops. The water demand ($m^3\ d^{-1}$) was defined as the product of the water consumption to harvest one unit of land and total land extension (Brouwer et al., 1992). Crop types and corresponding extensions were derived from georeferenced maps of the area (www.geoportale.regione.lombardia.it) and elaborated with QGIS 2.18. Periods of water withdrawal and crop rotation were simulated according to the irrigation calendars (Figure 1b) based on agronomic information of the area (Nelli and Sodi, 2007; Provincia di Milano, 2007; Borrelli et al., 2014; Moretti et al., 2015). Two water withdrawal scenarios were considered: (i) scenario *MR*, where silage maize and ryegrass were grown at the same time of rice and ryegrass and, (ii) scenario *MW*, where silage maize and ryegrass were grown at the same time of winter wheat. Moreover, different irrigation systems were simulated depending on crop types: (i) a monthly irrigation water pulse for silage maize, ryegrass and winter wheat and, (ii) a continuous irrigation for rice. Three types of soils were found predominantly in the study area, with more than one crop per type of soil (see Table S18). For this reason, crop simulations were

repeated for different soils. The simulated soil structure was also adapted to match the identified stratigraphy for a soil depth of 1 m, splitting (if needed) the widest horizons over two layers.

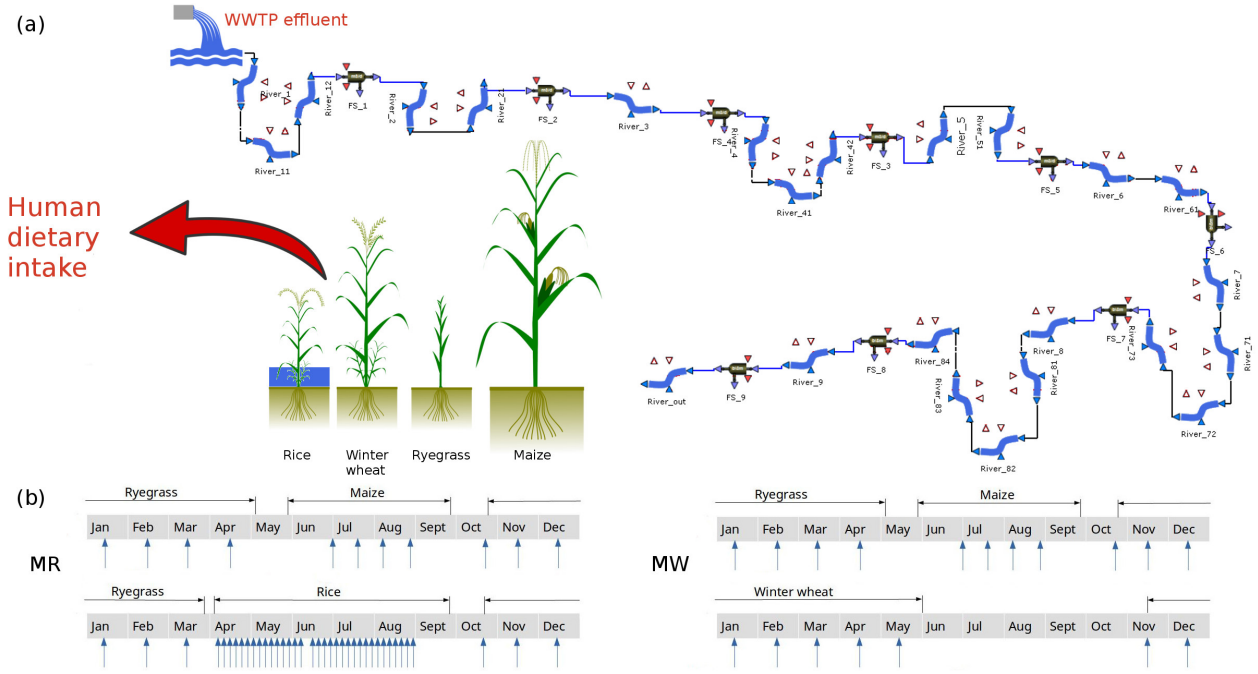


**Figure 1**. Outline of the wastewater reuse system (a) and irrigation calendars (b) for the two crop rotation scenarios.

### *2.2.3. Model input and parameters*

Concentrations of conventional pollutants in RWW (i.e. ammonia, nitrite, nitrate and phosphorus) represented a 24-hour time-proportional composite sample and were retrieved from the laboratory measurements conducted by WWTP staff. CEC concentrations in RWW were obtained from previous measurements at the outlet of the WWTP (Castiglioni et al., 2018a, 2018b) and assumed constant over the year. Such assumption can be held valid for CECs (e.g., DCF and CBZ) that show low to no seasonal fluctuations in usage (Sui et al., 2011). For antibiotics such as CLA, for which seasonal fluctuations were observed (McArdell et al., 2003), measurements may reflect a worst-case scenario as campaigns were conducted during winter time. Environmental conditions (Tables S16-17) were directly obtained from public databases or indirectly estimated (e.g., potential evaporation, soil temperature, bulk density and water retention properties). Crop-specific data (Table S19) were collected from literature preferring, where available, local sources. Soil initial conditions (CECs concentrations and water content) were assumed equal to the pseudo-steady state reached using the median CECs. For more details, the reader is referred to SM.

### *2.2.4. Uncertainty propagation*

The uncertainty associated to CEC concentrations in RWW and transformation rates (e.g., aerobic degradation in water, photodegradation and aerobic/anoxic degradation in sediments)

were propagated to the predicted concentration in the surface water channel through a Monte-Carlo based Uncertainty Analysis (UA). Uniform, triangular or empirical parameter distributions were chosen based on literature values (Tables S3-S15). For every CEC, 2000 runs were performed.
Resulting uncertainties in the predicted CEC concentrations along the river were then propagated, together with soil degradation rates and influential crop parameters, to CSPM predictions. Specifically, triangular distributions were considered for soil degradation rates and CEC concentrations. Crop parameters were considered as uniformly distributed with a variation of ±10% from literature data (Felle, 2001). Attention was paid to avoid parameter combinations that may lead to non-realistic scenarios (Steinwand et al., 2001). 2000 latin-hypercube Monte Carlo runs were performed for each CEC and soil type (Table S18). Physicochemical properties (Table S2) of perfluorinated compounds exhibited a high degree of uncertainty due to analytical limitations (Wang et al., 2011), and were thus included in UA. More details on UA are provided in SM.

## 2.3. Model objectives

The three main objectives of the developed integrated model were:
*I – Fate predictions and assessment of model performance:* long term simulations (≥ 1 year) were performed to assess CECs fate in surface water, irrigated crops and groundwater. Assessment of model performance was carried out by comparing model predictions with site-specific measurements, where available (as for DCF) and/or literature data. For the surface water channel, further verification was made by deriving first-order attenuation rates by fitting predicted median concentrations at different locations and comparing to experimental literature data. In this case, overall attenuation derives from the combination of different biotic and abiotic degradation processes.
As for the uptake in crops, the bioconcentration factor (BCF, $g_{dw}^{-1}$ $g^{-1}_{dw}$) was calculated as $C_{organ}/C_{soil}$, where $C_{organ}$ and $C_{soil}$ are the predicted dry weight concentrations in a given plant organ (root, stem, leaf, fruit) and in the first soil layer. There is currently limited consensus on calculation of BCFs since different approaches have been considered with respect to $C_{soil}$ values (Polesel et al., 2015). For this reason, both the simulated maximum and median soil concentrations were used for the BCF calculation, corresponding to $BCF_{max}$ and $BCF_{median}$, respectively. Calculated BCF was compared with literature (when not explicitly reported, empirical BCFs were derived from reported concentration data) except for CLA, which showed limited plant uptake (Limmer and Burken, 2014; Lamshoeft et al., 2018). Predicted leaching of CECs into groundwater was also compared with measurements from the nearby area.

*II – Ecological and human health risk assessment*: environmental risk assessment was carried out through the risk quotients (RQs) (Hernando et al., 2006; Kuzmanovic et al., 2013). RQs were calculated for each CEC as *PEC/PNEC*, where *PEC* is the predicted environmental concentration and *PNEC* the predicted no-effect concentration. *PNECs* were obtained from literature (Table S1) and *PEC*s were the predicted concentrations at the end of the surface water channel; specifically, maximum, median and minimum concentrations were predicted to obtain $RQ_{max}$, $RQ_{median}$ and $RQ_{min}$, respectively. Two alert thresholds of RQ above 0.1 and 1 were identified as

medium and high risk, respectively (Hernando et al., 2006). Monthly frequency of exceedance above the alert thresholds was calculated as additional risk indicator.
The human health risk associated to dietary intake was calculated with two different approaches: the threshold of toxicological concern (TTC) (Kroes et al., 2004; Malchi et al., 2014) and the hazard quotient (HQ) (Prosser et al., 2014b; Prosser and Sbiley, 2015). TTC values were obtained through the Cramer classes decision tree implemented in the Toxtree v3.1 software (Patlewicz et al., 2008) and used to calculate the crop ingestion required for posing a risk as (BW TTC)/ $C_{fw}$], where BW (kg) is the reference body weight (EFSA, 2012) and $C_{fw}$ (μg/$kg_{dw}$) is the CEC concentration in the edible part, based on fresh weight. These values were then compared with typical Italian food consumption rates for infants and adults (Leclercq et al., 2009). HQs were calculated as the ratio between the estimated daily intake (EDI) and the admissible daily intake (ADI), which is the amount of CECs that can be consumed daily over a person's lifespan without evocating an adverse effect. The level of concern was set to 0.1 as dietary ingestion represents a single pathway of exposure (Prosser and Sibley, 2015). Hazard Index (HI) was also calculated as the sum of HQs to provide a conservative first-tier estimate of the mixture risk (Prosser and Sibley, 2015; Evans et al., 2015). Median and 97.5% percentile were derived for HQ, TTC and HI values from UA propagation. Further details on the two methods are given in SM.

III – *Management scenarios analysis*
Two agronomic management strategies were simulated to assess their potential for human health risk mitigation compared to the existing surface irrigation:
(i) the adoption of sprinklers, which require a lower investment cost than drip irrigation, and are a more efficient irrigation system than surface irrigation (i.e. irrigation efficiency increases from 60% to 75% according to Brouwer et al., 1989);
(ii) one week extension of the period without irrigation before harvest (also known as crop-drying stage). Waiting periods before harvest are a commonly required health safety measure in case of biosolids application (Prosser et al., 2014b).
The benefits in terms of human health risk reduction of the existing WWTP, although not specifically designed to remove CECs, were simulated in a specific scenario, where untreated wastewater was directly used for irrigation. Specifically, CEC concentrations measured in WWTP influent (Castiglioni et al., 2018a) were used as input to the river model and first order attenuation rates (calculated beforehand) were used to estimate *PECs* at the end of the channel. Based on *PECs* as input, the CSPM was then used to predict concentrations in fruits, allowing to estimate dietary intake and health risk for infants as shown earlier.

## 3. Results and discussion

### 3.1. Sensitivity analysis

Among the 52 parameters of the river model in the IUWS_MP library, 12 parameters (Figure S2) had an impact on predicted CEC concentrations. The fraction of CEC sorbed onto total suspended solids (TSS) showed higher sensitivity if compared to the dissolved fraction sorbed to colloids, mainly due to sedimentation parameters, in agreement with De Schepper et al.

(2012). As to conventional pollutants, ammonium, nitrite and nitrate were impacted by microbial growth parameters, in agreement with Deksissa et al. (2004), while phosphorus was influenced by the sorption rate and sedimentation parameters (Figure S2).
For the CSPM model, variations of CECs concentrations were influenced by several soil and plants parameters (Figure S3), in agreement with previous modeling studies (Trapp, 2015) and experimental data (Chen et al., 2013; Goldstein et al., 2014; Dodgen et al., 2015; Lamshoeft et al., 2018). Notably, the effect of the Arrhenius temperature correction coefficient on soil concentrations (|PRCC| > 0.9) out-weighed the effect of the other parameters, as seen before (Legind et al., 2011). Predicted concentrations of the weakly acidic DCF showed considerable sensitivity to internal plant pH, which was further assessed.

## 3.2. Fate analysis

### *3.2.1. Surface water channel*

Verification of IUWS_MP for conventional pollutants was adequate for the intended purpose, showing predicted concentrations in agreement with the measurements (≤ 0.75 log units) and being able to follow seasonal trends (Figure S4).
Along the water channel, model predictions (Figure 2 and Figures S5-14) showed that all the investigated CECs were almost entirely found as dissolved in the water phase (~ 98% of the load released from the WWTP). The only exception was CLA, for which the fractions on colloids and TSS were, on average, equal to 6% and 17% of the total mass (Figure 2c). Most of the simulated CECs have lower sorption affinity than CLA ($logK_{ow}$ = 3.2), or they were negatively charged at the measured pH (i.e. electrical repulsion). These results were in good agreements with the measurements in the Ebro river (Ferreira da Silva et al., 2011), where most of the CECs were found as predominantly dissolved (84%, 87%, 95%, 95%, 95% of the total mass for DCF, CLA, PAR, CBZ and IBU, respectively). The width of concentration prediction bounds (about ± 200 % of the median) was mainly explained by the propagation of the uncertainties associated to the initial concentrations of CECs in RWW and by degradation rates. Low variation in predicted concentrations (~ 0.3 log units) resulted from the propagation of uncertainties of conventional pollutant parameters.
The temporal dynamics of predicted concentrations followed different daily and/or seasonal patterns depending on the simulated CEC. For example, photodegradation caused an important reduction in concentrations for DCF (52-89%) and FUR (25-87%) between night and day time, in agreement with the findings of Hanamoto et al. (2013). Predicted DCF concentrations during day time were also confirmed by the available measurements (Figure 2a). Photodegradation and biodegradation also caused seasonal patterns with the lowest concentrations during June, July and August (Figure 2a and 2b), when temperature and sunlight irradiation reached their maximum values (22-25 °C and up to 900 W $m^{-2}$, respectively). A considerable reduction was observed in summer months, as compared to December, for DCF (30-41%; summer median: 204-244 ng $L^{-1}$), and FUR (49-72%; summer median: 49.4-90.6 ng $L^{-1}$). Moreover, when rice was cultivated, median concentrations of DCF and FUR were 16% and 67% lower than when winter wheat was cultivated (orange and red lines in Figure 2). In fact, a high water withdrawal for rice cultivation led to a reduction of the water level and thus enhancing photodegradation

and sedimentation since rates of these two processes are inversely proportional to the water depth (Schwarzenbach, 2003).

Due to the low tendency to photodegrade (median $k_{pho,nearsurf} \leq 23.1\ d^{-1}$) and the overall slow biodegradation in water (median $k_{bio,\ water} \leq 0.32\ d^{-1}$), the other CECs showed smaller daily fluctuations (intra-day variation: ≤ 10 %), seasonal trends (reduction in summer months compared to December: ≤ 11%) and variations due to water withdrawal (concentration decrease during rice cultivation: ≤ 4%) (see Figures S5-S14).

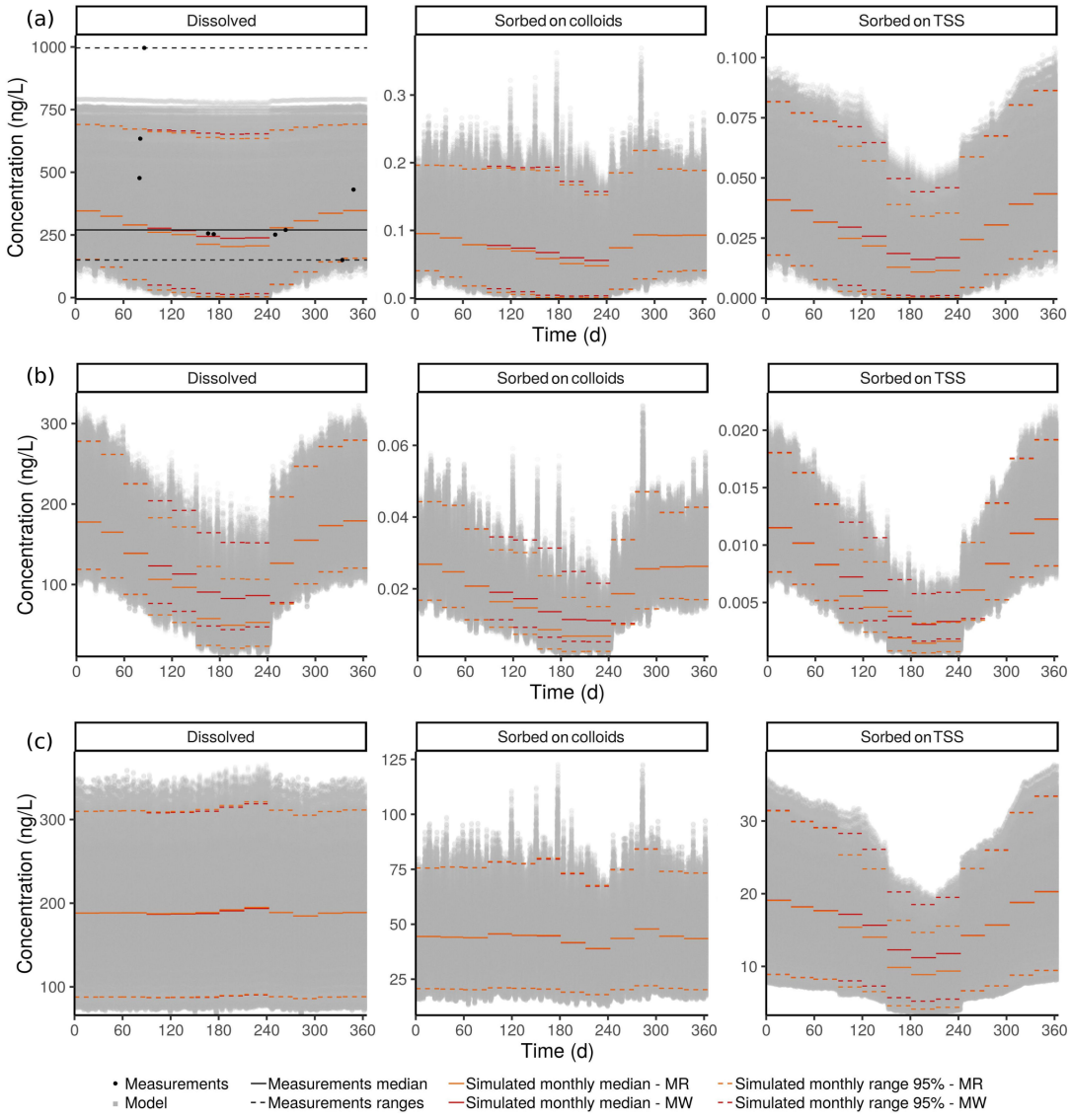


**Figure 2.** Annual variation (from January 1st to December 31st) of daytime DCF (a), FUR (b), CLA (c) concentrations at the end of the channel.

Predicted attenuation rates were in good agreement with literature data (Figure S15), with slight underestimation (≤ 1 order of magnitude). Differences might be due to the biofilm growth on submerged vegetation and sediment surface (Winkler et al., 2001; Sabaliunas et al., 2003; Kunkel and Radke, 2011; Writer et al., 2013), that enhances attenuation processes with respect to biodegradability processes accounted by our model.

Median attenuation rates varied throughout the year up to one order of magnitude due to different environmental conditions (temperature, sunlight intensity and water depth), with predicted maximum and minimum rates during July and December, respectively. Due to low CLA degradation (median $k_{pho,\ nearsurf}$ = 0.17 $d^{-1}$, median $k_{bio,\ water}$ = 3.85E$^{-02}$ $d^{-1}$), CLA attenuation rate variations were mostly caused by sedimentation, which was enhanced by the lower summer water depth, in agreement with Castiglioni et al. (2006). Similar seasonal variations of the attenuation rates were also observed by Matamoros et al. (2017) and Labadie and Budzinski (2005).

### *3.2.2. Crops*

In Figure 3a we report $BCF_{max}$ predictions for three CECs in different plant compartments, where the maximum simulated soil concentration is used for normalization (see Figures S16-S19 for the $BCF_{max}$ calculated with maximum soil concentrations for all the other CECs). Figure 3b-c presents $BCF_{median}$ values for fruits and leaves of the investigated crops based on the simulated median soil concentration, given the larger data availability for plausibility check (see Figures S16-S19 for roots and stems $BCFs_{median}$). Box-plots were obtained by aggregating BCFs based on crop type (i.e. maize, rice, ryegrass and wheat), and resulting ranges (i.e. width of the whiskers) included both variability (of CEC concentrations in the irrigation water, soil pH and soil organic content SOM) and uncertainty of model input.

Within crops (Figure 3a), predicted results for weakly acidic CECs, such as DCF, PFOA, FUR and IBU, mainly show accumulation in roots, which can be partly attributed to phloem translocation. For these CECs, a considerable BCF variation (more than factor 100) was generally obtained. This could be attributed to pH variability within the plant cell organs (Vreugdenhil and Koot-Gronsveld, 1989; Felle, 2001), which can strongly affect speciation of ionizable CECs and, consequently, the extent of CECs adsorption and translocation within the plant (Trapp, 2004). Moreover, large BCF variations for PFOA and PFOS were also associated to $logK_{ow}$ and $K_{HSA}$ uncertainty, which affect in-plant translocation and in-soil bioavailability (Trapp, 2009). TCS also showed maximum accumulation in roots, but mainly due to its high lipophilicity, which limits partitioning into xylem (Hsu et al., 1990). Conversely, neutral and hydrophilic CECs, such as CBZ, translocated upwards through the xylem to the leaves (Collins et al., 2006; Miller et al., 2016), where they showed the highest accumulation. In this case, variations of BCF were mainly caused by SOM variability, which influenced sorption of CECs in neutral form, such as estrogens (E1, E2 and EE2), TCS, PAR and CBZ (Goldstein et al., 2014), affecting bioavailability and uptake. SMX presented a more uniform accumulation among the plant organs due to both high phloem and xylem mobility (Kleier and Hsu, 1996; Goldstein et al., 2014). Regardless of the type of CEC, rice was generally the crop showing the highest uptake (Figure 3a), given that the irrigation system constantly floods the crop over the irrigational period, thus enhancing CECs loading. Conversely, the other crops were intermittently irrigated, and degradation and growth dilution lower uptake between irrigation events.

Box-plot medians (Figure 3b-c) were generally close (within 1 order of magnitude) to measurements, while for estrogens and PAR few to no measurements were available. Conversely, CBZ, TCS and SMX (having the highest data availability) showed measured values overall lower than predicted $BCF_{median}$. This may be due to metabolization within the plant

compartments, which has been experimentally observed for CBZ in leaves (Riemenschneider et al., 2016; Goldstein et al., 2014; Malchi et al., 2014), for TCS in roots (Macherius et al., 2012) and for SMX (Dodgen et al., 2013; Bircher et al., 2015; He et al., 2017; Li et al., 2018). In the model, metabolization within plants was assumed negligible since no kinetic data are available within the existing literature to account for such process. The approach used with respect to in-plant metabolism represents a realistic worst-case scenario. Moreover, in-plant metabolism does not always lead to degradation of the chemical but may lead to the formation of (i) conjugated metabolites that are prone to be transformed back to their parent analogue (Macherius et al., 2012); (ii) other metabolites that may be as hazardous as their respective parent (e.g., the case of carbamazepine metabolites; Malchi et al., 2015).

BCF calculation was highly affected by in-soil degradation, since it increases the differences between maximum and median soil concentration (hence, the difference between $BCF_{max}$ and $BCF_{median}$). In particular, $BCF_{median}$ variation for estrogens was the most affected (≥ 2 orders of magnitude) by in-soil degradation rates. The effect was more pronounced for maize, as the longer time between irrigation events allows for larger variations of the median soil concentration than for other crops. Overall, these results further confirm the need for a standard methodology for BCF calculation to allow for inter-study comparison of empirical results.

The model also predicted mass loss above $10^{-4}$ mg $m^{-2}$ $season^{-1}$ from soil to groundwater for CBZ, SMX, IBU, PFOS and PFOA (Figure S20), in agreement with the high GW concentrations measured in the area (Castiglioni et al., 2018b). Losses to groundwater were also predicted for DCF and FUR, while measurements were below detection limits, possibly due to further degradation outside the model boundary. Castiglioni et al. (2018b) also found traces of CLA and TCS in the groundwater, in disagreement with model predictions that showed almost complete accumulation in the surface soil layers, as confirmed by Chen et al. (2013) and Xu et al. (2009). The chemicals might stem from other sources (e.g. house imhoff tanks located in rural area) or reach groundwater by macropore transpor

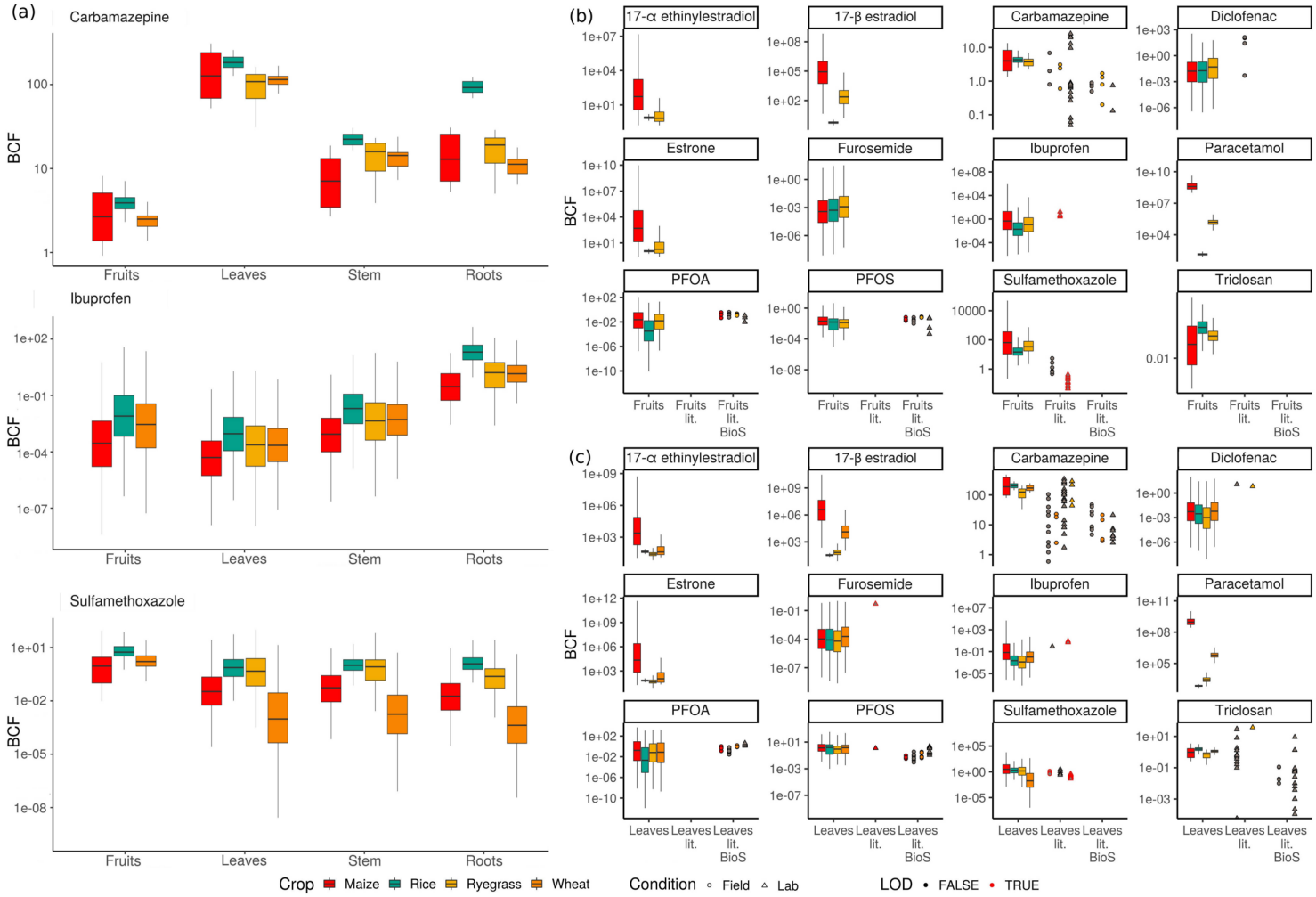


**Figure 3.** (a) Bioconcentration factors (BCFs, $g_{dw}/g_{dw}$) for CBZ, IBU and SMX in different crops and soil types. BCFs were calculated with respect to maximum soil concentrations. (b, c) Fruit and leaf BCFs ($g_{dw}/g_{dw}$) for all evaluated CECs in silage maize, winter wheat and rice in different soil types, and comparison with literature values (lit.). BCFs were calculated with respect to median soil concentrations. BioS indicates experimental studies conducted with the use of biosolids. Red borders indicate the use of a LOD value in the calculations. Refs: Bizkarguenaga et al. (2016), Blaine et al. (2013), Carter et al. (2014), Christou et al. (2017), Fu et al. (2016), Goldstein et al. (2014), Hurtado et al. (2017), Malchi et al. (2014), Mordechay et al. (2018), Navarro et al. (2017), Pannu et al. (2012), Shenker et al. (2011), Wen et al. (2014), Winker et al. (2010)..

## 3.3. Risk assessment

### *3.3.1. Ecological risk*

Three estrogens (E1, E2 and EE2), two antibiotics (SMX and CLA), one non-steroidal anti-inflammatory drug (IBU) and one antiseptic (TCS) showed $RQ_{median}$ above the alert thresholds at least once over the 1-year simulation. EE2 displayed the highest risk both in terms of magnitude and frequency of exceedance, with a daily median concentration always above the PNEC ($RQ_{median} \sim 27$), and a maximum concentration during winter corresponding to a $RQ_{max}$ of 46. Predicted $RQ_{median}$ for E2, CLA and TCS were approximately 1.5, with an average monthly frequency of exceeding the corresponding PNECs of 0.95, 0.79 and 0.77, respectively. IBU, E1 and SMX showed $RQ_{median}$ below 1, although a non-negligible ecological risk ($RQ_{max}$ ranging between 0.15 and 0.45) was shown. Other investigated CECs had an RQ below 0.1, showing low or negligible ecological risk (see Table S22). These results, in good agreement with what found by Riva et al. (2019) in the surrounding area, highlight that certain CECs may negatively affect aquatic organisms at a medium distance (approximately 12 km) from the WWTP.

### *3.3.2. Human health risk from dietary uptake*

The estimated consumption of rice and wheat required to exceed TTCs (Table S23) showed unrealistic values (>2 kg/d per person) for all the CECs but SMX. For this compound a consumption of 10 g/d and 50 g/d (considering the $97.5^{th}$ rice concentration percentile) might imply potential genotoxic effects (Malchi et al., 2015) on infants and adults, respectively. Conversely, SMX had an HQ below the alert threshold of 0.1 in accordance with the work of Christou et al. (2017). Consequently, experimental measurements should be performed in rice to clarify a possible risk related to SMX. The calculated negligible human health risk is in good agreement with the findings of Malchi et al. (2014) and Riemenschneider et al. (2016).
As for the predicted risk by the HQ approach (Table 1), results indicated negligible risk for all the CECs, although an HQ (infants) of 0.3 was calculated for EE2. A comparison with the TTC could not be done, since this latter approach is not valid for classes of compounds such as estrones (Kroes et al., 2004).
To conclude, the HI value (sum of all individual HQs, see Table 1) was below 1, showing no potential risk for human health from the investigated CECs. Moreover, the risk from indirect exposure (possible biotransfer of CECs from forage to milk and beef and, subsequently to humans) was not quantified since available empirical models (Travis and Arms, 1988; Hendriks et al., 2007) failed to properly describe fate of ionisable compounds and were not validated for the CECs here considered. Mechanistic models (Rosenbaum et al., 2009; Trapp et al., 2008) predict bioaccumulation in milk and meat solely for chemicals with strong partitioning into lipids, which is not the case for the investigated compounds.

**Table 1.** HQs and HIs for crops irrigated with water withdrawn at the end of the channel. P97.5 stands for values calculated with the 97.5$^{th}$ percentile CEC concentration.

| ECs | Rice | | Wheat | | Total | |
|---|---|---|---|---|---|---|
| | Median | P97.5 | Median | P97.5 | Median | P97.5 |
| Infants | | | | | | |
| SMX | 2.94E-03 | 2.03E-02 | 1.86E-04 | 1.58E-03 | 3.12E-03 | 2.19E-02 |
| DCF | 2.66E-06 | 6.35E-04 | 6.14E-08 | 1.26E-05 | 2.72E-06 | 6.48E-04 |
| IBU | 1.12E-09 | 5.27E-07 | 1.21E-10 | 5.94E-08 | 1.24E-09 | 5.86E-07 |
| PAR | 7.12E-07 | 1.05E-06 | 5.64E-08 | 9.08E-08 | 7.69E-07 | 1.14E-06 |
| CBZ | 2.62E-03 | 3.91E-03 | 2.21E-03 | 2.80E-03 | 4.84E-03 | 6.71E-03 |
| FUR | 5.37E-08 | 8.49E-05 | 1.25E-07 | 9.82E-05 | 1.79E-07 | 1.83E-04 |
| EE2 | 2.77E-02 | 2.57E-01 | 1.95E-03 | 3.85E-02 | 2.97E-02 | 2.95E-01 |
| E2 | 1.07E-05 | 2.53E-05 | 8.72E-07 | 2.02E-06 | 1.15E-05 | 2.73E-05 |
| E1 | 5.23E-04 | 4.82E-03 | 4.06E-05 | 7.80E-04 | 5.63E-04 | 5.60E-03 |
| PFOS | 6.98E-06 | 2.75E-04 | 5.44E-06 | 1.24E-04 | 1.24E-05 | 4.00E-04 |
| PFOA | 2.23E-08 | 1.22E-04 | 1.17E-06 | 2.66E-04 | 1.19E-06 | 3.88E-04 |
| TCS | 6.19E-09 | 1.79E-08 | 2.57E-09 | 1.04E-08 | 8.76E-09 | 2.83E-08 |
| | | | Hazard Index | | 3.82E-02 | 3.31E-01 |
| Adults | | | | | | |
| SMX | 4.45E-04 | 3.08E-03 | 8.88E-05 | 7.52E-04 | 5.34E-04 | 3.83E-03 |
| DCF | 4.03E-07 | 9.63E-05 | 2.93E-08 | 6.03E-06 | 4.33E-07 | 1.02E-04 |
| IBU | 1.70E-10 | 7.99E-08 | 2.93E-08 | 6.03E-06 | 2.27E-10 | 1.80E-07 |
| PAR | 1.08E-07 | 1.59E-07 | 2.69E-08 | 4.33E-08 | 1.35E-07 | 2.20E-07 |
| CBZ | 3.98E-04 | 5.93E-04 | 1.06E-03 | 1.33E-03 | 1.45E-03 | 1.93E-03 |
| FUR | 8.14E-09 | 1.29E-05 | 5.96E-08 | 4.69E-05 | 6.78E-08 | 5.97E-05 |
| EE2 | 4.20E-03 | 3.89E-02 | 9.32E-04 | 1.84E-02 | 5.13E-03 | 5.73E-02 |
| E2 | 1.62E-06 | 3.84E-06 | 4.16E-07 | 9.63E-07 | 2.03E-06 | 4.80E-06 |
| E1 | 7.93E-05 | 7.30E-04 | 1.94E-05 | 3.72E-04 | 9.86E-05 | 1.10E-03 |
| PFOS | 1.06E-06 | 1.31E-04 | 2.60E-06 | 5.94E-05 | 3.65E-06 | 1.90E-04 |
| PFOA | 3.38E-09 | 1.85E-05 | 5.58E-07 | 1.27E-04 | 5.62E-07 | 1.46E-04 |
| TCS | 9.38E-10 | 2.71E-09 | 1.23E-09 | 4.96E-09 | 2.17E-09 | 7.67E-09 |
| | | | Hazard Index | | 7.22E-03 | 6.47E-02 |

### 3.4. Risk management strategies

The adoption of a more efficient irrigation system (i.e. sprinklers) led to a calculated reduction of the human health risk due to the lower CECs load that reach the crops. Particularly, median HQs for infants decreased by 25% for EE2 and SMX. In the model simulations, direct deposition of chemicals on leaf surfaces due to sprinkling has not been considered and may lead to an additional uptake of chemicals via this pathway, while significant uptake into grains via surface deposition is unlikely. However, weak acids could reach the grains by phloem transport. We are not aware of studies addressing this process. On the other hand, the adoption of a crop-drying stage before rice harvest did not show any substantial reduction (< 2%) in the median rice

concentrations of EE2 (from $3.71 \cdot 10^{-4}$ ng/$g_{dw}$ to $3.65 \cdot 10^{-4}$ ng/$g_{dw}$) and SMX (from $5.21E^{-01}$ ng/$g_{dw}$ to $5.12E^{-01}$ ng/$g_{dw}$). In fact, at the later stages of crop growth the transpiration rate is minimum (Hidayati et al., 2016), consequently resulting in limiting the predicted CECs uptake during this stage. To best of our knowledge no experimental studies compared the CECs uptake under different irrigation systems preventing further verification of the model results.
Although not explicitly designed to remove CECs, the existing WWTP showed to be crucial for guaranteeing human health safety. In the scenario where the WWTP was absent, only few CECs (PFOS, PFOA, DCF, FUR and CBZ) had a HQ median risk below 0.1, while it was substantially above 1 for all the other CECs. For example, $HQ_{median}$ of TCS increased from 1.43 to 429, reaching in the worst-case scenario an $HQ_{max}$ of 842. Predicted rice concentrations increased up to 3 orders of magnitude, especially for TCS, IBU, E1 and PAR, which are efficiently removed (>99%) by the WWTP (Castiglioni et al., 2018b). These results were in agreement with the work of Goldstein et al. (2014) and Wu et al. (2014), in which higher CECs concentrations in TWW led to higher accumulation in crops. The risk for infants associated to SMX and PAR (considering the $97.5^{th}$ percentile of the concentration in rice) showed a required ingestion to exceed TTC lower than 1 g $d^{-1}$ and the HQs of E1, EE2 and SMX were 0.34, 0.26 and 0.33, respectively. Median and $97.5^{th}$ percentile for infants HIs increased up to 8 times, reaching values of 0.27 and 0.95. respectively. These results further indicate that irrigation with untreated wastewater requires specific attention when considering the risk posed by CECs.

## 4. Conclusions

This study proposed a new integrated model for simulating the fate of different contaminants of emerging concern under dynamic conditions when reclaimed wastewater is reused for irrigation purposes. By extending and integrating existing fate models, the model showed capability and flexibility in describing the fate of 13 contaminants, covering a wide range of physicochemical properties, across different compartments and over long time intervals.
Model predictions for contaminant occurrence in irrigation water and crops were generally verified with measured data, thus allowing for the evaluation of ecological and human health risk posed by wastewater discharge and reuse. Although dependent on the approach used, sulfamethoxazole and 17α-ethinylestradiol were associated to potential health risk from dietary intake of irrigated crops, particularly rice. While the existing wastewater treatment plant contributes significantly to reduce the overall risk, further reductions can be obtained by adopting more efficient irrigation practices.
Overall the proposed integrated approach represents a valuable decision support tool for assessing the safety of reclaimed wastewater reuse practices within the circular economy, particularly when considering recent developments in the regulation (EC, 2018).

# Supplementary information

## SI.1 Models extension

### SI.1.1 IUWS_MP

CECs are often ionized at environmentally relevant pH (Franco et al., 2010). While sorption of neutral chemicals occurs due to Van der Waals forces, in the presence of ions, the process is dominated by the stronger electrical forces. Hence, neutral molecules, anions and cations present different sorption behaviors which are furthermore affected by the degree of ionic speciation (Franco and Trapp, 2008). The Koc formula was updated accordingly to Franco et al. (2013) as shown in Eq. S1.

$$Koc_{acid} = \Phi_n 10^{0.54\ logKow+1.11} + \Phi_i 10^{0.11\ logKow+1.54} \qquad \text{(Eq. S1)}$$
$$Koc_{base} = 10^{logDow+2.78}$$

The sorption of the charged and neutral fractions of monovalent chemicals is described as a function of Kow or Dow, $pK_a$ and, in case of acids, also the solution pH. $\Phi_n$ and $\Phi_i$ are respectively the neutral and anionic CECs fractions calculated at $pH_{opt}$ = pH - 0.6, accordingly to the Henderson-Hasselbach equation. The range of applicability is $pK_a < 10$ for monovalent acids and $pK_a > 4$ for monovalent bases (Franco et al., 2013).
Environmental properties are intrinsically dynamic (Kunkel and Radke, 2011; Matamoros and Rodriguez, 2017) and the use of constant values would not properly describe realistic conditions. Hence, the use of external measurement inputs was allowed for the following properties:

- Sunlight intensity
- Water pH
- Air temperature
- Water temperature
- Wind speed

Irrigation is, also, seasonal dependent (Portmann et al., 2008). For this reason, the flow splitters, used to simulate the water withdrawal, were, thus, enhanced to describe a dynamic pattern throughout the year.

### SI.1.2 Coupled soil-plant model (CSPM)

Figure S1 shows the modelled flows mainly responsible for CECs traslocation inside the plants.

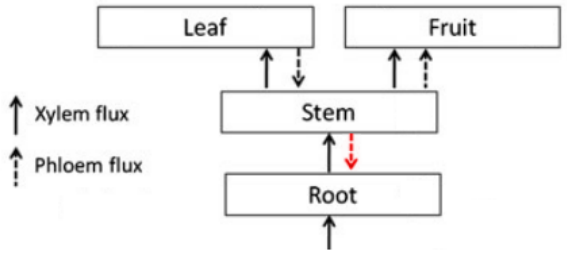


Figure S1. Modelled CECs flows inside the plants. In red the new phloem flux added.

As multiple crops are commonly grown on the same field within the same year (Borrelli et al., 2014), the model was extended to describe the succession of two different crops within the same year. Furthermore, an extra input was added to the model to account for the water and CECs mass added to the first soil layer through irrigation and the time-step used in the solution scheme was refined to prevent numerical issues.

Soil pH is not constant with depth, especially in agricultural field in which the surface layers are extensively plowed and fertilized (Zhang et al., 2017b). Therefore, a pH value was given to each of the five soil layers present in the model. Moreover, soil temperatures vary throughout the year due to the fluctuations of air temperature and solar radiation. As depth increases, temperatures are more uniform throughout the year, compared to the overlying layers (Xing and Spitler, 2017). Hence, a daily temperature was added for each of the layers 2-5, while the surface layer temperature was assumed equal to the air above.

## SI.2 Chemicals

Table S1. PNECs of selected CECs.

| | | PNEC value (ng/L) | Reference |
|---|---|---|---|
| clarithromycin | CLA | 200 | Zhao et al. (2017b) |
| sulfamethoxazole | SMX | 890 | Huang et al. (2018) |
| diclofenac | DCF | 9800 | Zhao et al. (2017b) |
| ibuprofen | IBU | 18 | Huang et al. (2018) |
| paracetamol | PAR | 367 | Riva et al. (2019) |
| carbamazepine | CBZ | 9000 | Zhao et al. (2017b) |
| furosemide | FUR | 45100 | Riva et al. (2019) |
| 17-β estradiol | E2 | 2 | Caldwell et al. (2012) |
| estrone | E1 | 6 | Caldwell et al. (2012) |
| 17-α ethinylestradiol | EE2 | 0.1 | Caldwell et al. (2012) |
| perfluorooctanoic acid | PFOA | 1.07E06 | Gredelj et al. (2018) |
| perfluorooctane sulfonate | PFOS | 1.6E04 | Gredelj et al. (2018) |
| triclosan | TCS | 2.6 | Gredelj et al. (2018) |

### SI.2.1 CECs physicochemical properties and degradation rates

Table S2 presents the physicochemical values used during the simulations. QSAR estimates of CLogP and ECOSAR of PFOS and PFOA were discarded as not reliable (Arp et al., 2006).

Table S2. Physicochemical properties of the selected CECs. All properties from Advanced Chemistry Development Inc. (2015), unless noted. (b) indicates a basic $pK_a$

| CEC | Mol mass (g/mol) | $pK_a$ | Vapor P (mmHg) | Log(Sw) (M) | Log(Kow) | Log(Koc) | Log($K_{HSA}$) |
|---|---|---|---|---|---|---|---|
| CLA | 747.95 | 8.5 (b) | 0 | -3.29 | 3.2 | | 2.77 |
| SMX | 253.28 | 5.7 | 1.9E-09 | -2.62 | 0.89 | 2.34[28], 1.79[28], 1.3[28], 1.4[28], 2.06[28], 3.47[28] | 2.86 |

Table S2. Cont.

| | | | | | | | |
|---|---|---|---|---|---|---|---|
| DCF | 296.15 | 4.4 | 1.59E-07 | -5.1 | 4.4 | | 4.91 |
| IBU | 206.28 | 4.3 | 1.39E-04 | -3.99 | 3.4 | | 4.74 |
| PAR | 151.06 | 10.2 | 1.43E-06 | -0.99 | 0.46 | 1.55[1] | 2.43 |
| CBZ | 236.27 | - | 5.78E-07 | -3.33 | 2.3 | | 3.91 |
| FUR | 330.74 | 3.5 | 0 | -3.66 | 2.03 | | 5.27 |
| E2 | 272.38 | 10 | 9.8E-09 | -4.64 | 3.36 | | 4.41 |
| E1 | 270.37 | 9.9 | 1.54E-08 | -3.95 | 3.13 | | 1.06 |
| EE2 | 296.40 | 10 | 3.7E-09 | -4.7 | 3.54 | | 3.55 |
| PFOA | 414.07 | 2.4, 0.5, 3.8[5], 0.5[6], 1.31[7], 1.01[4], <1[15], 2.5[12], 2.8[3], 0.9[8], 0[9], 0[13], -0.21[10], 2.14[11] | 3.14E-02[13], 3.11E-03[13], 3.14E-02[13], 2.4E-03[14], 2.25E-04[14], 9.02E-02[19], 1.5E-01[19] | -4.54, -1.98[2], -2.01[11], -2.09[2], -1.64[2], -2.73[8] | 4.6, 7.75, 4.3[14], 5.3[8], 4.59[14], 1.92[13], 6.26[15] | 2.06[17], 1.9[17], 2.17[17], 1.1[15], 3.2[15], 1.47[27] | 5.02, 4.0[20], 3.4[20], 3.42[21], 4.34[22], 3.57[23], 4.38[24], 5.16[24], 4.5[24] |
| PFOS | 500.13 | -5.7, -3.7, -3.41[8], 0.14[10], -3.3[12] | 2.6E-02[14], 2.54E-01[14], 2.34E-03[19], 1.13E-01[15] | -5.05, -3.84[8], -3.79[15] | 2.59, 7.03, 5.25[14], 5.26[14], 2.45[16], 4.67[15] | 1.6[15], 4.8[15], 2.57[17], 2.57[17], 3.1[17], 1.82[18] | 5.02, 7.1[20], 3.4[20], 3.51[25], 3.6[25], 3.66[23], 5.12[23], 3.7[26] |
| TCS | 289.54 | 8.8 | 4E-06 | -4.46 | 4.76 | | 4.81 |

References: 1: ECHA (2006), 2: Jensen et al. (2008), 3: Brace (1962), 4: Igarashi and Yotsuyanagi (1992), 5: Burns et al. (2009), 6: Vierke et al. (2013), 7: López-Fontán et al. (2005), 8: Wang et al. (2011), 9: Goss (2008), 10: Ahrens et al. (2012), 11: Nielsen (2012), 12: EFSA Scientific Commitee (2008), 13: Ding and Peijnenburg (2013), 14: Arp et al. (2006), 15: Rayne and Forest (2009b), 16: Jing et al. (2009), 17: Higgins and Luthy (2006), 18: Stevens and Coryell (2007), 19: Bhhatarai and Gramatica (2011), 20: Beesoon and Martin (2015), 21: Han et al. (2003), 22: Hebert and MacManus-Spencer (2010), 23: Chen and Guo (2009), 24: Bischel et al. (2010), 25: Wu et al. (2009), 26: Li et al. (2009), 27: Rahman et al. (2014), 28: Barron et al. (2009).

Table S3. CLA degradation rates.

| Near-surface photodegradation | | Biodegradation | | | | | |
|---|---|---|---|---|---|---|---|
| | | Sediments | | Water | | Soil | |
| $K_{pho,nearsurf}$ ($d^{-1}$) | Reference | $K_{bio,sed}$ ($d^{-1}$) | Reference | $K_{bio,wat}$ ($d^{-1}$) | Reference | $K_{bio,soil}$ ($d^{-1}$) | Reference |
| 0.23 | Calza et al. (2013) | 2.31E-03 – 2.31E-04 | JRC (2003) | Negligible | Alexy et al. (2004) | < 6.93E-4 – 7.80E-3 | Kodešová et al. (2016) |
| 0.13 | Gozlan and Koren (2016) | | | < 6.6E-03 | Calza et al. (2013) | | |
| | | | | < 9.9E-02 | Hanamoto et al. (2013) | | |
| | | | | 3.56E-3 – 1.39E-3 | Falås et al. (2013) | | |

Table S4. SMX degradation rates. (an) for anaerobic or anoxic conditions.

| Near-surface photodegradation | | Biodegradation | | | | | |
|---|---|---|---|---|---|---|---|
| | | Sediments | | Water | | Soil | |
| $K_{pho,nearsurf}$ ($d^{-1}$) | Reference | $K_{bio,sed}$ ($d^{-1}$) | Reference | $K_{bio,wat}$ ($d^{-1}$) | Reference | $K_{bio,soil}$ ($d^{-1}$) | Reference. |
| 4.62 – 5.33 | Baena-Nogueras et al. (2017) | 6.86E-2 – 0.14 | Lai and Hou (2008) | 8.66E-3 | Poirier-Larabie et al. (2016) | 6.08E-02 – 7.7E-02, 3.79E-2 – 4.53E-2 (an) | Lin and Gan (2011) |
| 1.28E-2 | Poirier-Larabie et al. (2016) | 0.63 | Radke et al. (2009) | Negligible | Baena-Nogueras et al. (2017) | 4.5E-03 – 0.15 | Kodešová et al. (2016) |
| 0.71 – 4.33 | Andreozzi et al. (2003) | 5.1E-02 – 7E-02, 4.15E-02 (an) | Zhang et al. (2013) | 1.24E-2 – 1.38E-2 | Adamek et al. (2016) | 0.2 – 0.73 | Li et al. (2015b) |
| 11.55, 2.77 – 5.78 | Lam and Mabury (2005) | 2.04E-02 | Li et al. (2015c) | 2.54E-3 | Radke et al. (2009) | 0.35 | Liu et al. (2010) |
| 9.90 – 17.33 | Ryan et al. (2011) | 3.65E-2 | Lam et al. (2004) | Negligible | Al-Ahmad et al. (1999) | | |
| 23.1 – 2.89 | Niu et al. (2013) | 3.09E-2 – 5.42E-02 | Xu et al. (2011) | 6.08E-2 | Zhang et al. (2013) | | |
| 7.22E-02 – 0.75 | Boreen et al. (2004) | 4.53E-03 | Su et al. (2016) | | | | |
| 2.39 – 6.93 | Bahnmüller et al. (2014) | | | | | | |
| 2.17 – 2.77 | Oliveira et al. (2019) | | | | | | |
| 0.39 – 1.73 | Bonvin et al. (2013) | | | | | | |
| 4.08 | Willach et al. (2018) | | | | | | |

Table S5. DCF degradation rates. (an) for anaerobic or anoxic conditions.

| Near-surface photodegradation | | Biodegradation | | | | | |
|---|---|---|---|---|---|---|---|
| | | Sediments | | Water | | Soil | |
| $K_{pho,nearsurf}$ ($d^{-1}$) | Reference | $K_{bio,sed}$ ($d^{-1}$) | Reference | $K_{bio,wat}$ ($d^{-1}$) | Reference | $K_{bio,soil}$ ($d^{-1}$) | Reference |
| 17.33 | Buser et al. (1998) | 3.73E-03 – 0.13 | Kunkel and Radke (2008) | Negligible | Baena-Nogueras et al. (2017) | 2.34E-2 – 0.14 | Lin and Gan (2011) |
| 86.64 | Poiger et al. (2001) | 3.45E-02, 1.54E-2 – 1.84E-02 (an) | Koumaki et al. (2017) | 4.08E-3 | Buser et al. (1998) | 3.39E-2 – 0.23 | Xu et al. (2009) |
| 1.73 | Poirier-Larabie et al. (2016) | 2.39E-02 – 7.7E-02 | Radke and Maier (2014) | 9.9E-03 | Poirier-Larabie et al. (2016) | 1.73 | Grossberger et al. (2014) |
| 99.02 – 115.52 | Baena-Nogueras et al. (2017) | 8E-3 – 2.6E-2 | Gröning et al. (2007) | | | | |
| 34.66 | Packer et al. (2003) | | | | | | |
| 0.35 – 3.47 | Andreozzi et al. (2003) | | | | | | |
| 2.31 - 23.1 | Koumaki et al. (2015) | | | | | | |
| 231.05 | Zhang et al. (2017a) | | | | | | |
| 266.59 – 277.26 | Zhang et al. (2011) | | | | | | |
| 6.93 | Vochezer (2010) | | | | | | |
| 11.55 | Radke et al. (2010) | | | | | | |

Table S6. IBU degradation rates. (an) for anaerobic or anoxic conditions.

| Near-surface photodegradation | | Biodegradation | | | | | |
|---|---|---|---|---|---|---|---|
| | | Sediments | | Water | | Soil | |
| $K_{pho,nearsurf}$ ($d^{-1}$) | Reference | $K_{bio,sed}$ ($d^{-1}$) | Reference | $K_{bio,wat}$ ($d^{-1}$) | Reference | $K_{bio,soil}$ ($d^{-1}$) | Reference |
| 1.68E-03 – 2.77E-02 | Yamamoto et al. (2009) | 3.65E-02 – 9.9E-02, 1.27E-03 – 3.35E-03 (an) | Conkle et al. (2012) | 1.2E-02 | Baena-Nogueras et al. (2017) | 4.56E-02 – 6.66E-02 | Lin and Gan (2011) |
| 7.97E-02 | Fono et al. (2006) | 0.43, 9.52E-03 – 2.11E-02 (an) | Koumaki et al. (2017) | 3.47E-02 | Buser et al. (1999) | 0.11 – 0.76 | Xu et al. (2009) |
| 5.13E-02 | Baena-Nogueras et al. (2017) | 0.14 – 0.28 | Kunkel and Radke (2008) | 3.47E-02 – 3.69E-02 | Yamamoto et al. (2009) | 2.28E-02 – 4.06E-04 | Carr et al. (2011) |
| 0.58 – 0.72 | Packer et al. (2003) | 8.56E-02 – 2.26, 1.47e-02 | Radke and Maier (2014) | | | 0.86 | Grossberger et al. (2014) |
| 6.30 | Peuravuori and Pihlaja (2009) | > 0.12 | Löffler et al. (2005) | | | | |
| 1.81E-02 | Koumaki et al. (2015) | 0.36 – 0.39 | Li et al. (2015c) | | | | |
| 1.12 | Lin and Reinhard (2005) | | | | | | |
| 6.93 | Jakimska et al. (2014) | | | | | | |

Table S7. PAR degradation rates.

| Near-surface photodegradation | | Biodegradation | | | | | |
|---|---|---|---|---|---|---|---|
| | | Sediments | | Water | | Soil | |
| $K_{pho,nearsurf}$ ($d^{-1}$) | Reference | $K_{bio,sed}$ ($d^{-1}$) | Reference | $K_{bio,wat}$ ($d^{-1}$) | Reference | $K_{bio,soil}$ ($d^{-1}$) | Reference |
| 0.58 – 17.32 | Baena-Nogueras et al. (2017) | 0.77 | Lam et al. (2004) | 1.2E-02 – 0.33 | Yamamoto et al. (2009) | >0.69 | Li et al. (2014) |
| 0.33 | Carlos et al. (2012) | 0.31 | Lin et al. (2010) | 2.47E-02 | Baena-Nogueras et al. (2017) | 3.65 – 3.85 | Li et al. (2015b) |
| 0.3 – 0.46 | Yamamoto et al. (2009) | 0.22 | Löffler et al. (2005) | | | | |
| Negligible | Kawabata et al. (2013) | | | | | | |
| 2.69E-02 | Peuravuori (2012) | | | | | | |
| 4.95E-02 – 0.69 | De Laurentiis et al. (2014) | | | | | | |
| 0.95 – 2.47 | Li et al. (2017b) | | | | | | |

Table S8. CBZ degradation rates. (an) for anaerobic or anoxic conditions.

| Near-surface photodegradation | | Biodegradation | | | | | |
|---|---|---|---|---|---|---|---|
| | | Sediments | | Water | | Soil | |
| $K_{pho,nearsurf}$ ($d^{-1}$) | Reference | $K_{bio,sed}$ ($d^{-1}$) | Reference | $K_{bio,wat}$ ($d^{-1}$) | Reference | $K_{bio,soil}$ ($d^{-1}$) | Reference |
| 0.17 | Calza et al. (2013) | 2.63E-03 – 4.2E-03, 1.58E-03 – 2.47E-03 (an) | Conkle et al. (2012) | 2.97E-03 – 5.55E-03 | Yamamoto et al. (2009) | 4E-03 – 1.5E-02 | Li et al. (2013) |
| 6.93E-03 – 3.47E-02 | Andreozzi et al. (2013) | Negl – 1.2E-02 | Radke and Maier (2014) | Negligible | Baena-Nogueras et al. (2017) | < 6.93E-04 – 5.37E-03 | Kodešová et al. (2016) |
| 7.92E-03 – 0.2 | Yamamoto et al. (2009) | 2.11E-03 | Löffler et al. (2005) | 1.1E-03 – 2.2E-03 | Durán-Álvarez et al. (2015) | < 3.47E-03 – 4.28E-03 | Grossberger et al. (2014) |
| Negligible – 1.39 | Baena-Nogueras et al. (2017) | Negl | Li et al. (2015c) | < 6.6E-03 | Calza et al. (2013) | | |
| 0.34 | Carlos et al. (2012) | 8.45E-03 | Lam et al. (2004) | | | | |
| 0.22 – 0.77 | Dong et al. (2015) | | | | | | |
| 0.16 | Durán-Álvarez et al. (2015) | | | | | | |
| 1.71E-02 | Peuravuori and Pihlaja (2009) | | | | | | |
| 0.87 | Doll and Frimmel (2003) | | | | | | |
| 0.14 – 2.77 | Lam and Mabury (2005) | | | | | | |
| 1.26E-02 | De Laurentiis et al. (2012) | | | | | | |

Table S9. FUR degradation rates.

| Near-surface photodegradation | | Biodegradation | | | | | |
|---|---|---|---|---|---|---|---|
| | | Sediments | | Water | | Soil | |
| $K_{pho,nearsurf}$ ($d^{-1}$) | Reference | $K_{bio,sed}$ ($d^{-1}$) | Reference | $K_{bio,wat}$ ($d^{-1}$) | Reference | $K_{bio,soil}$ ($d^{-1}$) | Reference |
| 86.64 | Hanamoto et al. (2013) | 4.33E-02 – 4.62E-02 | Li et al. (2015c) | < 0.1 | Hanamoto et al. (2013) | 4.91E-03 – 1.65E-02 | Polesel et al. (2015b) |
| 69.31 | Yagi et al. (1991) | 3.47E-02 – 4.95E-02 | Radke and Maier (2014) | 8.11E-04* | Khan and Ongerth (2004) | | |
| 34.66 | Jakimska et al. (2014) | 1.33E-02 – 4.62E-02 | Fenner et al. (2016) | | | | |

*: calculated correcting degradation rate with canal TSS

Table S10. E2 degradation rates. (an) for anaerobic or anoxic conditions.

| Near-surface photodegradation | | Biodegradation | | | | | |
|---|---|---|---|---|---|---|---|
| | | Sediments | | Water | | Soil | |
| $K_{pho,nearsurf}$ ($d^{-1}$) | Reference | $K_{bio,sed}$ ($d^{-1}$) | Reference | $K_{bio,wat}$ ($d^{-1}$) | Reference | $K_{bio,soil}$ ($d^{-1}$) | Reference |
| 2.77 – 17.32 | Liu et al. (2017) | 5.1E-02 – 5.33E-02, 1.75E-02 – 2.6E-02 (an) | Robinson et al. (2017) | ~ 1E-03 | Bradley et al. (2009) | 6.3 | Colucci and Topp (2002) |
| 2.17 – 2.77 | Leech et al. (2009) | 2.57 | Mashtare et al. (2013) | 7.97E-02 – 3.47 | Jurgens et al. (2002) | 0.17 – 0.46 | Carr et al. (2011) |
| 1.73 – 2.77 | Chowdhury et al. (2011) | 3.3E-02 | Czajka and Londry (2006) | 0.12 – 0.23 | Liu et al. (2011) | 0.46 – 3.15 | Colucci et al. (2001) |
| 2.17 – 2.77 | Whidbey et al. (2012) | 6.3, 1.05 – 1.87 (an) | Jurgens et al. (2002) | | | | |
| 8.66 | Lin and Reinhard (2005) | >1E-02 | Bradley et al. (2009) | | | | |
| 0.13 | Jurgens et al. (2002) | 1.87 – 7.7 | Zhang et al. (2016) | | | | |
| 0.83 – 1.24 | Li et al. (2017a) | | | | | | |
| 2.89 – 5.78 | Silva et al. (2016b) | | | | | | |

Table S11. EE2 degradation rates.

| Near-surface photodegradation | | Biodegradation | | | | | |
|---|---|---|---|---|---|---|---|
| | | Sediments | | Water | | Soil | |
| $K_{pho,nearsurf}$ ($d^{-1}$) | Reference | $K_{bio,sed}$ ($d^{-1}$) | Reference | $K_{bio,wat}$ ($d^{-1}$) | Reference | $K_{bio,soil}$ ($d^{-1}$) | Reference |
| 0.16 | Matamoros et al. (2009) | 6.42E-03 | Wu et al. (2015a) | Negligible | Wu et al. (2015a) | 0.83 | Colucci and Topp (2002) |
| 3.85 | Ren et al. (2016) | 0.16 | Mashtare et al. (2013) | 4.08E-02 | Jurgens et al. (2002) | 3.34E-03 – 3.07E-02 | Carr et al. (2011) |
| 0.72 | Zuo et al. (2013) | Negligible | Czajka and Londry (2006) | 6.42E-03 | Zuo et al. (2013) | 2.15E-02 – 0.37 | Colucci and Topp (2001) |
| 3.46 | Whidbey et al. (2012) | | | < 4.95E-02 | Matsuoka et al. (2005) | | |
| 6.93 | Lin and Reinhard (2005) | | | Negligible | Liu et al. (2011) | | |
| 0.13 | Jurgens et al. (2002) | | | | | | |
| 0.73 -3.46 | Ren et al. (2017a) | | | | | | |
| 2.4E-02 – 0.5 | Atkinson et al. (2011) | | | | | | |
| 0.89 – 7.7 | Silva et al. (2016b) | | | | | | |
| 0.77 | Grzybowski and Szydlowski (2014) | | | | | | |
| 0.63 – 0.69 | Ren et al. (2017b) | | | | | | |
| 1.39 | Wu et al. (2015a) | | | | | | |

Table S12. E1 degradation rates. (an) for anaerobic or anoxic conditions.

| Near-surface photodegradation | | Biodegradation | | | | | |
|---|---|---|---|---|---|---|---|
| | | Sediments | | Water | | Soil | |
| $K_{pho,nearsurf}$ ($d^{-1}$) | Reference | $K_{bio,sed}$ ($d^{-1}$) | Reference | $K_{bio,wat}$ ($d^{-1}$) | Reference | $K_{bio,soil}$ ($d^{-1}$) | Reference |
| 2.31 | Atkinson et al. (2011) | 6.8E-02 - 0.24, 3.14E-02 – 4.41E-02 (an) | Robinson et al. (2017) | 6.36E-02 – 6.93 | Jurgens et al. (2002) | 1.22E-02 – 0.22 | Carr et al. (2011) |
| 4.33 – 7.7 | Silva et al. (2016a) | 1.93E-02 | Mashtare et al. (2013) | 0.17 – 3.47 | de Mes et al. (2005) | 0.41 – 1.14 | Colucci et al. (2001) |
| 2.48 – 4.33 | Caupos et al. (2011) | 1.65, 4.88E-02 – 6.03E-02 (an) | Jurgens et al. (2002) | | | | |
| 13.86 – 34.66 | Chowdhury et al. (2011) | >1E-02 | Bradley et al. (2009) | | | | |
| 2.48 – 4.33 | Lin and Reinhard (2005) | | | | | | |

*: calculated correcting degradation rate with canal TSS

Table S13. PFOA degradation rates.

| Near-surface photodegradation | | Biodegradation | | | | | |
|---|---|---|---|---|---|---|---|
| | | Sediments | | Water | | Soil | |
| $K_{pho,nearsurf}$ ($d^{-1}$) | Reference | $K_{bio,sed}$ ($d^{-1}$) | Reference. | $K_{bio,wat}$ ($d^{-1}$) | Reference | $K_{bio,soil}$ ($d^{-1}$) | Reference |
| 4.22E-04 | Vaalgaama et al. (2011) | Negligible | Liou et al. (2010) | Negligible | Liou et al. (2010) | Negligible | Liou et al. (2010) |
| <1.98E-03 | Giesy et al. (2010) | | | | | | |

Table S14. PFOS degradation rates.

| Near-surface photodegradation | | Biodegradation | | | | | |
|---|---|---|---|---|---|---|---|
| | | Sediments | | Water | | Soil | |
| $K_{pho,nearsurf}$ ($d^{-1}$) | Reference | $K_{bio,sed}$ ($d^{-1}$) | Reference | $K_{bio,wat}$ ($d^{-1}$) | Reference | $K_{bio,soil}$ ($d^{-1}$) | Reference |
| 1642 | Brooke et al. (2004) | Negligible | Avendano et al. (2015) | Negligible | Avendano et al. (2015) | Negligible | Avendano et al. (2015) |

Table S15. TCS degradation rates.

| Near-surface photodegradation | | Biodegradation | | | | | |
|---|---|---|---|---|---|---|---|
| | | Sediments | | Water | | Soil | |
| $K_{pho,nearsurf}$ ($d^{-1}$) | Reference | $K_{bio,sed}$ ($d^{-1}$) | Reference | $K_{bio,wat}$ ($d^{-1}$) | Reference | $K_{bio,soil}$ ($d^{-1}$) | Reference |
| 23.1 - 115.52 | Baena-Nogueras et al. (2017) | 7.2E-03 | Wu et al. (2015a) | Negligible | Wu et al. (2015a) | 3.85E-02 | Wu et al. (2015a) |
| 23.1 | Koumaki et al. (2015) | 6.36E-02, Negligible (an) | Koumaki et al. (2018) | 1.92E-02 | Baena-Nogueras et al. (2017) | 4.42E-02 – 5.48E-02 | Xu et al. (2009) |
| 3.15 | Durán-Álvarez et al. (2015) | 1.22E-02 – 1.29E-02 | NICNAS (2009) | 0.69E-02 – 2.1E-02 | Durán-Álvarez et al. (2015) | 9.78E-03 – 1.74E-03 | Carr et al. (2011) |
| 3.3 | Latch et al. (2005) | | | | | 1.2E-02 – 2.17E-02 | Wu et al. (2009) |
| 69.31 | Lindström et al. (2002) | | | | | | |
| 23.1 | Singer et al. (2002) | | | | | | |
| 34.66 – 69.31 | Tixier et al. (2002) | | | | | | |
| 4.62 | Mezcua et al. (2004) | | | | | | |
| 3.01 | Martínez-Zapata et al. (2013) | | | | | | |
| 231.04 | Sanchez-Prado et al. (2006) | | | | | | |
| 0.2 | Wu et al. (2015a) | | | | | | |

## SI.3 Model parameters and model inputs

The environmental conditions used in RWQM1s1_MP are shown in Table S16. All values were taken from ARPA (Agenzia Regionale Protezione Ambiente) measurements databases for the year 2016. Regarding the CSPM, the model layers were adapted to the stratigraphy of the various soils with the parameters shown in Table S17. Photodegradation in rice paddies was assumed to be negligible due the sediment in suspension and plants shading. Eventual surface runoff of water was not modeled.

Table S16. Measurements and parameters used to characterize environmental conditions for the RWQM1s1_MP model

| Parameter | Source | Notes |
|---|---|---|
| Wind speed at 10 m above ground | ARPA | Hourly measurements |
| Air temperature | ARPA | Hourly measurements |
| Sunlight intensity | ARPA | Hourly measurements |
| Water temperature | ARPA | Monthly measurements at end of canal |
| pH | ARPA | Canal measurements average ±1 daily fluctuation (Simonsen and Harremoës, 1978) |
| TWW entering the canal | Mazzini et al. (2013) | Daily flow variations and rain events neglected |
| TWW CECs concentrations | Castiglioni et al. (2018a, 2018b) | Converted dissolved to total concentrations thanks to equations in Chapra (1997) |
| Algae, heterotrophs and nitrifying bacteria concentrations | | Initially left as default and then calibrated |
| Algae and bacterial growth parameters | Vanrollenghem et al. (2001) | |
| Phosphorous sorption and desorption | Chapra (1997) | |

Table S17. Environmental parameters and sources used for the CSPM. LOSAN is a publicly available soil database provided by ERSAF (Ente Regionale per i Servizi all'Agricoltura e alle Foreste), CRA-CMA stands for Unità di Ricerca per la Climatologia e la Meteorologia applicate all'Agricoltura

| Parameter | Source | Notes |
|---|---|---|
| Soil organic carbon | LOSAN | |
| Soil layer pH | LOSAN | |
| FC and PWP | LOSAN | Estimated from granulometries using correlations by Rawls et al. (1982) |
| Soil layers bulk density | LOSAN | Estimated from horizon-specific pedo-transfer functions from SOILQUALIMON report (Brenna et al., 2010) |
| Air temperature | ARPA | |
| Rainfall | ARPA | |
| Relative humidity | ARPA | |
| Potential evaporation | CRA-CMA | Obtained thanks to correction of potential evapotranspiration using $K_{c,ini}$ (1.05 rice, 0.3 other crops) (Legind et al., 2012; Polesel et al., 2015; Allen et al., 1998) |
| Soil layer temperature | CRA-CMA | Extrapolated from measurements at depths of 10 and 50 cm thanks to the sinusoidal functions in Xing and Spitler (2017). |

### SI.3.1 Soil properties

Table S18. Modeled soil properties.

| Horizon bottom depth (cm) | pH | Organic carbon (%) | Field capacity (L/L) | Wilting point (L/L) | Bulk density (g/cm3) |
|---|---|---|---|---|---|
| Soil 1: silage maize and ryegrass | | | | | |
| 13 | 7.3 | 4.9 | 0.36 | 0.14 | 1.09 |
| 38 | 6.9 | 0.64 | 0.23 | 0.10 | 1.52 |
| 60 | 7.8 | 0.64 | 0.31 | 0.13 | 1.32 |
| 75 | 7.6 | 0.5 | 0.38 | 0.21 | 1.80 |
| 100 | 7.5 | 0.37 | 0.32 | 0.14 | 1.59 |
| Soil 2: silage maize and ryegrass, winter wheat | | | | | |
| 20 | 6.6 | 1.27 | 0.24 | 0.09 | 1.45 |
| 40 | 6.6 | 1.27 | 0.24 | 0.09 | 1.45 |
| 60 | 6.7 | 0.16 | 0.18 | 0.09 | 1.48 |
| 80 | 6.7 | 0.16 | 0.18 | 0.09 | 1.48 |
| 100 | 6.7 | 0.16 | 0.18 | 0.09 | 1.48 |
| Soil 3: rice and ryegrass, winter wheat | | | | | |
| 35 | 6.1 | 2 | 0.26 | 0.11 | 1.33 |
| 45 | 6.9 | 0.72 | 0.21 | 0.08 | 1.49 |
| 67.5 | 7.2 | 0.63 | 0.16 | 0.06 | 1.41 |
| 90 | 7.2 | 0.63 | 0.16 | 0.06 | 1.41 |
| 100 | 7.4 | 0.44 | 0.23 | 0.12 | 1.49 |

Pseudo-steady state concentrations of the layers in each modeled soil were obtained with median concentration in TWW as irrigation concentration and median soil degradation rate and used as initial concentrations. For the crop rotation consisting of rice and ryegrass and winter wheat, the soil concentrations at the end of the rice and ryegrass years were used as represented the worst case soil concentration.

### SI.3.2 Plant parameters

Table S19. Parameters used for crop modeling. Parameters not noted were left as default.

| | Value | Reference | Notes |
|---|---|---|---|
| Maize | | | |
| Irrigation | 400 mm/season | Borrelli et al. (2014) | |
| Germination date | 20-05 | Borrelli et al. (2014) | |
| Harvest date | 30-09 | Borrelli et al. (2014) | |
| Transpiration coefficient | 60 L/kg fw | Legind et al. (2012) | |
| Water content roots | 0.84 g/g | Wang et al. (1991) | |
| Final root mass | 2.58 kg fw/m$^2$ | Legind et al. (2012) | |
| Growth rate | 0.081 1/d | Legind et al. (2012) | |
| Final stem mass | 3.61 kg fw/m$^2$ | Legind et al. (2012) | |
| Final leaf mass | 0.96 kg fw/m$^2$ | Legind et al. (2012) | |
| Final fruit mass | 1.78 kg fw/m$^2$ | Legind et al. (2012) | |
| Water content fruit | 0.76 | USDA (2018) | |
| Ryegrass | | | |
| Irrigation | 210 mm/season | FAO (2007) | Calculated subtracting rainfall from water requirements |
| Germination date | 9-12 with silage maize – 30/10 with rice | Borrelli et al. (2014), Nelli and Sodi (2007) | |
| Harvest date | 14-05 with silage maize – 31/03 with rice | Borrelli et al. (2014), Nelli and Sodi (2007) | |
| Final root mass | 2.35 kg fw/m$^2$ | | Assumed equal to winter wheat since same family (Poaceae) |
| Final stem mass | 1.8 kg fw/m$^2$ | Tabaglio et al. (2007), Abraha and Savage (2008) | Calculated assuming water content = 0.8 |
| Final leaf mass | 2.2 kg fw/m$^2$ | Tabaglio et al. (2007), Abraha and Savage (2008) | Calculated assuming water content = 0.8 |
| Initial fruit mass | 1E-05 kg fw/m$^2$ | Martiniello (1999) | To halt fruit development |

Table S19. Cont.

| | | | |
|---|---|---|---|
| Winter wheat | | | |
| Irrigation | 100 mm/season | Polesel et al. (2015) | |
| Germination date | 1-03 | Legind et al. (2012) | |
| Harvest date | 15-07 | Legind et al. (2012) | |
| Final root mass | 2.35 kg fw/m$^2$ | Legind et al. (2012) | |
| Final stem mass | 0.78 kg fw/m$^2$ | Legind et al. (2012) | |
| Final leaf mass | 1.81 kg fw/m$^2$ | Legind et al. (2012) | |
| Final fruit mass | 1.45 kg fw/m$^2$ | Legind et al. (2012) | |
| Rice | | | |
| Irrigation | 21.6 mm/day | Nelli and Sodi (2007) | |
| Germination date | 6-04 | Nelli and Sodi (2007) | |
| Harvest date | 30-09 | Nelli and Sodi (2007) | |
| Transpiration coefficient | 52 | Van der Vorm (1980) | |
| Roots/Stem/Leaf growth rate | 0.068 | Confalonieri and Bocchi (2005) | |
| Fruit growth rate | 0.13 | | Doubled compared to plant growth rate similarly to what observed for winter wheat and to match model ripening with agronomic data |
| Final root mass | 3.30 | Confalonieri and Bocchi (2005) | |
| Final stem mass | 1.76 | Confalonieri and Bocchi (2005) | |
| Final leaf mass | 1.92 | Confalonieri and Bocchi (2005) | |
| Final fruit mass | 0.94 | Confalonieri and Bocchi (2005) | |
| Water content root | 0.95 | Zhang and Webster (2002); Henry et al. (2012) | Calculated based on fresh weight measurements and roots to shoots ratio |
| Water content fruit | 0.23 | Rice Knowledge Bank (2017) | |

The ratio of phloem to xylem flux for PAR, SMX, IBU and FUR was set to 0.05, a median value between day and night. For the other CECs such ratio was set to 0 as considered non phloem-systemic based on the distinction by Kleier and Hsu (1996) relying on CECs Kow and $pK_a$. The phloem systemicity of DCF and PFOA was treated as uncertain as potentially affected by plant-specific parameters.

## SI.4 Uncertainty propagation

The preliminary uncertainty analysis (UA) of the IUWS_MP model for traditional pollutants was carried out varying the parameters in Table S20. Parameters uncertainty was based on Reichert and Vanrollenghem (2001) considering two classes of confidence: poorly known parameters were varied by 50% (Class 2), while better known parameters were varied by 20% (Class 1). CBZ, DCF and TCS, CECs with different physicochemical characteristics, were chosen amongst the thirteen selected to be tested. Random parameters combinations were obtained through 1000 Latin hypercube samplings for each CEC.

Table S20. Uncertainty classes of parameters for the uncertainty analysis of the traditional pollutants submodel.

| Parameter | Class | Parameter | Class |
|---|---|---|---|
| Heterotrophic bacteria input concentration | 2 | First stage nitrifiers (AOBs) input concentration | 2 |
| Phosphate adsorption rate | 2 | Algae input concentration | 2 |
| Saturation coefficient for aerobic growth of heterotrophs on dissolved organic substrate | 2 | Mean particle diameter | 2 |
| Slope | 1 | Saturation coefficient for growth of AOBs on ammonia | 2 |
| Maximum aerobic specific growth rate for heterotrophic biomass | 1 | Manning n value | 1 |
| Top canal width | 1 | Maximum aerobic specific growth rate for AOBs | 1 |
| Depth of canal filled to bank | 1 | | |

Successively, the uncertainty regarding the organic micropollutants IUWS_MP submodel and CSPM parameters on CECs concentrations were assessed through a Monte Carlo UA varying the parameters in Table S21. When no anoxic sediment biodegradation rates were found in literature, the aerobic values decreased by an order of magnitude were used. In case only one or two values were found, uniform distributions were used considering either a 10% variation or the range between the two values. The uncertainty of IUWS_MP was estimated thanks to 1000 runs for each water water withdraw scenario. The choice of the number of CSPM runs was based on the comparison of the percentiles from simulations consisting of an increasing amount of runs to the ones resulting from a 5000 runs simulation. As the percentiles from a 2000 runs simulation with Latin hypercube sampling differed negligibly from the 5000 runs simulation, the mentioned settings were chosen for the remaining simulations.

Table S21. Varied parameters during the IUWS_MP and CSPM Monte Carlo uncertainty analyses

| Parameter | Distribution | Source | Notes |
|---|---|---|---|
| TWW CEC concentrations | Triangular | Castiglioni et al. (2018a, 2018b) | Inf: minimum value/LOD<br>Mode: median value/0.5*LOQ<br>Sup: maximum value/LOQ |
| Water aerobic biodegr. rate<br>Sediment aerobic biodeg. rate<br>Sediment anoxic biodegr. rate<br>Soil dissipation rate<br>Photodegradation rate | Empirical, triangular | Tables S4 – S16 | Choice based on the quantity of experimental values found. Values outside 1.5*IQR (interquartile range) considered as outliers. Triangular distributions based on extreme values and medians |
| $pK_a$<br>Kow<br>Solubility<br>Vapor pressure<br>$K_{HSA}$<br>Kaw<br>(only perfluorinated chemicals) | Empirical, triangular | Table S3 | Choice based on the quantity of experimental values found |
| Irrigation concentration | Triangular | Surface water model | Inf: 2.5$^{th}$ percentile canal conc.<br>Mode: modal canal conc.<br>Sup: 97.5$^{th}$ percentile canal conc. |
| pH in cytosol<br>pH in vacuole<br>pH in phloem<br>pH in xylem | Uniform | Felle (2001), Felle et al. (2005), Johannes et al. (2001), Tournaire-Roux et al. (2003) | 10% variation is comparable to observed fluctuations |
| Transpiration coeff.<br>Root mass<br>Root growth rate<br>Stem growth rate<br>Leaves growth rate<br>Fruits growth rate | Uniform | | Variation equal to 10% to avoid numerical errors |
| Arrhenius temperature correction coeff. | Lognormal | EFSA (2007) | Median: 1.099<br>95$^{th}$ percentile: 1.144 |

Other parameters were varied during the analysis of specific CECs to either prevent numerical errors (SMX, PAR, E2), include uncertainty (PFOA, DCF) and improve model results (CLA, PFOS):

- PFOA and DCF phloem flux was set in 50% of the runs as 0;
- CLA's Koc was set to 10176 L/kg to match the value from the equations in Franco and Trapp (2008);
- SMX and PFOS KOC was varied as the other physicochemical properties;

- The soil structure during PAR simulations was modified to 3 layers of 33 cm whose soil properties were calculated as weighted average of the original layers. The dissipation rate was, also, set to the minimum value and the Koc from ECHA (2006) was used;
- The dissipation rate of E2 was limited to 1 $d^{-1}$.

Successively, the monthly medians of the total CECs concentrations taken at four locations along the canal were fitted with a first-order dissipation rate thanks to the use of Matlab R2016a and the estimated traveling times provided by IUWS_MP model. Yearly best- and worst-case attenuation rates were calculated for all the modeled CECs and compared to literature as a further validation.
Such attenuation rates and influent CECs concentrations (Castiglioni et al., 2018a) were used to estimate the expected concentrations along the canal in case of the absence of the upstream WWTP. Best- and worst-case scenarios were calculated respectively using low concentrations and high rates, and high concentrations and low rates. The median scenarios were obtained thanks to the median concentrations and the mean between the two attenuation rates.
The fruit CECs concentrations in case of the absence of the WWTP were estimated thanks to the expected median concentrations at the end of the canal which were used to reach a pseudo-steady state in the coupled soil-plant model. Successively, the median CECs concentration of the first layer at pseudo-steady state was multiplied by the median or the 97.5$^{th}$ percentile BCFs, calculated from the previous Monte Carlo uncertainty analyses, to estimate of the median and 97.5$^{th}$ percentile fruit concentration.

## SI.5 Sensitivity analyses (SA)

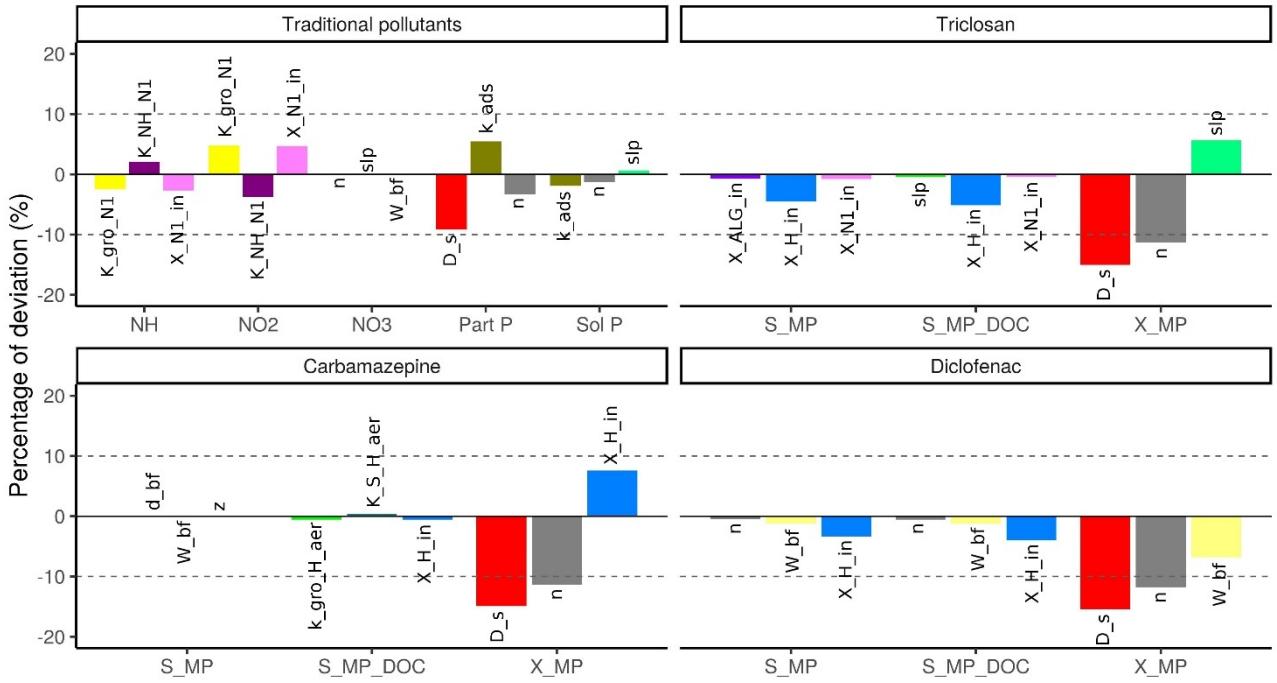


Figure S2. Deviation caused by increments of the parameters in the traditional pollutants submodel. S_MP, S_MP_DOC and X_MP indicate respectively the following fractions of a CEC: dissolved, sorbed on colloids and sorbed on TSS.

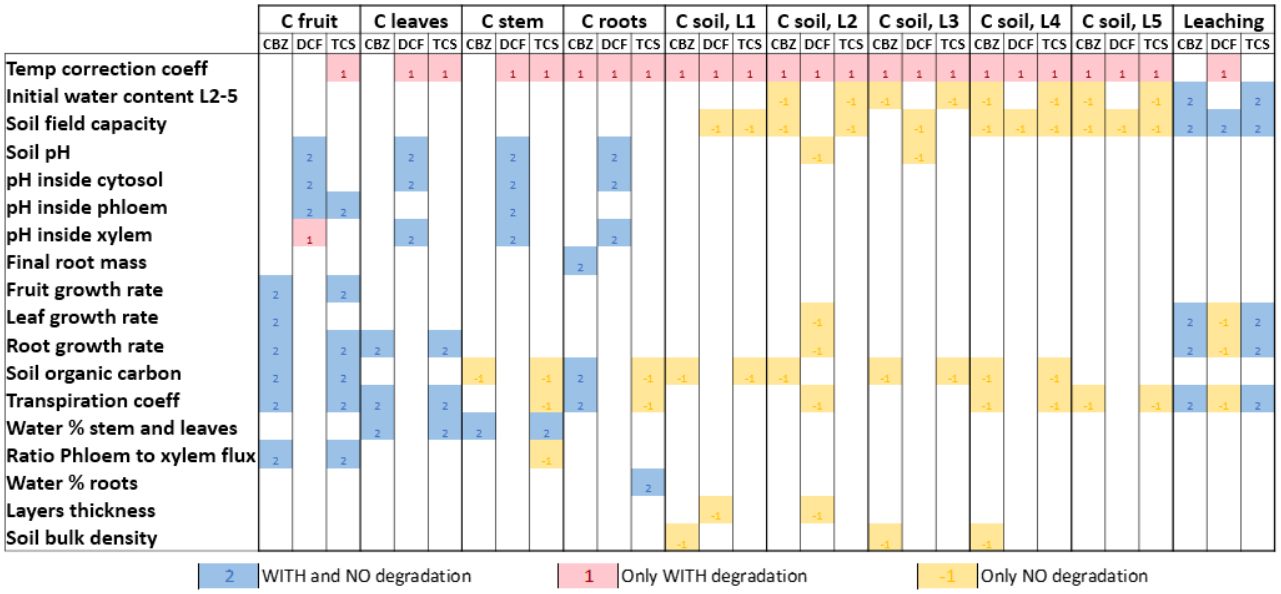


Figure S3. Coupled soil-plant model sensitive parameters in presence or absence of degradation.

## SI.6 Fate analysis

### SI.6.1 Traditional pollutants

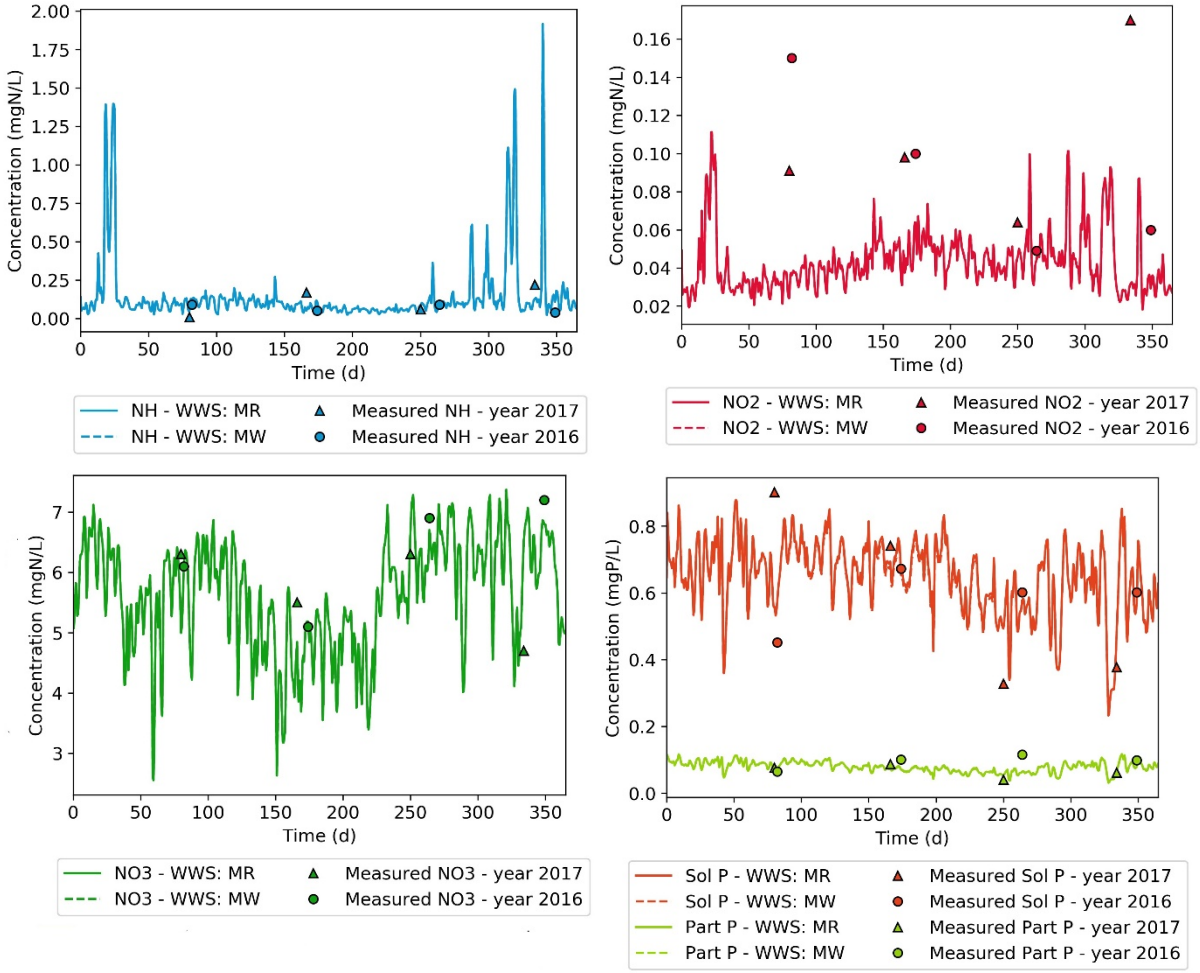


Figure S4. Traditional pollutants calibrated concentrations and measured values in canal. NH = ammonium, NO2 = nitrite, NO3 = nitrate, Sol P = soluble phosphorus, Part P = particulate phosphorus.

### SI.6.2 Uncertainty of CECs concentrations in canal

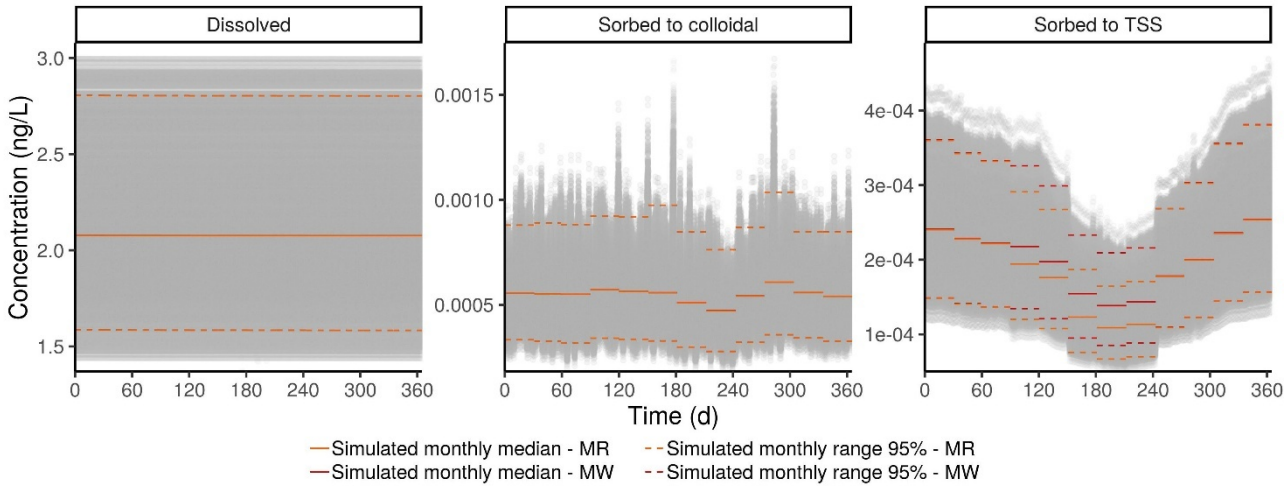


Figure S5. PFOS midday predicted concentration ranges. Days starting from January 1st until December 31st.

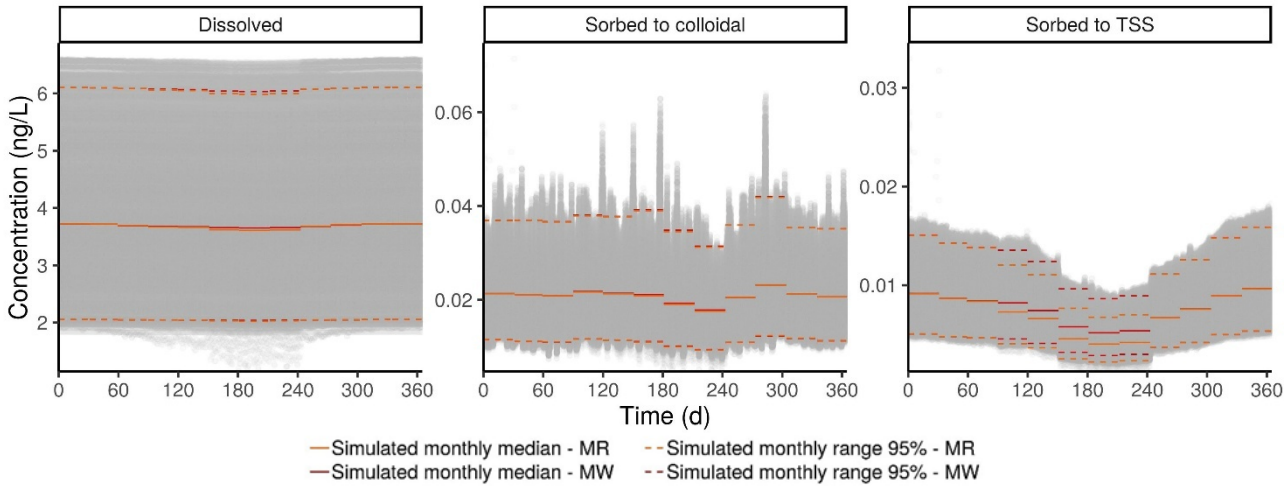


Figure S6. TCS midday predicted concentration ranges. Days starting from January 1st until December 31st.

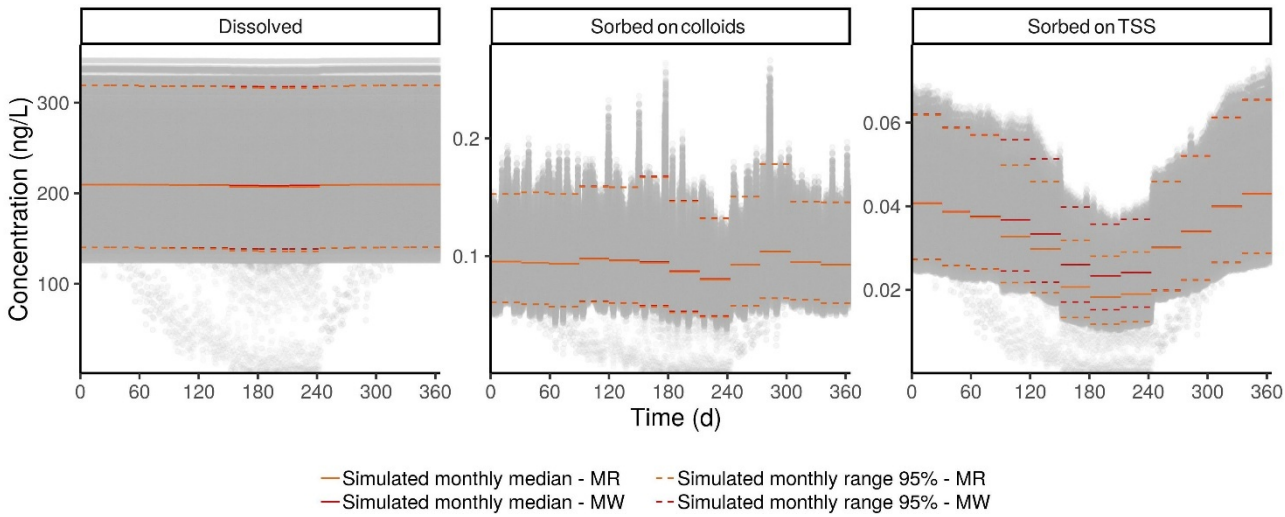


Figure S7. CBZ midday predicted concentration ranges. Days starting from January 1st until December 31st.

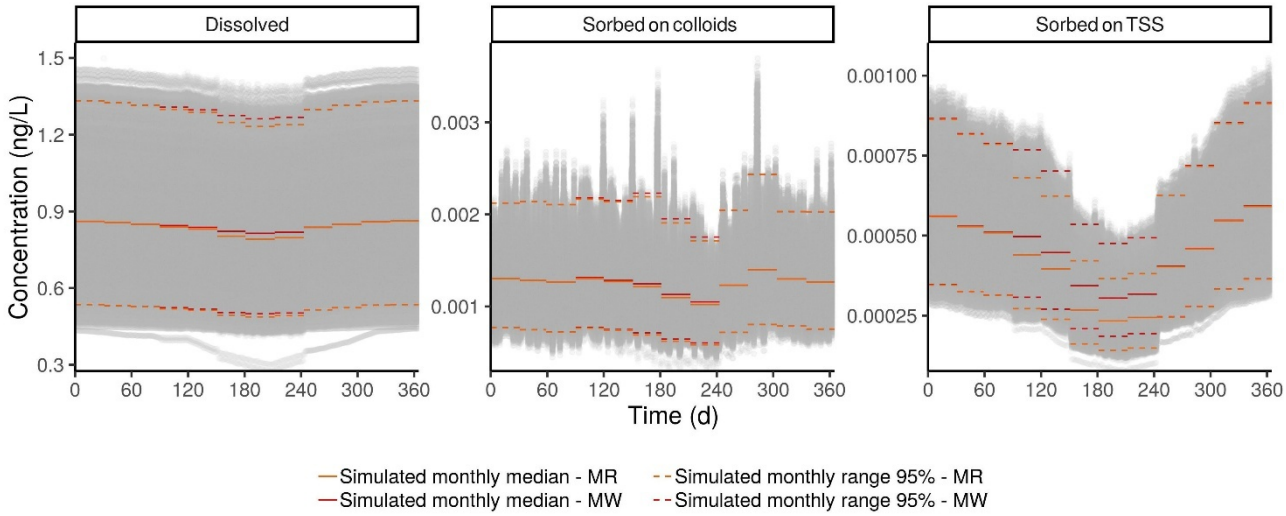


Figure S8. E1 midday predicted concentration ranges. Days starting from January 1st until December 31st.

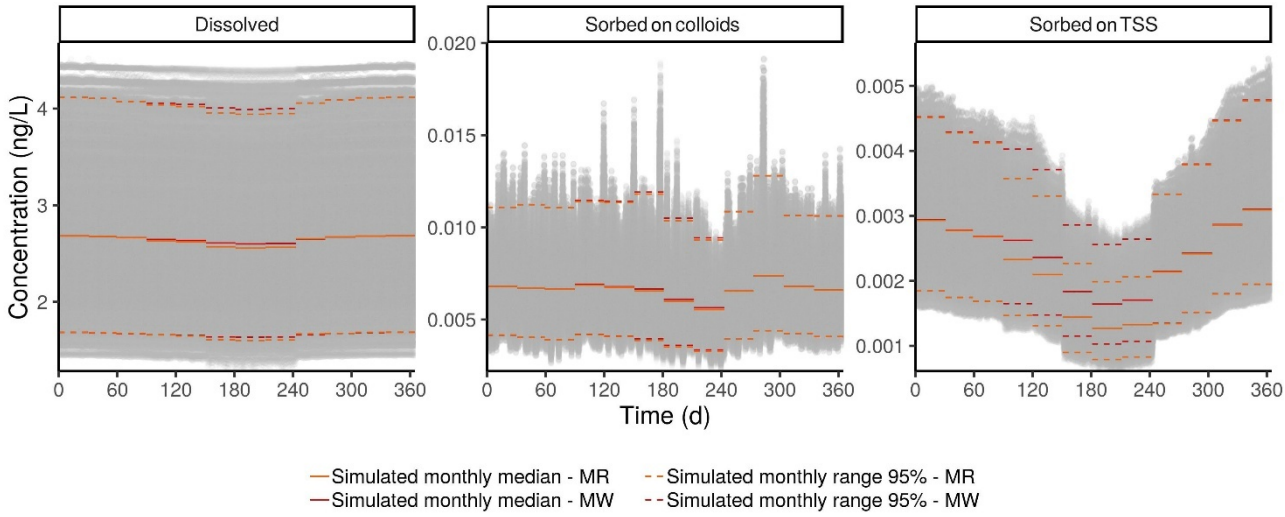


Figure S9. EE2 midday predicted concentration ranges. Days starting from January 1st until December 31st.

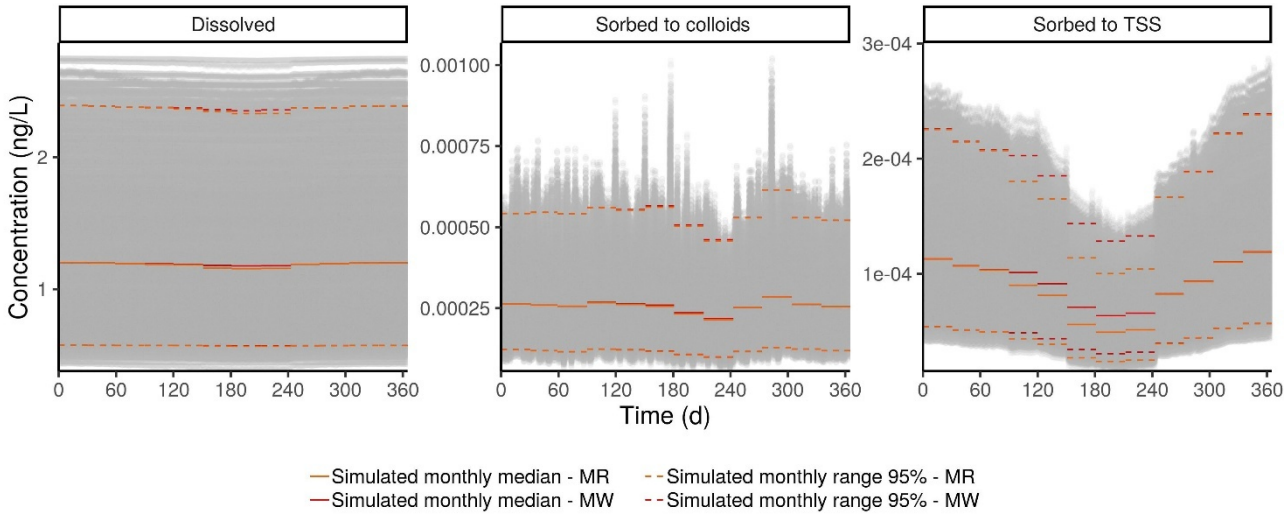


Figure S10. IBU midday predicted concentration ranges. Days starting from January 1st until December 31st.

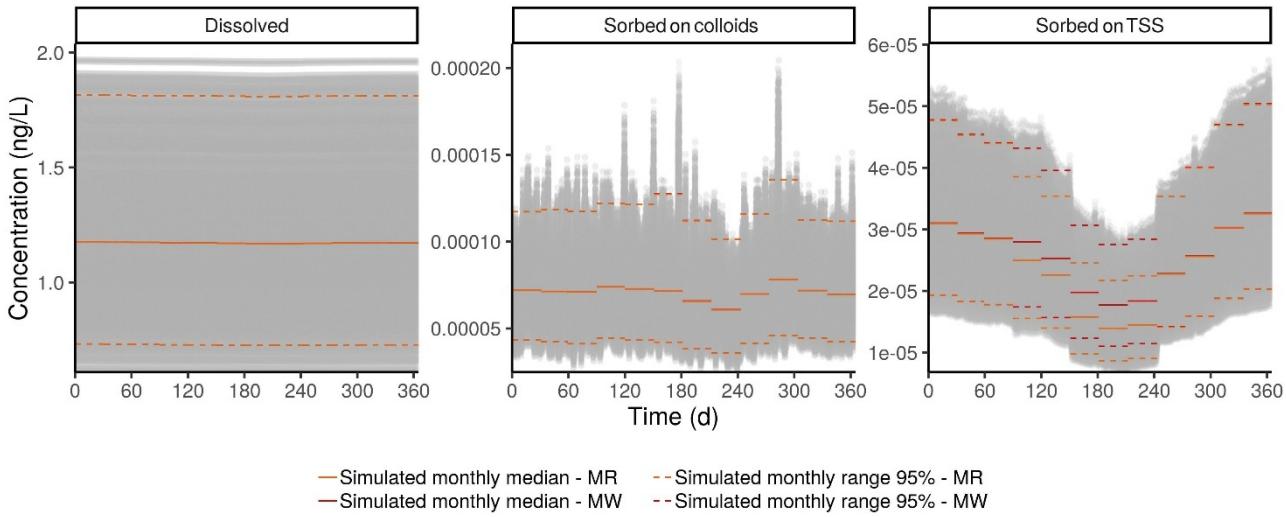


Figure S11. PAR midday predicted concentration ranges. Days starting from January 1st until December 31st.

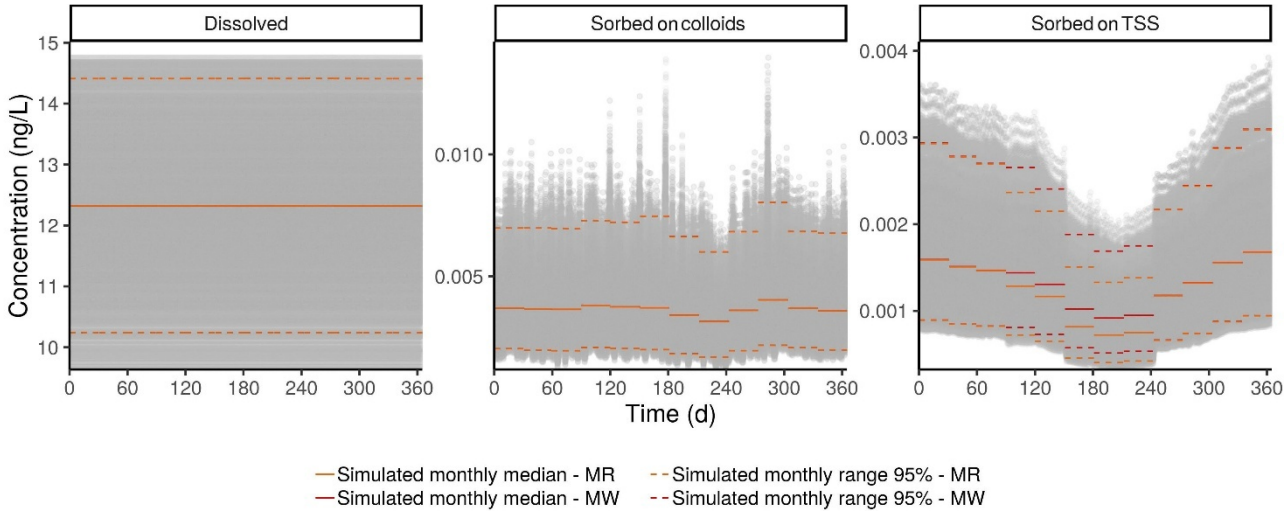


Figure S12. PFOA midday predicted concentration ranges. Days starting from January 1st until December 31st.

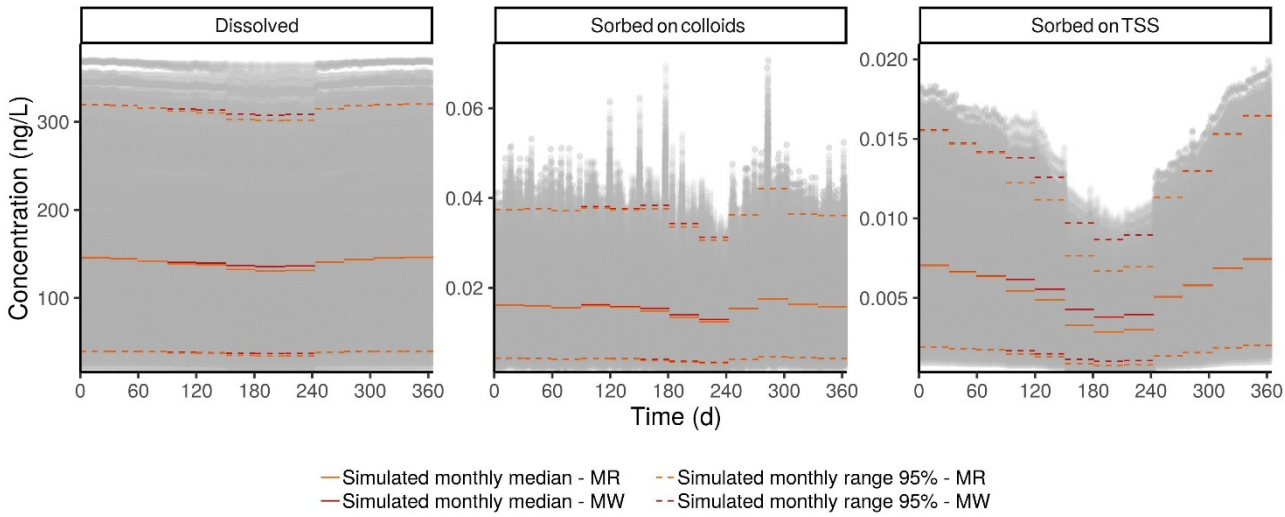


Figure S13. SMX midday predicted concentration ranges. Days starting from January 1st until December 31st.

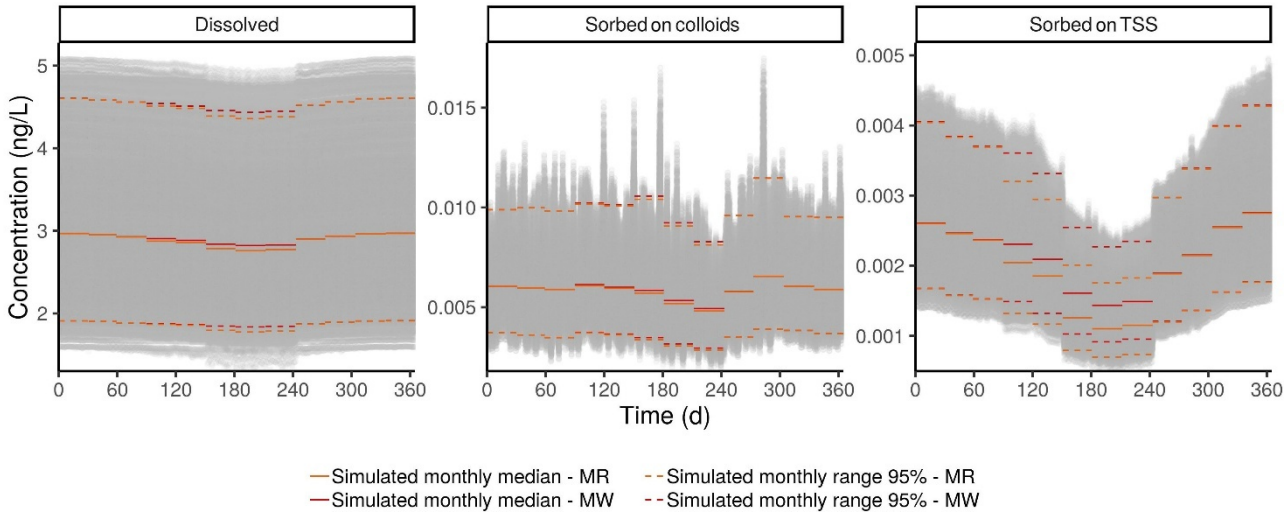


Figure S14. E2 midday predicted concentration ranges. Days starting from January 1st until December 31st.

### SI.6.3 Attenuation along the canal

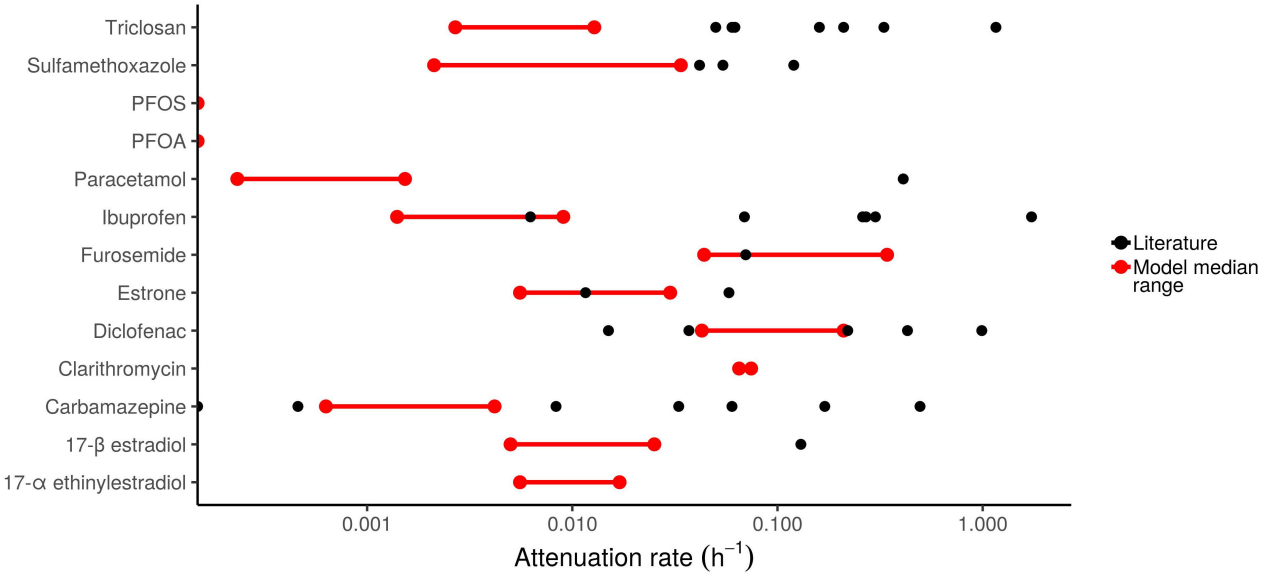


Figure S15. Predicted median attenuation rates compared to attenuation rates from literature. References: Acuña et al. (2015), Bester (2005), Fono et al. (2006), Guillet et al. (2019), Kunkel and Radke (2011), Lin et al. (2006), Morrall et al. (2004), Matamoros and Rodríguez (2017), Radke et al. (2010), Sabaliunas et al. (2003), Tixier et al. (2003), Williams et al. (2003), Writer et al. (2012, 2013).

### SI.6.4 Bioconcentration factors

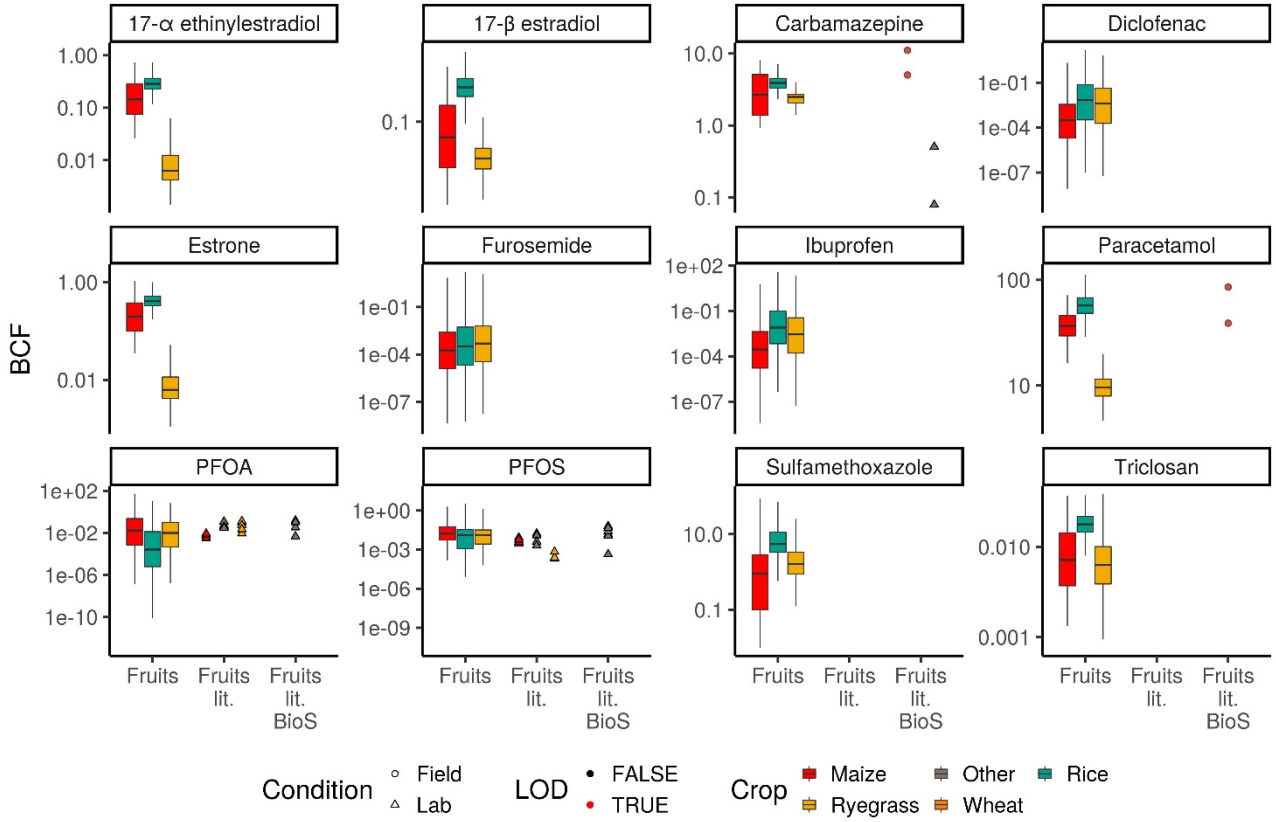


Figure S16. Fruit BCFs (gdw/gdw) for silage maize, winter wheat, ryegrass and rice with respect to maximum soil concentrations and literature (lit.) values. All simulated soils are shown. BioS indicates experimental studies conducted with the use of biosolids. Red borders indicate the use of an LOD value in the calculation of the BCF. References (including fruit BCFs in Figure 3): Blaine et al. (2013, 2014), Christou et al. (2017), Goldstein et al. (2014), Lechner and Knapp (2011), Mordechay et al. (2018), Navarro et al. (2017), Pannu et al. (2012), Prosser et al. (2014), Sabourin et al. (2012), Shenker et al. (2011), Stahl et al. (2009), Wen et al. (2014), Wu et al. (2010, 2012), Yager et al. (2014)

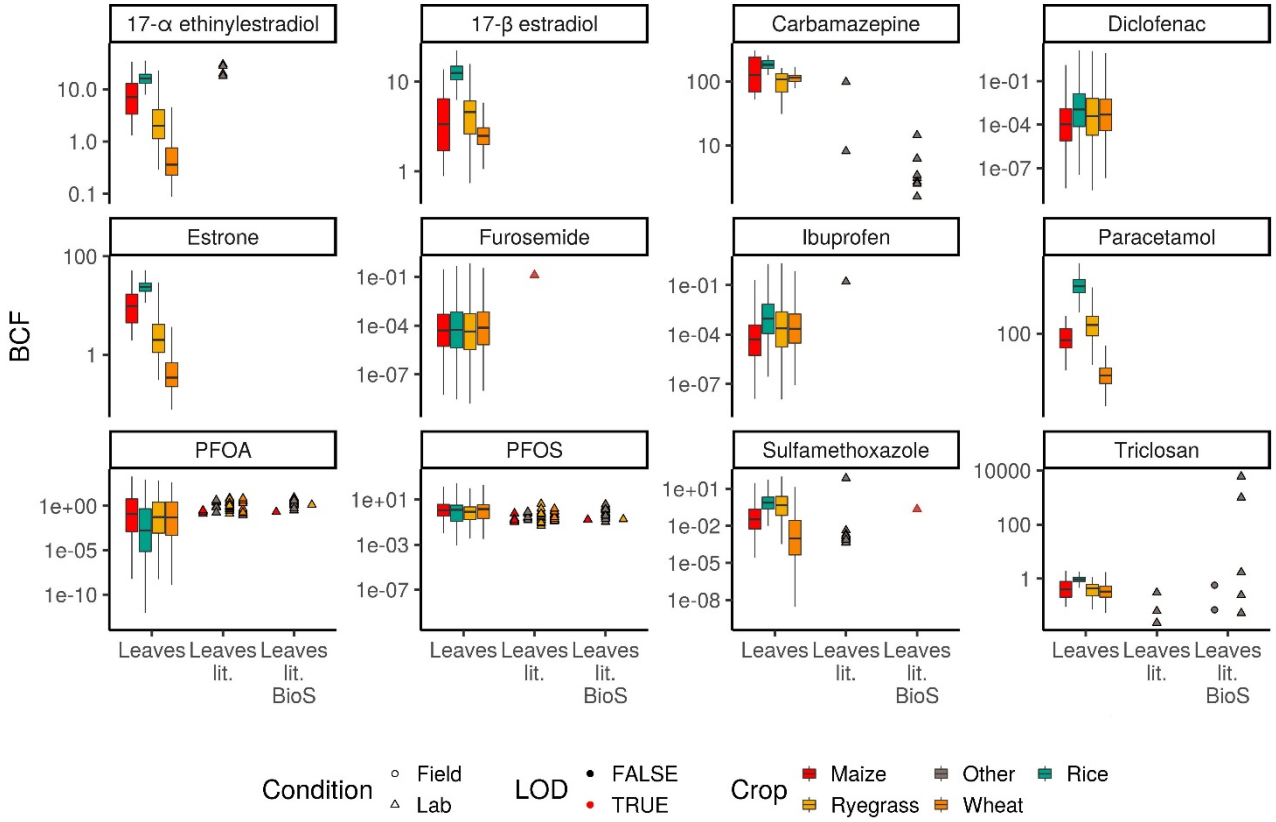


Figure S17. Leaf BCFs (gdw/gdw) for silage maize, winter wheat, ryegrass and rice with respect to maximum soil concentrations and literature (lit.) values. All simulated soils are shown. BioS indicates experimental studies conducted with the use of biosolids. Red borders indicate the use of an LOD value in the calculation of the BCF. References (including leaf BCFs in Figure 3): Aryal and Reinhold (2011), Bizkarguenaga et al. (2016), Blaine et al. (2013, 2014), Carter et al. (2014), Chitescu et al. (2012), Fu et al. (2016), Goldstein et al. (2014), Holling et al. (2012), Hurtado et al. (2017), Karnjanapiboonwong et al. (2011), Lechner and Knapp (2011), Macherius et al. (2012), Malchi et al. (2014), Mordechay et al. (2018), Navarro et al. (2017), Pannu et al. (2012), Prosser et al. (2014), Shenker et al. (2011), Stahl et al. (2009), Wen et al. (2014, 2016), Winker et al. (2010), Wu et al. (2010, 2012), Yoo et al. (2011), Zhao et al. (2014, 2017).

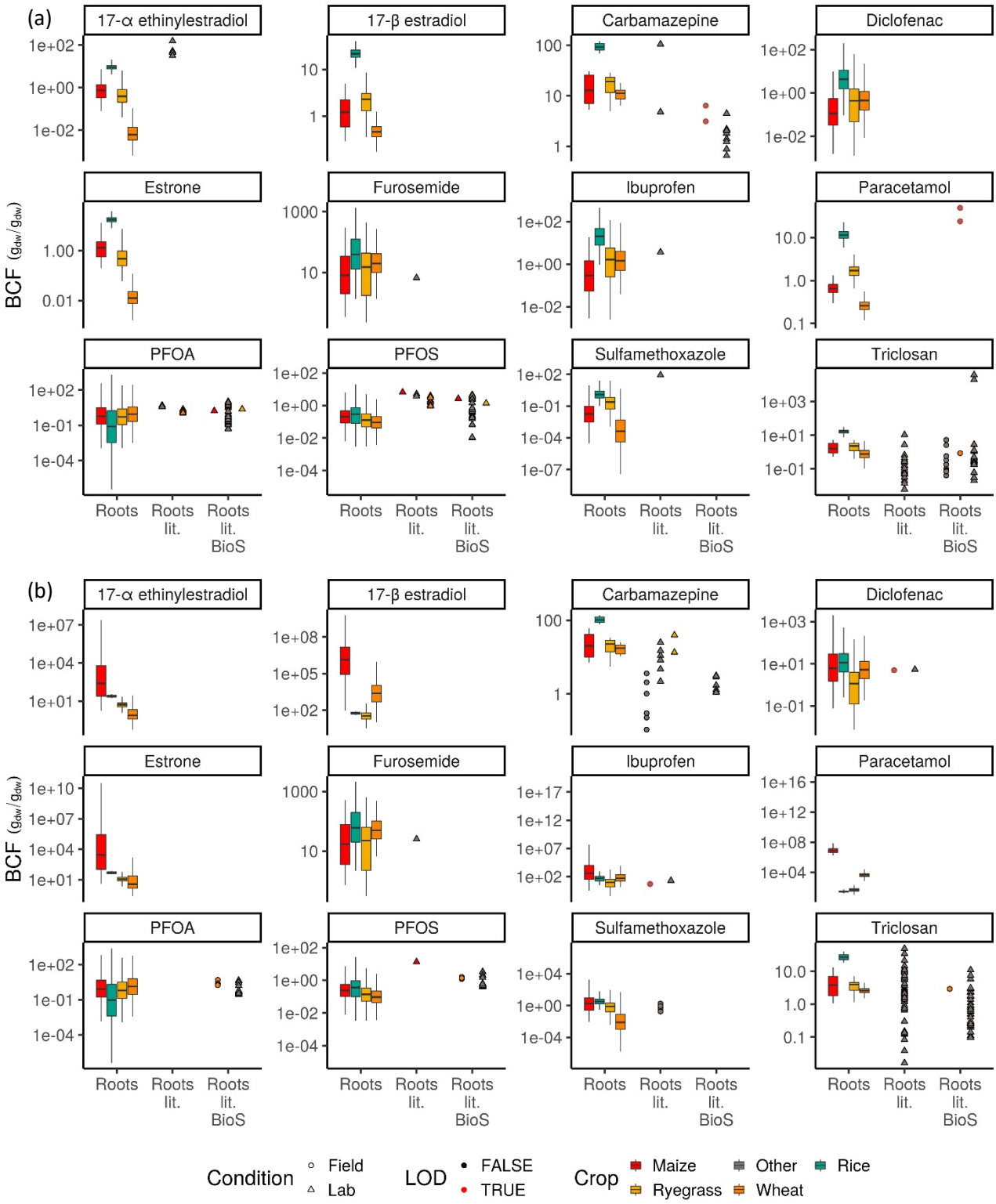


Figure S18. Root BCFs ($g_{dw}$ /$g_{dw}$) for silage maize, winter wheat, ryegrass and rice with respect to maximum (a) or median (b) soil concentrations and literature (lit.) values. All simulated soils are shown. BioS indicates experimental studies conducted with the use of biosolids. Red borders indicate the use of an LOD value in the calculation of the BCF. References: Aryal and Reinhold (2011), Bizkarguenaga et al. (2016), Blaine et al. (2014), Carter et al. (2014), Fu et al. (2016), Holling et al. (2012), Hurtado et al. (2017), Karnjanapiboonwong et al. (2011), Lechner and Knapp (2011), Macherius et al. (2012), Malchi et al. (2014), Pannu et al. (2012), Prosser et al. (2014), Sabourin et al. (2012), Shenker et al. (2011), Wen et al. (2014, 2016), Winker et al. (2010), Wu et al. (2010, 2012), Yager et al. (2014), Zhao et al. (2014, 2017).

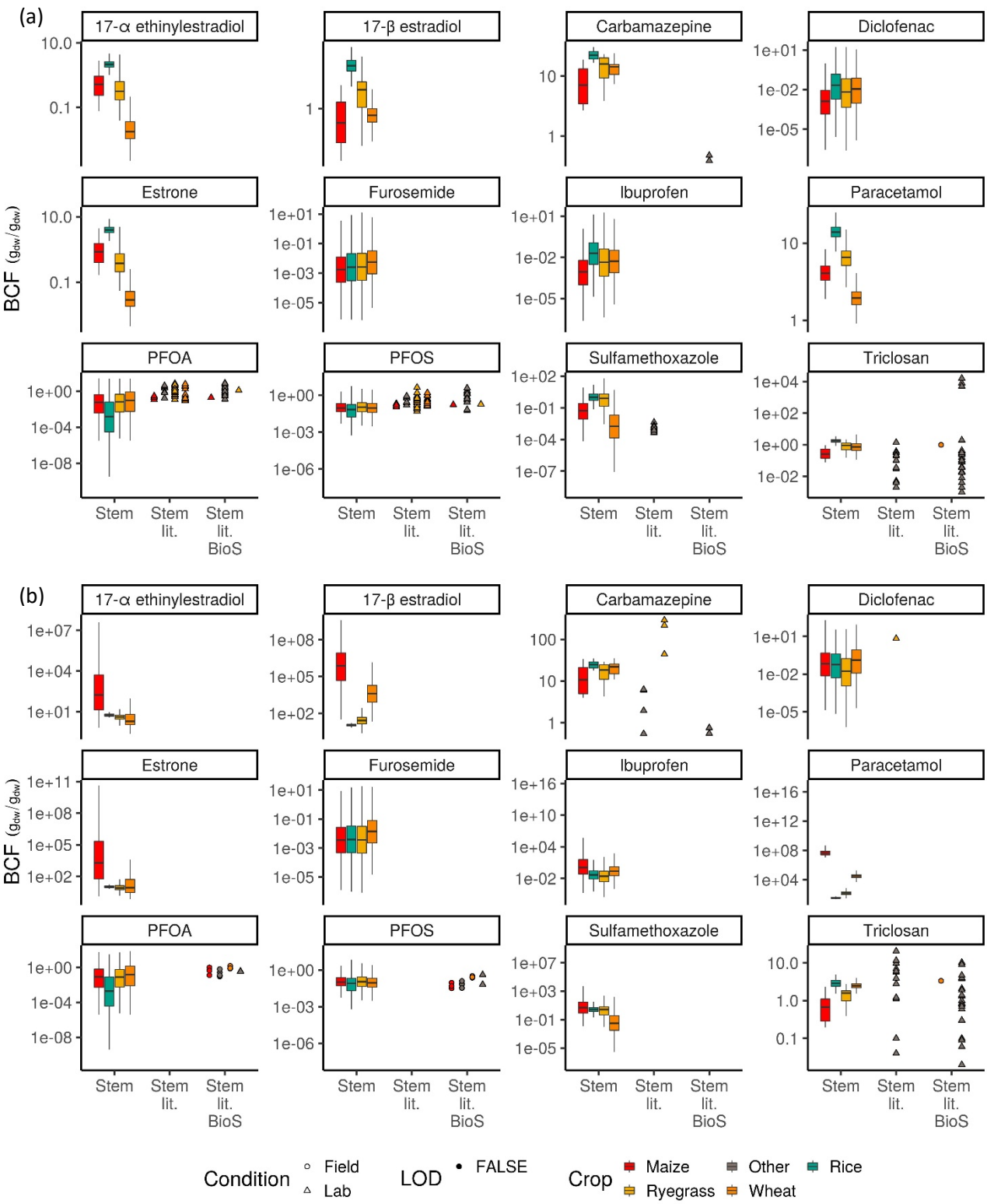


Figure S19. Stem BCFs ($g_{dw}/g_{dw}$) for silage maize, winter wheat, ryegrass and rice with respect to maximum (a) or median (b) soil concentrations and literature (lit.) values. All simulated soils are shown. BioS indicates experimental studies conducted with the use of biosolids. References: Aryal and Reinhold (2011), Blaine et al. (2013, 2014), Carter et al. (2014), Chitescu et al. (2012), Lechner and Knapp (2011), Navarro et al. (2017), Prosser et al. (2014), Shenker et al. (2011), Stahl et al. (2009), Wen et al. (2014, 2016), Winker et al. (2010), Wu et al. (2010), Yager et al. (2014), Yoo et al. (2011), Zhao et al. (2014, 2017).

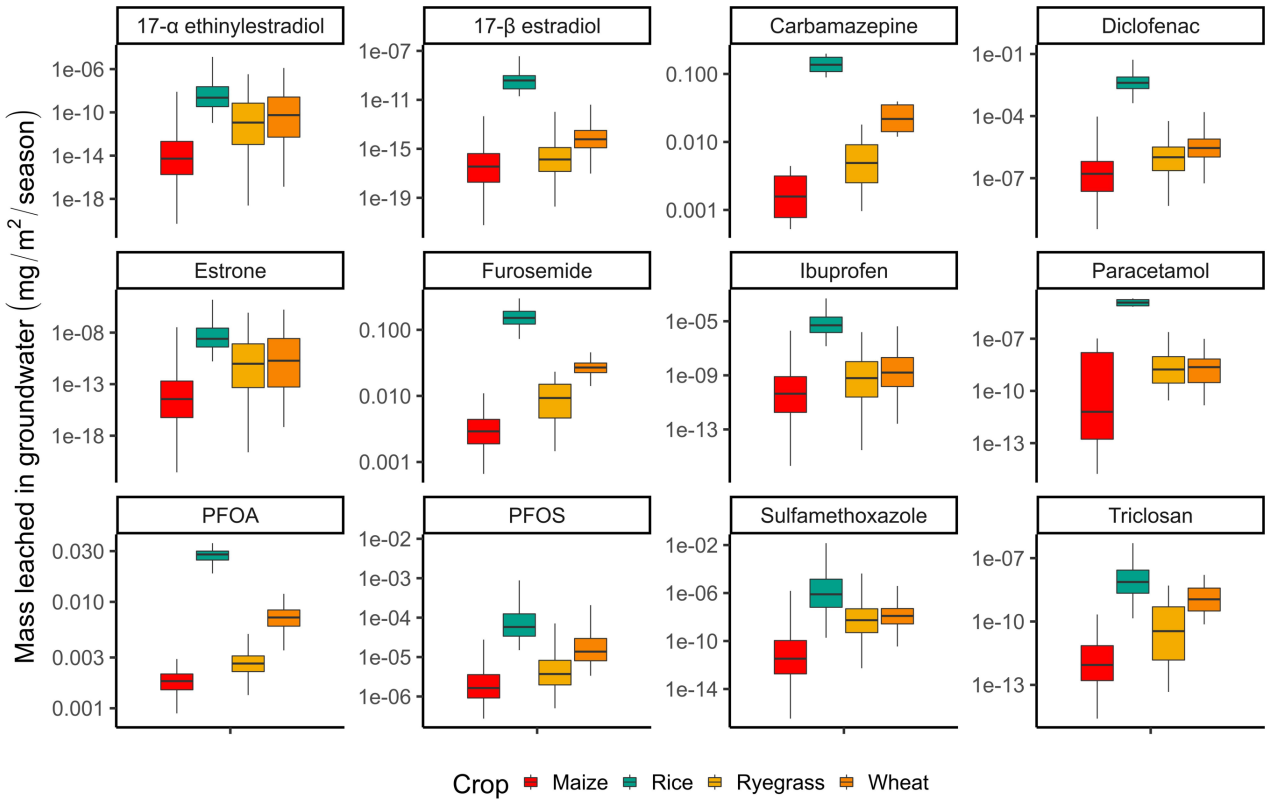


Figure S20. Total leached mass during each crop growing season.

## SI.7 Risk assessment

### SI.7.1 Environmental risk – Results

Table S22. Maximum, median and minimum RQs at the end of the canal and monthly frequency to exceed a given RQ.

| CEC | Max/Median/Min RQ | Monthly frequency of exceedance (%) | | | | | | | | | | | |
|---|---|---|---|---|---|---|---|---|---|---|---|---|---|
| | | Jan | Feb | Mar | Apr | May | Jun | Jul | Aug | Sept | Oct | Nov | Dec |
| RQ above 0.1 | | | | | | | | | | | | | |
| SMX | | | | | | | | | | | | | |
| | 0.42/0.16/0.018 | 74.1 | 73.9 | 73.5 | 73.5 | 73.4 | 72.7 | 72.4 | 72.6 | 73.7 | 73.9 | 74.2 | 74.1 |
| IBU | | | | | | | | | | | | | |
| | 0.15/0.07/0.021 | 16.9 | 16.7 | 16.5 | 16.4 | 16.3 | 15.9 | 15.8 | 15.9 | 16.2 | 16.4 | 16.7 | 16.8 |
| E1 | | | | | | | | | | | | | |
| | 0.25/0.14/0.046 | 91.7 | 91.5 | 91.3 | 90.8 | 90.5 | 89.2 | 88.4 | 88.8 | 90.6 | 91.2 | 91.5 | 91.7 |
| RQ above 1 | | | | | | | | | | | | | |
| CLA | | | | | | | | | | | | | |
| | 2.63/1.34/0.48 | 80 | 79.8 | 79.7 | 79.4 | 79 | 78.3 | 77.9 | 78 | 78.9 | 79.3 | 80 | 80.4 |
| EE2 | | | | | | | | | | | | | |
| | 45.88/26.74/12.86 | 100 | 100 | 100 | 100 | 100 | 100 | 100 | 100 | 100 | 100 | 100 | 100 |
| E2 | | | | | | | | | | | | | |
| | 2.57/1.48/0.65 | 95.8 | 95.6 | 95.4 | 95.1 | 94.9 | 94.1 | 93.6 | 93.8 | 95 | 95.3 | 95.7 | 95.8 |
| TCS | | | | | | | | | | | | | |
| | 2.56/1.43/0.44 | 77.9 | 77.7 | 77.6 | 77.3 | 77.1 | 76.5 | 76.5 | 76.6 | 77.3 | 77.6 | 77.7 | 77.9 |

### SI.7.2 Human health risk – Methods

Following the precautionary principle, human health risk was calculated with the assumption of no degradation between harvest and consumption and the complete bioaccessibility and bioavailability of the ingested CECs.
To calculate the ingestion required to exceed the threshold of toxicological concern (*TTC*), *TTC* was set equal to 30, 9.1, 1.5 and 0.0025 μg $kg_{bw}^{-1}$ $d^{-1}$, depending on the Cramer classes (I, II and III or genotoxic alerts) which the CEC belongs to (Kroes et al., 2004; Malchi et al., 2014).
Regarding the calculation of the hazard quotient (HQ), the ADI values were either found in Prosser and Sibley (2015) or in the reports produced by EFSA (2008), Environment Protection and Heritage Council of Australia (2008) and EMEA (2000) and, eventually, corrected as reported in Malchi et al. (2015).

### SI.7.3 Human health risk – Results

Table S23. Consumption (kg/d) required to exceed TTC for crops irrigated with water withdrawn at the end of the canal. P97.5 stands for values calculated with the 97.5$^{th}$ percentile CEC concentration.

| CEC | Infants | | | | Adults | | | |
|---|---|---|---|---|---|---|---|---|
| | Rice | | Wheat | | Rice | | Wheat | |
| | Median | P97.5 | Median | P97.5 | Median | P97.5 | Median | P97.5 |
| SMX | 0.07 | 0.01 | 1.92 | 0.23 | 0.38 | 0.05 | 11.2 | 1.32 |
| DCF | > 100 | 73.51 | > 100 | > 100 | > 100 | > 100 | > 100 | > 100 |
| IBU | > 100 | > 100 | > 100 | > 100 | > 100 | > 100 | > 100 | > 100 |
| PAR | 3.06 | 2.08 | 72.22 | 44.84 | 17.83 | 12.15 | > 100 | > 100 |
| CBZ | 8.59 | 5.77 | 19.03 | 15.06 | 50.12 | 33.65 | > 100 | 87.84 |
| FUR | > 100 | > 100 | > 100 | > 100 | > 100 | > 100 | > 100 | > 100 |
| PFOA | > 100 | > 100 | > 100 | > 100 | > 100 | > 100 | > 100 | > 100 |
| PFOS | > 100 | > 100 | > 100 | > 100 | > 100 | > 100 | > 100 | > 100 |
| TCS | > 100 | > 100 | > 100 | > 100 | > 100 | > 100 | > 100 | > 100 |

Table S24. HQs and His for crops irrigated with water withdrawn at the end of the canal. P97.5 stands for values calculated with the 97.5$^{th}$ percentile CEC concentration.

| CEC | Rice | | Wheat | | Total | |
|---|---|---|---|---|---|---|
| | Median | P97.5 | Median | P97.5 | Median | P97.5 |
| Infants | | | | | | |
| SMX | 2.94E-03 | 2.03E-02 | 1.86E-04 | 1.58E-03 | 3.12E-03 | 2,19E-02 |
| DCF | 2.66E-06 | 6.35E-04 | 6.14E-08 | 1.26E-05 | 2.72E-06 | 6.48E-04 |
| IBU | 1.12E-09 | 5.27E-07 | 1.21E-10 | 5.94E-08 | 1.24E-09 | 5.86E-07 |
| PAR | 7.12E-07 | 1.05E-06 | 5.64E-08 | 9.08E-08 | 7.69E-07 | 1.14E-06 |
| CBZ | 2.62E-03 | 3.91E-03 | 2.21E-03 | 2.80E-03 | 4.84E-03 | 6.71E-03 |
| FUR | 5.37E-08 | 8.49E-05 | 1.25E-07 | 9.82E-05 | 1.79E-07 | 1.83E-04 |
| EE2 | 2.77E-02 | 2.57E-01 | 1.95E-03 | 3.85E-02 | 2.97E-02 | 2.95E-01 |
| E2 | 1.07E-05 | 2.53E-05 | 8.72E-07 | 2.02E-06 | 1.15E-05 | 2.73E-05 |
| E1 | 5.23E-04 | 4.82E-03 | 4.06E-05 | 7.80E-04 | 5.63E-04 | 5.60E-03 |
| PFOS | 6.98E-06 | 2.75E-04 | 5.44E-06 | 1.24E-04 | 1.24E-05 | 4.00E-04 |
| PFOA | 2.23E-08 | 1.22E-04 | 1.17E-06 | 2.66E-04 | 1.19E-06 | 3.88E-04 |
| TCS | 6.19E-09 | 1.79E-08 | 2.57E-09 | 1.04E-08 | 8.76E-09 | 2.83E-08 |
| | | | | Hazard Index | 3.82E-02 | 3.31E-01 |
| Adults | | | | | | |
| SMX | 4.45E-04 | 3.08E-03 | 8.88E-05 | 7.52E-04 | 5.34E-04 | 3.83E-03 |
| DCF | 4.03E-07 | 9.63E-05 | 2.93E-08 | 6.03E-06 | 4.33E-07 | 1.02E-04 |
| IBU | 1.70E-10 | 7.99E-08 | 2.93E-08 | 6.03E-06 | 2.27E-10 | 1.80E-07 |
| PAR | 1.08E-07 | 1.59E-07 | 2.69E-08 | 4.33E-08 | 1.35E-07 | 2.20E-07 |
| CBZ | 3.98E-04 | 5.93E-04 | 1.06E-03 | 1.33E-03 | 1.45E-03 | 1.93E-03 |
| FUR | 8.14E-09 | 1.29E-05 | 5.96E-08 | 4.69E-05 | 6.78E-08 | 5.97E-05 |
| EE2 | 4.20E-03 | 3.89E-02 | 9.32E-04 | 1.84E-02 | 5.13E-03 | 5.73E-02 |
| E2 | 1.62E-06 | 3.84E-06 | 4.16E-07 | 9.63E-07 | 2.03E-06 | 4.80E-06 |
| E1 | 7.93E-05 | 7.30E-04 | 1.94E-05 | 3.72E-04 | 9.86E-05 | 1.10E-03 |
| PFOS | 1.06E-06 | 1.31E-04 | 2.60E-06 | 5.94E-05 | 3.65E-06 | 1.90E-04 |
| PFOA | 3.38E-09 | 1.85E-05 | 5.58E-07 | 1.27E-04 | 5.62E-07 | 1.46E-04 |
| TCS | 9.38E-10 | 2.71E-09 | 1.23E-09 | 4.96E-09 | 2.17E-09 | 7.67E-09 |
| | | | | Hazard Index | 7.22E-03 | 6.47E-02 |

## Reference

Abraha, M. G., Savage, M. J. (2008). The soil water balance of rainfed and irrigated oats, Italian rye grass and rye using the CropSyst model. Irrigation Science, 26(3), 203–212.

Acuña, V., von Schiller, D., García-Galán, M. J., Rodríguez-Mozaz, S., Corominas, L., Petrovic, M., Sabater, S. (2015). Occurrence and in-stream attenuation of wastewater-derived pharmaceuticals in Iberian rivers. Science of the Total Environment, 503–504, 133–141.

Adamek, E., Baran, W., Sobczak, A. (2016). Assessment of the biodegradability of selected sulfa drugs in two polluted rivers in Poland: Effects of seasonal variations, accidental contamination, turbidity and salinity. Journal of Hazardous Materials, 313, 147–158.

Ahrens, L., Harner, T., Shoeib, M., Lane, D. A., Murphy, J. G. (2012). Improved characterization of gas-particle partitioning for per- and polyfluoroalkyl substances in the atmosphere using annular diffusion denuder samplers. Environmental Science and Technology, 46(13), 7199–7206.

Aymerich, I., Acuña, V., Ort, C., Rodríguez-Roda, I., Corominas, L. (2017). Fate of organic microcontaminants in wastewater treatment and river systems: An uncertainty assessment in view of sampling strategy, and compound consumption rate and degradability. Water Res. 125, 152–161.

Al-Ahmad, A., Daschner, F. D., Kümmerer, K. (1999). Biodegradability of cefotiam, ciprofloxacin, meropenem, penicillin G, and sulfamethoxazole and inhibition of waste water bacteria. Archives of Environmental Contamination and Toxicology, 37(2), 158–163.

Alexy, R., Kümpel, T., Kümmerer, K. (2004). Assessment of degradation of 18 antibiotics in the Closed Bottle Test. Chemosphere, 57(6), 505–512.

Allen, R., Pereira, L. S., Raes, D., Smith, M. (1998). Crop Evapotranspiration - Guidelines for computing crop water requirements - FAO Irrigation and Drainage paper. Rome, Italy.

Andreozzi, R., Marotta, R., Paxéus, N. (2003). Pharmaceuticals in STP effluents and their solar photodegradation in aquatic environment. Chemosphere, 50(10), 1319–1330.

Arp, H. P. H., Niederer, C., Goss, K. (2006). Predicting the Partitioning Behavior of Various Highly Fluorinated. Environmental Science and Technology, 40(23), 7298–7304.

Aryal, N., Reinhold, D. M. (2011). Phytoaccumulation of antimicrobials from biosolids: Impacts on environmental fate and relevance to human exposure. Water Research, 45(17), 5545–5552.

Asano, T. (2002). Water from (waste)water - the dependable water resource. Water Science and Technology, 45(8):23-33.

Atkinson, S. K., Marlatt, V. L., Kimpe, L. E., Lean, D. R. S., Trudeau, V. L., Blais, J. M. (2011). Environmental factors affecting ultraviolet photodegradation rates and estrogenicity of estrone and ethinylestradiol in natural waters. Archives of Environmental Contamination and Toxicology, 60(1), 1–7.

Baena-Nogueras, R. M., González-Mazo, E., Lara-Martín, P. A. (2017). Degradation kinetics of pharmaceuticals and personal care products in surface waters: photolysis vs biodegradation. Science of the Total Environment, 590–591, 643–654.

Bach, P. M., Rauch, W., Mikkelsen, P. S., McCarthy, D. T., and Deletic, A. (2014). A critical review of integrated urban water modelling: Urban drainage and beyond. Environmental Modelling and Software, 54(4):88-107.

Bahlmann, A., Brack, W., Schneider, R.J. and Krauss, M. (2014) Carbamazepine and its metabolites in wastewater: Analytical pitfalls and occurrence in Germany and Portugal. Water Res 57, 104-114.

Bahnmüller, S., von Gunten, U., Canonica, S. (2014). Sunlight-induced transformation of sulfadiazine and sulfamethoxazole in surface waters and wastewater effluents. Water Research, 57, 183–192.

Barron, L., Havel, J., Purcell, M., Szpak, M., Kelleher, B., Paull, B. (2009). Predicting sorption of pharmaceuticals and personal care products onto soil and digested sludge using artificial neural networks. Analyst, 134(4), 663–670.

Beesoon, S., Martin, J. W. (2015). Isomer-Specific Binding Affinity of Perfluorooctanesulfonate (PFOS) and Perfluorooctanoate (PFOA) to Serum Proteins. Environmental Science & Technology, 49(9), 5722–5731.

Beck, M.B. (1976). Dynamic modelling and control applications in water quality maintenance. Water Res. 10, 575–595.

Ben Mordechay, E., Tarchitzky, J., Chen, Y., Shenker, M., Chefetz, B. (2018). Composted biosolids and treated wastewater as sources of pharmaceuticals and personal care products for plant uptake: A case study with carbamazepine. Environmental Pollution, 232, 164–172.

Benedetti, L., Meirlaen, J., Sforzi, F., Facchi, A., Gandolfi, C., & Vanrolleghem, P. A. (2004). Dynamic integrated modelling: a case study on the river Lambro. Novatech 2004, 1–8.

Bester, K. (2005). Fate of triclosan and triclosan-methyl in sewage treatment plants and surface waters. Archives of Environmental Contamination and Toxicology, 49(1), 9–17.

Bhhatarai, B., Gramatica, P. (2011). Prediction of Aqueous Solubility, Vapor Pressure and Critical Micelle Concentration for Aquatic Partitioning of Perfluorinated Chemicals. Environmental Science & Technology, 45(19), 8120–8128.

Bischel, H. N., MacManus-Spencer, L. A., Luthy, R. G. (2010). Noncovalent Interactions of Long-Chain Perfluoroalkyl Acids with Serum Albumin. Environmental Science & Technology, 44(13), 5263–5269.

Bizkarguenaga, E., Zabaleta, I., Mijangos, L., Iparraguirre, A., Fernández, L. A., Prieto, A., Zuloaga, O. (2016). Uptake of perfluorooctanoic acid, perfluorooctane sulfonate and perfluorooctane sulfonamide by carrot and lettuce from compost amended soil. Science of the Total Environment, 571, 444–451.

Blaine, A. C., Rich, C. D., Hundal, L. S., Lau, C., Mills, M. A., Harris, K. M., Higgins, C. P. (2013). Uptake of perfluoroalkyl acids into edible crops via land applied biosolids: Field and greenhouse studies. Environmental Science and Technology, 47(24), 14062–14069.

Blaine, A. C., Rich, C. D., Sedlacko, E. M., Hundal, L. S., Kumar, K., Lau, C., … Higgins, C. P. (2014). Perfluoroalkyl acid distribution in various plant compartments of edible crops grown in biosolids-amended soils. Environmental Science and Technology, 48(14), 7858–7865.

Boles Ponto, L.L., Schoenwald, R.D. (1990). Furosemide (Frusemide) A Pharmacokinetic/Pharmacodynamic Review (Part I). Clin. Pharmacokinet. 18, 381–408.

Bonvin, F., Omlin, J., Rutler, R., Schweizer, W. B., Alaimo, P. J., Strathmann, T. J., … Kohn, T. (2013). Direct photolysis of human metabolites of the antibiotic sulfamethoxazole: Evidence for abiotic back-transformation. Environmental Science and Technology, 47(13), 6746–6755.

Boreen, A. L., Arnold, W. A., McNeill, K. (2004). Photochemical fate of sulfa drugs in then aquatic environment: Sulfa drugs containing five-membered heterocyclic groups. Environmental Science and Technology, 38(14), 3933–3940.

Borrelli, L., Castelli, F., Ceotto, E., Cabassi, G., & Tomasoni, C. (2014). Maize grain and silage yield and yield stability in a long-term cropping system experiment in northern italy. European Journal of Agronomy, 55, 12–19.

Bottoni, P., Caroli, S., Caracciolo, A.B., (2010). Pharmaceuticals as priority water contaminants. Toxicol. Environ. Chem. 92, 549–565.

Brace, N. O. (1962). Long Chain Alkanoic and Alkenoic Acids with Perfluoroalkyl Terminal Segments. Journal of Organic Chemistry, 27(12), 4491–4498.

Bradley, P. M., Barber, L. B., Chapelle, F. H., Gray, J. L., Kolpin, D. W., McMahon, P. B. (2009). Biodegradation of 17beta-estradiol, estrone and testosterone in stream sediments. Environmental Science & Technology, 43(6), 1902–1910.

Brenna, S., Rocca, A., Sciaccaluga, Ma., Valagussa, M. (2010). SOILQUALIMON - Sistema di monitoraggio della qualità dei suoli in Lombardia. In Quaderni della Ricerca (Vol. 110).

Brian, J. V., Harris, C.A., Scholze, M., Backhaus, T., Booy, P., Lamoree, M., Pojana, G., Jonkers, N., Runnalls, T., Bonfà, A., Marcomini, A., Sumpter, J.P. (2005). Accurate prediction of the response of freshwater fish to a mixture of estrogenic chemicals. Environ. Health Perspect. 113, 721–728.

Brooke, D., Footitt, A., Nwaogu, T. A. (2004). Environmental Risk Evaluation Report: Perfluorooctanesulphonate (PFOS). In Environment Agency.

Brouwer, C., Hoevenaars, J.P.M. & Van Bosch, B.E., (1992) Scheme Irrigation Water Needs and Supply. Rome, Italy: FAO.

Brudler, S., Rygaard, M., Arnbjerg-Nielsen, K., Hauschild, M.Z., Ammitsøe, C., Vezzaro, L. (2019). Pollution levels of stormwater discharges and resulting environmental impacts. Sci. Total Environ. 663, 754–763.

Burns, D. C., Ellis, D. A., Webster, E., McMurdo, C. J. (2009). Response to Comment on "Experimental p K a Determination for Perfluorooctanoic Acid (PFOA) and the Potential Impact of p K a Concentration Dependence on Laboratory-Measured Partitioning Phenomena and Environmental Modeling." Environmental Science & Technology, 43(13), 5152–5154.

Buser, H. R., Poiger, T., Muller, M. D. (1999). Occurrence and environmental behavior of the chiral pharmaceutical drug ibuprofen in surface waters and in wastewater. Environmental Science and Technology, 33(15), 2529–2535.

Buser, H. R., Poiger, T., Müller, M. D. (1998). Occurrence and fate of the pharmaceutical drug diclofenac in surface waters: Rapid photodegradation in a lake. Environmental Science and Technology, 32(22), 3449–3456.

Butler, D. and Davies J.W. (2004). Urban Drainage (Second edition). CRC Press, London, UK.

Caldwell, D. J., Mastrocco, F., Anderson, P. D., Länge, R., Sumpter, J. P. (2012). Predicted-no-effect concentrations for the steroid estrogens estrone, 17β-estradiol, estriol, and 17α-ethinylestradiol. Environmental Toxicology and Chemistry, 31(6), 1396–1406.

Calza, P., Medana, C., Padovano, E., Giancotti, V., Minero, C. (2013). Fate of selected pharmaceuticals in river waters. Environmental Science and Pollution Research, 20(4), 2262–2270.

Candelieri, A. and Archetti, F. (2014). Identify typical urban water demand pattern for a reliable short-term forecasting – The icewater project approach. Procedia Engineering, 89, 1004–1012.

Carlos, L., Mártire, D. O., Gonzalez, M. C., Gomis, J., Bernabeu, A., Amat, A. M., Arques, A. (2012). Photochemical fate of a mixture of emerging pollutants in the presence of humic substances. Water Research, 46(15), 4732–4740.

Carr, D. L., Morse, A. N., Zak, J. C., Anderson, T. A. (2011). Biological degradation of common pharmaceuticals and personal care products in soils with high water content. Water, Air, and Soil Pollution, 217(1–4), 127–134.

Carter, L. J., Harris, E., Williams, M., Ryan, J. J., Kookana, R. S., Boxall, A. B. A. (2014). Fate and Uptake of Pharmaceuticals in Soil–Plant Systems. Journal of Agricultural and Food Chemistry, 62(4), 816–825.

Castiglioni, S., Bagnati, R., Fanelli, R., Pomati, F., Calamari, D., & Zuccato, E. (2006). Removal of pharmaceuticals in sewage treatment plants in Italy. Environmental Science and Technology, 40(1), 357–363.

Castiglioni, S., Bijlsma, L., Covaci, A., Emke, E., Hernández, F., Reid, M., Ort, C., Thomas, K.V., van Nuijs, A.L.N., de Voogt, P., Zuccato, E. (2012). Evaluation of uncertainties associated with the determination of community drug use through the measurement of sewage drug biomarkers. Environmental Science and Technology, 47, 1452–1460.

Castiglioni, S., Davoli, E., Riva, F., Palmiotto, M., Camporini, P., Manenti, A., & Zuccato, E. (2018a). Data on occurrence and fate of emerging contaminants in a urbanised area. Data in Brief, 17, 533–543.

Castiglioni, S., Davoli, E., Riva, F., Palmiotto, M., Camporini, P., Manenti, A., & Zuccato, E. (2018b). Mass balance of emerging contaminants in the water cycle of a highly urbanized and industrialized area of Italy. Water Research, 131:287-298.

Caupos, E., Mazellier, P., Croue, J. P. (2011). Photodegradation of estrone enhanced by dissolved organic matter under simulated sunlight. Water Research, 45(11), 3341–3350.

Celiz, M.D., Tso, J., Aga, D.S. (2009). Pharmaceutical metabolites in the environment: Analytical challenges and ecological risks. Environ. Toxicol. Chem. 28, 2473–2484.

Challis, J. K., Hanson, M. L., Friesen, K. J., Wong, C. S. (2014). A critical assessment of the photodegradation of pharmaceuticals in aquatic environments: defining our current understanding and identifying knowledge gaps. Environmental Science: Processes & Impacts, 16(4), 672–696.

Chapra, S. C. (1997). Surface Water-Quality Modeling. In McGraw-Hill Series in Water Resources and Environmental Engineering.

Chen, Y. M., Guo, L. H. (2009). Fluorescence study on site-specific binding of perfluoroalkyl acids to human serum albumin. Archives of Toxicology, 83(3), 255–261.

Chen, W., Xu, J., Lu, S., Jiao, W., Wu, L., & Chang, A. C. (2013). Fates and transport of PPCPs in soil receiving reclaimed water irrigation. Chemosphere, 93(10), 2621–2630.

Chowdhury, R. R., Charpentier, P. A., Ray, M. B. (2011). Photodegradation of 17β-estradiol in aquatic solution under solar irradiation: Kinetics and influencing water parameters. Journal of Photochemistry and Photobiology A: Chemistry, 219(1), 67–75.

Chowdhury, R. R., Charpentier, P., Ray, M. B. (2010). Photodegradation of estrone in solar irradiation. Industrial and Engineering Chemistry Research, 49(15), 6923–6930.

Christou, A., Agüera, A., Bayona, J.M., Cytryn, E., Fotopoulos, V., Lambropoulou, D., Manaia, C.M., Michael, C., Revitt, M., Schröder, P., Fatta-Kassinos, D. (2017). The potential implications of reclaimed wastewater reuse for irrigation on the agricultural environment: The knowns and unknowns of the fate of antibiotics and antibiotic resistant bacteria and resistance genes – A review. Water Res. 123:448-467.

Collins, C., Fryer, M., and Grosso, A. (2006). Plant uptake of non-ionic organic chemicals. Environmental Science and Technology, 40(1):45-52.

Colucci, M. S., Bork, H., Topp, E. (2001). Persistence of estrogenic hormones in agricultural soils: I. 17Beta-estradiol and estrone. J Environ Qual, 30(6), 2070–2076.

Colucci, M. S., Topp, E. (2002). Dissipation of part per trillion concentrations of estrogenic hormones from agricultural soils. Canadian Journal of Soil Science, 82(3), 335–340.

Colucci, M. S., Topp, E. (2001). Persistence of Estrogenic Hormones in Agricultural Soils: II. 17alpha-Ethynylestradiol. Journal of Environment Quality, 30(6), 2077–2080.

Confalonieri, R., Bocchi, S. (2005). Evaluation of CropSyst for simulating the yield of flooded rice in northern Italy. European Journal of Agronomy, 23(4), 315–326.

Conkle, J. L., Gan, J., Anderson, M. A. (2012). Degradation and sorption of commonly detected PPCPs in wetland sediments under aerobic and anaerobic conditions. Journal of Soils and Sediments, 12(7), 1164–1173.

COM (2015) 614 Closing the loop- An EU action plan for the Circular Economy. Communication from the Commission to the European Parliament, the Council, the European Economic and Social Committee and the Committee of the Regions. European Commission, Brussels, Belgium.

COM (2018) 337 Proposal for a REGULATION OF THE EUROPEAN PARLIAMENT AND OF THE COUNCIL on minimum requirements for water reuse. Proposal from the Commission to the European Parliament, the Council, the European Economic and Social Committee and the Committee of the Regions. European Commission, Brussels, Belgium.

Cormen, T. H., Leiserson, C. E., Rivest, R. L., Stein, C. (2001). Dijkstra's algorithm. Introduction to Algorithms (Second ed.). MIT Press and McGraw–Hill, 595-601.

Coutu, S., Wyrsch, V., Wynn, H.K., Rossi, L., Barry, D.A. (2013). Temporal dynamics of antibiotics in wastewater treatment plant influent. Sci. Total Environ. 458, 20–26.

Coutu, S., Pouchon, T., Queloz, P., Vernaz, N., (2016). Integrated stochastic modeling of pharmaceuticals in sewage networks. Stoch. Environ. Res. Risk Assess. 30, 1087–1097.

Czajka, C. P., Londry, K. L. (2006). Anaerobic biotransformation of estrogens. Science of the Total Environment, 367(2–3), 932–941.

D'Ascenzo, G., Di Corcia, A., Gentili, A., Mancini, R., Mastropasqua, R., Nazzari, M., Samperi, R. (2003). Fate of natural estogen conjugates in municipal sewage transport and treatment facilities. Science of the Total Environment, 320, 199–209.

Daughton, C. G. and Ternes, T. A. (1999). Pharmaceuticals and personal care products in the environment: agents of subtle change? Environmental Health Perspectives, 107(suppl 6):907-938.

Davidsen, S., Löwe, R., Thrysøe, C., Arnbjerg-Nielsen, K. (2017). Simplification of one-dimensional hydraulic networks by automated processes evaluated on 1D/2D deterministic flood models. Journal of Hydroinformatics, 19, 686–700.

Decision (EU) 2015/495 of 20 March 2015 establishing a watch list of substances for Union-wide monitoring in the field of water policy pursuant to Directive 2008/105/EC of the European Parliament and of the Council.

Decision (EU) 2018/840 of 5 June 2018 establishing a watch list of substances for Union-wide monitoring in the field of water policy pursuant to Directive 2008/105/EC of the European Parliament and of the Council and repealing Commission Implementing Decision (EU) 2015/495.

De Laurentiis, E., Chiron, S., Kouras-Hadef, S., Richard, C., Minella, M., Maurino, V., … Vione, D. (2012). Photochemical fate of carbamazepine in surface freshwaters: Laboratory measures and modeling. Environmental Science and Technology, 46(15), 8164–8173.

De Laurentiis, E., Prasse, C., Ternes, T. A., Minella, M., Maurino, V., Minero, C., … Vione, D. (2014). Assessing the photochemical transformation pathways of acetaminophen relevant to surface waters: Transformation kinetics, intermediates, and modelling. Water Research, 53, 235–248.

Delli Compagni, R., Polesel, F., von Borries, K.J.F., Zhang, Z., Turolla, A., Antonelli, M., Vezzaro, L., 2019. Modelling micropollutant fate in sewer systems – A new systematic approach to support conceptual model construction based on in-sewer hydraulic retention time. J. Environ. Manage. 246, 141–149.

Delli Compagni, R., Gabrielli, M., Polesel, F., Turolla, A., Trapp, S., Vezzaro, L., Antonelli, M. (2020). Risk assessment of contaminants of emerging concern in the context of wastewater reuse for irrigation: An integrated modelling approach. Chemosphere 242.

De Keyser, W., Gevaert, V., Verdonck, F., Nopens, I., De Baets, B., Vanrolleghem, P.A., Mikkelsen, P.S., Benedetti, L., (2010). Combining multimedia models with integrated urban water system models for micropollutants. Water Sci. Technol. 62, 1614–1622.

De Mes, T., Zeeman, G., Lettinga, G. (2005). Occurrence and fate of estrone, 17β-estradiol and 17α-ethynylestradiol in STPs for domestic wastewater. Reviews in Environmental Science and Bio/Technology, (4), 275–311.

De Schepper, V. C. J., Holvoet, K. M. A., Benedetti, L., Seuntjens, P., & Vanrolleghem, P. A. (2012). Extension of the River Water Quality Model No. 1 with the fate of pesticides. Journal of Hydroinformatics, 14(1), 48–64.

Deksissa, T., Meirlaen, J., Ashton, P. J., & Vanrolleghem, P. A. (2004). Simplifying dynamic river water quality modelling: A case study of inorganic nitrogen dynamics in the Crocodile River (South Africa). Water, Air, and Soil Pollution, 155(1–4), 303–320.

Ding, Y., Hayes, M. J., and Widhalm, M. (2011). Measuring economic impacts of drought: A review and discussion. Disaster Prevention and Management, 20(4):434-446.

Ding, G., Peijnenburg, W. J. G. M. (2013). Physicochemical Properties and Aquatic Toxicity of Poly- and Perfluorinated Compounds. Critical Reviews in Environmental Science and Technology, 43(6), 598–678.

Directive, 2008. 2008/105/EC of the European Parliament and of the Council of 16 December 2008 on environmental quality standards in the field ofwater policy, amending and subsequently repealing Council Directives 82/176/EEC, 83/513/ EEC, 84/156/EEC, 84/491/EEC, 86/280/EEC and amending Directive 2000/60/EC of

Directive, 2013. 2013/39/EU of the European Parliament and of the Council of 12 August 2013 amending Directives 2000/60/EC and 2008/105/EC as regards priority substances in the field of water policy. Off. J. Eur. Union L226, 1e17.

Dodgen, L. K., Ueda, A., Wu, X., Parker, D. R., and Gan, J. (2015). Effect of transpiration on plant accumulation and translocation of PPCP/EDCs. Environmental Pollution, 198:144-153.

Doll, T. E., Frimmel, F. H. (2003). Fate of pharmaceuticals - Photodegradation by simulated solar UV-light. Chemosphere, 52(10), 1757–1769.

Dong, M. M., Trenholm, R., Rosario-Ortiz, F. L. (2015). Photochemical degradation of atenolol, carbamazepine, meprobamate, phenytoin and primidone in wastewater effluents. Journal of Hazardous Materials, 282, 216–223.

Dudley, S., Sun, C., Jiang, J., & Gan, J. (2018). Metabolism of sulfamethoxazole in Arabidopsis thaliana cells and cucumber seedlings. Environmental Pollution, 242, 1748–1757.

Durán-Alvarez, J. C., Becerril-Bravo, E., Castro, V. S., Jiménez, B., and Gibson, R. (2009). The analysis of a group of acidic pharmaceuticals, carbamazepine, and potential endocrine disrupting compounds in wastewater irrigated soils by gas chromatography-mass spectrometry. Talanta, 78(3):1159-1166.

EC (European Commission), 2018. Proposal for a Regulation of the European Parliament and of the Council on minimum requirements for water reuse. Brussels, 28th May 2018.

ECHA. (2006). Paracetamol - Environmental fate & pathways. Retrieved December 18, 2018, from https://echa.europa.eu/registration-dossier/-/registered-dossier/12532/5/5/2

EFSA. (2008). Perfluorooctane sulfonate (PFOS), perfluorooctanoic acid (PFOA) and their salts. The EFSA Journal, 653, 1–131.

EFSA. (2007). Opinion on a request from EFSA related to the default Q10 value used to describe the temperature effect on transformation rates of pesticides in soil. The EFSA Journal, 622, 1–32.

EFSA Scientific Commitee. (2012). Guidance on selected default values to be used by the EFSA Scientific Committee, Scientific Panels and Units in the absence of actual measured data. EFSA Journal, 10(3), 2579.

Eggen, R.I.L., Hollender, J., Joss, A., Schärer, M., Stamm, C. (2014). Reducing the discharge of micropollutants in the aquatic environment: The benefits of upgrading wastewater treatment plants. Environ. Sci. Technol. 48, 7683–7689.

EMEA Committee for Veterinary Medicinal Products (2000). Furosemide – Summary Report. Technical Report September 1999.

Environment Protection and Heritage Council of Australia (2008). Australian Guidelines for Water Recycling: Managing Health and Environmental Risks (Phase 2) - Augmentation of Drinking Water Supplies. Technical Report 22.

Eriksson, E., Revitt, D.M., Ledin, A., Lundy, L., Lutzhoft, H.C.H., Wickman, T., Mikkelsen, P.S., (2011). Water management in cities of the future using emission control strategies for priority hazardous substances. Water Science and Technology, 64, 2109–2118.

European Commission Joint Research Centre. (2003). Technical guidance document on risk assessment in support of Commission Directive 93/67/ EEC on risk assessment for new notified substances and Commission Regulation (EC) No. 1488/94 on risk assessment for existing substances. Part II. EUR 20418 EN/2. European Chemicals Bureau, Part II, 7–179.

Evans, R. M., Scholze, M., & Kortenkamp, A. (2015). Examining the feasibility of mixture risk assessment: A case study using a tiered approach with data of 67 pesticides from the Joint FAO/WHO Meeting on Pesticide Residues (JMPR). Food and Chemical Toxicology, 84, 260–269.

Falås, P., Longrée, P., La Cour Jansen, J., Siegrist, H., Hollender, J., Joss, A. (2013). Micropollutant removal by attached and suspended growth in a hybrid biofilm-activated sludge process. Water Research, 47(13), 4498–4506.

FAO (2007). ECOCROP - Data Sheet - Lolium multiflorum. URL: http://ecocrop.fao.org/ecocrop/srv/en/dataSheet?id=7389. Last accessed: 05-10-2018.

Felle, H. H., Herrmann, A., Hückelhoven, R., Kogel, K. H. (2005). Root-to-shoot signalling: Apoplastic alkalinization, a general stress response and defence factor in barley (Hordeum vulgare). Protoplasma, 227(1), 17–24.

Felle, H. H. (2001). pH: Signal and messenger in plant cells. Plant Biology, 3(6), 577–591.

Fent K, Weston AA, Carminada D. (2006). Ecotoxicology of human pharmaceuticals. Aquat Toxicol, 76, 122–59.

Ferreira da Silva, B., Jelic, A., López-Serna, R., Mozeto, A. A., Petrovic, M., & Barceló, D. (2011). Occurrence and distribution of pharmaceuticals in surface water, suspended solids and sediments of the Ebro river basin, Spain. Chemosphere, 85(8), 1331–1339.

Fenner, K., Honti, M., Stamm, C., Varga, L., Bischoff, F. (2016). Suitability of laboratory simulation tests for the identification of persistence in surface waters.

Flores-Alsina, X., Saagi, R., Lindblom, E., Thirsing, C., Thornberg, D., Gernaey, K. V., and Jeppsson, U. (2014). Calibration and validation of a phenomenological influent pollutant disturbance scenario generator using full-scale data. Water Research, 51(0), 172–185.

Fono, L. J., Kolodziej, E. P., Sedlak, D. L. (2006). Attenuation of wastewater-derived contaminants in an effluent-dominated river. Environmental Science and Technology, 40(23), 7257–7262.

Franco, A., Struijs, J., Gouin, T., & Price, O. R. (2013). Evolution of the sewage treatment plant model SimpleTreat: Applicability domain and data requirements. Integrated Environmental Assessment and Management, 9(4), 560–568.

Franco, A., Ferranti, A., Davidsen, C., & Trapp, S. (2010). An unexpected challenge: Ionizable compounds in the REACH chemical space. International Journal of Life Cycle Assessment, 15(4), 321–325.

Franco, A., & Trapp, S. (2008). Estimation of the soil-water partition coefficient normalized to organic carbon for ionizable organic chemicals. Environ. Toxicol. Chem. 27, 1995-2004.

Frey, C. H., & Patil, S. R. (2002). Identification and Review of Sensitivity Analysis Methods. Risk Analysis, 22(3), 553–578.

Fu, Q., Wu, X., Ye, Q., Ernst, F., Gan, J. (2016). Biosolids inhibit bioavailability and plant uptake of triclosan and triclocarban. Water Research, 102, 117–124.

Gao, J., Li, J., Jiang, G., Shypanski, A.H., Nieradzik, L.M., Yuan, Z., Mueller, J.F., Ort, C., Thai, P.K. (2019). Systematic evaluation of biomarker stability in pilot scale sewer pipes. Water Res. 151, 447–455.

Galus, M., Jeyaranjaan, J., Smith, E., Li, H., Metcalfe, C., Wilson, J.Y. (2013) Chronic effects of exposure to a pharmaceutical mixture and municipal wastewater in zebrafish, Aquatic Toxicol, 132–133 212–222.

Gasperi, J., Zgheib, S., Cladiére, M., Rocher, V., Moilleron, R.., Chebbo, G. (2012). Priority pollutants in urban stormwater: Part 2 – Case of combined sewers. Water Res. 46, 6693–6703.

Gibson, R., Durán-Alvarez, J. C., Estrada, K. L., Chávez, A., and Jiménez Cisneros, B. (2010). Accumulation and leaching potential of some pharmaceuticals and potential endocrine disruptors in soils irrigated with wastewater in the Tula Valley, Mexico. Chemosphere, 81(11):1437-1445.

Giesy, J. P., Naile, J. E., Khim, J. S., Jones, P. D., Newsted, J. L. (2010). Aquatic Toxicology of Perfluorinated Chemicals. In D. M. Whitacre (Ed.), Reviews of Environmental Contamination and Toxicology (Vol. 202).

Göbel, A., McArdell, C.S., Joss, A., Siegrist, H., Giger, W. (2007). Fate of sulfonamides, macrolides, and trimethoprim in different wastewater treatment technologies. Sci. Total Environ. 372, 361–371.

Goldstein, M., Shenker, M., and Chefetz, B. (2014). Insights into the Uptake Processes of Wastewater-Borne Pharmaceuticals by Vegetables. Environmental Science and Technology, 48:5593-5600.

Gomes, R. L., Scrimshaw, M. D. and Lester J. N. (2009). Fate of conjugated natural and synthetic steroid estrogens in crude sewage and activated sludge batch studies. Environmental Science and Technology, 43, 3612–3618.

Gonzalez-Gil, L., Mauricio-Iglesias, M., Carballa, M., Lema, J.M. (2018). Why are organic micropollutants not fully biotransformed? A mechanistic modelling approach to anaerobic systems. Water Res.

Gonzalez-Garcia, M., Fernandez-Lopez, C., Polesel, F., Trapp, S. (2019). Predicting the uptake of emerging organic contaminants in vegetables irrigated with treated wastewater – Implications for food safety assessment. Environ. Res. 172, 175-181.

Goss, K. U. (2008). The pKa values of PFOA and other highly fluorinated carboxylic acids. Environmental Science and Technology, 42(2), 456–458.

Gosset, A., Durrieu, C., Orias, E., Bayard, E., Perrodin, Y. (2017). Identification and assessment of ecotoxicological hazards attributable to pollutants in urban wet weather discharges. Environ. Sci. Process. Impacts 19.

Gosling, S. N. and Arnell, N. W. (2016). A global assessment of the impact of climate change on water scarcity. Climatic Change, 134(3), 371-385.

Gozlan, I., Koren, I. (2016). Identification, Mechanisms and Kinetics of Macrolide Degradation Product Formation under Controlled Environmental Conditions. Journal of Environmental Analytical Chemistry, 03(01), 1–9.

Gredelj, A., Barausse, A., Grechi, L., Palmeri, L. (2018). Deriving predicted no-effect concentrations (PNECs) for emerging contaminants in the river Po, Italy, using three approaches: Assessment factor, species sensitivity distribution and AQUATOX ecosystem modelling. Environment International, 119(June), 66–78.

Gröning, J., Held, C., Garten, C., Claußnitzer, U., Kaschabek, S. R., Schlömann, M. (2007). Transformation of diclofenac by the indigenous microflora of river sediments and identification of a major intermediate. Chemosphere, 69(4), 509–516.

Grossberger, A., Hadar, Y., Borch, T., Chefetz, B. (2014). Biodegradability of pharmaceutical compounds in agricultural soils irrigated with treated wastewater. Environmental Pollution, 185, 168–177.

Grzybowski, W., Szydłowski, J. (2014). The impact of chromophoric dissolved organic matter on the photodegradation of 17α-ethinylestradiol (EE2) in natural waters. Chemosphere, 111, 13–17.

Guillet, G., Knapp, J. L. A., Merel, S., Cirpka, O. A., Grathwohl, P., Zwiener, C., Schwientek, M. (2019). Fate of wastewater contaminants in rivers: Using conservative-tracer based transfer functions to assess reactive transport. Science of The Total Environment, 656, 1250–1260.

Han, X., Snow, T. A., Kemper, R. A., Jepson, G. W. (2003). Binding of perfluorooctanoic acid to rat and human plasma proteins. Chemical Research in Toxicology, 16(6), 775–781.

Hanamoto, S., Nakada, N., Yamashita, N., & Tanaka, H. (2013). Modeling the photochemical attenuation of down-the-drain chemicals during river transport by stochastic methods and field measurements of pharmaceuticals and personal care products. Environmental Science and Technology, 47(23), 13571–13577.

Hebert, P. C., MacManus-Spencer, L. A. (2010). Development of a Fluorescence Model for the Binding of Medium- to Long-Chain Perfluoroalkyl Acids to Human Serum Albumin Through a Mechanistic Evaluation of Spectroscopic Evidence. Analytical Chemistry, 82(15), 6463–6471.

Hendriks, A. J., Smítková, H., & Huijbregts, M. A. J. (2007). A new twist on an old regression: Transfer of chemicals to beef and milk in human and ecological risk assessment. Chemosphere, 70(1), 46–56.

Henry, A., Cal, A. J., Batoto, T. C., Torres, R. O., Serraj, R. (2012). Root attributes affecting water uptake of rice (Oryza sativa) under drought. Journal of Experimental Botany, 63(13), 4751–4763.

Henze, M., Gujer, W., Takashi, M., van Loosdrecht, M. (2000). Activated Sludge Models ASM1, ASM2, ASM2d and ASM3, Scientific and Technical Reports No.9. IWA Publishing.

Henze, M., Gujer, W., Mino, T., Loosdrecht, M. van. (2002). Activated Sludge Models ASM1, ASM2, ASM2d and ASM3. In IWA Task Group on Mathematical Modelling for Design and Operation of Biological Wastewater Treatment. IWA Publishing.

Hermida, J., Tutor, J.C. (2003). How suitable are currently used carbamazepine immunoassays for quantifying carbamazepine-10,11-epoxide in serum samples? Ther. Drug Monit. 25, 384–388.

Hernando, M. D., Mezcua, M., Fernández-Alba, A. R., & Barceló, D. (2006). Environmental risk assessment of pharmaceutical residues in wastewater effluents, surface waters and sediments. Talanta, 69(2 SPEC. ISS.), 334–342.

Hidayati, N., Triadiati, & Anas, I. (2016). Photosynthesis and Transpiration Rates of Rice Cultivated Under the System of Rice Intensification and the Effects on Growth and Yield. HAYATI Journal of Biosciences, 23(2), 67–72.

Higgins, C. P., Luthy, R. G. (2006). Sorption of perfluorinated surfactants on sediments. Environmental Science and Technology, 40(23), 7251–7256.

Holling, C. S., Bailey, J. L., Heuvel, V., Kinney, C. A. (2012). Uptake of human pharmaceuticals and personal care products by cabbage (Brassica campestris) from fortified and biosolids-amended soils. Journal of Environmental Monitoring, 14, 3029–3036.

Hsu, F. C., Marxmiller, R. L., & Yang, A. Y. S. (1990). Study of Root Uptake and Xylem Translocation of Cinmethylin and Related Compounds in Detopped Soybean Roots Using a Pressure Chamber Technique. Plant Physiology, 93(4), 1573–1578.

Huang, Q., Bu, Q., Zhong, W., Shi, K., Cao, Z., Yu, G. (2018). Derivation of aquatic predicted no-effect concentration (PNEC) for ibuprofen and sulfamethoxazole based on various toxicity endpoints and the associated risks. Chemosphere, 193, 223–229.

Hurtado, C., Cañameras, N., Domínguez, C., Price, G. W., Comas, J., Bayona, J. M. (2017). Effect of soil biochar concentration on the mitigation of emerging organic contaminant uptake in lettuce. Journal of Hazardous Materials, 323(April 2016), 386–393.

Igarashi, S., Yotsuyanagi, T. (1992). Homogeneous liquid-liquid extraction by pH dependent phase separation with a fluorocarbon ionic surfactant and its application to the preconcentration of porphyrin compounds. Mikrochimica Acta, 106(1–2), 37–44.

Italian National Institute of Statistics (ISTAT), 1926. Open data. http://dati.istat.it/Index.aspx?DataSetCode=DCCV_INDACQDOM# (Accessed 15 April 2018).

IPCC (2014). Climate Change 2014: Impacts, Adaptation, and Vulnerability. Part A: Global and Sectoral Aspects. Contribution of Working Group II to the Fifth Assessment Report of the Intergovernmental Panel on Climate Change. Cambridge University Press, Cambridge, United Kingdom and New York, NY, USA.

Jakimska, A., Śliwka-Kaszyńska, M., Reszczyńska, J., Namieśnik, J., Kot-Wasik, A. (2014). Elucidation of transformation pathway of ketoprofen, ibuprofen, and furosemide in surface water and their occurrence in the aqueous environment using UHPLC-QTOF-MS Euroanalysis XVII. Analytical and Bioanalytical Chemistry, 406(15), 3667–3680.

Jelic, A., Rodriguez-Mozaz S., Barceló, D., Gutierrez, O. (2015). Impact of in-sewer transformation on 43 pharmaceuticals in a pressurized sewer under anaerobic conditions. Water Research 68, 98–108.

Jensen, A. A., Poulsen, P. B., Bossi, R. (2008). Survey and environmental/health assessment of fluorinated substances in impregnated consumer products and impregnating agents. In Survey of Chemical Substances in Consumer Products.

Jing, P., Rodgers, P. J., Amemiya, S. (2009). High lipophilicity of perfluoroalkyl carboxylate and sulfonate: Implications for their membrane permeability. Journal of the American Chemical Society, 131(6), 2290–2296.

Johannes, E., Collings, D. a, Rink, J. C., Allen, N. S. (2001). Cytoplasmic pH dynamics in maize pulvinal cells induced by gravity vector changes. Plant Physiology, 127(1), 119–130.

Johnson, A.C., Donnachie, R.L., Sumpter, J.P., Jürgens, M.D., Moeckel, C., Pereira, M.G. (2017). An alternative approach to risk rank chemicals on the threat they pose to the aquatic environment. Sci. Total Environ. 599–600, 1372–1381.

Jurgens, M. D., Holthaus, K. I. E., Johnson, A. C., Smith, J. J. L., Hetheridge, M., Williams, R. J. (2002). The potential for estradiol and ethyinylestradiol degradation in English Rivers. Environmental Toxicology and Chemistry, 21(3), 480–488.

Kapo, K. E., Paschka, M., Vamshi, R., Sebasky, M., McDonough K. (2017). Estimation of U.S. sewer residence time distributions for national-scale risk assessment of down-the-drain chemicals. Science of the Total Environment 603-604, 445-452.

Khan, S. J. and Ongerth J. E. (2004). Modelling of pharmaceutical residues in Australian sewage by quantities of use and fugacity calculations. Chemosphere, 54, 355-367.

Karnjanapiboonwong, A., Chase, D. A., Cañas, J. E., Jackson, W. A., Maul, J. D., Morse, A. N., Anderson, T. A. (2011). Uptake of 17α-ethynylestradiol and triclosan in pinto bean, Phaseolus vulgaris. Ecotoxicology and Environmental Safety, 74(5), 1336–1342.

Kasprzyk-Hordern, B., Dinsdale, R.M., Guwy, A.J. (2009). The removal of pharmaceuticals, personal care products, endocrine disruptors and illicit drugs during wastewater treatment and its impact on the quality of receiving waters. Water Res. 43, 363–380.

Kawabata, K., Sugihara, K., Sanoh, S., Kitamura, S., Ohta, S. (2013). Photodegradation of pharmaceuticals in the aquatic environment by sunlight and UV-A, -B and -C irradiation. The Journal of Toxicological Sciences, 38(2), 215–223.

Keller, V.D.J., Rees, H.G., Fox, K.K., Whelan, M.J. (2007). A new generic approach for estimating the concentrations of down-the-drain chemicals at catchment and national scale. Environ. Pollut. 148, 334–342.

Khan, S. J., Ongerth, J. E. (2004). Modelling of pharmaceutical residues in Australian sewage by quantities of use and fugacity calculations. Chemosphere, 54(3), 355–367.

Kleier, D. A., Hsu, F. C. (1996). Phloem Mobility of Xenobiotics. VII. The Design of Phloem Systemic Pesticides. Weed Science, 44(3), 749–756.

Kleier, D. A., & Hsu, F. C. (1996). Phloem Mobility of Xenobiotics. VII. The Design of Phloem Systemic Pesticides. Weed Science, 44(3), 749–756.

Kodešová, R., Kočárek, M., Klement, A., Golovko, O., Koba, O., Fér, M., … Grabic, R. (2016). An analysis of the dissipation of pharmaceuticals under thirteen different soil conditions. Science of the Total Environment, 544, 369–381.

Koormann, F., Rominger, J., Schowanek, D., Wagner, J.-O., Schröder, R., Wind, T., Silvani, M., Whelan, M.J. (2006). Modeling the fate of down-the-drain chemicals in rivers: An improved software for GREAT-ER. Environ. Model. Softw. 21, 925–936.

Koumaki, E., Mamais, D., Noutsopoulos, C. (2018). Assessment of the environmental fate of endocrine disrupting chemicals in rivers. Science of the Total Environment, 628–629, 947–958.

Koumaki, E., Mamais, D., Noutsopoulos, C. (2017). Environmental fate of non-steroidal anti-inflammatory drugs in river water/sediment systems. Journal of Hazardous Materials, 323, 233–241.

Koumaki, E., Mamais, D., Noutsopoulos, C., Nika, M. C., Bletsou, A. A., Thomaidis, N. S., … Stratogianni, G. (2015). Degradation of emerging contaminants from water under natural sunlight: The effect of season, pH, humic acids and nitrate and identification of photodegradation by-products. Chemosphere, 138, 675–681.

Kroes, R., Renwick, A. ., Cheeseman, M., Kleiner, J., Mangelsdorf, I., Piersma, A., … Würtzen, G. (2004). Structure-based thresholds of toxicological concern (TTC): guidance for application to substances present at low levels in the diet. Food and Chemical Toxicology, 42(1), 65–83.

Kunkel, U., & Radke, M. (2011). Reactive tracer test to evaluate the fate of pharmaceuticals in rivers. Environmental Science and Technology, 45(15), 6296–6302.

Kunkel, U., Radke, M. (2008). Biodegradation of Acidic Pharmaceuticals in Bed Sediments : Insight from a Laboratory Experiment. Environmental Science and Technology, 42(19), 7273–7279.

Kuzmanovic, M., Banjac, Z., Ginebreda, A., Petrovic, M., & Barcelo, D. (2013). Prioritization: Selection of Environmentally Occurring Pharmaceuticals to Be Monitored. In M. Petrovic, D. Barcelo, & S. Pérez (Eds.), Comprehensive Analytical Chemistry (2nd ed., Vol. 62, pp. 71–90).

Labadie, P., & Budzinski, H. (2005). Determination of steroidal hormone profiles along the Jalle d'Eysines River (near Bordeaux, France). Environmental Science and Technology, 39(14), 5113–5120.

Lai, H. T., Hou, J. H. (2008). Light and microbial effects on the transformation of four sulfonamides in eel pond water and sediment. Aquaculture, 283(1–4), 50–55.

Lam, M. W., Mabury, S. A. (2005). Photodegradation of the pharmaceuticals atorvastatin, carbamazepine, levofloxacin, and sulfamethoxazole in natural waters. Aquatic Sciences, 67(2), 177–188.

Lam, M. W., Young, C. J., Brain, R. A., Johnson, D. J., Hanson, M. A., Wilson, C. J., … Mabury, S. A. (2004). Aquatic persistance of eight pharmaceuticals in a microcosm study. Environmental Toxicology and Chemistry, 23(6), 1431–1440.

Lamshoeft, M., Gao, Z., Resseler, H., Schriever, C., Sur, R., Sweeney, P., … Reitz, M. U. (2018). Evaluation of a novel test design to determine uptake of chemicals by plant roots. Science of the Total Environment, 613–614, 10–19.

Latch, D. E., Packer, J. L., Stender, B. L., VanOverbeke, J., Arnold, W. A., McNeill, K. (2005). Aqueous photochemistry of triclosan: Formation of 2,4-dichlorophenol, 2,8-dichlorodibenzo-p-dioxin, and oligomerization products. Environmental Toxicology and Chemistry, 24(3), 517–525.

Launay, M.A., Dittmer, U. and Steinmetz, H. (2016) Organic micropollutants discharged by combined sewer overflows - Characterisation of pollutant sources and stormwater-related processes. Water Res 104, 82-92.

Lazarova, V. and Asano, T. (2013). Milestones in water reuse: main challenges, keys to success and trends of development. An overview. In Lazarova, V., Asano, T., Bahri, A., and Anderson, J., editors, "Milestones in Water Reuse", pages 1-22.

Leclercq, C., Arcella, D., Piccinelli, R., Sette, S., & Le Donne, C. (2009). The Italian National Food Consumption Survey INRAN-SCAI 2005–06: main results in terms of food consumption. Public Health Nutrition, 12(12), 2504–2532.

Lechner, M., Knapp, H. (2011). Carryover of Perfluorooctanoic Acid (PFOA) and Perfluorooctane Sulfonate (PFOS) from Soil to Plant and Distribution to the Different Plant Compartments Studied in Cultures of Carrots (Daucus carota ssp. Sativus), Potatoes (Solanum tuberosum), and Cucu. Journal of Agricultural and Food Chemistry, 59(20), 11011–11018.

Lee, H.J., Lee, E., Yoon, S.H., Chang, H.R., Kim, K., Kwon, J.H. (2012). Enzymatic and microbial transformation assays for the evaluation of the environmental fate of diclofenac and its metabolites. Chemosphere 87, 969–974.

Leech, D. M., Snyder, M. T., Wetzel, R. G. (2009). Natural organic matter and sunlight accelerate the degradation of 17ß-estradiol in water. Science of the Total Environment, 407(6), 2087–2092.

Legind, C. N., Kennedy, C. M., Rein, A., Snyder, N., & Trapp, S. (2011). Dynamic plant uptake model applied for drip irrigation of an insecticide to pepper fruit plants. Pest Management Science, 67(5), 521–527.

Lesser, L. E., Mora, A., Moreau, C., Mahlknecht, J., Hernández-Antonio, A., Ramirrez, A. I., and Barrios-Piña, H. (2018). Survey of 218 organic contaminants in groundwater derived from the world's largest untreated wastewater irrigation system: Mezquital Valley, Mexico. Chemosphere, 198:510-521.

Letsinger, S., Kay, P. (2019). Comparison of Prioritisation Schemes for Human Pharmaceuticals in the Aquatic Environment. Environ. Sci. Pollut. Res. 26, 3479–3491.

Li, J., Gao, J., Thai, P.K., Sun, X., Mueller, J.F., Yuan, Z., Jiang, G. (2018). Stability of illicit drugs as biomarkers in sewers: From lab to reality. Environmental Science and Technology, 52, 1561–1570.

Li, J., Gao, J., Thai, P.K., Shypanski, A., Nieradzik, L., Mueller, J.F. Yuan, Z., Jiang, G. (2019). Experimental investigation and modeling of the transformation of illicit drugs in a pilot-scale sewer system. Environ. Sci. Technol.

Li, F. H., Yao, K., Lv, W. Y., Liu, G. G., Chen, P., Huang, H. P., Kang, Y. P. (2015). Photodegradation of ibuprofen under UV-VIS irradiation: Mechanism and toxicity of photolysis products. Bulletin of Environmental Contamination and Toxicology, 94(4), 479–483.

Li, J., Zhang, Y., Huang, Q., Shi, H., Yang, Y., Gao, S., … Yang, X. (2017). Degradation of organic pollutants mediated by extracellular peroxidase in simulated sunlit humic waters: A case study with 17B-estradiol. Journal of Hazardous Materials, 331, 123–131.

Li, J., Dodgen, L., Ye, Q., Gan, J. (2013). Degradation kinetics and metabolites of carbamazepine in soil. Environmental Science and Technology, 47(8), 3678–3684.

Li, J., Ye, Q., Gan, J. (2014). Degradation and transformation products of acetaminophen in soil. Water Research, 49, 44–52.

Li, J., Ye, Q., Gan, J. (2015). Influence of organic amendment on fate of acetaminophen and sulfamethoxazole in soil. Environmental Pollution, 206, 543–550.

Li, L., Xu, Z. S., Song, G. W. (2009). Study on the Langmuir aggregation of fluorinated surfactants on protein. Journal of Fluorine Chemistry, 130(2), 225–230.

Li, Y., Pan, Y., Lian, L., Yan, S., Song, W., Yang, X. (2017). Photosensitized degradation of acetaminophen in natural organic matter solutions: The role of triplet states and oxygen. Water Research, 109, 266–273.

Li, Y., Chuang, Y. H., Sallach, J. B., Zhang, W., Boyd, S. A., & Li, H. (2018). Potential metabolism of pharmaceuticals in radish: Comparison of in vivo and in vitro exposure. Environmental Pollution, 242, 962–969.

Li, Z., Sobek, A., Radke, M. (2015). Flume experiments to investigate the environmental fate of pharmaceuticals and their transformation products in streams. Environmental Science and Technology, 49(10), 6009–6017.

Lin, A. Y. C., Plumlee, M. H., Reinhard, M. (2006). Natural attenuation of pharmaceuticals and alkylphenol polyethoxylate metabolites during river transport: Photochemical and biological transformation. Environmental Toxicology and Chemistry, 25(6), 1458–1464.

Lin, A. Y. C., Reinhard, M. (2005). Photodegradation of common environmental pharmaceuticals and estrogens in river water. Environmental Toxicology and Chemistry, 24(6), 1303–1309.

Lin, A. Y. C., Lin, C. A., Tung, H. H., Chary, N. S. (2010). Potential for biodegradation and sorption of acetaminophen, caffeine, propranolol and acebutolol in lab-scale aqueous environments. Journal of Hazardous Materials, 183(1–3), 242–250.

Lin, K., Gan, J. (2011). Sorption and degradation of wastewater-associated non-steroidal anti-inflammatory drugs and antibiotics in soils. Chemosphere, 83(3), 240–246.

Lienert, J., Güdel, K., Escher, B.I. (2007). Screening method for ecotoxicological hazard assessment of 42 pharmaceuticals considering human metabolism and excretory routes. Environ. Sci. Technol. 41, 4471–4478.

Lindström, A., Buerge, I. J., Poiger, T., Bergqvist, P. A., Müller, M. D., Buser, H. R. (2002). Occurrence and environmental behavior of the bactericide triclosan and its methyl derivative in surface waters and in wastewater. Environmental Science and Technology, 36(11), 2322–2329.

Liou, J. S. C., Szostek, B., DeRito, C. M., Madsen, E. L. (2010). Investigating the biodegradability of perfluorooctanoic acid. Chemosphere, 80(2), 176–183.

Liu, F., Ying, G.-G., Yang, J.-F., Zhou, L.-J., Tao, R., Wang, L., … Peng, P.-A. (2010). Dissipation of sulfamethoxazole, trimethoprim and tylosin in a soil under aerobic and anoxic conditions. Environmental Chemistry, 7(4), 370–376.

Liu, Y., Sun, W., Ni, J. (2011). Biodegradation of bisphenol A, 17β-estradiol, and 17α-ethynylestradiol in river water. International Journal of Environment and Pollution, 45, 225–236.

Liu, Y., Sun, H., Zhang, L., Feng, L. (2017). Photodegradation behaviors of 17β-estradiol in different water matrixes. Process Safety and Environmental Protection, 112, 335–341.

Limmer, M. A., & Burken, J. G. (2014). Plant Translocation of Organic Compounds: Molecular and Physicochemical Predictors. Environmental Science and Technology Letters, 1(2), 156–161.

Löffler, D., Römbke, J., Meller, M., Ternes, T. A. (2005). Environmental fate of pharmaceuticals in water/sediment systems. Environmental Science and Technology, 39(14), 5209–5218.

López-Fontán, J. L., Sarmiento, F., Schulz, P. C. (2005). The aggregation of sodium perfluorooctanoate in water. Colloid and Polymer Science, 283(8), 862–871.

Löwe, R., Vezzaro, L., Mikkelsen, P.S., Grum, M., Madsen, H. (2016). Probabilistic runoff volume forecasting in risk-based optimization for RTC of urban drainage systems. Environ. Model. Softw. 80, 143–158.

Luo, Y., Guo, W., Ngo, H.H., Nghiem, L.D., Hai, F.I., Zhang, J., Liang, S., Wang, X.C. (2014a). A review on the occurrence of micropollutants in the aquatic environment and their fate and removal during wastewater treatment. Sci. Total Environ.

Luo, Y., Guo, W., Ngo, H.H., Nghiem, L.D., Hai, F.I., Zhang, J., Liang, S., Wang, X.C. (2014b). A review on the occurrence of micropollutants in the aquatic environment and their fate and removal during wastewater treatment. Sci. Total Environ.

Macherius, A., Eggen, T., Lorenz, W. G., Reemtsma, T., Winkler, U., & Moeder, M. (2012). Uptake of Galaxolide, Tonalide, and Triclosan by Carrot, Barley, and Meadow Fescue Plants. Journal of Agricultural and Food Chemistry, 60(32), 7785–7791.

MacKay, A.A., Vasudevan, D. (2012). Polyfunctional Ionogenic Compound Sorption: Challenges and New Approaches To Advance Predictive Models. Environ. Sci. Technol. 46, 9209–9223.

Majewsky, M., Gallé, T., Bayerle, M., Goel, R., Fischer, K., Vanrolleghem, P.A. (2011). Xenobiotic removal efficiencies in wastewater treatment plants: Residence time distributions as a guiding principle for sampling strategies.

Malchi, T., Maor, Y., & Chefetz, B. (2015). Comments on "Human health risk assessment of pharmaceuticals and personal care products in plant tissue due to biosolids and manure amendments, and wastewater irrigation." Environment International, 82, 110–112.

Malchi, T., Maor, Y., Tadmor, G., Shenker, M., & Chefetz, B. (2014). Irrigation of Root Vegetables with Treated Wastewater: Evaluating Uptake of Pharmaceuticals and the Associated Human Health Risks. Environmental Science & Technology, 48(16), 9325–9333.

Mannina, G., Alida, C., Viviani, G. (2017). Micropollutants throughout an integrated urban drainage model: Sensitivity and uncertainty analysis. Journal of Hydrology, 554, 397-405.

Margot, J., Rossi, L., Barry, D.A., Holliger, C. (2015). A review of the fate of micropollutants in wastewater treatment plants. Wiley Interdiscip. Rev. Water 2, 457–487.

Martin, C., Vanrolleghem, P.A., (2014). Analysing, completing, and generating influent data for WWTP modelling: A critical review. Environmental Modelling and Software, 60, 188–201.

Martínez-Zapata, M., Aristizábal, C., Peñuela, G. (2013). Photodegradation of the endocrine-disrupting chemicals 4n-nonylphenol and triclosan by simulated solar UV irradiation in aqueous solutions with Fe(III) and in the absence/presence of humic acids. Journal of Photochemistry and Photobiology A: Chemistry, 251, 41–49.

Martiniello, P. (1999). Effects of irrigation and harvest management on dry- matter yield and seed yield of annual clovers grown in pure stand and in mixtures with graminaceous species in a Mediterranean environment. Grass and Forage Science, 54, 52–61.

Masseroni, D., Ricart, S., de Cartagena, F. R., Monserrat, J., Gonçalves, J. M., de Lima, I., … Gandolfi, C. (2017). Prospects for improving gravity-fed surface irrigation systems in mediterranean european contexts. Water (Switzerland), 9(1), 20.

Mashtare, M. L., Lee, L. S., Nies, L. F., Turco, R. F. (2013). Transformation of 17α-Estradiol, 17β-estradiol, and estrone in sediments under nitrate- and sulfate-reducing conditions. Environmental Science and Technology, 47(13), 7178–7185.

Miller, E. L., Nason, S. L., Karthikeyan, K. G., and Pedersen, J. A. (2016). Root Uptake of Pharmaceuticals and Personal Care Product Ingredients. Environmental Science and Technology, 50(2):525-541.

Matamoros, V., & Rodríguez, Y. (2017). Influence of seasonality and vegetation on the attenuation of emerging contaminants in wastewater effluent-dominated streams. A preliminary study. Chemosphere, 186, 269–277.

Matsuoka, S., Kikuchi, M., Kimura, S., Kurokawa, Y., Kawai, S. (2005). Determination of Estrogenic Substances in the Water of Muko River Using in Vitro Assays, and the Degradation of Natural Estrogens by Aquatic Bacteria. Journal of Health Science, 51(2), 178–184.

Mazaleuskaya, L.L., Sangkuhl, K., Thorn, C.F., Fitzgerald, G.A., Altman, R.B., Klein, T.E. (2015). PharmGKB summary: Pathways of acetaminophen metabolism at the therapeutic versus toxic doses. Pharmacogenet. Genomics 25, 416–426.

Mazzini, R., Pedrazzi, L., Lazarova, V. (2013). Production of high quality recycled water for agricultural irrigation in Milan. In V. Lazarova, T. Asano, A. Bahri, J. Anderson (Eds.), Milestones in Water Reuse (pp. 179–190).

McArdell, C. S., Molnar, E., Suter, M. J. F., & Giger, W. (2003). Occurrence and Fate of Macrolide Antibiotics in Wastewater Treatment Plants and in the Glatt Valley Watershed, Switzerland. Environmental Science and Technology, 37(24), 5479–5486.

McCall, A. K., Scheidegger, A., Madry, M.M., Steuer, A.E., Weissbrodt, D.G., Vanrolleghem, P.A., Kraemer, T., Morgenroth, E., Ort, C. (2016). Influence of different sewer biofilms on transformation rates of drugs. Environmental Science and Technology, 50, 13351–13360.

McCall, A. K., Palmitessa, R., Blumensaat, F., Morgenroth, E., Ort, C. (2017). Modeling in-sewer transformations at catchment scale – implications on drug consumption estimates in wastewater-based epidemiology, Water Research, 122, 655–668.

Menzies, J., McDonough, K., McAvoy, D., Federle, T.W. (2017). Biodegradation of nonionic and anionic surfactants in domestic wastewater under simulated sewer conditions. Biodegradation, 28, 1–14.

Mejia Avendaño, S., Zhong, G., Liu, J. (2015). Comment on "Biodegradation of perfluorooctanesulfonate (PFOS) as an emerging contaminant." Chemosphere, 138, 1037–1038.

Mezcua, M., Gómez, M. J., Ferrer, I., Aguera, A., Hernando, M. D., Fernández-Alba, A. R. (2004). Evidence of 2,7/2,8-dibenzodichloro-p-dioxin as a photodegradation product of triclosan in water and wastewater samples. Analytica Chimica Acta, 524(1–2 SPEC. ISS.), 241–247.

Monteiro, S. C. and Boxall, A. B. (2010). Occurrence and Fate of Human Pharmaceuticals in the Environment. In Whitacre, D. M., editor, "Reviews of Environmental Contamination and Toxicology", volume 202, pages 54-154. Springer, New York, NY.

Moretti, B., Grignani, C., Bechini, L., & Sacco, D. (2015). Efficacia e convenienza delle catch crop. L'informatore Agrario, (36), 52–56.

Morrall, D., McAvoy, D., Schatowitz, B., Inauen, J., Jacob, M., Hauk, A., Eckhoff, W. (2004). A field study of triclosan loss rates in river water (Cibolo Creek, TX). Chemosphere, 54(5), 653–660.

Mose Pedersen, B., n.d. Screening for humane laegemidler i vandmiljøet 2.

Mutzner, L., Vermeirssen, E.L.M., Ort, C., (2019). Passive samplers in sewers and rivers with highly fluctuating micropollutant concentrations – Better than we thought. J. Hazard. Mater. 361, 312–320.

National Food Institute, Technical University of Denmark (2018). Danish (Q)SAR Database. URL: http://qsar.food.dtu.dk. Last accessed: 23-03-2019.

Navarro, I., de la Torre, A., Sanz, P., Porcel, M. Á., Pro, J., Carbonell, G., Martínez, M. D. L. Á. (2017). Uptake of perfluoroalkyl substances and halogenated flame retardants by crop plants grown in biosolids-amended soils. Environmental Research, 152(October 2016), 199–206.

Nelli, E. and Sodi, F. (2007). Riso - Oryza sativa L. - Atlante delle coltivazioni erbacee - Piante industriali. URL: http://www.agraria.org/coltivazionierbacee/riso.htm. Last accessed: 5-10-2018.

Nelder, J. A., Mead, R. (1964). A simplex method for function minimization. The Computer Journal, 7, 308–313.

NICNAS. (2009). Triclosan, Priority Existing Chemical Assessment Report.

Nielsen, C. J. (2012). PFOA Isomers, Salts, and Precursors.

Niu, J., Zhang, L., Li, Y., Zhao, J., Lv, S., Xiao, K. (2013). Effects of environmental factors on sulfamethoxazole photodegradation under simulated sunlight irradiation: Kinetics and mechanism. Journal of Environmental Sciences, 25(6), 1098–1106.

O'Brien, J. W., Banks, A. P. W., Novic, A. J., Mueller, J. F., Jiang, G., Ort, C., Eaglesham, G., Yuan, Z., and Thai, P. K. (2017). Impact of in-Sewer Degradation of Pharmaceutical and Personal Care Products (PPCPs) Population Markers on a Population Model. Environmental Science and Technology, 51 (7), 3816-3823.

Obropta, C.C., Kardos, J.S., (2007). Review of urban stormwater quality models: Deterministic, stochastic, and hybrid approaches. Journal of the American Water Resource Association, 43, 1508–1523.

Oekotoxzentrum, 2019. Proposals for Acute and Chronic Quality Standards. https://www.ecotoxcentre.ch/expert-service/quality-standards/proposals-for-acute-and-chronic-quality-standards/

Oliveira, C., Lima, D. L. D., Silva, C. P., Calisto, V., Otero, M., Esteves, V. I. (2019). Photodegradation of sulfamethoxazole in environmental samples: The role of pH, organic matter and salinity. Science of the Total Environment, 648, 1403–1410.

Ort, C., Hollender, J., Schaerer, M., Siegrist, H. (2009). Model-based evaluation of reduction strategies for micropollutants from wastewater treatment plants in complex river networks. Environmental Science and Technology, 43, 3214–3220.

Ort C., Schaffner, C., Giger, W., Gujer, W. (2005). Modeling stochastic load variations in sewer systems. Water Science and Technology, 52, 113-122.

Ort, C., Lawrence, M.G., Rieckermann, J., Joss, A. (2010). Sampling for pharmaceuticals and personal care products (PPCPs) and illicit drugs in wastewater systems: Are your conclusions valid? A critical review. Environ. Sci. Technol. 44, 6024–6035.

Ort, C., Lawrence, M.G., Reungoat, J., Mueller, J.F., (2010a). Sampling for PPCPs in wastewater systems: Comparison of different sampling modes and optimization strategies. Environ. Sci. Technol. 44, 6289–6296.

Ort, C., Lawrence, M.G., Rieckermann, J., Joss, A., (2010b). Sampling for pharmaceuticals and personal care products (PPCPs) and illicit drugs in wastewater systems: Are your conclusions valid? A critical review. Environ. Sci. Technol. 44, 6024–6035.

Packer, J. L., Werner, J. J., Latch, D. E., McNeill, K., Arnold, W. A. (2003). Photochemical fate of pharmaceuticals in the environment: Naproxen, diclofenac, clofibric acid, and ibuprofen. Aquatic Sciences, 65(4), 342–351.

Paltiel, O., Fedorova, G., Tadmor, G., Kleinstern, G., Maor, Y., Chefetz, B. (2016). Human Exposure to Wastewater-Derived Pharmaceuticals in Fresh Produce: A Randomized Controlled Trial Focusing on Carbamazepine. Environ. Sci. Technol. 50, 4476–4482.

Pannu, M. W., Toor, G. S., O'Connor, G. A., Wilson, P. C. (2012). Toxicity and bioaccumulation of biosolids-borne triclosan in food crops. Environmental Toxicology and Chemistry, 31(9), 2130–2137.

Patlewicz, G., Jeliazkova, N., Safford, R. J., Worth, A. P., & Aleksiev, B. (2008). An evaluation of the implementation of the Cramer classification scheme in the Toxtree software. SAR and QSAR in Environmental Research, 19(5–6), 495–524.

Petrie, B., Barden, R., Kasprzyk-Hordern, B. (2015). A review on emerging contaminants in wastewaters and the environment: Current knowledge, understudied areas and recommendations for future monitoring. Water Research, 72, 3–27.

Patrolecco, L., Capri, S., Ademollo, N. (2015). Occurrence of selected pharmaceuticals in the principal sewage treatment plants in Rome (Italy) and in the receiving surface waters. Environ. Sci. Pollut. Res. 22, 5864–5876.

Peuravuori, J., Pihlaja, K. (2009). Phototransformations of selected pharmaceuticals under low-energy UVA-vis and powerful UVB-UVA irradiations in aqueous solutions-the role of natural dissolved organic chromophoric material. Analytical and Bioanalytical Chemistry, 394(6), 1621–1636.

Peuravuori, J. (2012). Aquatic photochemistry of paracetamol in the presence of dissolved organic chromophoric material and nitrate. Environmental Science and Pollution Research, 19(6), 2259–2270.

Phillips, P.J., Chalmers, A.T., Gray, J.L., Kolpin, D.W., Foreman, W.T., Wall, G.R., (2012). Combined sewer overflows: An environmental source of hormones and wastewater micropollutants. Environ. Sci. Technol. 46, 5336–5343.

Piña, B., Bayona, J.M., Christou, A., Fatta-Kassinos, D., Guillon, E., Lambropoulou, D., Michael, C., Polesel, F., Sayen, S. (2018). On the contribution of reclaimed wastewater irrigation to the potential exposure of humans to antibiotics, antibiotic resistant bacteria and antibiotic resistance genes – NEREUS COST Action ES1403 position paper. Journal of Environmental Chemical Engineering.

Pizza, F. (2014). Agricultural reuse of treated wastewater : the case of Milano-Nosedo municipal wastewater treatment plant. In D. Santoro, Trojan Technologies, & Western University (Eds.), Wastewater and Biosolids Treatment and Reuse: Bridging Modeling and Experimental Studies. ECI Symposium Series.

Plośz, B. G., Leknes, H., Thomas, K. V. (2010). Impacts of competitive inhibition, parent compound formation and partitioning behaviour on the removal of antibiotics in municipal wastewater treatment. Environmental Science and Technology, 44 (2), 734–742.

Plośz, B. G., Langford, K. H., Thomas, K. V. (2012). An activated sludge modeling framework for xenobiotic trace chemicals (ASM-X): Assessment of diclofenac and carbamazepine. Biotechnology and Bioengineering, 109 (11), 2757–2769.

Plósz, B.G., Benedetti, L., Daigger, G.T., Langford, K.H., Larsen, H.F., Monteith, H., Ort, C., Seth, R., Steyer, J.-P., Vanrolleghem, P.A., Eawag, C.O. (2013). Modelling micro-pollutant fate in wastewater collection and treatment systems: status and challenges. Water Sci. Technol.

Poiger, T., Buser, H. R., Müller, M. D. (2001). Photodegradation of the pharmaceutical drug diclofenac in a lake: Pathway, field measurements, and mathematical modeling. Environmental Toxicology and Chemistry, 20(2), 256–263.

Poirier-Larabie, S., Segura, P. A., Gagnon, C. (2016). Degradation of the pharmaceuticals diclofenac and sulfamethoxazole and their transformation products under controlled environmental conditions. Science of the Total Environment, 557–558, 257–267.

Polesel, F., Andersen, H. R., Trapp, S., Plósz, B. G. (2016). Removal of Antibiotics in Biological Wastewater Treatment Systems—A Critical Assessment Using the Activated Sludge

Modeling Framework for Xenobiotics (ASM-X). Environmental Science and Technology, 50 (19), 10316-10334.

Polesel, F., Plósz, B.G., Trapp, S. (2015). From consumption to harvest: Environmental fate prediction of excreted ionizable trace organic chemicals. Water Research 84, 85-98.

Pomiès, M., Choubert, J.-M., Wisniewski, C., Coquery, M. (2013). Modelling of micropollutant removal in biological wastewater treatments: A review. Sci. Total Environ. 443, 733–748.

Portmann, F., Siebert, S., Bauer, C., Döll, P. (2008). Global dataset of monthly growing areas of 26 irrigated crops. Frankfurt Hydrology Paper, 06, 400.

Pouzol, T., Lévi, Y., Bertrand-Krajewski, J. L. (2018). A Dynamic Pharmaceuticals Loads Source Generator. 11th International Conference on Urban Drainage Modelling, Palermo (Italy).

Prosser, R. S., Lissemore, L., Topp, E., & Sibley, P. K. (2014a). Bioaccumulation of triclosan and triclocarban in plants grown in soils amended with municipal dewatered biosolids. Environmental Toxicology and Chemistry, 33(5), 975–984.

Prosser, R. S., & Sibley, P. K. (2015). Human health risk assessment of pharmaceuticals and personal care products in plant tissue due to biosolids and manure amendments, and wastewater irrigation. Environment International, 75, 223–233.

Prosser, R. S., Trapp, S., & Sibley, P. K. (2014b). Modeling Uptake of Selected Pharmaceuticals and Personal Care Products into Food Crops from Biosolids-Amended Soil. Environmental Science & Technology, 48(19), 11397–11404.

Provincia di Milano (2007). Piano di Settore Agricolo. Relazione Generale.

Radke, M., Lauwigi, C., Heinkele, G., Múrdter, T. E., Letzel, M. (2009). Fate of the antibiotic sulfamethoxazole and its two major human metabolites in a water sediment test. Environmental Science and Technology, 43(9), 3135–3141.

Radke, M., Maier, M. P. (2014). Lessons learned from water/sediment-testing of pharmaceuticals. Water Research, 55, 63–73.

Radke, M., Ulrich, H., Wurm, C., Kunkel, U. (2010). Dynamics and attenuation of acidic pharmaceuticals along a river stretch. Environmental Science and Technology, 44(8), 2968–2974.

Rahman, M. F., Peldszus, S., Anderson, W. B. (2014). Behaviour and fate of perfluoroalkyl and polyfluoroalkyl substances (PFASs) in drinking water treatment: A review. Water Research, 50, 318–340.

Ramin, P., Libonati Block A., Polesel F., Causanilles A., Emke, E., de Voogt, P., Plosz, B.G. (2016). Transformation and sorption of illicit drug biomarkers in sewer systems: Understanding the role of suspended solids in raw wastewater. Environmental Science and Technology, 50 (24), 13397–13408.

Ramin, P., Libonati Block A., Causanilles A., Valverde-Perez, B., Emke, E., de Voogt, P., Polesel F., Plosz, B.G. (2017). Transformation and sorption of illicit drug biomarkers in sewer biofilms. Environmental Science and Technology 51, 10572–10584.

Ramin, P., Valverde-Pérez, B., Polesel, F., Locatelli, L., Benedek, &, Plósz, G. (2015). A systematic model identification method for chemical transformation pathways-the case of heroin biomarkers in wastewater. Science report.

Rawls, W. J., Brakensiek, D. L., Saxton, K. E. (1982). Estimation of soil water properties. American Society of Agricultural and Biological Engineers, 25(5), 1316–1320.

Rayne, S., Forest, K. (2009). Congener-specific organic carbon-normalized soil and sediment-water partitioning coefficients for the C 1 through C 8 perfluoroalkyl carboxylic and sulfonic acids. Journal of Environmental Science and Health, Part A, 44(13), 1374–1387.

Rayne, S., Forest, K. (2009). Perfluoroalkyl sulfonic and carboxylic acids: A critical review of physicochemical properties , levels and patterns in waters and wastewaters , and treatment methods Perfluoroalkyl sulfonic and carboxylic acids : A critical review of physicochemical prop. 4529.

Reichert, P., Vanrolleghem, P. (2001). Identifiability and uncertainty analysis of the River Water Quality Model No. 1 (RWQM1). Water Science and Technology, 43(7), 329–338.

Reichert, P., Borchardt, D., Henze, M., Rauch, W., Shanahan, P., Somlyódy, L., Vanrolleghem, P. (2001). River Water Quality Model no. 1 (RWQM1): II. Biochemical process equations. Water Sci. Technol. 43, 11–30.

Reynolds D. (2015). Gaussian Mixture Models. In: Li S.Z., Jain A.K. (editors) Encyclopedia of Biometrics. Springer, Boston, MA.

Ren, D., Bi, T., Gao, S., Li, X., Huang, B., Pan, X. (2016). Photodegradation of 17α-ethynylestradiol in nitrate aqueous solutions. Environmental Engineering Research, 21(2), 188–195.

Ren, D., Huang, B., Xiong, D., He, H., Meng, X., Pan, X. (2017). Photodegradation of 17α-ethynylestradiol in dissolved humic substances solution: Kinetics, mechanism and estrogenicity variation. Journal of Environmental Sciences, 54, 196–205.

Ren, D., Huang, B., Yang, B., Pan, X., Dionysiou, D. D. (2017). Mitigating 17A-ethynylestradiol water contamination through binding and photosensitization by dissolved humic substances. Journal of Hazardous Materials, 327, 197–205.

René, P. Schwarzenbach, Beate I. Escher, Kathrin Fenner, Thomas B. Hofstetter, C. Annette Johnson, U. von G. and B., Wehrli (2006). The Challenge of Micropollutants in Aquatic Systems. Science (80-85). 313, 1072–1077.

Rice Knowledge Bank. (2017). Measuring moisture content. Retrieved October 15, 2018, from http://www.knowledgebank.irri.org/step-by-step-production/postharvest/milling/milling-and-quality/measuring-moisture-content-in-milling

Riemenschneider, C., Al-Raggad, M., Moeder, M., Seiwert, B., Salameh, E., & Reemtsma, T. (2016). Pharmaceuticals, Their Metabolites, and Other Polar Pollutants in Field-Grown Vegetables Irrigated with Treated Municipal Wastewater. Journal of Agricultural and Food Chemistry, 64(29), 5784–5792.

Riva, F., Zuccato, E., Davoli, E., Fattore, E., & Castiglioni, S. (2019). Risk assessment of a mixture of emerging contaminants in surface water in a highly urbanized area in Italy. Journal of Hazardous Materials, 361, 103–110.

Robinson, J. A., Ma, Q., Staveley, J. P., Smolenski, W. J., Ericson, J. (2017). Degradation and transformation of 17A-estradiol in water–sediment systems under controlled aerobic and anaerobic conditions. Environmental Toxicology and Chemistry, 36(3), 621–629.

Rogowska, J., Cieszynska-Semenowicz, M., Ratajczyk, W., Wolska, L. (2019). Micropollutants in treated wastewater. Ambio.

Rosenbaum, R. K., Mckone, T. E., & Jolliet, O. (2009). CKow: A dynamic model for chemical transfer to meat and milk. Environmental Science and Technology, 43(21), 8191–8198.

Ryan, C. C., Tan, D. T., Arnold, W. A. (2011). Direct and indirect photolysis of sulfamethoxazole and trimethoprim in wastewater treatment plant effluent. Water Research, 45(3), 1280–1286.

Sabaliunas, D., Webb, S. F., Hauk, A., Jacob, M., and Eckhoff, W. S. (2003). Environmental fate of Triclosan in the River Aire Basin, UK. Water Research, 37(13):3145–3154.

Sabourin, L., Duenk, P., Bonte-Gelok, S., Payne, M., Lapen, D. R., Topp, E. (2012). Uptake of pharmaceuticals, hormones and parabens into vegetables grown in soil fertilized with municipal biosolids. Science of the Total Environment, 431, 233–236.

Saagi, R., Flores-Alsina, X., Fu, G., Butler, D., Gernaey, K. V, and Jeppsson, U. (2016). Catchment & sewer network simulation model to benchmark control strategies within urban wastewater systems. Environmental Modelling and Software, 78, 16–30.

Saagi, R., Flores-Alsina, X., Kroll, S., Gernaey, K.V., Jeppsson, U. (2017). A model library for simulation and benchmarking of integrated urban wastewater systems. Environ. Model. Softw. 93, 282–295.

Saltelli, A., Andres, T. H., & Homma, T. (1993). Sensitivity analysis of model output: An investigation of new techniques. Computational Statistics & Data Analysis, 15(2), 211–238.

Sanchez-Prado, L., Llompart, M., Lores, M., García-Jares, C., Bayona, J. M., Cela, R. (2006). Monitoring the photochemical degradation of triclosan in wastewater by UV light and sunlight using solid-phase microextraction. Chemosphere, 65(8), 1338–1347.

Sauvé, S., Desrosiers, M., (2014). A review of what is an emerging contaminant. Chem. Cent. J. 8, 1–7.

Schneider R., Schur N., Reinau D., Gut S., Schwenkglenks M., Meier R. C., (2018). *Helsana-Arzneimittelreport für die Schweiz,* Report, Basel, Switzerland.

Schowanek, D., Fox, K., Holt, M., Schroeder, F.R., Koch, V., Cassani, G., Matthies, M., Boeije, G., Vanrolleghem, P., Young, A., Morris, G., Gandolfi, C., Feijtel, T.C.J. (2001). GREAT-ER: a new tool for management and risk assessment of chemicals in river basins - Contribution to GREAT-ER #10. Water Sci. Technol. 43, 179–185.

Schwarzenbach, R. P., Gschwend, P. M., & Imboden, D. M. (2003). Environmental Organic Chemistry (Second Edition).

Sengeløv, G., Halling-Sørensen, B., Aarestrup, F. (2003). Susceptibility of Escherichia coli and Enterococcus faecium isolated from pigs and broiler chickens to tetracycline degra- dation products and distribution of tetracycline resistance determinants in E. coli from food animals. Vet. Microbiol. 95, 91–101.

Shanahan, P., Borchardt, D., Henze, M., Rauch, W., Reichert, P., Somlyódy, L., Vanrolleghem, P., Shanahan D.; Henze,M.; Rauch,W.; Reichert,P.; Somlyody,L.; Vanrolleghem,P., P.. B. (2001). River Water Quality Model no. 1 (RWQM1): I. Modelling approach. Water Sci. Technol. 43, 1–9.

Shenker, M., Harush, D., Ben-ari, J., Chefetz, B. (2011). Chemosphere Uptake of carbamazepine by cucumber plants – A case study related to irrigation with reclaimed wastewater. Chemosphere, 82(6), 905–910.

Siemens, J., Huschek, G., Siebe, C., and Kaupenjohann, M. (2008). Concentrations and mobility of human pharmaceuticals in the world's largest wastewater irrigation system, Mexico City-Mezquital Valley. Water Research, 42(8-9):2124-2134.

Silva, C. P., Lima, D. L. D., Otero, M., Esteves, V. I. (2016). Photosensitized Degradation of 17β-estradiol and 17α-ethinylestradiol: Role of Humic Substances Fractions. Journal of Environment Quality, 45(2), 693–700.

Silva, C. P., Lima, D. L. D., Groth, M. B., Otero, M., Esteves, V. I. (2016). Effect of natural aquatic humic substances on the photodegradation of estrone. Chemosphere, 145, 249–255.

Simonsen, J. F., Harremoës, P. (1978). Oxygen and pH fluctuations in rivers. Water Research, 12(7), 477–489.

Sin, G., Gernaey, K. V., Neumann, M. B., van Loosdrecht, M. C. M., & Gujer, W. (2011). Global sensitivity analysis in wastewater treatment plant model applications: Prioritizing sources of uncertainty. Water Research, 45(2), 639–651.

Singer, H., Müller, S., Tixier, C., Pillonel, L. (2002). Triclosan: Occurrence and fate of a widely used biocide in the aquatic environment: Field measurements in wastewater treatment plants, surface waters, and lake sediments. Environmental Science and Technology, 36(23), 4998–5004.

Snip, L.J.P., Flores-Alsina, X., Plósz, B.G., Jeppsson, U., Gernaey, K.V. (2014). Modelling the occurrence, transport and fate of pharmaceuticals in wastewater systems. Environmental Modelling and Software 62, 112–127.

Snip, L.J.P, Flores-Alsina, X., Aymerich, I., Rodríguez-Mozaz, S., Barceló, D., Plósz, B.G., Corominas, Ll., Rodriguez-Roda, I., Jeppsson, U., Gernaey, K.V. (2016). Generation of synthetic influent data to perform (micro)pollutant wastewater treatment modelling studies. Science of the Total Environment, 569-570, 278-290.

Speight, T.M., Sjöqvist, F. (2006). Clinical pharmacokinetics: The first 30 years. Clin. Pharmacokinet. 45, 645–647.

SPG 2013. Sewage Pattern Generator software available from Eawag http://www.eawag.ch/en/department/sww/software/ Accessed: on March, 2019.

Stadler, L.B., Ernstoff, A.S., Aga, D.S., Love, N.G. (2012). Micropollutant Fate in Wastewater Treatment: Redefining "Removal."

Stahl, T., Heyn, J., Thiele, H., Hüther, J., Failing, K., Georgii, S., Brunn, H. (2009). Carryover of perfluorooctanoic acid (PFOA) and perfluorooctane sulfonate (PFOS) from soil to plants. Archives of Environmental Contamination and Toxicology, 57(2), 289–298.

Stamm, C., Rasanen, K., Burdon, F.J., Altermatt, F., Jokela, J., Joss, A., Ackermann, M., Eggen, R.I.L., Eawag. (2016). Unravelling the Impacts of Micropollutants in Aquatic Ecosystems: Interdisciplinary Studies at the Interface of Large-Scale Ecology.

STAT-TAB. https://www.bfs.admin.ch/bfs/en/home.html. Accessed on March, 2019.

Steinwand, A. L., Harrington, R. F., & Groeneveld, D. P. (2001). Transpiration coefficients for three Great Basin shrubs. Journal of Arid Environments, 49(3), 555–567.

Stevens, J. B., Coryell, A. (2007). Surface Water Quality Criterion for Perfluorooctane Sulfonic Acid.

Su, T., Deng, H., Benskin, J. P., Radke, M. (2016). Biodegradation of sulfamethoxazole photo-transformation products in a water/sediment test. Chemosphere, 148, 518–525.

Sui, Q., Huang, J., Deng, S., Chen, W., & Yu, G. (2011). Seasonal variation in the occurrence and removal of pharmaceuticals and personal care products in different biological wastewater treatment processes. Environmental Science and Technology, 45(8), 3341–3348.

Tabaglio, V., Ligabue, M., Reggiani, R., Piazza, C., Tassi, D., Ruozzi, F. (2007). Quale loglio italico scegliere per la campagna 2007-08. L'informatore Agrario, 35, 40–43.

Testa, B., Pedretti, A., Vistoli, G. (2012). Reactions and enzymes in the metabolism of drugs and other xenobiotics. Drug Discov. Today.

Thai, P.K., Jiang, G., Gernjak, W., Yuan, Z., Lai, F.Y., Mueller, J.F. (2014). Effects of sewer conditions on the degradation of selected illicit drug residues in wastewater. Water Research, 48, 538–547.

Tixier, C., Singer, H. P., Canonica, S., Müller, S. R. (2002). Phototransformation of triclosan in surface waters: A relevant elimination process for this widely used biocide - Laboratory studies, field measurements, and modeling. Environmental Science and Technology, 36(16), 3482–3489.

Tixier, C., Singer, H. P., Oellers, S., Müller, S. R. (2003). Occurrence and Fate of Carbamazepine, Clofibric Acid, Diclofenac, Ibuprofen, Ketoprofen, and Naproxen in Surface Waters. Environmental Science & Technology, 37(6), 1061–1068.

Tournaire-Roux, C., Sutka, M., Javot, H., Gout, E., Gerbeau, P., Luu, D. T., … Maurel, C. (2003). Cytosolic pH regulates root water transport during anoxic stress through gating of aquaporins. Nature, 425(6956), 393–397.

Trapp, S. (2017). Coupled soil-plant uptake model for monovalent ionics. First release June 2017 at https://homepage.env.dtu.dk/stt/2017Release_Plant_Model/index.htm

Trapp, S. (2015). Calibration of a plant uptake model with plant- and site-specific data for uptake of chlorinated organic compounds into radish. Environmental Science and Technology, 49(1), 395–402.

Trapp S. (2009) Bioaccumulation of Polar and Ionizable Compounds in Plants. In: Devillers J. (eds) Ecotoxicology Modeling. Emerging Topics in Ecotoxicology (Principles, Approaches and Perspectives), vol 2. Springer, Boston, MA.

Trapp S, Ma L Bomholtz, Legind CN. (2008). Coupled mother-child model for bioaccumulation of POPs in nursing infants. Environmental Pollution 156, 90-98.

Trapp, S. (2004). Plant Uptake and Transport Models for Neutral and Ionic Chemicals. Environmental Science and Pollution Research, 11(1), 33–39.

Trapp, S., & Horobin, R. W. (2005). A predictive model for the selective accumulation of chemicals in tumor cells. European Biophysics Journal, 34(7), 959–966.

Trapp, S., & Matthies, M. (1998). Chemodynamics and Environmental Modelling. An introduction. New York, NY: Springer-Verlag.

Travis, C. C., & Arms, A. D. (1988). Bioconcentration of Organics in Beef, Milk, and Vegetation. Environmental Science and Technology, 22(3), 271–274.

USDA (2018). National Nutrient Database for Standard Reference Legacy Release - Basic Report: 11167, Corn, sweet, yellow, raw. URL: https://ndb.nal.usda.gov/ndb/foods/show/11167. Last accessed: 18-10-2018

Vaalgamaa, S., Vähätalo, A. V., Perkola, N., Huhtala, S. (2011). Photochemical reactivity of perfluorooctanoic acid (PFOA) in conditions representing surface water. Science of the Total Environment, 409(16), 3043–3048.

Van der Vorm, P. D. J. (1980). Uptake of Si by five plant species, as influenced by variations in Si-supply. Plant and Soil, 56(1), 153–156.

Vanrolleghem, P.A., Borchardt, D., Henze, M., Rauch, W., Reichert, P., Shanahan, P., Somly□dy, L. (2001). River Water Quality Model No. 1 (RWQM1): III. Biochemical submodel selection. Water Sci. Technol. 43, 31–40.

Vanrolleghem, P.A., Kamradt, B., Solvi, A., Muschalla, D. (2002). Making the best of two Hydrological Flow Routing Models : Nonlinear Outflow-Volume Relationships and Backwater Effects Model.

Vanrolleghem, P., Borchardt, D., Henze, M., Rauch, W., Reichert, P., Shanahan, P., Somlyódy, L. (2001). River Water Quality Model no. 1 (RWQM1): III. Biochemical submodel selection. Water Science and Technology, 43(5), 31–40.

Verlicchi, P., Al Aukidy, M., Zambello, E. (2012). Occurrence of pharmaceutical compounds in urban wastewater: Removal, mass load and environmental risk after a secondary treatment-A review. Sci. Total Environ.

Verlicchi, P., Ghirardini, A. (2019). Occurrence of micropollutants in wastewater and evaluation of their removal efficiency in treatment trains: The influence of the adopted sampling mode. Water (Switzerland) 11, 1–17.

Vezzaro, L., Benedetti, L., Gevaert, V., De Keyser, W., Verdonck, F., De Baets, B., … Mikkelsen, P. S. (2014). A model library for dynamic transport and fate of micropollutants in integrated urban wastewater and stormwater systems. Environmental Modelling and Software, 53, 98–111.

Vezzaro, L., Eriksson, E., Ledin, A., Mikkelsen, P.S. (2011). Modelling the fate of organic micropollutants in stormwater ponds. Sci. Total Environ. 409.

Vieno, N., Sillanpää, M. (2014). Fate of diclofenac in municipal wastewater treatment plant - A review. Environ. Int. 69, 28–39.

Vierke, L., Berger, U., Cousins, I. T. (2013). Estimation of the acid dissociation constant of perfluoroalkyl carboxylic acids through an experimental investigation of their water-to-air transport. Environmental Science and Technology, 47(19), 11032–11039.

Vochezer, K. (2010). Modelling of Carbamazepine and Diclofenac in a River Network by Modelling of Carbamazepine and Diclofenac in a River Network. Swedish University of Agricultural Sciences, Uppsala.

Voinov, A., Shugart, H.H., 2013. "Integronsters", integral and integrated modeling. Environ. Model. Softw. 39, 149–158.

Vreugdenhil, D., & Koot-Gronsveld, E. A. M. (1989). Measurements of pH, Sucrose and Potassium-Ions in the Phloem Sap of Castor Bean (Ricinus-Communis) Plants. Physiologia Plantarum, 77, 385–388.

Wang, X. -L, Canny, M. J., McCully, M. E. (1991). The water status of the roots of soil-grown maize in relation to the maturity of their xylem. Physiologia Plantarum, 82(2), 157–162.

Wang, Z., MacLeod, M., Cousins, I. T., Scheringer, M., & Hungerbühler, K. (2011). Using COSMOtherm to predict physicochemical properties of poly- and perfluorinated alkyl substances (PFASs). Environmental Chemistry, 8(4), 389–398.

Wen, B., Li, L., Zhang, H., Ma, Y., Shan, X., Zhang, S. (2014). Field study on the uptake and translocation of per fluoroalkyl acids (PFAAs) by wheat (Triticum aestivum L.) grown in biosolids-amended soils. Environmental Pollution, 184, 547–554.

Wen, B., Wu, Y., Zhang, H., Liu, Y., Hu, X., Huang, H. (2016). The roles of protein and lipid in the accumulation and distribution of per fluorooctane sulfonate (PFOS) and per fluorooctanoate

(PFOA) in plants grown in biosolids-amended soils *. Environmental Pollution, 216, 682–688.

Whidbey, C. M., Daumit, K. E., Nguyen, T. H., Ashworth, D. D., Davis, J. C. C., Latch, D. E. (2012). Photochemical induced changes of in vitro estrogenic activity of steroid hormones. Water Research, 46(16), 5287–5296.

WHO Collaborating Centre for Drug Statistics Methodology, Oslo, Norway. https://www.whocc.no/ddd/definition_and_general_considera/. Accessed on March, 2019.

Willach, S., Lutze, H. V., Eckey, K., Löppenberg, K., Lüling, M., Wolbert, J. B., … Schmidt, T. C. (2018). Direct Photolysis of Sulfamethoxazole Using Various Irradiation Sources and Wavelength Ranges - Insights from Degradation Product Analysis and Compound-Specific Stable Isotope Analysis. Environmental Science and Technology, 52(3), 1225–1233.

Williams, R.J., Keller, V.D.J., Johnson, A.C., Young, A.R., Holmes, M.G.R., Wells, C., Gross-Sorokin, M., Benstead, R. (2009). A national risk assessment for intersex in fish arising from steroid estrogens. Environ. Toxicol. Chem. 28, 220–230.

Williams, R. J., Johnson, A. C., Smith, J. J. L., Kanda, R. (2003). Steroid estrogens profiles along river stretches arising from sewage treatment works discharges. Environmental Science and Technology, 37(9), 1744–1750.

Winkler, M., Lawrence, J. R., & Neu, T. R. (2001). Selective degradation of ibuprofen and clofibric acid in two model river biofilm systems. Water Research, 35(13), 3197–3205.

Wolfs, V., Villazon, M.F., Willems, P. (2013) Development of a semi-automated model identification and calibration tool for conceptual modelling of sewer systems. Water Science and Technology, 68, 167–175.

Writer, J. H., Antweiler, R. C., Ferrer, I., Ryan, J. N., & Thurman, E. M. (2013). In-stream attenuation of neuro-active pharmaceuticals and their metabolites. Environmental Science and Technology, 47(17), 9781–9790.

Writer, J. H., Ryan, J. N., Keefe, S. H., Barber, L. B. (2012). Fate of 4-nonylphenol and 17β-estradiol in the Redwood River of Minnesota. Environmental Science and Technology, 46(2), 860–868.

Wu, C., Huang, X., Lin, J., Liu, J. (2015). Occurrence and Fate of Selected Endocrine-Disrupting Chemicals in Water and Sediment from an Urban Lake. Archives of Environmental Contamination and Toxicology, 68(2), 225–236.

Wu, C., Spongberg, A. L., Witter, J. D., Sridhar, B. B. M. (2012). Transfer of wastewater associated pharmaceuticals and personal care products to crop plants from biosolids treated soil. Ecotoxicology and Environmental Safety, 85, 104–109.

Wu, C., Spongberg, A. L., Witter, J. D. (2009). Adsorption and Degradation of Triclosan and Triclocarban in Soils and Biosolids-Amended Soils. Journal of Agricultural and Food Chemistry, 57, 4900–4905.

Wu, C., Spongberg, A. L., Witter, J. D., Fang, M., Czajkowski, K. P. (2010). Uptake of Pharmaceutical and Personal Care Products by Soybean Plants from Soils Applied with Biosolids and Irrigated with Contaminated Water. Environmental Science & Technology, 44(16), 6157–6161.

Wu, L., Gao, H.-W., Gao, N., Chen, F.-F., Chen, L. (2009). Interaction of perfluorooctanoic acid with human serum albumin. BMC Structural Biology, 9(1), 31.

Wu, X., Conkle, J. L., Ernst, F., & Gan, J. (2014). Treated wastewater irrigation: Uptake of pharmaceutical and personal care products by common vegetables under field conditions. Environmental Science and Technology, 48(19), 11286–11293.

Xing, L., Spitler, J. D. (2017). Prediction of undisturbed ground temperature using analytical and numerical modeling. Part I: Model development and experimental validation. Science and Technology for the Built Environment, 23(5), 787–808.

Xu, B., Mao, D., Luo, Y., Xu, L. (2011). Sulfamethoxazole biodegradation and biotransformation in the water-sediment system of a natural river. Bioresource Technology, 102(14), 7069–7076.

Xu, J., Wu, L., Chang, A. C. (2009). Degradation and adsorption of selected pharmaceuticals and personal care products (PPCPs) in agricultural soils. Chemosphere, 77(10), 1299–1305.

Yager, T. J. B., Furlong, E. T., Kolpin, D. W., Kinney, C. A., Zaugg, S. D., Burkhardt, M. R. (2014). Dissipation of Contaminants of Emerging Concern in Biosolids Applied to Nonirrigated Farmland in Eastern Colorado. JAWRA Journal of the American Water Resources Association, 50(2), 343–357.

Yagi, N., Kenmotsu, H., Sekikawa, H., Takada, M. (1991). Studies on the Photolysis and Hydrolysis of Furosemide in Aqueous Solution. Chemical & Pharmaceutical Bulletin, 39, 454–457.

Yamamoto, H., Nakamura, Y., Moriguchi, S., Nakamura, Y., Honda, Y., Tamura, I., … Sekizawa, J. (2009). Persistence and partitioning of eight selected pharmaceuticals in the aquatic environment: Laboratory photolysis, biodegradation, and sorption experiments. Water Research, 43(2), 351–362.

Yoo, H., Washington, J. W., Jenkins, T. M., Ellington, J. J. (2011). Quantitative determination of perfluorochemicals and fluorotelomer alcohols in plants from biosolid-amended fields using LC/MS/MS and GC/MS. Environmental Science and Technology, 45(19), 7985–7990.

Zgheib, S., Moilleron, R.., Chebbo, G. (2012). Priority pollutants in urban stormwater: Part 1 – Case of separate storm sewers. Water Res. 46, 6683–6692.

Zhang, Y., Geißen, S.U., Gal, C. (2008). Carbamazepine and diclofenac: Removal in wastewater treatment plants and occurrence in water bodies. Chemosphere.

Zhang, N., Li, J. M., Liu, G. G., Chen, X. L., Jiang, K. (2017a). Photodegradation of diclofenac in aqueous solution by simulated sunlight irradiation: Kinetics, thermodynamics and pathways. Water Science and Technology, 75(9), 2163–2170.

Zhang, Y., Biswas, A., Adamchuk, V. I. (2017b). Implementation of a sigmoid depth function to describe change of soil pH with depth. Geoderma, 289, 1–10.

Zhang, N., Liu, G., Liu, H., Wang, Y., He, Z., Wang, G. (2011). Diclofenac photodegradation under simulated sunlight: Effect of different forms of nitrogen and Kinetics. Journal of Hazardous Materials, 192(1), 411–418.

Zhang, W., Webster, E. P. (2002). Shoot and root growth of rice (Oryza sativa) in response to V-10029. Weed Technology, 16(4), 768–772.

Zhang, Y., Xu, J., Zhong, Z., Guo, C., Li, L., He, Y., … Chen, Y. (2013). Degradation of sulfonamides antibiotics in lake water and sediment. Environmental Science and Pollution Research, 20(4), 2372–2380.

Zhang, Y., Sangster, J. L., Gauza, L., Bartelt-Hunt, S. L. (2016). Impact of sediment particle size on biotransformation of 17β-estradiol and 17β-trenbolone. Science of the Total Environment, 572, 207–215.

Zhao, S., Fan, Z., Sun, L., Zhou, T., Xing, Y., Liu, L. (2017a). Interaction effects on uptake and toxicity of perfluoroalkyl substances and cadmium in wheat (Triticum aestivum L.) and rapeseed (Brassica campestris L.) from co-contaminated soil. Ecotoxicology and Environmental Safety, 137(July 2016), 194–201.

Zhao, S., Fang, S., Zhu, L., Liu, L., Liu, Z., Zhang, Y. (2014). Mutual impacts of wheat (Triticum aestivum L .) and earthworms (Eisenia fetida) on the bioavailability of per fluoroalkyl substances (PFASs) in soil. Environmental Pollution, 184, 495–501.

Zhao, W., Wang, B., Wang, Y., Deng, S., Huang, J., Yu, G. (2017b). Deriving acute and chronic predicted no effect concentrations of pharmaceuticals and personal care products based on species sensitivity distributions. Ecotoxicology and Environmental Safety, 144(February), 537–542.

Zonja, B., Pe, S. (2015). Human Metabolite Lamotrigine-N 2-glucuronide Is the Principal Source of Lamotrigine-Derived Compounds in Wastewater Treatment Plants and Surface Water.

Zoppou, C. (2001). Review of urban storm water models. Environmental Modelling and Software, 16 (3), 195–231.

Zuccato, E., Castiglioni, S., Bagnati, R., Melis, M., Fanelli, R. (2010). Source, occurrence and fate of antibiotics in the Italian aquatic environment. J. Hazard. Mater. 179, 1042–1048.

Zuo, Y., Zhang, K., Zhou, S. (2013). Determination of estrogenic steroids and microbial and photochemical degradation of 17α-ethinylestradiol (EE2) in lake surface water, a case study. Environmental Sciences: Processes and Impacts, 15(8), 1529–1535.

Żur, J., Piński, A., Marchlewicz, A., Hupert-Kocurek, K., Wojcieszyńska, D., Guzik, U. (2018). Organic micropollutants paracetamol and ibuprofen-toxicity, biodegradation, and genetic background of their utilization by bacteria. Environ. Sci. Pollut. Res. Int. 25, 21498–21524.